

Dynamically orthogonal field equations for stochastic fluid flows and particle dynamics

by

Themistoklis P. Sapsis

Dipl., National Technical University of Athens (2005)

Submitted to the Department of Mechanical Engineering
in partial fulfillment of the requirements for the degree of

Doctor of Philosophy in Mechanical Engineering

at the

MASSACHUSETTS INSTITUTE OF TECHNOLOGY

February 2011

© Massachusetts Institute of Technology 2011. All rights reserved.

Author
Department of Mechanical Engineering
31 October, 2010

Certified by
Pierre F.J. Lermusiaux
Associate Professor
Thesis Supervisor

Accepted by
David E. Hardt
Chairman, Department Committee on Graduate Theses

Dynamically orthogonal field equations for stochastic fluid flows and particle dynamics

by

Themistoklis P. Sapsis

Submitted to the Department of Mechanical Engineering
on 31 October, 2010, in partial fulfillment of the
requirements for the degree of
Doctor of Philosophy in Mechanical Engineering

Abstract

In the past decades an increasing number of problems in continuum theory have been treated using stochastic dynamical theories. This is because dynamical systems governing real processes always contain some elements characterized by uncertainty or stochasticity. Uncertainties may arise in the system parameters, the boundary and initial conditions, and also in the external forcing processes. Also, many problems are treated through the stochastic framework due to the incomplete or partial understanding of the governing physical laws. In all of the above cases the existence of random perturbations, combined with the complex dynamical mechanisms of the system often leads to their rapid growth which causes distribution of energy to a broadband spectrum of scales both in space and time, making the system state particularly complex. Such problems are mainly described by Stochastic Partial Differential Equations and they arise in a number of areas including fluid mechanics, elasticity, and wave theory, describing phenomena such as turbulence, random vibrations, flow through porous media, and wave propagation through random media. This is but a partial listing of applications and it is clear that almost any phenomenon described by a field equation has an important subclass of problems that may profitably be treated from a stochastic point of view.

In this work, we develop a new methodology for the representation and evolution of the complete probabilistic response of infinite-dimensional, random, dynamical systems. More specifically, we derive an exact, closed set of evolution equations for general nonlinear continuous stochastic fields described by a Stochastic Partial Differential Equation. The derivation is based on a novel condition, the Dynamical Orthogonality (DO), on the representation of the solution. This condition is the ‘key’ to overcome the redundancy issues of the full representation used while it does not restrict its generic features. Based on the DO condition we derive a system of field equations consisting of a Partial Differential Equation (PDE) for the mean field, a family of PDEs for the orthonormal basis that describe the stochastic subspace where uncertainty ‘lives’ as well as a system of Stochastic Differential Equations that defines how the uncertainty evolves in the time varying stochastic subspace. If additional restrictions are assumed on the form of the representation, we recover both the Proper-Orthogonal-Decomposition (POD) equations and the generalized Polynomial-Chaos (PC) equations; thus the new methodology generalizes these two approaches. For the efficient treatment of the strongly transient character on the systems described above we derive adaptive criteria for the variation of the stochastic dimensionality that characterizes the system response. Those criteria follow directly from the dynamical equations describing the system.

We illustrate and validate this novel technique by solving the 2D stochastic Navier-Stokes equations in various geometries and compare with direct Monte Carlo simulations. We also

apply the derived framework for the study of the statistical responses of an idealized ‘double gyre’ model, which has elements of ocean, atmospheric and climate instability behaviors.

Finally, we use our new stochastic description for flow fields to study the motion of inertial particles in flows with uncertainties. Inertial or finite-size particles in fluid flows are commonly encountered in nature (e.g., contaminant dispersion in the ocean and atmosphere) as well as in technological applications (e.g., chemical systems involving particulate reactant mixing). As it has been observed both numerically and experimentally, their dynamics can differ markedly from infinitesimal particle dynamics. Here we use recent results from stochastic singular perturbation theory in combination with the DO representation of the random flow, in order to derive a reduced order inertial equation that will describe efficiently the stochastic dynamics of inertial particles in arbitrary random flows.

Thesis Supervisor: Pierre F.J. Lermusiaux

Title: Associate Professor

Acknowledgments

I wish to extend warm thanks to my advisors Pierre Lermusiaux and George Haller for this wonderful journey. It all started four years ago when I began to work with George on the nonlinear dynamics of small particles. A year after I joined MSEAS group and I start my research on stochastic flows with Pierre. I am indebted to both of them for giving me a well balanced mix of freedom and guidance on my research, allowing me to put time on new ideas while maintaining the scientific ‘entropy’ on reasonable and efficient levels. Special thanks to George for doing that remotely with such an enthusiasm but also for teaching me to present results in a rigorous but nevertheless attractive way. Special thanks to Pierre for teaching me that mathematical modeling can and should always be performed in connection with physical intuition and understanding of the considered phenomenon. I am also grateful to the members of my thesis committee, Dennis McLaughlin, Nicholas Patrikalakis, and Carl Wunsch for their constructive comments and advise.

I owe a huge debt of gratitude to Alex Vakakis for his advise and support especially during some difficult times of my graduate life. I met him many years ago when I took his Nonlinear Dynamics classes as undergrad in Greece and since then he has been a mentor, friend, and collaborator. I am grateful to my diploma thesis advisor Makis Athanassoulis whose classes, seminars, and endless hours put on joint research on various applied math topics and especially on stochastic systems were important background for the work done in this thesis.

I wish to extend warm thanks to my officemate and friend, Matt Ueckermann, for his help and support on the numerical part of the thesis. Matt’s enthusiasm on scientific computing led to a two-three orders of magnitude speed increase of the original codes. This was not enough for him though so he implemented the developed algorithms using his finite-volume framework, ending up with an even faster and more accurate code which was used for some of the results included in this work.

I feel indebted to all my collaborators: Larry Bergman for collaboration on random vibrations and also his advise and support, Jerry Gollub and Nick Ouellette for working on experimental data analysis for particles, Jeff Peng and John Dabiri for providing data and collaborating on the predator-prey interactions problem around a jellyfish, Sotiria Koloutsou-Vakakis for collaboration on transportation of pollutants, and Raf Ferrari for discussions and collaboration on ocean mixing and Lagrangian Coherent Structures.

Thanks also to all the members in the Nonlinear Dynamics Lab and the MSEAS group for four wonderful years. Special thanks to my officemates who helped create a great working environment: Mani Mathur, Wenbo Tang, Lisa Burton, Eric Heubel, Arpit Agarwal, Thomas Sondergaard, Konur Yigit, Tapovan Lolla, Latifah Hamzah, and Melissa Kaufman. I also want to thank Leslie Regan and Marcia Munger for solving every administrative problem.

I would like to acknowledge ONR (N00014-07-1-1061, N00014-08-1-1097, N00014-07-1-0241 (QPE)), AFOSR (FA 9550-06-0092), and NSF (DMS-04- 04845) for supporting my research. I have very much appreciated the opportunity to attend many conferences and meetings; discussing my work with other scientists has been an important part of my graduate career. I especially thanks MIT for awarding me the Presidential Fellowship ‘George and Marie Vergottis’ for the first two years.

I also want to show my gratitude to Kimon Bekelis and George Gikas for endless hours of discussions on academic and non-academic issues, and for always being there as friends whenever I need them.

This list would not be complete without a special thanks to my family here at US, uncle Foti, aunt Laura, Sonia, Rob and Alex for their unconditional love and support in many situations. Last but not least, I am grateful to my parents and my brother Panteli. I have no way to thank them for their invaluable role in my life but to dedicate this dissertation to them.

Contents

1	Introduction	17
1.1	Preview of chapters	18
2	Representations of stochastic fields	21
2.1	Introduction	21
2.2	The family of probability density functions	23
2.3	The moment system	25
2.3.1	Connection with the family of characteristic functions	26
2.4	The characteristic functional	27
2.4.1	Determination of the moments system	28
2.4.2	Determination of the family of characteristic functions	29
2.4.3	Characteristic functionals with explicit description	29
2.5	The Karhunen Loeve expansion	30
2.5.1	A geometrical interpretation	31
2.5.2	Application to fluid flows	33
3	Evolution of stochastic fields	37
3.1	Introduction	37
3.2	Definitions and problem statement	40
3.3	The stochastic subspace and the dynamical orthogonality condition	41
3.4	Dynamically orthogonal field equations	43
3.4.1	The case of independent increment excitation (white noise)	46
3.5	Consistency with existing methodologies	49
3.5.1	Generalized polynomial chaos expansion	49
3.5.2	Proper orthogonal decomposition	50
4	Evolution of the stochastic dimensionality	51
4.1	Introduction	51
4.2	Cost scaling with the stochastic dimensionality	52
4.3	Update of the stochastic subspace using stability properties of the SPDE	53
4.3.1	Conditions for the evolution of the stochastic dimensionality	54
4.3.2	Selection of new stochastic dimensions	55
4.4	Update of the stochastic subspace using data and measurements	58
4.4.1	Data and measurements formulation	58
4.4.2	Update of the stochastic information inside \mathbf{V}_S	59
4.4.3	Expansion of the stochastic subspace \mathbf{V}_S	61

5	Application of dynamically orthogonal field equations to random fluid flows	63
5.1	Formulation	63
5.2	Derivation of DO Navier-Stokes equations	65
5.2.1	Stochastic pressure field	65
5.2.2	Evolution of the mean field $\bar{\mathbf{u}}(\mathbf{x}, t; \omega)$	67
5.2.3	Evolution of the stochastic subspace basis $\mathbf{u}_i(\mathbf{x}, t; \omega)$	67
5.2.4	Evolution of the stochastic coefficients $Y_i(\mathbf{x}, t; \omega)$	68
5.3	The case of stochastic boundary conditions	69
5.4	Unstable perturbations for Navier-Stokes equations	70
5.5	Transfer of energy in Navier-Stokes	72
5.5.1	Energy exchanges between the DO modes and the mean flow	73
5.5.2	Energy exchanges between the DO modes	74
5.5.3	Stochastic energy in Navier-Stokes	75
5.6	Application I: Lid driven cavity flow with stochastic initial conditions	76
5.6.1	Evolution of a small stochastic perturbation	79
5.6.2	Convergence with respect to the stochastic dimensionality	83
5.7	Application II: Flow past a circular disk with stochastic initial conditions	86
5.8	Application III: Instabilities in the forced double gyre flow in a basin	94
5.8.1	Model	97
5.8.2	An overview of deterministic analysis	98
5.8.3	Bifurcation analysis of the stochastic response	101
5.8.4	Stochastic response for larger Reynolds number	111
6	Finite-size particles in stochastic flows	119
6.1	Introduction	119
6.2	Summary of results for finite-size particles in deterministic flows	120
6.2.1	Reduced order dynamics	121
6.2.2	Instabilities on the dynamics of finite-size particles	127
6.2.3	Clustering of finite-size particles	129
6.3	Dynamics of finite-size particles in stochastic flows	131
6.3.1	Stochastic velocity field	131
6.3.2	Markov (diffusion) approximation	132
6.3.3	Stochastic slow manifold	135
6.3.4	Stochastic inertial equation	137
6.3.5	Stochastic source inversion	139
6.4	Higher order Lagrangian stochastic models	139
6.5	Clustering due to stochasticity of the flow	140
6.6	Application: Particles in the double gyre flow	142
6.6.1	Stochastic slow manifold in the flow	142
6.6.2	Convergence to the stochastic slow manifold	147
6.6.3	Validation of stochastic inertial equation	147
6.6.4	Clustering due to the combined effect of inertial and flow stochasticity	150
7	Conclusions	155
7.1	Future directions	156

A	DO equations for 3D Navier-Stokes in component wise form	159
A.1	Stochastic pressure field	161
A.2	Evolution of the mean field $\bar{\mathbf{u}}(\mathbf{x}, t; \omega)$	163
A.3	Evolution of the stochastic subspace basis $\chi_i(\mathbf{x}, t; \omega)$	163
A.4	Evolution of the stochastic coefficients $Y_i(\mathbf{x}, t; \omega)$	165
B	Numerical implementation of 2D DO for Navier-Stokes	167
B.1	Initial conditions formulation	167
B.1.1	Storage of orthonormal basis	168
B.2	Evolution of stochastic state	168
B.3	Diagonalization of covariance matrix - Adaptive criteria	168
B.4	Storage - Plotting	170
C	Normal local stability of general invariant manifolds	171
C.1	Set-up and definitions	171
C.2	Normally stable and normally unstable subsets	172
C.3	Computing the NILE	175
C.4	Locating stable and unstable neighborhoods of $M(t)$	176
C.5	Stability properties of non-neutrally buoyant particles	177

List of Figures

2-1	Ellipsoid that contains the main spread ('mass') of the probability measure; defined by the principal directions and the associated eigenvalues of the correlation operator.	32
3-1	a) The stochastic subspace \mathbf{V}_S spanned by fields $\mathbf{u}_i(\mathbf{x}, t)$ that corresponds to important variance. b) The variation of the $\mathbf{u}_i(\mathbf{x}, t)$ inside V_S can always be covered by a rotation of the stochastic coefficients $Y_i(t; \omega)$	44
4-1	Computational time (sec) for the lid-driven cavity flow described in Chapter 5, using different number of modes (red curve). The blue line indicates the linear 'best fit' in the log-log plot and it has an inclination equal to 1.986 (2 is the theoretical prediction).	54
4-2	Decomposition of the stochastic subspace \mathbf{V}_S based on the data subspace \mathbf{V}_O	59
4-3	Update of the probability density function $f_{\mathbf{Y}}(\mathbf{y}, t)$ using data or measurements.	62
5-1	Energy exchanges between DO modes and the mean flow in stochastic, homogeneous, Navier-Stokes equations. The energy flow from the mean to the modes is characterized by the second order statistics while variance exchange among the modes is characterized by the third order statistics.	77
5-2	Driven cavity flow, problem configuration.	77
5-3	Initial conditions for the mean and the basis of the stochastic subspace V_S in terms of the field streamfunction.	78
5-4	Evolution of principal variances $\sigma_i^2(t)$, $i = 1, \dots, 5$ (blue curves) and mean field energy (red curve) for the flow in a cavity.	79
5-5	Mean field and basis of the stochastic subspace V_S in terms of the streamfunction and vorticity field; two-dimensional marginals of the five dimensional joint pdf $f(\mathbf{y}, t)$ at time $t = 2$	80
5-6	Mean field and basis of the stochastic subspace V_S in terms of the streamfunction and vorticity field; two-dimensional marginals of the five dimensional joint pdf $f(\mathbf{y}, t)$ at time $t = 8$	81
5-7	Mean velocity field (streamfunction) computed using Monte-Carlo method (250 and 500 samples) and the DO field equations ($s = 5$ modes) at $t = 1$	82
5-8	Upper plots: mean flow for $t = 0.7$ in terms of the streamfunction for i) the four modes solution and ii) the five modes solution. Lower plot: the red curves represent the time series for the variances $\sigma_i^2(t)$, $i = 1, \dots, 5$ of the five-modes solution $\mathbf{v}(\mathbf{x}, t; \omega)$ while the blue curves represent the projection of the four modes solution $\mathbf{u}(\mathbf{x}, t; \omega)$ to the modes $\mathbf{v}_i(\mathbf{x}, t)$	84

5-9	Upper plots: mean flow for $t = 5.98$ in terms of the streamfunction for i) the four modes solution and ii) the five modes solution. Lower plot: the red curves represent the time series for the variances $\sigma_i^2(t)$, $i = 1, \dots, 5$ of the five-modes solution $\mathbf{v}(\mathbf{x}, t; \omega)$ while the blue curves represent the projection of the four modes solution $\mathbf{u}(\mathbf{x}, t; \omega)$ to the modes $\mathbf{v}_i(\mathbf{x}, t)$	85
5-10	Mean flow for various stochastic dimensionalities and for $t = 1$	86
5-11	Mean flow for various stochastic dimensionalities and for $t = 2$	87
5-12	Mean flow for various stochastic dimensionalities and for $t = 6$	88
5-13	Left column: mean flow for various stochastic dimensionalities $\dim(\mathbf{V}_S)$ at $t = 2$. The four right columns on the right show the four most energetic modes $\mathbf{u}_i(\mathbf{x}, t)$ in terms of their streamfunction as well as their associated variance $E^\omega [Y_i^2(t; \omega)]$ as a function of time.	89
5-14	Left column: mean flow for various stochastic dimensionalities $\dim(\mathbf{V}_S)$ at $t = 6$. The four right columns on the right show the four most energetic modes $\mathbf{u}_i(\mathbf{x}, t)$ in terms of their streamfunction as well as their associated variance $E^\omega [Y_i^2(t; \omega)]$ as a function of time.	90
5-15	Left column: mean flow for various stochastic dimensionalities $\dim(\mathbf{V}_S)$ at $t = 8$. The four right columns on the right show the four most energetic modes $\mathbf{u}_i(\mathbf{x}, t)$ in terms of their streamfunction as well as their associated variance $E^\omega [Y_i^2(t; \omega)]$ as a function of time.	91
5-16	Upper plot: instantaneous error of the solution with respect to the number of modes used and time. Lower plot: time averaged error with respect to the number of DO modes.	92
5-17	A typical realization of the flow past a circular disk.	92
5-18	Initial conditions for the mean and the basis of the stochastic subspace V_S in terms of the field streamfunction.	93
5-19	Evolution of principal variances $\sigma_i^2(t)$, $i = 1, \dots, 5$ (blue curves) and mean field energy (red curve) for the flow behind a disk.	94
5-20	Mean field and basis of the stochastic subspace V_S in terms of the streamfunction; two-dimensional marginals of the five dimensional joint pdf $f(\mathbf{y}, t)$ at time $t = 2$	95
5-21	Mean field and basis of the stochastic subspace V_S in terms of the streamfunction; two-dimensional marginals of the five dimensional joint pdf $f(\mathbf{y}, t)$ at time $t = 4$	96
5-22	Mean velocity field (streamfunction) computed using the DO field equations ($s = 5$) and Monte-Carlo method (500 samples) at $t = 1$	96
5-23	Bifurcation diagram for the QG model with values of the parameters as in Tables 5.1 and 5.2 (from Simonnet and Dijkstra [133]).	99
5-24	Spectral behavior of the eigenmodes involved into the various bifurcations of the antisymmetric branch for the barotropic QG model (from Simonnet and Dijkstra [133]).	100
5-25	Stochastic response of the QG model for $Re = 25$. The left top plot shows the mean flow in terms of the vorticity (colormap) and the streamlines (black solid curves). The right-top plot indicates the energy of the mean flow (red curve) and the variance of the stochastic mode. The bottom plot indicates the first DO mode together with the pdf for the stochastic coefficient.	101
5-26	Stochastic response of the QG system for $Re = 35$ after the system has reached steady state statistics.	102

5-27	Oscillation of the DO mode during convergence to the steady state attractor for $Re = 35$	103
5-28	Addition of an extra mode at the time instant where the existing mode exceeds the predefined variance (Flow $Re = 38$).	104
5-29	Mode removal due to very low variance (Flow $Re = 38$).	105
5-30	The variance of the stochastic perturbation becomes comparable with the energy of the mean flow. At this point mutual interactions between the mean flow and the perturbation begin to occur.	106
5-31	Steady state regime for $Re = 38$. Note that the perturbation retains its symmetric character even though the variance of the mode is comparable with energy of the mean flow.	107
5-32	Stochastic response for $Re = 40$. Note that the first mode has symmetric spatial properties which are accompanied by symmetric pdf while the second mode has antisymmetric spatial properties with non-symmetric pdf.	108
5-33	Initial stage of motion for $Re = 55$	109
5-34	As time evolves more modes have to be added in order to achieve the given tolerance (in terms of variance).	110
5-35	Convergence to a deterministic attractor after a transient stochastic regime for $Re = 65$	111
5-36	Response for $Re = 85$. In this case the convergence to the deterministic attractor occurs earlier with the initial stochastic regime being much shorter in time.	112
5-37	Convergence to a deterministic attractor for $Re = 100$	113
5-38	Stochastic attractor after a temporal convergence to deterministic dynamics ($Re = 200$).	114
5-39	Summary of the stochastic analysis for the double gyre flow over various Reynolds numbers.	114
5-40	Initial regime of the stochastic response for $Re = 10^4$	115
5-41	The modes added are localized around the boundary of the formed gyres of the mean flow.	115
5-42	After the mean flow energy exceeds a certain limit an instability breaks the symmetry of the third mode as it is shown in the corresponding pdf plot.	116
5-43	The instability shown in the previous figure is the starting point for the non-Gaussian statistics shown here.	117
6-1	(a) The geometry of the domain D_0 (b) The attracting set of fixed points M_0 ; each point p in M_0 has a n -dimensional stable manifold $f_0^s(p)$ (unperturbed stable fiber at p) satisfying $(\mathbf{x}, \phi) = const$	124
6-2	(a) The geometry of the slow manifold M_ϵ (b) A trajectory intersecting a stable fiber $f_\epsilon^s(p)$ converges to the trajectory through the fiber base point p	124
6-3	Sudden changes in the velocity field delay convergence to the slow manifold.	126
6-4	Particle velocity (blue solid curve) attracted by a concentrated layer of probability, a stochastic slow manifold. The red solid curve denotes the mean of the manifold and the dotted curves define the local spread of probability around the mean.	136
6-5	Clustering manifold is independent from the flow direction.	141
6-6	Stochastic double gyre for the illustration of the inertial particles motion; $Re = 25$ (See chapter 5 for details).	143

6-7	Mean value of the stochastic slow manifold governing the motion of inertial particles for the double gyre stochastic flow.	144
6-8	Variance of the stochastic slow manifold describing of motion inertial particles for $t = 100.0$ and $t = 100.5$	145
6-9	Variance of the stochastic slow manifold describing of motion inertial particles for $t = 101.0$ and $t = 101.5$	146
6-10	(a) Rapid convergence to the stochastic slow manifold during the initial phase of motion. The colormap denotes the local variance of the slow manifold $\sigma_s(\mathbf{x}, t)$. The vertical coordinate shows the distance of the stochastic dynamics from the mean slow manifold. (b) x - component of the particle velocity, resolved according to Maxey-Riley equation for a particular flow realization (blue solid curve). The red lines indicate the local spread of probability around the mean slow manifold at the particle's location. (c) same as (b) but now the distance from the slow manifold is shown.	148
6-11	Same as 6-10 but for a later time instant.	149
6-12	Comparison of stochastic inertial equation (6.40) and direct Monte-Carlo simulation for $t = 100, 101, 102$	151
6-13	Same as Figure 6-12 for $t = 103, 104$	152
6-14	Concentration field for finite size particles (heavy particles) for two different time instants. The blue lines indicate streamlines for the mean flow. The red lines indicate clustering manifolds for the stochastic flow field.	153
B-1	Computational algorithm for the adaptive DO equations.	169
C-1	Trajectories jump away from $M(t)$ over the unstable subset $M_u(t)$, but return to $M(t)$ over the stable subset $M_s(t)$. The figure assumes that $M(t)$ is a normally hyperbolic attracting manifold, in which case the jumping trajectory keeps approaching the same underlying trajectory on $M(t)$ by the invariant foliation of the stable manifold $W^s(M(t))$	173
C-2	The operator $\Pi_{F_t^{t+s}(p)}^{t+s} DF_t^{t+s} _{N_p M(t)}$ maps vectors in the normal space $N_p M(t)$ to vectors in the normal space $N_{F_t^{t+s}(p)} M(t+s)$. The NILE $\sigma(p; t)$ is the exponential rate at which the norm of the above operator grows in the limit of infinitesimally small s . Therefore, $\sigma(p; t)$ measures the exponential rate at which the normal component of vectors normal to the manifold $M(t)$ grows over very short times. (The time τ is arbitrary within the interval $[t, t + s]$.)	174
C-3	The manifold $M(t)$ as a local graph over the x variables.	175

List of Tables

5.1	Reference values of parameters in the barotropic QG model (dimensional). . .	98
5.2	Reference values of parameters in the barotropic QG model (non-dimensional). . .	98
6.1	Reference values of parameters in the barotropic QG model used for the study of finite-size particles (dimensional).	143

Chapter 1

Introduction

Dynamical systems play a central role in applications of mathematics to natural and engineering sciences. However, dynamical systems governing real processes always contain some elements characterized by uncertainty or stochasticity. Uncertainties may arise in the system parameters, the boundary and initial conditions, and also in the ‘external forcing’ processes. Also, many problems are treated through the stochastic framework due to the incomplete or partial understanding of the governing physical laws. In all of the above cases the existence of random perturbations, combined with the complex dynamical mechanisms of the system itself can often lead to a rapid growth of the uncertainty in the dynamics and state of the system. Such rapid growth can distribute the uncertainties to a broadband spectrum of scales both in space and time, making the system state particularly complex.

In the past decades an increasing number of problems in continuum theory have been treated using stochastic dynamical theories. Such problems are mainly described by stochastic partial differential equations (SPDEs) and they arise in a number of areas including fluid mechanics, elasticity, and wave theory, describing phenomena such as turbulence, random vibrations, flow through porous media, and wave propagation through random media. This is but a partial listing of applications and it is clear that almost any phenomenon described by a field equation has an important subclass of problems that may profitably be treated from a stochastic point of view.

Probably the most characteristic representative from this family of problems are turbulent flows. In turbulence the spatial and temporal dependence of the instantaneous values of the fluid dynamics fields have a very complex nature. Moreover, if turbulent flow is setup repeatedly under the same conditions, the exact values of these fields will be different each time. However, even though the details of the flow maybe different over various runs, it has been observed that their statistical properties remain similar, or at least coherent over certain finite-time and space scales. These observations lead to the natural conjecture that statistical modeling or statistical averaging over appropriate spatial and temporal scales maybe more efficient for the description of these phenomena.

In this work, we develop a new methodology for the representation and evolution of the complete probabilistic response of infinite-dimensional, random, dynamical systems. More specifically, we derive an exact, closed set of evolution equations for general nonlinear continuous stochastic fields described by a Stochastic Partial Differential Equation (SPDE). By hypothesizing a decomposition of the solution field into a mean and stochastic dynamical component that are both time and space dependent, we derive a system of field equations consisting of a Partial Differential Equation (PDE) for the mean field, a family of PDEs for

the orthonormal basis that describe the stochastic subspace where the stochasticity ‘lives’ as well as a system of Stochastic Differential Equations that defines how the stochasticity evolves in the time varying stochastic subspace. These new Dynamically Orthogonal (DO) evolution equations are derived directly from the original SPDE, using nothing more than a dynamically orthogonal condition on the representation of the solution. This condition is the ‘key’ to overcome the redundancy issues of the full representation used while it does not restrict its generic features. Therefore, we do not assume an a priori representation neither for the stochastic coefficients, nor for the spatial structure of the solution; all this information is obtained directly by the system equations, boundary and initial conditions. If additional restrictions are assumed on the form of the representation, we recover both the Proper-Orthogonal-Decomposition (POD) equations and the generalized Polynomial-Chaos (PC) equations. For the efficient treatment of the strongly transient character on the systems described above, we derive adaptive criteria for the variation of the stochastic dimensionality that characterizes the system response. Those criteria follow directly from the dynamical equations describing the system. We also describe how information obtained from full-field data inputs can be merged with the numerically evolved stochastic fields within the context of DO equations.

Since the basis of the stochastic subspace is evolving according to the system SPDE, fewer modes are needed to capture most of the stochastic energy relative to the classic POD method that fixes the form of the basis a priori, especially for the case of transient responses. On the other hand, since the stochasticity inside the dynamically varying stochastic subspace is described by a reduced-order, exact set of SDEs, we avoid the large computational cost of PC methods to capture non-Gaussian behavior. Therefore, by allowing the stochastic subspace to change we obtain a better understanding of the physics of the problem over different dynamical regimes without having the well known cost or divergence issues resulted from irrelevant representations of spatial (in POD method) or stochastic structure (in PC method). We illustrate and validate this novel technique by solving the 2D Navier-Stokes equations in various geometries and compare with direct Monte Carlo simulations. We also apply the derived framework for the study of the statistical responses of an idealized ‘double gyre’ model, which has elements of ocean, atmospheric and climate instability behaviors.

Finally, we use our new stochastic description for flow fields to study the motion of inertial particles in flows with uncertainties. Inertial or finite-size particles in fluid flows are commonly encountered in nature (e.g., contaminant dispersion in the atmosphere) as well as in technological applications (e.g., chemical systems involving particulate reactant mixing) and as it has been observed both numerically and experimentally, their dynamics can differ markedly from infinitesimal particle dynamics. Here we use recent results from stochastic singular perturbation theory in combination with the DO representation of the random flow, in order to derive a reduced order inertial equation that will describe efficiently the stochastic dynamics of inertial particles in arbitrary random flows.

1.1 Preview of chapters

This thesis is organized as follows. In Chapter 2 we give the necessary notation and summarize basic properties for random fields. We present in detail a generalized form of the Karhunen Loeve expansion, which is a fundamental tool for the reduction of the stochastic dimensionality that characterizes a given problem. We also present a geometrical interpretation of its properties and we illustrate how it can be used for the efficient time and space

dependent representation of random fields that characterize fluid motion and have a priori properties such as non-divergence.

Chapter 3 is the central theoretical part of the thesis. Here we derive an exact, closed set of evolution equations for general continuous stochastic fields described by a Stochastic Partial Differential Equation (SPDE). The derivation is based on a novel condition, the dynamical orthogonality, on the representation of the solution, which as we prove, it comes naturally without imposing any constraints on the form of the response. Based on this condition we derive a system of field equations consisting of a Partial Differential Equation (PDE) for the mean field, a family of PDEs for the orthonormal basis that describe the stochastic subspace as well as a system of Stochastic Differential Equations that defines how the stochasticity evolves in the time varying stochastic subspace. We also prove that under additional restrictions on the form of the representation, the DO field equations reproduce both the Proper-Orthogonal-Decomposition equations and the generalized Polynomial-Chaos equations; thus the new methodology unifies these two approaches.

The scope of Chapter 4 is to develop adaptive criteria for the dimensionality of the stochastic subspace in the context of the dynamically orthogonal field equations. We present adaptive criteria for the contraction and expansion of the stochastic subspace and we also illustrate how the new stochastic dimensions should be chosen (when the stochastic subspace should be expanded) according to stability arguments. These criteria are based on the current stochastic response of the system and they use a priori hypotheses on the spectrum of the orthogonal complement of the stochastic subspace. Note that we restrict ourselves to the ‘internal’ adaptation, i.e. we assume that the realizations of the full fields resulting from our simulations are the new information used in the adaptation. This is different from adaptation to external irregular data.

In Chapter 5 we apply the Dynamically Orthogonal field equations to the case of two dimensional random flows described by Navier-Stokes equations with and without the Coriolis force due to a rotating reference frame. In the first two sections we formulate the problem and we derive closed, evolution equations for the mean field, the scalar stochastic coefficients, and the DO modes. We also discuss the case of stochastic boundary conditions and we prove that this family of problems can always be reformulated as problems with deterministic boundary conditions and suitable forcing. Subsequently, we present numerical results for specific geometries and forcing configurations and we will examine convergence properties of the proposed methodology. In the last section of the chapter we consider an idealized model for the description of the temporal variability of the wind-driven, vertically averaged, ocean circulation. The aim of this section is to study the stochastic response of this model for different forcing parameters and Reynolds regimes. Through the developed stochastic framework we shall prove that in the unstable regimes, as those are predicted by the deterministic theory, the system converges to a stochastic steady state response which is characterized by finite variance that is smaller than the energy of the mean flow. For larger Reynolds or forcing amplitude, we find that this variance may become comparable with the energy of the mean flow giving rise to periodic or even chaotic responses.

In Chapter 6 we apply our theoretical and numerical results derived for the description of stochastic flows in order to study the motion of finite-size particles in flows with uncertainty. Specifically, we examine the coupled effects due to inertia and flow stochasticity. In the first part of the chapter we summarize theoretical results for particles in deterministic flows. Subsequently we present results for the stochastic case. Specifically, we prove that the velocity of finite-size particles is governed by a stochastic slow manifold, a ‘layer’ of probability around the deterministic slow manifold derived previously for deterministic

flows. Based on a stochastic reduction on this manifold we derive a stochastic inertial equation that governs the motion of particles and which includes new terms expressing the coupled effect of particles inertia and stochasticity. In the second part of the chapter we first illustrate numerically the convergence of the particles stochastic velocity to the stochastic slow manifold. We validate the derived inertial equation for a specific example and we analyze the coupled effects of particles inertia and flow stochasticity on the preferential concentration of particles. In Chapter 7 we summarize the contributions of this work.

Chapter 2

Representations of stochastic fields

Abstract

The primary purpose of this chapter is to give the necessary notation and summarize basic properties for random fields. In the first section we give the definition of a stochastic phenomenon. Subsequently we provide with a brief description of the mathematical tools used for the representation of stochastic fields such as probability density functions, moments, and the characteristic functional. We also prove that those different descriptions are equivalent. The next section refers to Karhunen Loeve expansion, which is a fundamental tool for the reduction of the stochastic dimensionality that characterizes a given problem. We give a geometrical interpretation of its properties and we illustrate how it can be used for the efficient representation of random fields that characterize fluid motion and have a priori properties such non-divergenceness.

2.1 Introduction

Many problems arising in nature and technology can be profitably treated from a stochastic point of view. A common characteristic for these problems is the presence of uncertainties in the system parameters, and disordered or random perturbations in the dynamical variables that describe the system state. Also, many problems are treated through the stochastic framework due to the incomplete or partial understanding of the governing physical laws or simply because the stochastic approach is the most efficient way of doing computations (e.g. turbulence). In all of the above cases the existence of random perturbations, combined with the nonlinearities of the system often leads to their rapid growth which causes distribution of energy to a broadband spectrum of scales both in space and time, making the system state particularly complex.

Probably the most characteristic representative from this family of problems are turbulent flows. In turbulence the spatial and temporal dependence of the instantaneous values of the fluid dynamics fields have a very complex nature. Moreover, if turbulent flow is setup repeatedly under the same conditions, the exact values of these fields will be different each time (see e.g. Monin and Yaglom [102]). However, even though the details of the flow maybe different over various runs, it has been observed that their statistical properties remain similar leading to the natural conjecture that statistical modeling or statistical averaging over appropriate spatial and temporal scales ('spectral windows', [105]) maybe more efficient for the description of these phenomena.

The primary purpose of this chapter is to introduce the mathematical tools used for the

description of random fields. Before we proceed to the definition of a random or stochastic fields we shall first give a more formal definition of what we mean by a random or stochastic phenomenon. We consider a sequence of runs for the same experiment Π^ω (where ω denotes an arbitrary realization) that describe a given phenomenon, $\Pi^{\omega_1}, \Pi^{\omega_2}, \dots, \Pi^{\omega_n}, \dots$ and the corresponding sequence of results $R^{\omega_1}, R^{\omega_2}, \dots, R^{\omega_n}, \dots$. In many cases the following relation holds for the outcomes of the various runs

$$d(R^{\omega_i}, R^{\omega_j}) < \varepsilon_\omega \quad \text{for all } i, j \quad (2.1)$$

where d is a suitable metric (i.e. distance, see e.g. [104]) and ε_ω is a predefined level of tolerance. The above behavior leads to the commonly expected result that different runs of the same experiment leads to close results. From the above discussion we have the following definition [7]

Definition 1 *A phenomenon will be called deterministic if, for every experiment Π^ω that is associated with it, any sequence of experimental runs Π^{ω_i} satisfies eq. (2.1) with sufficiently small ε_ω . In contrary if relation (2.1) is not valid for one or more experiments then the phenomenon will be called nondeterministic.*

Therefore, the definition of a deterministic or nondeterministic phenomenon depends strongly on the tolerance level ε_ω as well as on the metric d . Even though an experiment associated with a nondeterministic phenomenon presents important variability in terms of results, this picture may change if we consider mean values of the outcomes for a large sequence of runs, e.g. the ensemble mean

$$\overline{R_N^\omega} = \frac{R^{\omega_1} + R^{\omega_2} + \dots + R^{\omega_N}}{N}$$

Then, it is possible to have sufficiently close mean values $\overline{R_N^\omega}$ over different sequences of runs $\{\Pi^\omega\}_i$ for the same experiment Π^ω

$$d\left(\overline{R_{N_i}^\omega}, \overline{R_{N_j}^\omega}\right) < \varepsilon_\omega \quad \text{for any large experimental sequences } \{\Pi^\omega\}_i, \{\Pi^\omega\}_j$$

In this case the experiment is said to present statistical stability [163]. Using this concept we proceed to the definition of a stochastic or random phenomenon ([163], [7])

Definition 2 *A nondeterministic phenomenon will be called stochastic or random if the results of any associated experiment with it Π^ω , present statistical stability.*

We shall now define the appropriate tools for the mathematical modeling of stochastic phenomena. In the theoretical modeling of random phenomena the basic role is played by the probability space $(\Omega, \mathcal{E}_\Omega, \mathcal{P})$. The set Ω , which we call sample space, includes all the possible outcomes of a given phenomenon. \mathcal{E}_Ω is a σ -algebra of subsets of Ω [67], i.e. a set of subsets that has the following properties i) $\Omega \in \mathcal{E}_\Omega$, ii) if $A \in \mathcal{E}_\Omega$ then its complement is also in \mathcal{E}_Ω , iii) Every countable union of the elements of \mathcal{E}_Ω , i.e. every $A_i \in \mathcal{E}_\Omega$, is in \mathcal{E}_Ω . Based on these two concepts we define the probability measure P_Ω as a set function from \mathcal{E}_Ω to the interval $[0, 1]$ which satisfies the three axioms of probability ([67], [135]).

For every physical realization $\omega \in \Omega$, we may correspond a quantity $u(\omega) \in \mathcal{U}$, where \mathcal{U} is a suitable set (e.g. a subset of \mathbb{R} , a set of functions, or a set of fields). Therefore the abstract set Ω contains all the possible physical realizations of the phenomenon, while

\mathcal{U} contains their corresponding mathematical description. For example, in the case of a random flow, $\omega \in \Omega$ will represent a particular physical realization of the flow, while $u(\omega)$ will represent a specific mathematical quantity associated with the flow e.g. the velocity field. This leads to the concept of a stochastic process or stochastic field. Specifically, we have the following formal definition

Definition 3 *A stochastic field is a function $\mathbf{u}(\mathbf{x}, t; \omega) = \{u_j(x, t; \omega)\}_{j=1}^m \in \mathbb{R}^m$, $\mathbf{x} \in D \subset \mathbb{R}^n$, $t \in T$, $\omega \in \Omega$, defined on a sample space Ω , a spatial domain D , and a time interval T , such that, for every $\mathbf{x} \in D \subset \mathbb{R}^n$, $t \in T$ and every real vector $\mathbf{r} \in \mathbb{R}^m$ the set $\{\omega : u_j(x, t; \omega) < r_j, j = 1, \dots, m\}$ is inside \mathcal{E}_Ω .*

Having a stochastic field, there are at least three different kinds of methods to obtain statistically averaged properties. They are space averages, time averages, and ensemble averages. The usefulness of space averages is limited to fields that are statistically homogeneous or at least approximately homogeneous over scales larger than those of the random features. Similarly, time averages are useful only if the stochastic field is in effect statistically stationary over time scales much larger than the time scale of the stochastic properties. In both of the above cases averaging over the appropriate ‘spectral window’ (i.e. range of spatial and temporal scales, [105]) may significantly simplify the problem. The third type of average, ensemble averages, does not assume anything on the statistical characteristics of the random field (e.g. homogeneity or stationarity) and for this reason it is the most versatile. In what follows every averaged quantity will be in the sense of ensemble average and will be denoted as

$$E^\omega [u(\omega)] = \lim_{N \rightarrow \infty} \frac{u(\omega_1) + u(\omega_2) + \dots + u(\omega_N)}{N}$$

where $\omega_i \in \Omega$ are specific realizations. In the following sections we will present the essential tools used for the analysis and description of stochastic fields in terms of their statistical and physical properties.

2.2 The family of probability density functions

In this section we will give the definitions of probability density functions and also present the essential notation that will be used in the rest of the thesis. Given a stochastic vector field $\mathbf{u}(\mathbf{x}, t; \omega)$ defined as above, we have for every collection of spatial positions $\mathbf{x}_1, \mathbf{x}_2, \dots, \mathbf{x}_N$ and time instants t_1, t_2, \dots, t_N the joint probability distribution function

$$F_{\mathbf{u}(\mathbf{x}_1, t_1), \dots, \mathbf{u}(\mathbf{x}_N, t_N)}(\mathbf{u}_1, \dots, \mathbf{u}_N) = \mathcal{P}[\{\omega : \mathbf{u}(\mathbf{x}_1, t_1; \omega) < \mathbf{u}_1 \cap \dots \cap \mathbf{u}(\mathbf{x}_N, t_N; \omega) < \mathbf{u}_N\}]$$

where each inequality is meant in the component-wise sense, i.e. $u_j(x_1, t_1; \omega) < u_{1j}$, $j = 1, \dots, m$. This family (the term ‘family’ follows from the fact that the joint distribution function is defined for arbitrary combinations of time instants and space locations) will always satisfy the Kolmogorov compatibility conditions [67]

1) the symmetry condition: if $\{i_1, i_2, \dots, i_N\}$ is a permutation of numbers $1, 2, \dots, N$ then for arbitrary $N \geq 1$

$$F_{\mathbf{u}(\mathbf{x}_1, t_1), \dots, \mathbf{u}(\mathbf{x}_N, t_N)}(\mathbf{u}_1, \dots, \mathbf{u}_N) = F_{\mathbf{u}(\mathbf{x}_{i_1}, t_{i_1}), \dots, \mathbf{u}(\mathbf{x}_{i_N}, t_{i_N})}(\mathbf{u}_{i_1}, \dots, \mathbf{u}_{i_N}).$$

2) the consistency condition: for $M < N$ we have

$$\lim_{\substack{\mathbf{u}_j \rightarrow \infty \\ j > M}} F_{\mathbf{u}(\mathbf{x}_1, t_1), \dots, \mathbf{u}(\mathbf{x}_M, t_M), \dots, \mathbf{u}(\mathbf{x}_N, t_N)}(\mathbf{u}_1, \dots, \mathbf{u}_N) = F_{\mathbf{u}(\mathbf{x}_1, t_1), \dots, \mathbf{u}(\mathbf{x}_M, t_M)}(\mathbf{u}_1, \dots, \mathbf{u}_M).$$

The above family of probability distribution functions defines uniquely the stochastic field $\mathbf{u}(\mathbf{x}, t; \omega)$. Therefore a complete statistical characterization of a random field involves the characterization of the full family of probability distribution functions.

In the special case where $F_{\mathbf{u}(\mathbf{x}_1, t_1), \dots, \mathbf{u}(\mathbf{x}_N, t_N)}(\mathbf{u}_1, \dots, \mathbf{u}_N)$ is differentiable with respect to its arguments $(\mathbf{u}_1, \dots, \mathbf{u}_N)$ for every collection of spatial locations and time instants we can alternatively use the probability density function (see e.g. [109])

$$f_{\mathbf{u}(\mathbf{x}_1, t_1), \dots, \mathbf{u}(\mathbf{x}_N, t_N)}(\mathbf{u}_1, \dots, \mathbf{u}_N) = \frac{\partial^N}{\partial \mathbf{u}_1 \dots \partial \mathbf{u}_N} F_{\mathbf{u}(\mathbf{x}_1, t_1), \dots, \mathbf{u}(\mathbf{x}_N, t_N)}(\mathbf{u}_1, \dots, \mathbf{u}_N)$$

where

$$\frac{\partial \cdot}{\partial \mathbf{u}} = \frac{\partial^m}{\partial u_1 \partial u_2 \dots \partial u_m}.$$

Note that for the special case of scalar fields described by the probability distribution function

$$F_{u(\mathbf{x}_1, t_1), \dots, u(\mathbf{x}_N, t_N)}(u_1, \dots, u_N) = \mathcal{P}[\{\omega : u(\mathbf{x}_1, t_1; \omega) < u_1 \cap \dots \cap u(\mathbf{x}_N, t_N; \omega) < u_N\}],$$

the definition of the probability density function has the simpler form

$$f_{u(\mathbf{x}_1, t_1), \dots, u(\mathbf{x}_N, t_N)}(u_1, \dots, u_N) = \frac{\partial^N}{\partial u_1 \dots \partial u_N} F_{u(\mathbf{x}_1, t_1), \dots, u(\mathbf{x}_N, t_N)}(u_1, \dots, u_N).$$

In the general case the family of probability density functions satisfies the following conditions

1) the non-negativity condition

$$f_{\mathbf{u}(\mathbf{x}_1, t_1), \dots, \mathbf{u}(\mathbf{x}_N, t_N)}(\mathbf{u}_1, \dots, \mathbf{u}_N) \geq 0$$

2) the normalization property

$$\int_{\mathbb{R}^{N \cdot m}} f_{\mathbf{u}(\mathbf{x}_1, t_1), \dots, \mathbf{u}(\mathbf{x}_N, t_N)}(\mathbf{u}_1, \dots, \mathbf{u}_N) d\mathbf{u}_1 \dots d\mathbf{u}_N = 1$$

3) the marginal property

$$\int_{\mathbb{R}^{(N-M) \cdot m}} f_{\mathbf{u}(\mathbf{x}_1, t_1), \dots, \mathbf{u}(\mathbf{x}_N, t_N)}(\mathbf{u}_1, \dots, \mathbf{u}_N) d\mathbf{u}_{M+1} \dots d\mathbf{u}_N = f_{\mathbf{u}(\mathbf{x}_1, t_1), \dots, \mathbf{u}(\mathbf{x}_M, t_M)}(\mathbf{u}_1, \dots, \mathbf{u}_M)$$

For the fields that we will consider in the present work we will assume that the probability distribution functions of every order (i.e. for any number of joint time instants and space locations - e.g. second order are the joint probability density functions involving two time instants and space locations) exist and they are also differentiable. In this case an alternative tool for the description of a stochastic field is given by the family of characteristic functions

defined as

$$\begin{aligned}\phi_{\mathbf{u}(\mathbf{x}_1, t_1), \dots, \mathbf{u}(\mathbf{x}_N, t_N)}(\xi_1, \dots, \xi_N) &= \mathcal{F} [f_{\mathbf{u}(\mathbf{x}_1, t_1), \dots, \mathbf{u}(\mathbf{x}_N, t_N)}(\cdot, \dots, \cdot)] \\ &= E^\omega \left[\exp \left(i \sum_{j=1}^N \mathbf{u}_j(\mathbf{x}_j, t_j; \omega)^T \xi_j \right) \right]\end{aligned}$$

where \mathcal{F} denotes the Fourier transform. The family of characteristic functions possess the following properties

1) the normalization property

$$\phi_{\mathbf{u}(\mathbf{x}_1, t_1), \dots, \mathbf{u}(\mathbf{x}_N, t_N)}(\mathbf{0}, \dots, \mathbf{0}) = 1$$

2) the boundness property

$$|\phi_{\mathbf{u}(\mathbf{x}_1, t_1), \dots, \mathbf{u}(\mathbf{x}_N, t_N)}(\xi_1, \dots, \xi_N)| \leq 1 \text{ for all } (\xi_1, \dots, \xi_N) \in \mathbb{R}^{N \cdot m}$$

3) the symmetry property

$$\phi_{\mathbf{u}(\mathbf{x}_1, t_1), \dots, \mathbf{u}(\mathbf{x}_N, t_N)}(\xi_1, \dots, \xi_N) = \phi_{\mathbf{u}(\mathbf{x}_1, t_1), \dots, \mathbf{u}(\mathbf{x}_N, t_N)}^*(-\xi_1, \dots, -\xi_N)$$

where * denotes the complex-conjugate.

4) the marginal property

$$\phi_{\mathbf{u}(\mathbf{x}_1, t_1), \dots, \mathbf{u}(\mathbf{x}_N, t_N)}(\xi_1, \dots, \xi_M, 0, \dots, 0) = \phi_{\mathbf{u}(\mathbf{x}_1, t_1), \dots, \mathbf{u}(\mathbf{x}_M, t_M)}(\xi_1, \dots, \xi_M).$$

5) positive definiteness: for every vector $\mathbf{c} \in \mathbb{Z}^M$ (with \mathbf{c}^* denoting the complex conjugate of \mathbf{c}) we have

$$\sum_{j=1}^M \sum_{i=1}^M \phi_{\mathbf{u}(\mathbf{x}_1, t_1), \dots, \mathbf{u}(\mathbf{x}_N, t_N)}(\xi_{1i} - \xi_{1j}, \dots, \xi_{Mi} - \xi_{Mj}) c_i c_j^* \geq 0$$

for any collection of vectors $\mathbb{R}^m \ni \xi_{ij}, i, j = 1, \dots, M$.

2.3 The moment system

The next important concept for the description of stochastic or random fields is the statistical moments. For a stochastic vector field $\mathbf{u}(\mathbf{x}, t; \omega)$ defined as above, we have the statistical moments of the first order

$$\bar{\mathbf{u}}(\mathbf{x}, t) = E^\omega [\mathbf{u}(\mathbf{x}, t; \omega)] = \int_{\mathbb{R}} \mathbf{u} f_{\mathbf{u}(\mathbf{x}, t)}(\mathbf{u}) d\mathbf{u} \in \mathbb{R}^m$$

It is often necessary to investigate the joint behavior of the field at two different spatiotemporal locations. For this case we define the correlation operator (or second moment)

$$\begin{aligned}\mathbf{R}_{\mathbf{u}(\mathbf{x}_1, t_1; \omega)\mathbf{u}(\mathbf{x}_2, t_2; \omega)} &= E^\omega \left[\mathbf{u}(\mathbf{x}_1, t_1; \omega) \mathbf{u}(\mathbf{x}_2, t_2; \omega)^T \right] \\ &= \int_{\mathbb{R}^{m^2}} \mathbf{u}_1 \mathbf{u}_2^T f_{\mathbf{u}(\mathbf{x}_1, t_1)\mathbf{u}(\mathbf{x}_2, t_2)}(\mathbf{u}_1, \mathbf{u}_2) d\mathbf{u}_1 d\mathbf{u}_2 \in \mathbb{R}^{m \times m}.\end{aligned}$$

An alternative definition is given by the correlation coefficient which is a normalized version of the correlation operator.

In many occasions it is often more convenient to work with central moments. The second order central moments are described by the covariance operator (or central second moment)

$$\mathbf{C}_{\mathbf{u}(\mathbf{x}_1, t_1; \omega)\mathbf{u}(\mathbf{x}_2, t_2; \omega)} = E^\omega \left[(\mathbf{u}(\mathbf{x}_1, t_1; \omega) - \bar{\mathbf{u}}(\mathbf{x}_1, t_1; \omega)) (\mathbf{u}(\mathbf{x}_2, t_2; \omega) - \bar{\mathbf{u}}(\mathbf{x}_2, t_2; \omega))^T \right]$$

Since, for what will follow we will make extensive use of the above operator at the same time instants $t_1 = t_2$ but at different locations we will use the following notation for the spatial covariance

$$\begin{aligned}\mathbf{C}_{\mathbf{u}(\cdot, t; \omega)\mathbf{u}(\cdot, t; \omega)}(\mathbf{x}, \mathbf{y}) &= \mathbf{C}_{\mathbf{u}(\mathbf{x}, t; \omega)\mathbf{u}(\mathbf{y}, t; \omega)} \\ &= E^\omega \left[(\mathbf{u}(\mathbf{x}, t; \omega) - \bar{\mathbf{u}}(\mathbf{x}, t; \omega)) (\mathbf{u}(\mathbf{y}, t; \omega) - \bar{\mathbf{u}}(\mathbf{y}, t; \omega))^T \right].\end{aligned}$$

The above quantities define the second-order statistical characteristics for the field $\mathbf{u}(\mathbf{x}, t; \omega)$. Their knowledge is sufficient for a complete stochastic description for the case of Gaussian fields (see e.g. [109]). However, for the general case, the complete family of moments is required. Specifically, a complete stochastic description of $\mathbf{u}(\mathbf{x}, t; \omega)$ requires the knowledge of all moments of order r

$$\begin{aligned}E^\omega [u_{j_1}(\mathbf{x}_1, t_1; \omega) u_{j_2}(\mathbf{x}_2, t_2; \omega) \dots u_{j_r}(\mathbf{x}_r, t_r; \omega)] \\ = \int_{\mathbb{R}^{m \cdot r}} u_{j_1} u_{j_2} \dots u_{j_r} f_{\mathbf{u}(\mathbf{x}_1, t_1)\mathbf{u}(\mathbf{x}_2, t_2)\dots\mathbf{u}(\mathbf{x}_r, t_r)}(\mathbf{u}_1, \mathbf{u}_2, \dots, \mathbf{u}_r) d\mathbf{u}_1 d\mathbf{u}_2 \dots d\mathbf{u}_r\end{aligned}$$

for every combination of spatial locations $\mathbf{x}_1, \mathbf{x}_2, \dots, \mathbf{x}_r$, time instants t_1, t_2, \dots, t_r , indices $\mathbf{j} = (j_1, j_2, \dots, j_r)$, (with $j_k \in \{1, \dots, m\}$) and $r = 1, 2, \dots$. Note that in the above definition u_{j_1} denotes the j_1 component of \mathbf{u}_1 and so on.

2.3.1 Connection with the family of characteristic functions

We saw previously that the system of statistical moments is connected to the family of probability density functions. This is also true for the family of characteristic functions. Specifically, we can express any statistical moment as (see e.g. [136])

$$\begin{aligned}E^\omega [u_{j_1}(\mathbf{x}_1, t_1; \omega) u_{j_2}(\mathbf{x}_2, t_2; \omega) \dots u_{j_r}(\mathbf{x}_r, t_r; \omega)] \\ = \frac{1}{i^r} \frac{\partial^r}{\partial \xi_{1j_1} \partial \xi_{2j_2} \dots \partial \xi_{rj_r}} \phi_{\mathbf{u}(\mathbf{x}_1, t_1), \dots, \mathbf{u}(\mathbf{x}_r, t_r)}(\xi_1, \dots, \xi_N)_{\xi_j=0}\end{aligned}$$

where ξ_{1j_1} is the j_1 component of the vector ξ_1 and so on. The above property is a direct consequence of the definition of the characteristic function through the Fourier transform

of the corresponding density. Hence we have presented three different approaches for the complete probabilistic description of a stochastic field and we have also recalled their connection. For all the presented approaches the definition is given in terms of a system that includes all possible combinations of spatial locations and time instants. In the next section we describe an infinite dimensional tool that captures the complete probabilistic information in a single functional.

2.4 The characteristic functional

We saw that the tools presented so far follow a bottom-up approach in the sense that we define the global statistical behavior through the definition of finite-dimensional joint statistical quantities such as probability density functions at various locations and time instants or moments associated with them. A top-down approach will involve the consideration of an infinite dimensional quantity that will be able to reproduce all the finite-dimensional information. Such a quantity is the characteristic functional defined directly in terms of the full probability measure \mathcal{P} . More specifically, we have the following definition ([136], [102], [120])

Definition 4 For a stochastic field $\mathbf{u}(\mathbf{x}, t; \omega) = \{u_j(x, t; \omega)\}_{j=1}^m \in \mathbb{R}^m$, $\mathbf{x} \in D \subset \mathbb{R}^n$, $t \in T$, $\omega \in \Omega$, the characteristic functional is defined as

$$\begin{aligned} \Phi_{\mathbf{u}}[\theta] &= E^{\omega} \left[\exp \left(i \int_{\mathbb{R}^m} \int_T \mathbf{u}(\mathbf{x}, t; \omega)^T \theta(\mathbf{x}, t) dt d\mathbf{x} \right) \right] \\ &= \int_{\Omega} \exp \left(i \int_{\mathbb{R}^m} \int_T \mathbf{u}(\mathbf{x}, t; \omega)^T \theta(\mathbf{x}, t) dt d\mathbf{x} \right) d\mathcal{P}(\omega) \end{aligned}$$

where $\theta(\mathbf{x}, t) \in \mathbb{R}^m$, $\mathbf{x} \in D \subset \mathbb{R}^n$, $t \in T$, is an arbitrary field.

Therefore, we see that the characteristic functional is a generalization of the family of characteristic functions and therefore it has the same properties i.e.

1) the normalization property

$$\Phi_{\mathbf{u}}[\mathbf{0}] = 1$$

2) the boundness property

$$|\Phi_{\mathbf{u}}[\theta]| \leq 1 \text{ for all } \theta$$

3) the symmetry property

$$\Phi_{\mathbf{u}}[\theta] = \overline{\Phi_{\mathbf{u}}[-\theta]}$$

4) positive definiteness: for every vector $\mathbf{c} \in \mathbb{Z}^M$ (with \mathbf{c}^* denoting the complex conjugate of \mathbf{c}) we have

$$\sum_{j=1}^M \sum_{i=1}^M \Phi_{\mathbf{u}}[\theta_i - \theta_j] c_i c_j^* \geq 0$$

for arbitrary fields θ_i $i = 1, \dots, M$. As mentioned at the beginning, the characteristic functional contains the full probabilistic information. In fact, through the characteristic functional we can derive the complete system of moments, as well as the family of characteristic functions and through them the corresponding family of probability density functions.

2.4.1 Determination of the moments system

We shall now illustrate how the characteristic functional can be used to derive expressions for the moment system. By considering the first Frechet derivative (see e.g. [26]) of the characteristic functional we have

$$\begin{aligned} \frac{\delta \Phi_{\mathbf{u}}}{\delta \theta} [\theta; \varphi] &= \lim_{s \rightarrow 0} \frac{\Phi_{\mathbf{u}} [\theta + s\varphi] - \Phi_{\mathbf{u}} [\theta]}{s} = \\ &= \left. \frac{d}{ds} E^\omega \left[\exp \left(i \int_{\mathbb{R}^m} \int_T \mathbf{u}(\mathbf{x}, t; \omega)^T [\theta(\mathbf{x}, t) + s\varphi(\mathbf{x}, t)] dt d\mathbf{x} \right) \right] \right|_{s=0} \\ &= i E^\omega \left[\int_{\mathbb{R}^m} \int_T \mathbf{u}(\mathbf{x}, t; \omega)^T \varphi(\mathbf{x}, t) dt d\mathbf{x} \exp \left(i \int_{\mathbb{R}^m} \int_T \mathbf{u}(\mathbf{x}, t; \omega)^T \theta(\mathbf{x}, t) dt d\mathbf{x} \right) \right] \end{aligned}$$

Considering the above expression for $\theta = \mathbf{0}$ we obtain

$$\frac{\delta \Phi_{\mathbf{u}}}{\delta \theta} [\mathbf{0}; \varphi] = i E^\omega \left[\int_{\mathbb{R}^m} \int_T \mathbf{u}(\mathbf{x}, t; \omega)^T \varphi(\mathbf{x}, t) dt d\mathbf{x} \right]$$

Setting $\varphi_j(\mathbf{x}, t) = \delta(\mathbf{x} - \mathbf{x}_0) \delta(t - t_0) \delta_{jk} = \delta_{k, \mathbf{x}_0, t_0}$ we obtain

$$\frac{\delta \Phi_{\mathbf{u}}}{\delta \theta} [\mathbf{0}; \delta_{k, \mathbf{x}_0, t_0}] = i E^\omega [u_k(\mathbf{x}_0, t_0; \omega)]$$

thus

$$E^\omega [u_k(\mathbf{x}_0, t_0; \omega)] = \frac{1}{i} \frac{\delta \Phi_{\mathbf{u}}}{\delta \theta} [\mathbf{0}; \delta_{k, \mathbf{x}_0, t_0}].$$

where δ_{jk} is the Kronecker delta and $\delta(t - t_0)$ is the Dirac delta function. Depending on the smoothness of the characteristic functional we may consider higher order Frechet derivatives in order to obtain higher order moments. Specifically, we have

$$\begin{aligned} \frac{\delta^2 \Phi_{\mathbf{u}}}{\delta \theta^2} [\mathbf{0}; \varphi_1, \varphi_2] &= \\ &= i^2 E^\omega \left[\int_{\mathbb{R}^m} \int_T \mathbf{u}(\mathbf{x}, t; \omega)^T \varphi_1(\mathbf{x}, t) \int_{\mathbb{R}^m} \int_T \mathbf{u}(\mathbf{x}, t; \omega)^T \varphi_2(\mathbf{x}, t) dt d\mathbf{x} \right] \end{aligned}$$

from which we obtain the correlation (second moment) operator

$$\mathbf{R}_{u_k(\mathbf{x}_1, t_1; \omega) u_l(\mathbf{x}_2, t_2; \omega)} = \frac{1}{i^2} \frac{\delta^2 \Phi_{\mathbf{u}}}{\delta \theta^2} [\mathbf{0}; \delta_{k, \mathbf{x}_1, t_1}, \delta_{l, \mathbf{x}_2, t_2}].$$

We may generalize the above procedure to obtain expressions for any moment characterizing the field $\mathbf{u}(\mathbf{x}, t; \omega)$

$$E^\omega [u_{j_1}(\mathbf{x}_1, t_1; \omega) u_{j_2}(\mathbf{x}_2, t_2; \omega) \dots u_{j_r}(\mathbf{x}_r, t_r; \omega)] = \frac{1}{i^r} \frac{\delta^r \Phi_{\mathbf{u}}}{\delta \theta^r} [\mathbf{0}; \delta_{j_1, \mathbf{x}_1, t_1}, \dots, \delta_{j_r, \mathbf{x}_r, t_r}]$$

From the above equation we also conclude that the existence of moments is connected to the smoothness degree of the characteristic functional at the origin.

2.4.2 Determination of the family of characteristic functions

Another important property of the characteristic functional is its connection with the family of characteristic functions. Specifically, we can generate any finite dimensional characteristic function simply by considering the characteristic functional for delta-type fields, i.e. $\theta_k(\mathbf{x}, t) = \delta(\mathbf{x} - \mathbf{x}_0) \delta(t - t_0) \delta_{jk} = \delta_{k, \mathbf{x}_0, t_0}$. For one-dimensional characteristic functions we will have

$$\begin{aligned} \Phi_{\mathbf{u}} [\xi_0 \delta_{k, \mathbf{x}_0, t_0}] &= \\ &= E^\omega \left[\exp \left(i \xi_0 \int_{\mathbb{R}^m} \int_T \mathbf{u}(\mathbf{x}, t; \omega)^T \delta_{k, \mathbf{x}_0, t_0} dt d\mathbf{x} \right) \right] \\ &= E^\omega [\exp (i \xi_0 u_k(\mathbf{x}_0, t_0; \omega))] \\ &= \phi_{u_k(\mathbf{x}_0, t_0)}(\xi_0) \end{aligned}$$

Using the same approach we may derive more complex, finite-dimensional, characteristic functions

$$\phi_{u_{j_1}(\mathbf{x}_1, t_1), \dots, u_{j_N}(\mathbf{x}_N, t_N)}(\xi_1, \dots, \xi_N) = \Phi_{\mathbf{u}} \left[\sum_{k=1}^N \xi_k \delta_{j_k, \mathbf{x}_k, t_k} \right].$$

where ξ_i have been defined in Section 2.2. Having the full family of finite-dimensional characteristic functions, we may also obtain the corresponding family of probability density functions by inverse Fourier transform. Hence we have illustrated how the characteristic functional contains the full probabilistic information and it can reproduce any finite-dimensional quantity connected with the stochastic field.

2.4.3 Characteristic functionals with explicit description

Although the characteristic functional provides a complete stochastic description for a random field its main disadvantage is the lack of explicit formulas that can be used for the representation of general stochastic fields. In this section we present the characteristic functional for two special cases of fields: Gaussian random field and a more generalized form of characteristic functional that is capable of capturing more complex statistics.

Gaussian characteristic functional

Gaussian probability measures ([120]) play a very important role in the theory of probability in infinite dimensional spaces. The major reason is the existence of an analytic expression for the characteristic functional. The technical reason behind this feature is the property of Gaussian measures to be defined completely through the first and second order statistical characteristics. Below we give the definition of a Gaussian characteristic functional. We first consider a deterministic field $\mathbf{m}(\mathbf{x}, t) \in \mathbb{R}^m$, $\mathbf{x} \in D \subset \mathbb{R}^n$, $t \in T$ that will play the role of the mean field as well as a self-adjoint (symmetric), positive-definite operator with finite-trace (see e.g. [104]), $\mathbf{C}(\mathbf{x}_1, t_1, \mathbf{x}_2, t_2) \in \mathbb{R}^{m \times m}$, $\mathbf{x}_1, \mathbf{x}_2 \in D \subset \mathbb{R}^n$, $t_1, t_2 \in T$ that will play the role of the covariance operator. Then we have the following result (see e.g. [120])

Theorem 5 *The characteristic functional associated with a normally distributed random*

field $\mathbf{u}(\mathbf{x}, t; \omega)$ having mean $\mathbf{m}(\mathbf{x}, t; \omega)$ and covariance operator $\mathbf{C}(\mathbf{x}_1, t_1, \mathbf{x}_2, t_2)$ is given by

$$\begin{aligned} \log \Phi_{\mathbf{u}}[\theta] &= i \int_{\mathbb{R}^m} \int_T \mathbf{m}(\mathbf{x}, t)^T \theta(\mathbf{x}, t) dt d\mathbf{x} \\ &\quad - \frac{1}{2} \int_{\mathbb{R}^{2m}} \int_{T^2} \theta(\mathbf{x}_1, t_1)^T \mathbf{C}(\mathbf{x}_1, t_1, \mathbf{x}_2, t_2) \theta(\mathbf{x}_2, t_2) dt_1 dt_2 d\mathbf{x}_1 d\mathbf{x}_2 \end{aligned}$$

Note that based on the explicit expression for the Gaussian characteristic functional we may construct more general representations of characteristic functionals by considering convex superpositions of different Gaussian characteristic functionals. For more details we refer to Sobczyk, 1991 [136] (p. 21).

Tatarskii characteristic functional

We will now describe a more general form of characteristic functional representation, first introduced by Tatarskii, 1995 [142]. This representation creates a wide class of characteristic functionals and its derivation is based on the construction of a specific random function (see [142] for the description of the random function). Here we will state only the representation, details for the derivation can be found in [142].

Theorem 6 *Let a weight function $W(\mathbf{x}, t) : D \times T \rightarrow [0, \infty)$ normalized to 1, an arbitrary function $\mathbf{g}(\mathbf{x}_1, t_1, \mathbf{x}_2, t_2) : D^2 \times T^2 \rightarrow \mathbb{R}^m$, and a characteristic function $\phi_v(\cdot, t)$ describing a scalar stochastic process. Then the functional*

$$\log \Phi_{\mathbf{u}}[\theta] = \int_{\mathbb{R}^m} \int_T W(\mathbf{x}_1, t_1) \phi_v \left(\int_{\mathbb{R}^m} \int_T \mathbf{g}(\mathbf{x}_1, t_1, \mathbf{x}_2, t_2)^T \theta(\mathbf{x}_2, t_2) dt_2 d\mathbf{x}_2, t_1 \right) dt_1 d\mathbf{x}_1$$

represents a characteristic functional.

The above functional has been used successfully for the representation of random wave fields [142] but also for the derivation of characteristic functionals of probability measures that are well known measures in finite dimensions, such as the Gamma measure, the Abel measure and the Cauchy measure [39]. However, the expression above may be still too restrictive in order to represent effectively stochastic fields of general form.

2.5 The Karhunen Loeve expansion

A different approach for the description of a stochastic field follows the Karhunen-Loeve expansion. This is a linear decomposition of the stochastic field into deterministic fields multiplied by scalar stochastic coefficients. The deterministic fields carry all the spatial information while the scalar coefficients contain the stochastic information of the response. In this case the description of uncertainty is done through an expansion directly on the state-space variables and not through the joint probabilities at various spatial locations and time instants. As we shall see in the present section, the Karhunen-Loeve expansion has the great advantage to separate the probabilistic structure of the problem from the stochastic one. Moreover, for sufficiently smooth samples of the stochastic field, the convergence of the Karhunen-Loeve series is very rapid. Specifically, we have the following representation Theorem (see [143], [59]; see also [73], [81], [76] for oceanic applications)

Theorem 7 *An arbitrary spatially mean-square continuous random field $\mathbf{u}(\mathbf{x}, t; \omega)$, $\mathbf{x} \in D \subset \mathbb{R}^n, t \in T, \omega \in \Omega$ can be represented in the form of a series*

$$\mathbf{u}(\mathbf{x}, t; \omega) = \bar{\mathbf{u}}(\mathbf{x}, t) + \sum_{i=1}^{\infty} Y_i(t; \omega) \mathbf{u}_i(\mathbf{x}, t)$$

which is mean-square convergent for each $\mathbf{x} \in D \subset \mathbb{R}^n, t \in T$ and

$$Y_i(t; \omega) = \int_D [\mathbf{u}(\mathbf{x}, t; \omega) - \bar{\mathbf{u}}(\mathbf{x}, t)]^T \mathbf{u}_i(\mathbf{x}, t) d\mathbf{x}$$

are zero-mean stochastic processes, mutually orthogonal, with $E^\omega [Y_i(t; \omega) Y_j(t; \omega)] = \delta_{ij} \lambda_i^2(t)$; where $\{\mathbf{u}_i(\mathbf{x}, t), \lambda_i^2(t)\}_{i=1}^{\infty}$ are the eigenpairs associated with the following eigenvalue problem

$$\int_D \mathbf{C}_{\mathbf{u}(\cdot, t; \omega) \mathbf{u}(\cdot, t; \omega)}(\mathbf{x}, \mathbf{y}) \mathbf{u}_i(\mathbf{y}, t) d\mathbf{y} = \lambda_i^2(t) \mathbf{u}_i(\mathbf{x}, t)$$

Note, in the above representation both the deterministic fields and the stochastic coefficients are time-dependent. Although many authors consider a special case of the above representation where the stochastic coefficients do not evolve with time (see e.g. [59], [134]) here we will use this time-dependent representation in order to obtain (in the next chapter) evolution equations for all the quantities involved. We emphasize that a mean-square continuous random field $\mathbf{u}(\mathbf{x}, t; \omega)$ has by definition samples which are mean square integrable, i.e. the realizations of the random field $\mathbf{u}(\mathbf{x}, t; \omega)$ are such that $\int_D \mathbf{u}(\mathbf{x}, t)^T \mathbf{u}(\mathbf{x}, t) d\mathbf{x} < \infty$.

We will denote the Hilbert space of spatially square integrable fields as \mathbf{L}^2 .

Note, that since $\mathbf{C}_{\mathbf{u}(\cdot, t; \omega) \mathbf{u}(\cdot, t; \omega)}(\mathbf{x}, \mathbf{y})$ is always self-adjoint (symmetric) and positive definite, we will have a countable infinity of eigenpairs with all the eigenvalues being real positive and the associated eigenfields orthogonal to each other. Also, $\lim_{i \rightarrow \infty} \lambda_i^2 = 0$ [104].

2.5.1 A geometrical interpretation

As we saw, Karhunen-Loeve expansion, apart from the analytic requirement for square integrability, does not impose restrictions on the stochastic structure of the random coefficients, i.e. to be necessarily Gaussian. If we want to give a more geometrical picture of its properties, the Karhunen-Loeve expansion finds the principal directions $\mathbf{u}_i(\mathbf{x}, t)$ in the infinite dimensional space \mathbf{L}^2 and orders them so that along the direction described by $\mathbf{u}_i(\mathbf{x}, t)$, we have larger spread of probability relative to the direction $\mathbf{u}_{i+1}(\mathbf{x}, t)$, for all i . Specifically, if we denote with

$$\sigma^2[\mathbf{u}(\mathbf{x}, t)] = \int_{D^2} \mathbf{u}(\mathbf{x}, t)^T \mathbf{C}_{\mathbf{u}(\cdot, t; \omega) \mathbf{u}(\cdot, t; \omega)}(\mathbf{x}, \mathbf{y}) \mathbf{u}(\mathbf{y}, t) d\mathbf{x} d\mathbf{y}$$

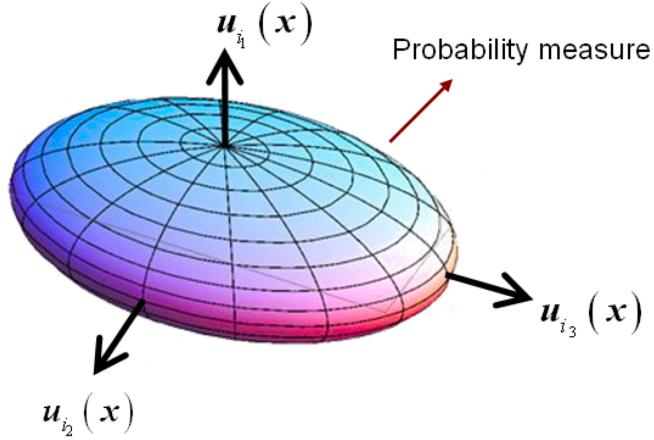


Figure 2-1: Ellipsoid that contains the main spread (‘mass’) of the probability measure; defined by the principal directions and the associated eigenvalues of the correlation operator.

the spread or variance of the probability measure associated with the random field $\mathbf{u}(\mathbf{x}, t; \omega)$, along the direction $\mathbf{u}(\mathbf{x}, t)$, we have the following property

$$\begin{aligned}
 \mathbf{u}_1(\mathbf{x}, t) \text{ is such that } \lambda_1^2(t) &= \sigma^2[\mathbf{u}_1(\mathbf{x}, t)] = \max_{\mathbf{L}^2} \sigma^2[\mathbf{u}(\mathbf{x}, t)] \\
 \mathbf{u}_2(\mathbf{x}, t) \text{ is such that } \lambda_2^2(t) &= \sigma^2[\mathbf{u}_2(\mathbf{x}, t)] = \max_{[\text{span}\{\mathbf{u}_1\}]^\perp} \sigma^2[\mathbf{u}(\mathbf{x}, t)] \\
 &\vdots \\
 \mathbf{u}_{i+1}(\mathbf{x}, t) \text{ is such that } \lambda_{i+1}^2(t) &= \sigma^2[\mathbf{u}_{i+1}(\mathbf{x}, t)] = \max_{[\text{span}\{\mathbf{u}_j\}_{j=1}^i]^\perp} \sigma^2[\mathbf{u}(\mathbf{x}, t)] \\
 &\vdots
 \end{aligned}$$

where $\text{span}\{\mathbf{u}_j\}_{j=1}^i$ denotes the linear subspace spanned by the eigenfields $\{\mathbf{u}_j\}_{j=1}^i$ and $^\perp$ denotes the orthogonal complement. Therefore, the spectral decomposition of the covariance operator provides us with a sequence of fields along which we have a monotonic decrease on the spread of the probability measure. Note that no information about the shape of the probability measure is given in this level of analysis since the spread of probability is the maximum information that the second-order statistics can provide. Thus, we may think the set of eigenpairs as an ellipsoid in infinite dimensions, with the directions of the principal axes defined by $\{\mathbf{u}_j\}_{j=1}^\infty$ and the amplitudes along these axes defined by $\{\lambda_j^2\}_{j=1}^\infty$. This ellipsoid bounds the probability measure, in the sense that the main spread (‘mass’) of the probability measure is contained in the ellipsoid interior (Figure 2-1).

Since, the ellipsoid has always a finite number of axes which are greater than an arbitrary constant $\epsilon > 0$ (this is a sequence of the property $\lim_{i \rightarrow \infty} \lambda_i^2 = 0$) we may argue that Karhunen-Loeve expansion gives a finite dimensional ellipsoid where the main mass of the probability measure is contained. Hence, we are interested to characterize the detailed characteristics of the probability measure (such as higher order moments or joint probability

density functions) only along those directions which are associated with important spread of probability or variance, i.e. for the part of the probability measure contained in the ellipsoid.

2.5.2 Application to fluid flows

In stochastic partial differential equations and especially in stochastic fluid flows we are interested to describe and characterize random fields that have given spatial properties such as divergence free or irrotational fields. Using the Karhunen-Loeve expansion we are able to represent very efficiently fields that have such properties. Moreover, through this representation we shall prove properties which are satisfied by the covariance operator as well as higher order moments describing the random field. Finally, as we shall illustrate the Karhunen-Loeve series provides us with a very efficient tool to create random samples of fields with given properties such as divergence-free fields.

We first recall the following fundamental result for flow fields [10]

Theorem 8 *Any spatially differentiable flow field $\mathbf{u}(\mathbf{x}, t)$ can always be decomposed as*

$$\mathbf{u}(\mathbf{x}, t) = \mathbf{u}_r(\mathbf{x}, t) + \mathbf{u}_d(\mathbf{x}, t) + \mathbf{u}_b(\mathbf{x}, t)$$

where

i) $\mathbf{u}_r(\mathbf{x}, t)$ is a divergence-free velocity field which can be expressed as

$$\nabla \cdot \mathbf{u}_r(\mathbf{x}, t) = 0 \Leftrightarrow \mathbf{u}_r(\mathbf{x}, t) = \nabla \times \psi(\mathbf{x}, t)$$

with $\psi(\mathbf{x}, t)$ being the field streamfunction,

ii) $\mathbf{u}_d(\mathbf{x}, t)$ is a rotational-free field which can be expressed as

$$\nabla \times \mathbf{u}_d(\mathbf{x}, t) = 0 \Leftrightarrow \mathbf{u}_d(\mathbf{x}, t) = \nabla q(\mathbf{x}, t)$$

with $\Delta q(\mathbf{x}, t) = \text{div } \mathbf{u}_d(\mathbf{x}, t)$ being the flow divergence,

iii) $\mathbf{u}_b(\mathbf{x}, t)$ is the potential flow part, that depends only from the boundary conditions and which can be written as

$$\begin{aligned} \nabla \times \mathbf{u}_b(\mathbf{x}, t) = 0 \\ \nabla \cdot \mathbf{u}_b(\mathbf{x}, t) = 0 \end{aligned} \Rightarrow \mathbf{u}_b(\mathbf{x}, t) = \nabla \phi(\mathbf{x}, t) \text{ with } \Delta \phi(\mathbf{x}, t) = 0.$$

Using the above property in combination with Karhunen-Loeve expansion we may write every sufficiently smooth (i.e. spatially differentiable in the mean square sense) random field as

$$\begin{aligned} \mathbf{u}(\mathbf{x}, t; \omega) = \nabla \times \bar{\psi}(\mathbf{x}, t) + \nabla \bar{q}(\mathbf{x}, t) + \nabla \bar{\phi}(\mathbf{x}, t) \\ + \sum_{i=1}^{\infty} Y_i(t; \omega) [\nabla \times \psi_i(\mathbf{x}, t) + \nabla q_i(\mathbf{x}, t) + \nabla \phi_i(\mathbf{x}, t)] \end{aligned} \quad (2.2)$$

Such a random field that is divergence-free will satisfy the equation

$$\nabla \cdot \mathbf{u}(\mathbf{x}, t; \omega) = 0, \quad \mathbf{x} \in D \subset \mathbb{R}^3, t \in T, \omega \in \Omega$$

Using the expansion (2.2) we obtain

$$\nabla \cdot \mathbf{u}(\mathbf{x}, t; \omega) = \Delta \bar{q}(\mathbf{x}, t) + \sum_{i=1}^{\infty} Y_i(t; \omega) \Delta q_i(\mathbf{x}, t) = 0 \quad (2.3)$$

Since the above equation holds for arbitrary $\omega \in \Omega$ the above quantity is always zero if and only if the mean and the stochastic modes are divergence free

$$\Delta \bar{q}(\mathbf{x}, t) = \Delta q_i(\mathbf{x}, t) = 0, \quad i = 1, \dots$$

In addition here, the last set of equations is accompanied by homogeneous boundary conditions since the non-homogeneous components are satisfied by the fields $\bar{\phi}, \phi_i, i = 1, \dots$. Therefore we will need to have here:

$$\bar{q}(\mathbf{x}, t) = q_i(\mathbf{x}, t) = 0, \quad i = 1, \dots$$

for all $\mathbf{x} \in D \subset \mathbb{R}^3, t \in T$.

Using similar arguments for the case of irrotational or potential flow fields, i.e. by taking the curl or the divergence of the Karhunen-Loeve expansion, we obtain the following result.

Theorem 9 *Let $\mathbf{u}(\mathbf{x}, t; \omega)$ be a random field. Then the following statements are true:*

i) if $\nabla \cdot \mathbf{u}(\mathbf{x}, t; \omega) = 0, \omega \in \Omega$ then the flow can be expanded as

$$\begin{aligned} \mathbf{u}(\mathbf{x}, t; \omega) &= \nabla \times \bar{\psi}(\mathbf{x}, t) + \nabla \bar{\phi}(\mathbf{x}, t) \\ &+ \sum_{i=1}^{\infty} Y_i(t; \omega) [\nabla \times \psi_i(\mathbf{x}, t) + \nabla \phi_i(\mathbf{x}, t)] \end{aligned} \quad (2.4)$$

where $\Delta \bar{\phi}(\mathbf{x}, t) = \Delta \phi_i(\mathbf{x}, t) = 0, i = 1, \dots$

ii) if $\nabla \times \mathbf{u}(\mathbf{x}, t; \omega) = 0, \omega \in \Omega$ then the flow can be expanded as

$$\begin{aligned} \mathbf{u}(\mathbf{x}, t; \omega) &= \nabla \bar{q}(\mathbf{x}, t) + \nabla \bar{\phi}(\mathbf{x}, t) \\ &+ \sum_{i=1}^{\infty} Y_i(t; \omega) [\nabla q_i(\mathbf{x}, t) + \nabla \phi_i(\mathbf{x}, t)] \end{aligned} \quad (2.5)$$

where $\Delta \bar{\phi}(\mathbf{x}, t) = \Delta \phi_i(\mathbf{x}, t) = 0, i = 1, \dots$

iii) if $\nabla \times \mathbf{u}(\mathbf{x}, t; \omega) = 0$, and $\nabla \cdot \mathbf{u}(\mathbf{x}, t; \omega) = 0, \omega \in \Omega$ then the flow can be expanded as

$$\mathbf{u}(\mathbf{x}, t; \omega) = \nabla \bar{\phi}(\mathbf{x}, t) + \sum_{i=1}^{\infty} Y_i(t; \omega) \nabla \phi_i(\mathbf{x}, t). \quad (2.6)$$

where $\Delta \bar{\phi}(\mathbf{x}, t) = \Delta \phi_i(\mathbf{x}, t) = 0, i = 1, \dots$

Moment properties of random flows with given hydrodynamic characteristics

We shall now use the representations derived in the last Theorem to derive properties for the covariance operator that is associated with the random field $\mathbf{u}(\mathbf{x}, t; \omega)$. Using representation

(2.4) for divergence-free random fields we will have the covariance function given by

$$\begin{aligned} & \mathbf{C}_{\mathbf{u}(\cdot,t;\omega)\mathbf{u}(\cdot,t;\omega)}(\mathbf{x}, \mathbf{y}) \\ &= \sum_{k=1}^{\infty} \sum_{l=1}^{\infty} E^{\omega} [Y_k(t;\omega) Y_l(t;\omega)] [\nabla \times \psi_k(\mathbf{x}, t) + \nabla \phi_k(\mathbf{x}, t)] [\nabla \times \psi_l(\mathbf{y}, t) + \nabla \phi_l(\mathbf{y}, t)]^T \\ &= \sum_{k=1}^{\infty} \lambda_k^2 [\nabla \times \psi_k(\mathbf{x}, t) + \nabla \phi_k(\mathbf{x}, t)] [\nabla \times \psi_k(\mathbf{y}, t) + \nabla \phi_k(\mathbf{y}, t)]^T \end{aligned}$$

We also have

$$\operatorname{div} [\nabla \times \psi_k(\mathbf{x}, t) + \nabla \phi_k(\mathbf{x}, t)] = 0, \quad k = 1, \dots$$

Therefore, we obtain the following property of covariance functions characterizing incompressible random fields

$$\nabla_{\mathbf{x}} \cdot \mathbf{C}_{\mathbf{u}(\cdot,t;\omega)\mathbf{u}(\cdot,t;\omega)}(\mathbf{x}, \mathbf{y}) = \nabla_{\mathbf{y}} \cdot \mathbf{C}_{\mathbf{u}(\cdot,t;\omega)\mathbf{u}(\cdot,t;\omega)}^T(\mathbf{x}, \mathbf{y}) = \mathbf{0}$$

or in index notation

$$\frac{\partial}{\partial x_i} C_{u_i(\cdot,t;\omega)u_j(\cdot,t;\omega)}(\mathbf{x}, \mathbf{y}) = \frac{\partial}{\partial y_j} C_{u_i(\cdot,t;\omega)u_j(\cdot,t;\omega)}(\mathbf{x}, \mathbf{y}) = 0$$

where $\nabla_{\mathbf{x}}$ denotes the divergence operator with respect to the spatial variables \mathbf{x} (note that \mathbf{x}, \mathbf{y} are 3-dimensional vectors representing spatial variables).

Using similar arguments we have the following property for irrotational fields

$$\nabla_{\mathbf{x}} \times \mathbf{C}_{\mathbf{u}(\cdot,t;\omega)\mathbf{u}(\cdot,t;\omega)}(\mathbf{x}, \mathbf{y}) = \nabla_{\mathbf{y}} \times \mathbf{C}_{\mathbf{u}(\cdot,t;\omega)\mathbf{u}(\cdot,t;\omega)}^T(\mathbf{x}, \mathbf{y}) = \mathbf{0}_{3 \times 3}$$

or in index notation

$$\varepsilon_{ijk} \frac{\partial}{\partial x_j} C_{u_k(\cdot,t;\omega)u_l(\cdot,t;\omega)}(\mathbf{x}, \mathbf{y}) = \varepsilon_{ijl} \frac{\partial}{\partial y_j} C_{u_k(\cdot,t;\omega)u_l(\cdot,t;\omega)}(\mathbf{x}, \mathbf{y}) = 0$$

where ε_{ijk} is the Levi-Civita symbol. Using these results we can generalize the above arguments and derive similar properties for higher order moments of random fields.

Monte Carlo simulation of random flows with given hydrodynamic characteristics

As we saw, the Karhunen Loeve expansion separates the stochastic from the spatial structure of the problem allowing us to represent uncertainty very effectively. This representation property can be used for the efficient simulation of random fields with given properties such as incompressibility. In the more traditional approach for sample generation of random fields, the spectral decomposition method is used (see e.g. [115]). In this framework the statistics of the random field are assumed to be Gaussian with spatially homogeneous character. This assumption allows for the description of the second-order statistics of the random field through the spatial Fourier transform of the covariance operator. The generation of samples is then based on the decomposition of the full spectrum function into smaller (narrow banded) components each one having random phase which is uniformly distributed. This technique is very popular for the simulation of random water waves (see e.g. [106]).

Using the Karhunen Loeve expansion, in the time-dependent form presented above, we may generate samples by performing Monte-Carlo simulation to the random coefficients $Y_i(t; \omega)$ and with fixed modes $\mathbf{u}_i(\mathbf{x}, t)$ that respect a priori the spatial characteristics of the random field such as divergence-free or rotational-free but also the time-dependent characteristics of the problem. We emphasize that through this approach, no assumptions are required for the spatial characteristics of uncertainty, such as homogeneity. Moreover, the non-Gaussian character of the random field is fully respected since this is expressed completely through the random simulation of the scalar coefficients $Y_i(t; \omega)$. This is not the case for other approaches used such as the POD method where the field is represented as

$$\mathbf{u}(\mathbf{x}, t; \omega) = \bar{\mathbf{u}}(\mathbf{x}) + \sum_{i=1}^s Y_i(t; \omega) \mathbf{u}_i(\mathbf{x})$$

or the polynomial-chaos method where the following representation is used

$$\mathbf{u}(\mathbf{x}, t; \omega) = \bar{\mathbf{u}}(\mathbf{x}, t) + \sum_{i=1}^s Y_i(\omega) \mathbf{u}_i(\mathbf{x}, t).$$

In both of the above cases the lack of time dependence on either the deterministic fields or the stochastic coefficients restrict the representation capabilities. This is not the case for the general Karhunen Loeve expansion where all quantities evolve with time. allowing for very efficient representation of any given field. These properties will also be of particular importance for the generation of samples used to represent the initial conditions for evolution problems as we shall see in the next chapter.

Chapter 3

Evolution of stochastic fields

Abstract

In this chapter we derive an exact, closed set of evolution equations for general continuous stochastic fields described by a Stochastic Partial Differential Equation (SPDE). By hypothesizing a decomposition of the solution field into a mean and stochastic dynamical component, we derive a system of field equations consisting of a Partial Differential Equation (PDE) for the mean field, a family of PDEs for the orthonormal basis that describe the stochastic subspace where the stochasticity ‘lives’ as well as a system of Stochastic Differential Equations that defines how the stochasticity evolves in the time varying stochastic subspace. These new evolution equations are derived directly from the original SPDE, using nothing more than a dynamically orthogonal condition on the representation of the solution. If additional restrictions are assumed on the form of the representation, we recover both the Proper-Orthogonal-Decomposition equations and the generalized Polynomial-Chaos equations. The material presented in the chapter is part of the article Sapsis and Lermusiaux, 2009 [129].

3.1 Introduction

In the past decades an increasing number of problems in continuum theory have been treated using stochastic dynamical theories. Applications of this kind include problems where even though the details of the response maybe different over various runs, their statistical properties obtained by averaging over appropriate spatial and temporal scales (‘spectral windows’, [105]) remain similar. To this end one may decide to use the stochastic framework to model the effect of the smaller and/or faster scales of the system response as well as the effect of larger and/or slower scales of the boundary conditions. Such problems are mainly described by stochastic partial differential equations (SPDEs) and they arise in a number of areas including fluid mechanics, elasticity, and wave theory to describe phenomena such as turbulence ([9], [102], [154], [46], [3], [46]), random vibrations ([137], [86], [118]), flow through porous media ([16], [165]), and wave propagation through random media ([135], [68], [45]). This is but a partial listing of applications and it is clear that almost any phenomenon described by a field equation has an important subclass of problems that may profitably be treated from a stochastic point of view. This includes problems for which the dynamics is not fully resolved or not sufficiently known to warrant solely a deterministic approach as well as problems for which initial, boundary or parametric uncertainties are significant.

A basic goal of uncertainty quantification is to estimate joint probability distributions for the field variables, given the probabilistic information for the initial state and forcing of the system as well as for the SPDE random coefficients. A complete probabilistic description of the response would either require the knowledge of the response characteristic functional or equivalently the knowledge of the whole Kolmogorov hierarchy of the joint probability distributions of the response stochastic fields at any collection of time instances and spatial locations ([16], [67]). Given the SPDE that governs the system, it was first shown by Hopf [60] that for the stochastic Navier Stokes equations, a functional differential equation can be derived that governs the characteristic functional for the response. His approach was later adapted to the problems of stochastic wave propagation by Tatarskii [141] and Lee [72]. This approach, known as the statistical approach to turbulence, has also been developed further by many authors (see, e.g., [85], [44], [69]) and provides with infinite dimensional transport equations for the characteristic functional that characterizes the stochastic solution. Even though these functional equations contain the full probabilistic information for the dynamical system and their derivation from the SPDE is straightforward ([16]), their infinite dimensional character prevents from a feasible method of solution.

The Monte-Carlo simulation technique is a more practical method that can be readily applied to solve such problems to an arbitrary degree of accuracy, provided a sufficiently large number of samples is used. During the past years significant advances have been made in improving the efficiency of Monte-Carlo schemes. This includes new sequential Monte-Carlo methods (e.g. Particle Filters, see e.g. [38]) where the probability density function of the response is approximated by a mixture of weighted Dirac functions. A most recent development is the usage of a mixture of weighted Gaussian kernels instead of Dirac functions to provide a more reliable representation of the response pdf ([30],[150]). In recent years, such particle filters and their variants have been applied to stochastic estimations in various fields including ocean and atmosphere dynamics ([61]) and structural dynamics ([29]).

Another approach is based on the generation and evolution of an optimal set of input samples of reduced dimensionality such that the scales and dynamical processes where the dominant, most energetic, uncertainties occur are continuously spanned. This is motivated by the multi-scale, intermittent, non-stationary and non-homogeneous uncertainty fields for ocean dynamics (e.g. [77]). The methodology, referred to as Error Subspace Statistical Estimation (ESSE) ([81],[74],[76],[79]), uses a Karhunen Loeve (KL) expansion but with time-varying and adaptive basis functions (see Chapter 2, Theorem 7). The functions are evolved using stochastic, data-assimilative, ensemble predictions initialized by a multi-scale scheme and evolved through a Monte-Carlo approach. Similar ideas have been later applied to the modeling of diffusion processes in random heterogenous media ([47], [48]). These methods approximate the response pdf without making any explicit assumption about its form and can thus be used in general nonlinear, non-Gaussian systems. However, a major issue is that the evolution of the dominant uncertainties is through a Monte-Carlo scheme and therefore a larger number of samples can still be required for accurate prediction.

Order reduction methods have also been utilized to derive reduced-order models which have lower complexity relative to the original SPDE model and which reveal the underlying structure of the system dynamics. A classical approach is the statistical technique of Karhunen-Loeve expansion or Proper Orthogonal Decomposition (POD) (see [109], [89],

[59]) where the response of the dynamical system is usually assumed to have the form

$$\mathbf{u}(\mathbf{x}, t; \omega) = \sum_{i=1}^s X_i(t; \omega) \mathbf{u}_i(\mathbf{x}), \quad \omega \in \Omega \quad (3.1)$$

where $X_i(t; \omega)$ are stochastic processes and the family $u_i(\mathbf{x})$ are time-independent functions computed from data collected in the course of experiments or from direct numerical simulations. Specifically, $u_i(\mathbf{x})$ s are orthonormal fields that provide an optimal modal decomposition in the sense that a finite collection of these modes can capture the dominant components of the complete infinite-dimensional process. A Galerkin projection of the original governing equations to the low-dimensional subspace identified by the POD basis functions $u_i(\mathbf{x})$ provides the reduced order evolution equations for the unknown stochastic coefficients $X_i(t; \omega)$. Note that POD is most commonly used in the deterministic framework to derive reduced order dynamical equations. In this case the averaging is usually performed over time and more rarely over realizations. The POD concept has been applied to a wide range of areas such as turbulence ([89], [134], [19], [59]), and control of chemical processes ([50], [132], [166]). However, the main drawback of the POD method is that the basis functions are chosen a priori and therefore may not be able to efficiently represent the evolving responses generated by nonlinear dynamical processes.

Another main approach is the Polynomial Chaos (PC) expansion pioneered by Ghanem and Spanos [52] in the context of solid mechanics. It is based on the original theory of Wiener on polynomial chaos ([156], [25], [157]). The stochastic field describing the system response is treated as an element in the Hilbert space of random functions and is approximated by its projection onto a finite subspace spanned by orthogonal polynomials. Specifically, instead of imposing a representation for fixed fields $\mathbf{u}_i(\mathbf{x})$ as for the POD method, the stochastic processes $X_i(t; \omega)$ are spectrally represented in terms of fixed multi-dimensional Hermite polynomials,

$$\mathbf{u}(\mathbf{x}, t; \omega) = \sum_{i=1}^s \Phi_i(\zeta(\omega)) \mathbf{u}_i(\mathbf{x}, t), \quad \omega \in \Omega \quad (3.2)$$

where Φ_i are orthogonal polynomials and $\zeta(\omega)$ are given random variables. A Galerkin projection of the governing equations to the low-dimensional subspace defined by the Φ_i s transforms the original SPDE to a set of coupled deterministic PDEs for the unknown family $\mathbf{u}_i(\mathbf{x}, t)$. The method has been applied to a series of applications including fluid mechanics ([31], [91], [162], [66], [34]), structural mechanics ([52], [51], [130]), and wave propagation in random media ([92]). Although for any arbitrary random process with finite second-order moments, the PC expansion converges in accord with Cameron-Martin theorem [25], it has been demonstrated that the convergence rate is optimal (i.e. a given error tolerance is achieved with the smallest number of terms in the series) for Gaussian processes [88], while for other types of processes the convergence rate may be substantially slower. A recent development by Xiu and Karniadakis ([161], [162]) proposes a generalized PC expansion where basis functions from the Askey family of hypergeometric polynomials are used. It is shown that suitable basis functions different from the Hermite polynomials can increase substantially the rate of convergence. Depending on the form of the SPDE, its stochastic coefficients, and the initial stochastic conditions, there is an optimum choice of basis functions through which an optimum rate of convergence can be achieved. However, this choice must be made a priori and this can be a very challenging task especially for non-stationary complex dynamical systems with large number of degrees of freedom (e.g.

atmospheric or oceanic dynamics).

Here we will utilize the general Karhunen-Loeve expansion presented in Chapter 2 (Theorem 7 and references therein),

$$\mathbf{u}(\mathbf{x}, t; \omega) = \bar{\mathbf{u}}(\mathbf{x}, t) + \sum_{i=1}^s Y_i(t; \omega) \mathbf{u}_i(\mathbf{x}, t), \quad \omega \in \Omega \quad (3.3)$$

in order to derive evolution equations for the $Y_i(t; \omega)$, $\bar{\mathbf{u}}(\mathbf{x}, t)$ and $\mathbf{u}_i(\mathbf{x}, t)$ without making any assumptions on their form: the original SPDE governing $\mathbf{u}(\mathbf{x}, t; \omega)$ is the only information utilized. Using a new dynamical orthogonality condition for the fields $\mathbf{u}_i(\mathbf{x}, t)$, we overcome the redundancy of representation (3.3) and derive an exact set of evolution equations that has the form of an s -dimensional stochastic differential equation for the random coefficients $Y_i(t; \omega)$ coupled with $s+1$ deterministic PDEs for the fields $\bar{\mathbf{u}}(\mathbf{x}, t)$ and $\mathbf{u}_i(\mathbf{x}, t)$, where s is the number of modes that we retain in representation (3.3). In this way, the basis that describes the stochastic subspace is dynamically evolved and is not chosen a priori: it adapts to the stochasticity introduced by the stochastic initial conditions and coefficients, and evolves according to the SPDE governing $\mathbf{u}(\mathbf{x}, t; \omega)$. The stochastic coefficients $Y_i(t; \omega)$ are also evolved according to dynamical equations derived directly from the original SPDE allowing us to use any SDE numerical scheme for their solution (e.g. particle methods). For the special case of stochastic excitation that is delta correlated in time, i.e. white noise, an equivalent non-linear Fokker-Planck-Kolmogorov equation describes the evolution of the joint probability density function for the stochastic processes $Y_i(t; \omega)$.

The derived field equations are consistent with the dynamical orthogonality condition which also implies the preservation of the classical orthonormality condition for the fields $\mathbf{u}_i(\mathbf{x}, t)$. If additional suitable assumptions, either on the form of the fields $\bar{\mathbf{u}}(\mathbf{x}, t)$ and $\mathbf{u}_i(\mathbf{x}, t)$, or on the form of $Y_i(t; \omega)$ are utilized, our novel equations reproduce the reduced-order equations obtained by application of the POD or PC method, respectively.

3.2 Definitions and problem statement

Let $(\Omega, \mathcal{E}_\Omega, \mathcal{P})$ be the probability space and let $\mathbf{x} \in D \subseteq \mathbb{R}^n$ denote the spatial variable and $t \in T$ the time. In applications, the most important cases are where $n = 2, 3$ therefore in what follows we will assume that $\mathbf{x} \in D \subseteq \mathbb{R}^n$, $n = 2, 3$. The set of all continuous, square integrable random fields, i.e. $\int_D E^\omega \left[\mathbf{u}(\mathbf{x}, t; \omega) \mathbf{u}(\mathbf{x}, t; \omega)^T \right] d\mathbf{x} < \infty$ for all $t \in T$ (where \bullet^T

denotes the complex conjugate operation) and the covariance operator

$$\mathbf{C}_{\mathbf{u}(\cdot, t; \omega) \mathbf{v}(\cdot, s; \omega)}(\mathbf{x}, \mathbf{y}) = E^\omega \left[(\mathbf{u}(\mathbf{x}, t; \omega) - \bar{\mathbf{u}}(\mathbf{x}, t))^T (\mathbf{v}(\mathbf{y}, s; \omega) - \bar{\mathbf{v}}(\mathbf{y}, s)) \right], \quad \mathbf{x}, \mathbf{y} \in D, \quad t, s \in T \quad (3.4)$$

form a Hilbert space ([120], [135]) that will be denoted by \mathbf{H} .

For every two elements $\mathbf{u}(\mathbf{x}, t; \omega)$, $\mathbf{v}(\mathbf{x}, t; \omega) \in \mathbf{H}$ we define the spatial inner product as

$$\langle \mathbf{u}(\bullet, t; \omega), \mathbf{v}(\bullet, t; \omega) \rangle = \int_D \mathbf{u}(\mathbf{x}, t; \omega)^T \mathbf{v}(\mathbf{x}, t; \omega) d\mathbf{x}$$

where the integral on the right hand side is defined in the mean square sense ([87]). For the case where the integrands are deterministic the mean square integral is reduced to the

classical Riemann integral. In what follows we will use Einstein's convection for summation, i.e. $\sum_i a_i b_i = a_i b_i$ except if the limits of summation need to be shown. A double index that is not summed-up will be denoted as $a_{\bar{i}} b_{\bar{i}}$. We define the projection operator $\mathbf{\Pi}$ of a field $\mathbf{u}(\mathbf{x}, t)$, $\mathbf{x} \in D$ to an m -dimensional linear subspace spanned by the orthonormal family $\{\mathbf{w}_j(\mathbf{x}, t; \omega)\}_{j=1}^m$, $\mathbf{x} \in D$ as follows

$$\begin{aligned} \mathbf{\Pi}_{\{\mathbf{w}_j(\mathbf{x}, t; \omega)\}_{j=1}^m} [\mathbf{u}(\mathbf{x}, t; \omega)] &= \sum_{j=1}^m \mathbf{w}_j(\mathbf{x}, t; \omega) \langle \mathbf{w}_j(\bullet, t; \omega), \mathbf{u}(\bullet, t; \omega) \rangle \\ &= \mathbf{w}_j(\mathbf{x}, t; \omega) \langle \mathbf{w}_j(\bullet, t; \omega), \mathbf{u}(\bullet, t; \omega) \rangle. \end{aligned}$$

The SPDE describing the system evolution is assumed to have the form

$$\frac{\partial \mathbf{u}(\mathbf{x}, t; \omega)}{\partial t} = \mathcal{L}[\mathbf{u}(\mathbf{x}, t; \omega); \omega], \quad \mathbf{x} \in D, \quad t \in \mathcal{T}, \quad \omega \in \Omega \quad (3.5)$$

where \mathcal{L} is a general (nonlinear), differential operator. Additionally, the initial state of the system at t_0 is described by the random field

$$\mathbf{u}(\mathbf{x}, t_0; \omega) = \mathbf{u}_0(\mathbf{x}; \omega), \quad \mathbf{x} \in D, \quad \omega \in \Omega \quad (3.6)$$

and the boundary conditions are given by

$$\mathcal{B}[\mathbf{u}(\xi, t; \omega)] = \mathbf{h}(\xi, t; \omega), \quad \xi \in \partial D, \quad \omega \in \Omega \quad (3.7)$$

where \mathcal{B} is a linear differential operator. For all of the above quantities we assume that random coefficients have statistical moments of every order.

3.3 The stochastic subspace and the dynamical orthogonality condition

As we saw in the last section of Chapter 2 Karhunen-Loeve representation provide us with a tool to represent every random field $\mathbf{u}(\mathbf{x}, t; \omega) \in \mathbf{H}$ at a given time t by a series of the form

$$\mathbf{u}(\mathbf{x}, t; \omega) = \bar{\mathbf{u}}(\mathbf{x}, t) + \sum_{i=1}^{\infty} Y_i(t; \omega) \mathbf{u}_i(\mathbf{x}, t), \quad \omega \in \Omega \quad (3.8)$$

where $\mathbf{u}_i(\mathbf{x}, t)$ are the eigenfunctions, and $Y_i(t; \omega)$ are zero-mean, stochastic processes with variance $E^\omega [Y_i^2(t; \omega)]$ equal to the corresponding eigenvalue $\lambda_i^2(t)$ of the eigenvalue problem

$$\int_D \mathbf{C}_{\mathbf{u}(\cdot, t)\mathbf{u}(\cdot, t)}(\mathbf{x}, \mathbf{y}) \mathbf{u}_i(\mathbf{x}, t) d\mathbf{x} = \lambda_i^2(t) \mathbf{u}_i(\mathbf{y}, t), \quad \mathbf{y} \in D. \quad (3.9)$$

Moreover, we discussed that the important mass of the probability measure can always be captured by a finite dimensional subspace in the sense that for every $\sigma_{cr} > 0$ there is always a positive integer s such that the finite truncation of (3.8) that contains the first s terms is σ_{cr} -close (in the mean square sense, i.e. in the norm $\|\cdot\|_2^2 = \langle \bullet, \bullet \rangle$) to the field $\mathbf{u}(\mathbf{x}, t; \omega)$. Therefore, every random field $\mathbf{u}(\mathbf{x}, t; \omega) \in \mathbf{H}$ can be approximated arbitrarily well, by a

finite series of the form

$$\mathbf{u}(\mathbf{x}, t; \omega) = \bar{\mathbf{u}}(\mathbf{x}, t) + \sum_{i=1}^s Y_i(t; \omega) \mathbf{u}_i(\mathbf{x}, t), \quad \omega \in \Omega \quad (3.10)$$

where s is a sufficiently large, non-negative integer. Based on the above discussion we define the stochastic subspace $\mathbf{V}_S = \text{span} \{\mathbf{u}_i(\mathbf{x}, t)\}_{j=1}^s$ as the linear space spanned by the s eigenfields that correspond to the s largest eigenvalues. A graphical interpretation of the stochastic subspace is given in Figure 3-1a where we represent the space \mathbf{V}_S as a plane along which the probability measure presents important spread. On the other hand along any direction included in \mathbf{V}_S^\perp , represented as the red axis, the spread of probability is smaller (in the mean square sense) than σ_{cr} . Hence, \mathbf{V}_S defines the appropriate subspace where the stochasticity of the random field ‘lives’ at time t , following ESSE ideas ([81, 75]). Our goal now is two-fold:

1. For fixed dimensionality s study how the stochasticity evolves inside \mathbf{V}_S . More specifically we seek the equations governing the evolution of the stochastic vector $\{Y_j(t; \omega)\}_{j=1}^s$.
2. Study how \mathbf{V}_S evolves inside \mathbf{H} through the variation of the basis $\{\mathbf{u}_j(\mathbf{x}, t)\}_{j=1}^s$.

Clearly, representation (3.10) with all quantities $(\bar{\mathbf{u}}(\mathbf{x}, t), \{\mathbf{u}_j(\mathbf{x}, t)\}_{j=1}^s, \{Y_j(t; \omega)\}_{j=1}^s)$ varying is redundant and therefore we cannot derive independent equations from the SPDE describing their evolution. Hence, it is essential to impose additional constraints in order to get a well posed problem for the unknown quantities.

To this end we examine more carefully the source of redundancy in representation (3.10). Specifically, we notice that the variation of the stochastic coefficients $\{Y_j(t; \omega)\}_{j=1}^s$ can express exclusively the evolution of uncertainty within the stochastic space \mathbf{V}_S . On the other hand, by varying the basis $\{\mathbf{u}_j(\mathbf{x}, t)\}_{j=1}^s$ we can express both the evolution of uncertainty within \mathbf{V}_S and also normal to \mathbf{V}_S . Therefore, we see that the source of redundancy comes from the evolution of uncertainty that can be described by both the variation of the stochastic coefficients and the basis. To overcome this difficulty we need to restrict the evolution of the basis $\{\mathbf{u}_j(\mathbf{x}, t)\}_{j=1}^s$ to be normal to the space \mathbf{V}_S since the evolution within \mathbf{V}_S can be described completely by a rotation of the stochastic coefficients as it is shown in Figure 3-1b. The above requirement can be elegantly expressed through the following condition

$$\frac{d\mathbf{V}_S}{dt} \perp \mathbf{V}_S \Leftrightarrow \left\langle \frac{\partial \mathbf{u}_i(\bullet, t)}{\partial t}, \mathbf{u}_j(\bullet, t) \right\rangle = 0, \quad i = 1, \dots, s, \quad j = 1, \dots, s. \quad (3.11)$$

We will refer to the above condition as the dynamically orthogonal (DO) condition. Note, that the DO condition implies the preservation of orthonormality for the basis $\{\mathbf{u}_j(\mathbf{x}, t)\}_{j=1}^s$ since

$$\frac{\partial}{\partial t} \langle \mathbf{u}_i(\bullet, t), \mathbf{u}_j(\bullet, t) \rangle = \left\langle \frac{\partial \mathbf{u}_i(\bullet, t)}{\partial t}, \mathbf{u}_j(\bullet, t) \right\rangle + \left\langle \frac{\partial \mathbf{u}_j(\bullet, t)}{\partial t}, \mathbf{u}_i(\bullet, t) \right\rangle = 0, \quad i = 1, \dots, s, \quad j = 1, \dots, s.$$

To summarize the above discussion, in what follows we will use the DO representation defined by equation (3.10) and the additional properties

1. $\{Y_j(t; \omega)\}_{j=1}^s$ are zero-mean stochastic processes.

2. $\{\mathbf{u}_j(\mathbf{x}, t)\}_{j=1}^s$ are deterministic fields satisfying the DO condition (3.11) which are initially orthonormal, i.e. $\langle \mathbf{u}_i(\bullet, t_0), \mathbf{u}_j(\bullet, t_0) \rangle = \delta_{ij}$.

3.4 Dynamically orthogonal field equations

In this section we use representation (3.10) to derive reduced order field equations describing the mean state of the system, its stochastic characteristics and their interactions. As it is proven in the following theorem, the DO expansion results in a set of independent, explicit equations for all the unknown quantities. In particular, using the DO expansion we reformulate the original SPDE to an s -dimensional stochastic differential equation for the random coefficients $Y_i(t; \omega)$ coupled with $s + 1$ deterministic PDEs for the fields $\bar{\mathbf{u}}(\mathbf{x}, t)$ and $\mathbf{u}_i(\mathbf{x}, t)$.

Theorem 10 (DO evolution equations) *Under the assumptions of the DO representation the original SPDE (3.5)-(3.7) is reduced to the following system of equations*

$$\frac{dY_i(t; \omega)}{dt} = \langle \mathcal{L}[\mathbf{u}(\bullet, t; \omega); \omega] - E^\omega[\mathcal{L}[\mathbf{u}(\bullet, t; \omega); \omega]], \mathbf{u}_i(\bullet, t) \rangle, \quad (3.12)$$

$$\frac{\partial \bar{\mathbf{u}}(\mathbf{x}, t)}{\partial t} = E^\omega[\mathcal{L}[\mathbf{u}(\mathbf{x}, t; \omega); \omega]], \quad (3.13)$$

$$\frac{\partial \mathbf{u}_i(\mathbf{x}, t)}{\partial t} = \Pi_{\mathbf{V}_S^\perp} [E^\omega[\mathcal{L}[\mathbf{u}(\mathbf{x}, t; \omega); \omega] Y_j(t; \omega)]] \mathbf{C}_{Y_i(t)Y_j(t)}^{-1} \quad (3.14)$$

where $\Pi_{\mathbf{V}_S^\perp}[\mathbf{F}(\mathbf{x})] = \mathbf{F}(\mathbf{x}) - \Pi_{\mathbf{V}_S}[\mathbf{F}(\mathbf{x})] = \mathbf{F}(\mathbf{x}) - \langle \mathbf{F}(\bullet), \mathbf{u}_k(\bullet, t) \rangle \mathbf{u}_k(\mathbf{x}, t)$ and $\mathbf{C}_{Y_i(t)Y_j(t)} = E^\omega[Y_i(t; \omega) Y_j(t; \omega)]$. The associated boundary conditions have the form

$$\begin{aligned} \mathcal{B}[\bar{\mathbf{u}}(\xi, t; \omega)]|_{\xi \in \partial D} &= E^\omega[\mathbf{h}(\xi, t; \omega)] \\ \mathcal{B}[\mathbf{u}_i(\xi, t)]|_{\xi \in \partial D} &= E^\omega[Y_j(t; \omega) \mathbf{h}(\xi, t; \omega)] \mathbf{C}_{Y_i(t)Y_j(t)}^{-1} \end{aligned}$$

and the initial conditions are given by

$$\begin{aligned} Y_i(t_0; \omega) &= \langle \mathbf{u}_0(\bullet; \omega) - \bar{\mathbf{u}}_0(\bullet), \mathbf{u}_{i0}(\bullet) \rangle \\ \bar{\mathbf{u}}(\mathbf{x}, t_0) &= \bar{\mathbf{u}}_0(\bullet) \equiv E^\omega[\mathbf{u}_0(\mathbf{x}; \omega)] \\ \mathbf{u}_i(\mathbf{x}, t_0) &= \mathbf{u}_{i0}(\mathbf{x}) \end{aligned}$$

for all $i = 1, \dots, s$, where $\mathbf{u}_{i0}(\mathbf{x})$ are the eigenfields of the correlation operator $\mathbf{C}_{\mathbf{u}(\cdot, t_0)\mathbf{u}(\cdot, t_0)}$ defined by the eigenvalue problem (3.9).

Proof: First we insert the DO representation to the evolution equation (3.5). We obtain (using Einstein's summation notation defined in Chapter 2)

$$\frac{\partial \bar{\mathbf{u}}(\mathbf{x}, t)}{\partial t} + \frac{dY_i(t; \omega)}{dt} \mathbf{u}_i(\mathbf{x}, t) + Y_i(t; \omega) \frac{\partial \mathbf{u}_i(\mathbf{x}, t)}{\partial t} = \mathcal{L}[\mathbf{u}(\mathbf{x}, t; \omega); \omega]. \quad (3.15)$$

By applying the mean value operator we obtain the second equation of the theorem (equation 3.13), i.e. an evolution equation for the mean part of the representation.

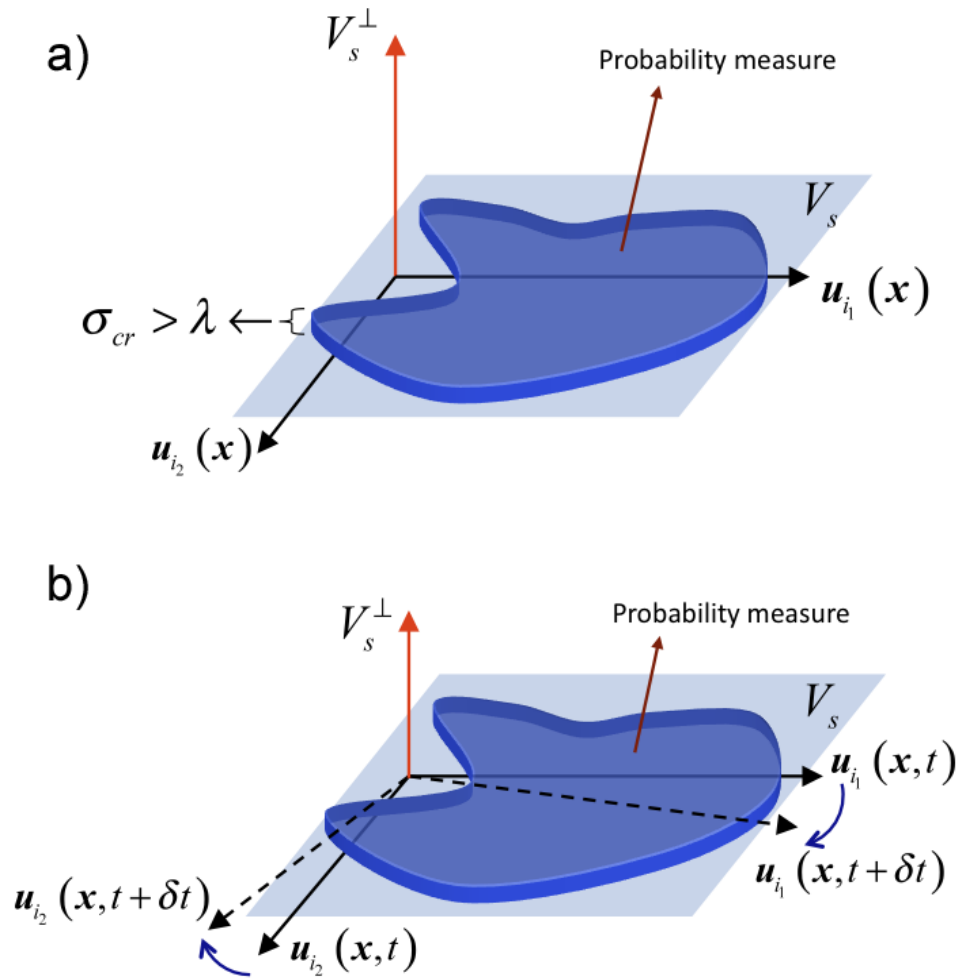


Figure 3-1: a) The stochastic subspace \mathbf{V}_S spanned by fields $\mathbf{u}_i(\mathbf{x}, t)$ that corresponds to important variance. b) The variation of the $\mathbf{u}_i(\mathbf{x}, t)$ inside V_s can always be covered by a rotation of the stochastic coefficients $Y_i(t; \omega)$.

By considering the inner product of the evolution equation (3.15) with each of the fields $\{\mathbf{u}_j(\mathbf{x}, t)\}_{j=1}^s$ we have

$$\begin{aligned} & \left\langle \frac{\partial \bar{\mathbf{u}}(\bullet, t)}{\partial t}, \mathbf{u}_j(\bullet, t) \right\rangle + \frac{dY_i(t; \omega)}{dt} \langle \mathbf{u}_i(\bullet, t), \mathbf{u}_j(\bullet, t) \rangle + Y_i(t; \omega) \left\langle \frac{\partial \mathbf{u}_i(\bullet, t)}{\partial t}, \mathbf{u}_j(\bullet, t) \right\rangle \\ & = \langle \mathcal{L}[\mathbf{u}(\mathbf{x}, t; \omega); \omega], \mathbf{u}_j(\bullet, t) \rangle. \end{aligned}$$

Now, the second term on the left hand side vanishes because of orthonormality except one term for which $i = j$. Moreover, the DO condition implies that the third term vanishes completely. Therefore we have the family of s stochastic differential equations

$$\frac{dY_j(t; \omega)}{dt} + \left\langle \frac{\partial \bar{\mathbf{u}}(\bullet, t)}{\partial t}, \mathbf{u}_j(\bullet, t) \right\rangle = \langle \mathcal{L}[\mathbf{u}(\bullet, t; \omega); \omega], \mathbf{u}_j(\bullet, t) \rangle, \quad j = 1, \dots, s.$$

Note that by using (3.13) or by applying the mean value operator to the above equation, we obtain

$$\left\langle \frac{\partial \bar{\mathbf{u}}(\bullet, t)}{\partial t}, \mathbf{u}_j(\bullet, t) \right\rangle = E^\omega [\langle \mathcal{L}[\mathbf{u}(\bullet, t; \omega); \omega], \mathbf{u}_j(\bullet, t) \rangle], \quad j = 1, \dots, s.$$

The quantity $\left\langle \frac{\partial \bar{\mathbf{u}}(\bullet, t)}{\partial t}, \mathbf{u}_j(\bullet, t) \right\rangle$ expresses the variation of $\bar{\mathbf{u}}$ towards directions of the stochastic subspace \mathbf{V}_S . Hence, the equation for $\mathbf{Y}(t; \omega)$ will take the final form (3.12).

As a next step, we multiply equation (3.15) with $Y_j(t; \omega)$ and apply the mean value operator to get

$$E^\omega \left[\frac{dY_i(t; \omega)}{dt} Y_j(t; \omega) \right] \mathbf{u}_i(\mathbf{x}, t) + E^\omega [Y_i(t; \omega) Y_j(t; \omega)] \frac{\partial \mathbf{u}_i(\mathbf{x}, t)}{\partial t} = E^\omega [\mathcal{L}[\mathbf{u}(\mathbf{x}, t; \omega); \omega] Y_j(t; \omega)]$$

which can be written as

$$\mathbf{C}_{Y_i(t)Y_j(t)} \frac{\partial \mathbf{u}_i(\mathbf{x}, t)}{\partial t} + \mathbf{C}_{\frac{dY_i(t)}{dt}Y_j(t)} \mathbf{u}_i(\mathbf{x}, t) = E^\omega [\mathcal{L}[\mathbf{u}(\mathbf{x}, t; \omega); \omega] Y_j(t; \omega)] \quad (3.16)$$

where $\mathbf{C}_{Y_i(t)Y_j(t)} = E^\omega [Y_i(t; \omega) Y_j(t; \omega)]$. By considering the inner product of the last equation with the field $\mathbf{u}_k(\mathbf{x}, t)$, and using DO condition, we obtain an exact expression for $\mathbf{C}_{\frac{dY_k(t)}{dt}Y_j(t)}$

$$\mathbf{C}_{\frac{dY_k(t)}{dt}Y_j(t)} = E^\omega [\langle \mathcal{L}[\mathbf{u}(\mathbf{x}, t; \omega); \omega], \mathbf{u}_k(\bullet, t) \rangle Y_j(t; \omega)]. \quad (3.17)$$

Note that this result (3.17) can also be obtained from the definition of $\mathbf{C}_{\frac{dY_k(t)}{dt}Y_j(t)}$ and from equation 3.12. Now, inserting the last expression to equation (3.16) will result in the equation

$$\begin{aligned} \mathbf{C}_{Y_i(t)Y_j(t)} \frac{\partial \mathbf{u}_i(\mathbf{x}, t)}{\partial t} & = E^\omega [\mathcal{L}[\mathbf{u}(\mathbf{x}, t; \omega); \omega] Y_j(t; \omega)] - \mathbf{\Pi}_{\mathbf{V}_S} [E^\omega [\mathcal{L}[\mathbf{u}(\mathbf{x}, t; \omega); \omega] Y_j(t; \omega)]] \\ & = \mathbf{\Pi}_{\mathbf{V}_S^\perp} [E^\omega [\mathcal{L}[\mathbf{u}(\mathbf{x}, t; \omega); \omega] Y_j(t; \omega)]] \end{aligned}$$

where

$$\mathbf{\Pi}_{\mathbf{V}_S^\perp} [F(\mathbf{x})] = \mathbf{F}(\mathbf{x}) - \langle \mathbf{F}(\bullet), \mathbf{u}_k(\bullet, t) \rangle \mathbf{u}_k(\mathbf{x}, t).$$

Moreover, since $\mathbf{C}_{Y_i(t)Y_j(t)}$ is positive-definite it can always be inverted and therefore we obtain the final expression (3.14) for the evolution of the fields $\mathbf{u}_i(\mathbf{x}, t)$.

Finally, by applying the mean value operator on equation (3.7) for $\mathbf{x} \in \partial D$ we obtain the boundary condition for the evolution of the mean field

$$\mathcal{B}[\bar{\mathbf{u}}(\xi, t; \omega)]|_{\xi \in \partial D} = E^\omega[\mathbf{h}(\xi, t; \omega)].$$

Additionally, by multiplying equation (3.7) with $Y_j(t; \omega)$ and applying the mean value operator we obtain for $\mathbf{x} \in \partial D$

$$E^\omega[Y_j(t; \omega) \mathbf{h}(\xi, t; \omega)] = \mathbf{C}_{Y_i(t)Y_j(t)} \mathcal{B}[\mathbf{u}_i(\xi, t)]|_{\xi \in \partial D}.$$

Therefore,

$$\mathcal{B}[\mathbf{u}_i(\xi, t)]|_{\xi \in \partial D} = E^\omega[Y_j(t; \omega) \mathbf{h}(\xi, t; \omega)] \mathbf{C}_{Y_i(t)Y_j(t)}^{-1}.$$

The initial conditions for the quantities involved are found by approximating the initial field $\mathbf{u}_0(\mathbf{x}; \omega)$ by a truncated Karhunen-Loeve expansion containing s terms. Therefore, the initial conditions $\mathbf{u}_{i0}(\mathbf{x})$ for the fields $\mathbf{u}_i(\mathbf{x}, t)$ will be the s most energetic eigenfields of the correlation operator $\mathbf{C}_{\mathbf{u}(\cdot, t_0)\mathbf{u}(\cdot, t_0)}$ defined by the eigenvalue problem

$$\int_D \mathbf{C}_{\mathbf{u}(\cdot, t_0)\mathbf{u}(\cdot, t_0)}(\mathbf{x}, \mathbf{y}) \mathbf{u}_{i0}(\mathbf{x}) d\mathbf{x} = \lambda_i^2 \mathbf{u}_{i0}(\mathbf{y}), \quad \mathbf{y} \in D.$$

The initial conditions for the stochastic coefficients $Y_i(t; \omega)$ will be given by the projection of the field $\mathbf{u}_0(\mathbf{x}; \omega) - \bar{\mathbf{u}}_0(\mathbf{x})$ to the orthonormal eigenfields $\mathbf{u}_{i0}(\mathbf{x})$ as follows

$$Y_i(t_0; \omega) = \langle \mathbf{u}_0(\bullet; \omega) - \bar{\mathbf{u}}_0(\bullet), \mathbf{u}_{i0}(\bullet) \rangle,$$

and the initial condition for the mean field will be given by $\bar{\mathbf{u}}(\mathbf{x}, t_0) = \bar{\mathbf{u}}_0(\mathbf{x}) \equiv E^\omega[\mathbf{u}_0(\mathbf{x}; \omega)]$. □

As it can be easily verified the evolution equations derived above are consistent with the DO condition that was initially assumed. Also, the initialization procedure for our DO field equations follows the multivariate ESSE approach, e.g. [75, 78].

It should be emphasized that the knowledge of the full set of quantities associated with the DO expansion, i.e. $\{Y_j(t; \omega)\}_{j=1}^s$, $\bar{\mathbf{u}}(\mathbf{x}, t)$, and $\mathbf{u}_i(\mathbf{x}, t)$ can lead, through simple random variable transformations ([109]), to analytic expressions of any statistical quantity of interest (e.g. pdfs of velocity field at particular positions of the domain, spectral representations of the stochasticity etc.) in terms of these DO expansion quantities (see Chapter 5).

3.4.1 The case of independent increment excitation (white noise)

A special class of SPDE of great importance is the case where the operator \mathcal{L} can be linearly split to a deterministic part and to a stochastic part having the form of derivative of an independent increment process ([116]), e.g. Brownian motion or Poisson process. More specifically we consider the special case of a system excited by an independent increment (with respect to time) stochastic process and having deterministic boundary conditions,

described by the evolution equation

$$\frac{\partial \mathbf{u}(\mathbf{x}, t; \omega)}{\partial t} = \mathcal{D}[\mathbf{u}(\mathbf{x}, t; \omega)] + \sum_{r=1}^R \Phi_r(\mathbf{x}, t) \frac{dW_r(t; \omega)}{dt}, \quad \mathbf{x} \in D, \quad t \in T, \quad \omega \in \Omega \quad (3.18)$$

$$\mathbf{u}(\mathbf{x}, t_0; \omega) = \mathbf{u}_0(\mathbf{x}; \omega), \quad \mathbf{x} \in D, \quad \omega \in \Omega$$

$$\mathcal{B}[\mathbf{u}(\xi, t; \omega)] = \mathbf{h}_D(\xi, t), \quad \xi \in \partial D, \quad \omega \in \Omega$$

where \mathcal{D} is a deterministic, differential operator, $\mathbf{h}_D(\xi, t)$ is a deterministic quantity defining the boundary conditions, $\{\Phi_r(\mathbf{x}, t)\}_{r=1}^R$ are deterministic, sufficiently smooth fields, and $\{W_r(t; \omega)\}_{r=1}^R$ are taken for simplicity to be independent Brownian motions (although the proof follows exactly the same steps for general independent increment processes). In this case an alternative description of the stochasticity inside \mathbf{V}_S , can be given in terms of the probability density function $f_{\mathbf{Y}}(y_1, y_2, \dots, y_s, t)$ for the stochastic vector $\{Y_j(t; \omega)\}_{j=1}^s$. For simplicity in what follows we will also use the following notation

$$\mathcal{D}[\mathcal{U}(\mathbf{x}, t), \mathbf{Y}(t; \omega)] \equiv \mathcal{D}\left[\bar{\mathbf{u}}(\mathbf{x}, t) + \sum_{i=1}^s Y_i(t; \omega) \mathbf{u}_i(\mathbf{x}, t)\right] = \mathcal{D}[\mathbf{u}(\mathbf{x}, t; \omega)]$$

with $\mathcal{U}(\mathbf{x}, t)$ referring to the $s+1$ fields $\bar{\mathbf{u}}(\mathbf{x}, t)$, $\{\mathbf{u}_j(\mathbf{x}, t)\}_{j=1}^s$. We then obtain the following result.

Corollary 11 *Under the assumption of the DO representation the SPDE (3.18) is reduced to the following system of equations*

$$\begin{aligned} \frac{\partial f_{\mathbf{Y}}}{\partial t} = & -\frac{\partial}{\partial y_j} \left[f_{\mathbf{Y}} \left\langle \mathcal{D}[\mathcal{U}(\bullet, t), \mathbf{y}] - \int_{\mathbb{R}^s} f_{\mathbf{Y}}(v, t) \mathcal{D}[\mathcal{U}(\bullet, t), v] dv, \mathbf{u}_i(\bullet, t) \right\rangle \right] \\ & + \frac{1}{2} \frac{\partial^2}{\partial y_i \partial y_j} [f_{\mathbf{Y}} Q_{ij}(t)] \end{aligned} \quad (3.19)$$

$$\frac{\partial \bar{\mathbf{u}}(\mathbf{x}, t)}{\partial t} = \int_{\mathbb{R}^s} f_{\mathbf{Y}}(v, t) \mathcal{D}[\mathcal{U}(\mathbf{x}, t), v] dv, \quad (3.20)$$

$$\frac{\partial \mathbf{u}_i(\mathbf{x}, t)}{\partial t} = \mathbf{\Pi}_{\mathbf{V}_S^\perp} \left[\int_{\mathbb{R}^s} v_j f_{\mathbf{Y}}(v, t) \mathcal{D}[\mathcal{U}(\mathbf{x}, t), v] dv \right] \mathbf{C}_{Y_i(t)Y_j(t)}^{-1} \quad (3.21)$$

where $Q_{ij}(t) = \langle \Phi_r(\bullet, t), \mathbf{u}_i(\bullet, t) \rangle \langle \Phi_r(\bullet, t), \mathbf{u}_j(\bullet, t) \rangle$ and $\mathbf{C}_{Y_i(t)Y_j(t)} = \int_{\mathbb{R}^s} v_i v_j f_{\mathbf{Y}}(v, t) dv$.

The associated boundary conditions have the form

$$\mathcal{B}[\bar{\mathbf{u}}(\xi, t; \omega)]|_{\xi \in \partial D} = \mathbf{h}_D(\xi, t)$$

$$\mathcal{B}[\mathbf{u}_i(\xi, t)]|_{\xi \in \partial D} = 0$$

and the initial conditions are given by

$$\begin{aligned} f_{\mathbf{Y}}(\mathbf{y}, t_0) &= f_{\mathbf{Y}_0}(\mathbf{y}) \\ \bar{\mathbf{u}}(\mathbf{x}, t_0) &= E^\omega[\mathbf{u}_0(\mathbf{x}; \omega)] \\ \mathbf{u}_i(\mathbf{x}, t_0) &= \mathbf{u}_{i0}(\mathbf{x}) \end{aligned}$$

for all $i = 1, \dots, s$, where $\mathbf{u}_{i0}(\mathbf{x})$ are defined in Theorem 1 and $f_{\mathbf{Y}_0}(\mathbf{y})$ is the probability density function associated with the random vector $Y_i(t_0; \omega) = \langle \mathbf{u}_0(\bullet; \omega) - \bar{\mathbf{u}}_0(\bullet), \mathbf{u}_{i0}(\bullet) \rangle$.

Proof: By using the special form of the SPDE (3.18) and the zero mean property of the Brownian motion we obtain from equation (3.12)

$$\begin{aligned} \frac{dY_i(t; \omega)}{dt} &= \langle \mathcal{D}[\mathcal{U}(\mathbf{x}, t), \mathbf{Y}(t; \omega)] - E^\omega[\mathcal{D}[\mathcal{U}(\mathbf{x}, t), \mathbf{Y}(t; \omega)]], \mathbf{u}_i(\bullet, t) \rangle \\ &\quad + \langle \Phi_r(\bullet, t), \mathbf{u}_i(\bullet, t) \rangle \frac{dW_r(t; \omega)}{dt}. \end{aligned}$$

This last equation is an Ito stochastic differential equation and can be written equivalently as a transport equation for the probability density function $f_{\mathbf{Y}}(y_1, y_2, \dots, y_s, t)$

$$\begin{aligned} \frac{\partial f_{\mathbf{Y}}}{\partial t} + \frac{\partial}{\partial y_j} [f_{\mathbf{Y}} \{ \langle \mathcal{D}[\mathcal{U}(\bullet, t), \mathbf{y}] - E^\omega[\mathcal{D}[\mathcal{U}(\bullet, t), \mathbf{y}]], \mathbf{u}_i(\bullet, t) \rangle \}] & \quad (3.22) \\ = \frac{1}{2} \frac{\partial^2}{\partial y_i \partial y_j} [f_{\mathbf{Y}} \langle \Phi_r(\bullet, t), \mathbf{u}_i(\bullet, t) \rangle \langle \Phi_r(\bullet, t), \mathbf{u}_j(\bullet, t) \rangle]. & \end{aligned}$$

Note, that

$$E^\omega[\mathcal{D}[\mathcal{U}(\mathbf{x}, t), \mathbf{Y}(t; \omega)]] = \int_{\mathbb{R}^s} f_{\mathbf{Y}}(v, t) \mathcal{D}[\mathcal{U}(\mathbf{x}, t), v] dv$$

and hence equation (3.19) follows. Equation for the mean field follows directly from the corresponding equation (3.13) and the zero-mean property of the Brownian motion. Finally, using equation (3.14) we obtain

$$\begin{aligned} \frac{\partial \mathbf{u}_i(\mathbf{x}, t)}{\partial t} &= \mathbf{\Pi}_{\mathbf{V}_S^\perp} [E^\omega[\mathcal{D}[\mathbf{u}(\mathbf{x}, t; \omega)] Y_j(t; \omega)]] \mathbf{C}_{Y_i(t)Y_j(t)}^{-1} \\ &\quad + \mathbf{\Pi}_{\mathbf{V}_S^\perp} \left[\langle \Phi_r(\bullet, t), \mathbf{u}_i(\bullet, t) \rangle E^\omega \left[\frac{dW_r(t; \omega)}{dt} Y_j(t; \omega) \right] \right] \mathbf{C}_{Y_i(t)Y_j(t)}^{-1}. \end{aligned}$$

The second term on the right hand side vanishes due to the non-anticipative property of Brownian motion ([135]). Moreover,

$$E^\omega[\mathcal{D}[\mathbf{u}(\mathbf{x}, t; \omega)] Y_j(t; \omega)] = \int_{\mathbb{R}^s} v_j f_{\mathbf{Y}}(v, t) \mathcal{D}[\mathcal{U}(\mathbf{x}, t), v] dv.$$

Additionally, for the boundary conditions, we obtain from Theorem 1

$$\mathcal{B}[\mathbf{u}_i(\xi, t)]|_{\xi \in \partial D} = E^\omega[Y_j(t; \omega) \mathbf{h}_D(\xi, t)] \mathbf{C}_{Y_i(t)Y_j(t)}^{-1} = \mathbf{h}_D(\xi, t) E^\omega[Y_j(t; \omega)] \mathbf{C}_{Y_i(t)Y_j(t)}^{-1} = 0.$$

Therefore, equation (3.21) follows. Finally the initial conditions are defined as in Theorem 1 with the stochastic vector $Y_i(t_0; \omega) = \langle \mathbf{u}_0(\bullet; \omega) - \bar{\mathbf{u}}_0(\bullet), \mathbf{u}_{i0}(\bullet) \rangle$ described now by the

associated probability density function $f_{\mathbf{Y}_0}(\mathbf{y})$. \square

Note that a transport equation for the probability density function can also be obtained for the case of general time correlation structure for the excitation using recent results for stochastic dynamical systems ([65], [127]).

3.5 Consistency with existing methodologies

The derivation of our new dynamically orthogonal field equations (3.12)-(3.14) was based exclusively on the representation of the solution by the DO expansion. In what follows, we show that by imposing additional restrictions on the representation, either those of the PC or the POD expansion, we recover the set of equations that are obtained for each of these expansions. Therefore, the DO field equations (3.12)-(3.14) can be considered as a general methodology that unifies two of the most important and widely used methods for evolving uncertainty in stochastic continuous systems governed by a SPDE or a system of SPDEs.

3.5.1 Generalized polynomial chaos expansion

In the generalized PC method, introduced by Xiu and Karniadakis [161] the stochastic processes $\{Y_j(t; \omega)\}_{j=1}^s$ are chosen a priori and often fixed in time, based on the statistical characteristics of the system input process. Specifically, the stochastic processes are chosen to have the statistically time-independent form

$$Y_j(t; \omega) = \Phi_j(\zeta(\omega)) \quad (3.23)$$

where Φ_j are orthogonal polynomials from the Askey-scheme and $\zeta(\omega)$ are given random variables [161]. In this case, the following orthogonality relation in the random space holds between the stochastic coefficients

$$E^\omega [\Phi_i(\zeta(\omega)) \Phi_j(\zeta(\omega))] = E^\omega [\Phi_i(\zeta(\omega))^2] \delta_{ij}.$$

The reduced order PC equations (e.g. [91],[162],[21],[66],[103]) are usually derived by substituting a representation as (3.10) but with the stochastic coefficients given by (3.23) to the SPDE (3.5) and then projecting it to the stochastic orthogonal basis functions $\Phi_j(\zeta(\omega))$ using the inner-product. Following these steps we obtain

$$E^\omega [\Phi_i(\zeta(\omega))^2] \frac{\partial \mathbf{u}_i(\mathbf{x}, t; \omega)}{\partial t} = E^\omega [\mathcal{L}[\mathbf{u}(\mathbf{x}, t; \omega); \omega] \Phi_i(\zeta(\omega))]. \quad (3.24)$$

To now show that the DO expansion can reduce to the PC expansion, we start from the DO field equations (3.12)-(3.14) but we restrict them with (3.23). Then the equation for the stochastic coefficients $\{Y_j(t; \omega)\}_{j=1}^s$ is not used since those are chosen *a priori* in a classic PC equation. Then, our equation for the mean field (3.13) provides directly the equation in the set (3.24) that corresponds to $\Phi_i(\zeta(\omega))$ being the constant polynomial. Finally, to obtain the remaining equations in (3.24), we start with the third of the DO field equations (3.14) in the form

$$\mathbf{C}_{Y_i(t)Y_j(t)} \frac{\partial \mathbf{u}_i(\mathbf{x}, t)}{\partial t} = E^\omega [\mathcal{L}[\mathbf{u}(\mathbf{x}, t; \omega); \omega] Y_j(t; \omega)] - \mathbf{\Pi}_{\mathbf{V}_S} [E^\omega [\mathcal{L}[\mathbf{u}(\mathbf{x}, t; \omega); \omega] Y_j(t; \omega)]] \quad (3.25)$$

But, from (3.17), we have $E^\omega [\langle \mathcal{L} [\mathbf{u}(\mathbf{x}, t; \omega); \omega], \mathbf{u}_k(\bullet, t) \rangle Y_j(t; \omega)] = \mathbf{C} \frac{dY_k(t)}{dt} Y_j(t) = 0$ since the stochastic characteristics of $\Phi_i(\zeta(\omega))$ do not change with time. Therefore, we have $\mathbf{\Pi}_{\mathbf{V}_S} [E^\omega [\mathcal{L} [\mathbf{u}(\mathbf{x}, t; \omega); \omega] Y_j(t; \omega)]] = 0$ in (3.25). Hence, equation (3.25) and the mean equation (3.13) reduce to the family of PC equations (3.24).

3.5.2 Proper orthogonal decomposition

The POD method uses *a priori* chosen fields $\{\mathbf{u}_j(\mathbf{x})\}_{j=1}^s$, generated either from an ensemble of experiments or from direct numerical simulations ([59]) and provides equations either for the stochastic or the deterministic coefficients $\{Y_j(t; \omega)\}_{j=1}^s$. In what follows we show how our DO equations reduce to the standard POD method (given the standard POD assumptions) for the stochastic case since the deterministic equations follow as a special case.

In a standard POD method, one chooses an expansion having the form

$$\mathbf{u}(\mathbf{x}, t; \omega) = \sum_{i=1}^s X_i(t; \omega) \mathbf{u}_i(\mathbf{x}) \quad (3.26)$$

where $\{\mathbf{u}_j(\mathbf{x})\}_{j=1}^s$ are fixed, orthonormal fields and $\{X_j(t; \omega)\}_{j=1}^s$ are stochastic processes (in general with non-zero mean). The reduced order POD evolutions equations are then usually obtained by Galerkin projection of the original SPDE (3.5) onto the orthonormal fields $\mathbf{u}_j(\mathbf{x})$. In this way we obtain the set of equations

$$\frac{dX_j(t; \omega)}{dt} = \langle \mathcal{L} [\mathbf{u}(\mathbf{x}, t; \omega); \omega], \mathbf{u}_j(\mathbf{x}, t) \rangle. \quad (3.27)$$

To now show that the DO expansion can reduce to the POD method, we start from Theorem 1 and the DO field equations but we restrict them with (3.26). We consider just equations (3.12) and (3.13) since $\{\mathbf{u}_j(\mathbf{x})\}_{j=1}^s$ have already be imposed from the POD method. Moreover, we note that the coefficients $\{X_j(t; \omega)\}_{j=1}^s$ of the POD method are connected to the stochastic coefficients $\{Y_j(t; \omega)\}_{j=1}^s$ of Theorem 1 through the relation

$$X_j(t; \omega) = Y_j(t; \omega) + \langle \bar{\mathbf{u}}(\mathbf{x}, t), \mathbf{u}_j(\mathbf{x}) \rangle.$$

Then, by differentiating $X_j(t; \omega)$ and using equations (3.12), (3.13) we recover equation (3.27)

$$\begin{aligned} \frac{dX_j(t; \omega)}{dt} &= \frac{dY_j(t; \omega)}{dt} + \left\langle \frac{\partial \bar{\mathbf{u}}(\mathbf{x}, t)}{\partial t}, \mathbf{u}_j(\mathbf{x}, t) \right\rangle \\ &= \langle \mathcal{L} [\mathbf{u}(\bullet, t; \omega); \omega] - E^\omega [\mathcal{L} [\mathbf{u}(\bullet, t; \omega); \omega]], \mathbf{u}_j(\bullet, t) \rangle \\ &\quad + \langle E^\omega [\mathcal{L} [\mathbf{u}(\mathbf{x}, t; \omega); \omega]], \mathbf{u}_j(\mathbf{x}, t) \rangle \\ &= \langle \mathcal{L} [\mathbf{u}(\bullet, t; \omega); \omega], \mathbf{u}_j(\bullet, t) \rangle. \end{aligned}$$

Chapter 4

Evolution of the stochastic dimensionality

Abstract

The scope of this chapter is to develop adaptive criteria for the dimensionality of the of the stochastic subspace in the context of the dynamically orthogonal (DO) field equations. In the first section we discuss the cost scaling of the DO field equations with respect to the number of stochastic dimensions used. Subsequently, we present adaptive criteria for the contraction and expansion of the stochastic subspace and we also illustrate how the new stochastic dimensions should be chosen (when the stochastic subspace should be expanded) according to stability arguments. Finally, we also discuss the issue of updating both the stochastic subspace and the probabilistic information (i.e. the stochastic coefficients) through the usage of full-field data if those are available. The material presented in this chapter is partially contained in Sapsis and Lermusiaux, 2009, 2010 [129], [126].

4.1 Introduction

In Chapter 2 we saw how we can approximate the full probability measure by its projection to a finite dimensional subspace, the stochastic subspace or error subspace of the problem. Using this property we derived an exact closed set of field equations that evolve the probabilistic structure for fixed stochastic dimensionality s . In this chapter we will discuss how this stochastic dimensionality should vary with respect to time according to the correct response of the system. More formally we may think of the stochastic dimensionality as the minimal number of latent variables needed to approximate satisfactory the system at a given time instant.

The estimation of the number of latent variables is an essential step in the process of reduced-order modeling for stochastic systems since most order-reduction methods need that number as an external and *a priori* user-defined parameter. However, there are many situations where the dimensionality of the stochastic subspace needs to be adapted as the system evolves. A typical example is a stochastic system initiated with deterministic initial conditions where the stochastic subspace is initially an empty set and as time evolves acquires non-zero dimensionality. Another commonly encountered problem where it is essential to adapt the stochastic dimensionality, is a stochastic system exhibiting transient dynamics either due to time varying external excitation or inherent instabilities.

Typical applications of this kind are atmospheric and oceanic systems where the strongly transient and non-stationary character of the dynamics requires adaptive modeling of the dimensionality. For oceanic data assimilation applications a convergence criterion based on the second-order statistical characteristics of the system state is defined and utilized to control and adapt the stochastic dimensionality (see [81], [74], [75], [76], [78]).

Other estimators of the stochastic dimension come from fractal geometry including the capacity dimension [112] and the correlation dimension [53]. Other methods that are not primarily intended to compute the fractal dimension can also be used to evaluate the dimensionality of the stochastic subspace. One of the most commonly used is the Principal Component Analysis (PCA) [71] mainly because of its simplicity. PCA is a linear method, meaning that the estimator cannot identify nonlinear dependencies but only gives a global dimensionality of an object. However, as we illustrated in Chapter 2 this can be sufficient information since the nonlinear dependencies may be expressed through the joint probability density function defined in the reduced order, time-varying, space.

4.2 Cost scaling with the stochastic dimensionality

The most important obstacle towards the numerical solution of stochastic dynamical systems and especially of high dimensionality such as SPDEs is the exponential growth of the number of unknowns with respect to the stochastic dimensionality of the problem. This is also known as curse of dimensionality [14] and refers to the exponential growth of hypervolume as a function of dimensionality. Therefore in a direct simulation approach where N degrees of freedom are involved in every stochastic dimension, the storage cost of having s stochastic dimensions will be given by

$$S_{direct}(N) = \mathcal{O}(N^s).$$

Hence, for high or infinite-dimensional systems, the storage, and thus, the computational cost is prohibited. In the Polynomial-Chaos method, where the stochastic element is projected into a given set of random functions the storage cost grows polynomially as (see e.g. [162])

$$S_{PC}(N) = N \sum_{q=1}^p \frac{1}{k!} \prod_{r=0}^{k-1} (s+r) \sim \mathcal{O}(Ns^p),$$

where p is the order of the polynomial-chaos approximation and s the stochastic dimensionality of the problem. Therefore, the growth rate strongly depends on the order p which may need to be sufficiently large in order to capture adequately complex statistical responses. For the same method, the associated computational cost for evolving the degrees of freedom depends on the order of the non-linearity, q , characterizing the evolution equation (e.g. for Navier-Stokes $q = 2$) and it will scale as

$$C_{PC}(N) \sim \mathcal{O}([Ns^p]^q).$$

where the exponent q comes from the fact that for a q -order polynomial term in the system equation and a representation consisting of Ns^p terms the number of multiplications required for the computation of this term will be $[Ns^p]^q$.

In the ESSE approach the storage cost grows linearly with respect to the stochastic dimension s . Since the evolution of the probabilistic information is done through Monte-

Carlo simulation the computational cost does not depend on the stochastic dimensionality but rather on the number of Monte-Carlo samples that will allow us to get a satisfactory approximation of the stochastic response.

In the case of the DO field equations the storage cost grows linearly with respect to the stochastic dimension s , while the computational cost grows polynomially with an exponent that does not depend on s but rather on the nonlinearity q associated with the governing equations. More specifically, as we presented in the previous section, the representation (3.10) consists of $s + 1$ deterministic fields, and a stochastic process that takes values in \mathbb{R}^s . Even though the stochastic process $\mathbf{Y}(t; \omega)$ carries the curse of dimensionality, the small to moderate size of s (even for realistic oceanic applications $s \sim O(10) - O(10^3)$ is sufficient, [82]) allows for storage of the probabilistic structure through a fixed number of samples (see Appendix B). Therefore, the main storage cost comes from the $s + 1$ time dependent fields. Thus,

$$S_{DO}(N) = \mathcal{O}(Ns),$$

Consequently, for a system operator \mathcal{L} having polynomial nonlinearities of maximum order q the computational cost will be given by

$$C_{DO}(N) = \mathcal{O}([Ns]^q).$$

where the computational cost follows from similar arguments as in the case of the PC method.

From the above discussion we conclude that in the DO methodology the storage cost grows linearly independently from the complexity of the stochastic solution or the nonlinearity of the system operator, while the number of numerical operations grows polynomially with an exponent that depends exclusively on the order of nonlinearity of the system operator.

In Figure 4-1 we present the computational cost in seconds with respect to the number of modes for a dynamical system described by Navier-Stokes equations. More specifically, we consider the stochastic lid-driven cavity flow which is described in detail in Chapter 5. The red curve indicates the measured time for a particular run while the blue line is the best linear fit. The inclination of the best linear fit is equal to 1.986 and compares satisfactory with the theoretical prediction i.e. the order of nonlinearity which for Navier-Stokes is 2.

4.3 Update of the stochastic subspace using stability properties of the SPDE

In this section we will study criteria for the dimensionality selection of the stochastic subspace \mathbf{V}_S as the system evolves. The proposed conditions for the contraction and expansion of the stochastic subspace will be based on the covariance matrix $\mathbf{C}_{Y_i(t)Y_j(t)} = E^\omega [Y_i(t; \omega) Y_j(t; \omega)]$, i.e. on the second order characteristics of the stochastic field. Note that $\mathbf{C}_{Y_i(t)Y_j(t)}$ provides information about both the intensity of the uncertainty that characterizes a stochastic field but also the principal directions in \mathbf{H} over which this stochasticity is distributed.

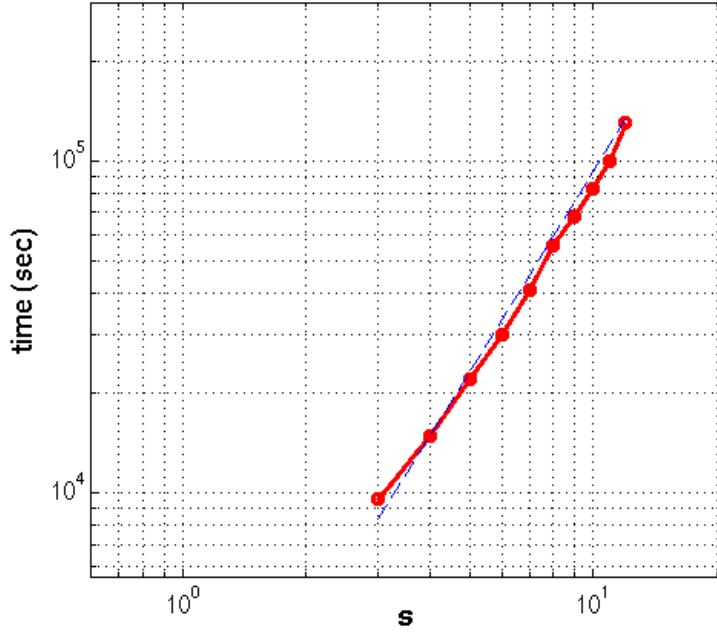


Figure 4-1: Computational time (sec) for the lid-driven cavity flow described in Chapter 5, using different number of modes (red curve). The blue line indicates the linear 'best fit' in the log-log plot and it has an inclination equal to 1.986 (2 is the theoretical prediction).

4.3.1 Conditions for the evolution of the stochastic dimensionality

For the covariance matrix $\mathbf{C}_{Y_i(t)Y_j(t)}$ we have the set of eigenvalues $\rho_j^2(t)$, $j = 1, \dots, s$ and the corresponding eigenvectors $\phi_j(t)$, $j = 1, \dots, s$, given by the eigenvalue problem

$$\mathbf{C}_{Y_i(t)Y_j(t)}\phi_{kj}(t) = \rho_k^2(t)\phi_{\bar{k}i}(t).$$

To relate the above eigenvalues and eigenvectors with those of the covariance operator $\mathbf{C}_{\mathbf{u}(\cdot,t)\mathbf{u}(\cdot,t)}(\mathbf{x}, \mathbf{y})$ we observe by definition of our representation of $\mathbf{u}(\mathbf{x}, t; \omega)$ (having order s) that

$$\begin{aligned} \mathbf{C}_{\mathbf{u}(\cdot,t)\mathbf{u}(\cdot,t)}(\mathbf{x}, \mathbf{y}) &= E^\omega \left[Y_i(t; \omega) Y_j(t; \omega) \mathbf{u}_i(\mathbf{x}, t) \mathbf{u}_j(\mathbf{y}, t)^T \right] \\ &= \mathbf{C}_{Y_i(t)Y_j(t)} \mathbf{u}_i(\mathbf{x}, t) \mathbf{u}_j(\mathbf{y}, t)^T \end{aligned}$$

Then we can easily check that the eigenvalue problem

$$\int_D \mathbf{C}_{\mathbf{u}(\cdot,t)\mathbf{u}(\cdot,t)}(\mathbf{x}, \mathbf{y}) \mathbf{u}_i(\mathbf{x}, t) d\mathbf{x} = \lambda_i^2(t) \mathbf{u}_i(\mathbf{y}, t), \quad \mathbf{y} \in D$$

has s non-zero eigenvalues given by $\rho_j^2(t)$, $j = 1, \dots, s$ with the corresponding eigenfields given by

$$v_j(\mathbf{x}, t) = \phi_{ij}(t) \mathbf{u}_i(\mathbf{x}, t), \quad j = 1, \dots, s$$

where $\phi_{ij}(t)$ is the i element of the j eigenvector $\phi_j(t)$.

In what follows, we provide one condition for the decrease and one for the increase of the size of the stochastic subspace, considering arbitrary contraction time t_c and expansion time t_e at which this can happen.

Condition 12 (Contraction of \mathbf{V}_S) *The stochastic dimension $s = \dim \mathbf{V}_S$ will be decreased by one when at $t = t_c$ the minimum eigenvalue becomes less than a pre-defined critical value σ_{cr}^2*

$$\min_i \rho_i^2(t_c) < \sigma_{cr}^2.$$

In this way we set a threshold of variance below which uncertainty is sufficiently small to be neglected. The stochastic subspace basis elements $\mathbf{u}_i(\mathbf{x}, t_c)$ as well as the stochastic coefficients $Y_i(t_c; \omega)$ have to be updated accordingly. We assume that $(\rho_s^2(t_c), v_s(\mathbf{x}, t_c))$ is the eigenpair that we neglect because $\rho_s^2(t_c) < \sigma_{cr}^2$. Moreover, we denote as $\mathbf{u}_i^+(\mathbf{x}, t_c)$ and $Y_i^+(t_c; \omega)$, $i = 1, \dots, s-1$ the basis elements of the stochastic subspace \mathbf{V}_{S-1}^+ and the corresponding stochastic coefficients respectively after the application of the contraction criterion. By choosing the basis elements $\mathbf{u}_i^+(\mathbf{x}, t_c)$ to be identical with the eigenfields $v_i(\mathbf{x}, t_c)$, $i = 1, \dots, s-1$ we have the stochastic subspace \mathbf{V}_{S-1}^+ which is contracted relative to \mathbf{V}_S exactly by the eigendirection $v_s(\mathbf{x}, t_c)$ that corresponds to the minimum eigenvalue (note that orthonormality of $v_i(\mathbf{x}, t_c)$, $i = 1, \dots, s-1$ is preserved). Then, the state of the system at $t = t_c$ will be described by

$$\mathbf{u}^+(\mathbf{x}, t_c; \omega) = \bar{\mathbf{u}}(\mathbf{x}, t_c) + \sum_{i=1}^{s-1} Y_i^+(t_c; \omega) v_i(\mathbf{x}, t_c), \quad \omega \in \Omega$$

where the stochastic coefficients can be easily found by projecting the stochastic part of the solution $\mathbf{u}(\mathbf{x}, t_c; \omega) - \bar{\mathbf{u}}(\mathbf{x}, t_c)$ to the basis $v_j(\mathbf{x}, t_c)$, $j = 1, \dots, s-1$

$$Y_j^+(t_c; \omega) = \phi_{ij}(t_c) Y_i(t_c; \omega), \quad i = 1, \dots, s-1$$

Condition 13 (Expansion of \mathbf{V}_S) *The stochastic dimension $s = \dim \mathbf{V}_S$ will be increased by one when at $t = t_e$ the minimum eigenvalue becomes greater than a pre-defined critical value $\Sigma_{cr}^2 > \sigma_{cr}^2$.*

$$\min_i \rho_i^2(t_e) \geq \Sigma_{cr}^2 > \sigma_{cr}^2.$$

The additional stochastic dimension is chosen for simplicity to have a stochastic coefficient $Y_{s+1}^+(t_e; \omega)$ that is normally distributed with variance σ_{cr}^2 . Moreover, it is assumed statistically independent from the existing stochastic coefficients. Both of the above assumptions are based on the fact that the stochastic intensity along the new direction is small (σ_{cr}^2). However, the selection of the the additional basis field $\mathbf{u}_{s+1}^+(\mathbf{x}, t_e)$ is not straightforward and will be made based on stability arguments of the system operator \mathcal{L} .

4.3.2 Selection of new stochastic dimensions

We will now describe the directions in \mathbf{H} which are not included in the stochastic subspace \mathbf{V}_S and which have the larger tendency to grow (most unstable) in terms of the variance. In what follows we will assume that uncertainty is small and uniform in the orthogonal complement of the stochastic subspace (the one that until now is not considered stochastic). Based on this assumption we may chose the new direction based only on the largest growth rate (see e.g. [73], [63]).

First we give some definitions that will be essential to our analysis.

Suppose $\Phi(\mathbf{u}) : \mathbf{H} \rightarrow \mathbf{H}$ is an operator from the space of square integrable stochastic fields \mathbf{H} to itself. The operator Φ will be called Frechet differentiable (see e.g. [26]) if for any $\mathbf{u} \in \mathbf{H}$ there exists a bounded, linear operator $\frac{\delta\Phi(\mathbf{u})}{\delta\mathbf{u}}[\mathbf{h}] : \mathbf{H} \rightarrow \mathbf{H}$ such that the following limit exists

$$\lim_{\varepsilon \rightarrow 0} \frac{\left\| \Phi(\mathbf{u} + \varepsilon\mathbf{h}) - \Phi(\mathbf{u}) - \frac{\delta\Phi(\mathbf{u})}{\delta\mathbf{u}}[\mathbf{h}] \right\|_2}{\varepsilon} = 0.$$

where $\|\mathbf{u}\|_2^2 = \langle \mathbf{u}, \mathbf{u} \rangle$ is the norm induced by the inner product of the Hilbert space \mathbf{H} . In this case we will have (Cartan, 1971 [26])

$$\Phi(\mathbf{u} + \varepsilon\mathbf{h}) - \Phi(\mathbf{u}) = \varepsilon \frac{\delta\Phi(\mathbf{u})}{\delta\mathbf{u}}[\mathbf{h}] + \mathcal{O}(\varepsilon^2). \quad (4.1)$$

In what follows we will study the normal stability of \mathbf{V}_S , i.e. the stability of the reduced system to perturbations which are normal to \mathbf{V}_S . To this end we will use Normal Infinitesimal Lyapunov Exponents (NILE) that have been used in the study of normal stability properties of invariant manifolds ([57]). More specifically, we consider a small perturbation of an element in \mathbf{V}_S at the time instant t_e that has the form

$$\tilde{\mathbf{u}}(\mathbf{x}, t_e; \omega) = \varepsilon \Upsilon(t_e; \omega) \vartheta(\mathbf{x}, t_e) + \mathbf{u}(\mathbf{x}, t_e; \omega).$$

where $\mathbf{u} \in \mathbf{V}_S$, ε is a small real number, $\vartheta(\mathbf{x}, t_e)$ is a deterministic field that is normal to the stochastic subspace \mathbf{V}_S , and $\Upsilon(t_e; \omega)$ is a square-integrable random variable that is independent from the stochastic processes $Y_i(t; \omega)$, $i = 1, \dots, s$, $t \leq t_e$. Then from the $s + 1$ dimensional DO equations we will have

$$\varepsilon \frac{d\Upsilon(t; \omega)}{dt} = \langle \mathcal{L}[\tilde{\mathbf{u}}(\bullet, t; \omega); \omega] - E^\omega[\mathcal{L}[\tilde{\mathbf{u}}(\bullet, t; \omega); \omega]], \vartheta(\bullet, t) \rangle$$

Then, by expanding $\mathcal{L}[\tilde{\mathbf{u}}(\bullet, t; \omega); \omega]$ around \mathbf{u} using equation (4.1) we obtain

$$\mathcal{L}[\tilde{\mathbf{u}}(\mathbf{x}, t; \omega); \omega] = \mathcal{L}[\mathbf{u}(\mathbf{x}, t; \omega); \omega] + \varepsilon \Upsilon(t; \omega) \frac{\delta\mathcal{L}[\mathbf{u}(\mathbf{x}, t; \omega); \omega]}{\delta\mathbf{u}}[\vartheta(\mathbf{x}, t)] + \mathcal{O}(\varepsilon^2)$$

Moreover, since $\Upsilon(t; \omega)$ is zero-mean we will have for the limit $t \rightarrow t_e$

$$\lim_{t \rightarrow t_e} E^\omega[\mathcal{L}[\tilde{\mathbf{u}}(\mathbf{x}, t; \omega); \omega]] = \lim_{t \rightarrow t_e} E^\omega[\mathcal{L}[\mathbf{u}(\mathbf{x}, t; \omega); \omega]] + \mathcal{O}(\varepsilon^2)$$

Now inserting these latter two equations in the equation for $\Upsilon(t; \omega)$ we have for $t \rightarrow t_e$

$$\begin{aligned} \varepsilon \frac{d\Upsilon(t; \omega)}{dt} \Big|_{t=t_e} &= \langle \mathcal{L}[\mathbf{u}(\bullet, t_e; \omega); \omega] - E^\omega[\mathcal{L}[\mathbf{u}(\bullet, t_e; \omega); \omega]], \vartheta(\bullet, t_e) \rangle \\ &+ \varepsilon \Upsilon(t_e; \omega) \left\langle \frac{\delta\mathcal{L}[\mathbf{u}(\bullet, t_e; \omega); \omega]}{\delta\mathbf{u}}[\vartheta(\bullet, t_e)], \vartheta(\bullet, t_e) \right\rangle + \mathcal{O}(\varepsilon^2) \end{aligned}$$

Then we multiply with $2\Upsilon(t; \omega)$ and apply the mean value operator to obtain for the limit

$t \rightarrow t_e, \varepsilon \rightarrow 0$

$$\left. \frac{dE^\omega [\Upsilon^2(t; \omega)]}{dt} \right|_{t=t_e} = 2E^\omega [\Upsilon^2(t_e; \omega)] \left\langle E^\omega \left[\frac{\delta \mathcal{L}[\mathbf{u}(\bullet, t_e; \omega); \omega]}{\delta \mathbf{u}} [\vartheta(\bullet, t_e)] \right], \vartheta(\bullet, t_e) \right\rangle$$

Therefore the NILE in this case will be given by

$$\sigma_{t_e}[\mathbf{u}] = 2 \max_{\substack{\vartheta \in V_s^\perp \\ \|\vartheta\|=1}} \mathcal{Q}[\vartheta] \equiv 2 \max_{\substack{\vartheta \in V_s^\perp \\ \|\vartheta\|=1}} \left\langle E^\omega \left[\frac{\delta \mathcal{L}[\mathbf{u}(\bullet, t; \omega); \omega]}{\delta \mathbf{u}} [\vartheta(\bullet, t)] \right], \vartheta(\bullet, t) \right\rangle \quad (4.2)$$

The last quantity is a measure of the maximum potential growth of perturbations which are not contained in \mathbf{V}_S . Using the above quantity we can predict based on the current state of the system and the current form of the stochastic subspace \mathbf{V}_S which perturbation $\vartheta(\mathbf{x}, t_e)$ will grow faster and therefore we can update or expand the stochastic subspace accordingly.

Another approach that is commonly used in the weather prediction literature is based on the instantaneous left singular vector of the tangent linear model considered over a finite time interval extending from the current time to a future time instant (the so called ‘linear regime’). This approach is based on the assumption of linearized dynamics over this short time interval that allows to find the perturbation that will have the maximum growth over this finite interval (See e.g. [83], [73], [63]).

Numerical computation of the NILE

In order to compute the NILE we first approximate \mathbf{V}_S^\perp by a finite base $\{\vartheta_i(\mathbf{x}, t_e)\}_{i=1}^q$. This can also be seen as the first iteration of the breeding procedure ([63], [81]); this ‘first step’ approach is also utilized in ESSE method except that in the present work we do the analysis in continuous time.

Note that such basis can always be constructed using any finite base that approximates the space of square integrable deterministic fields \mathbf{L}^2 (e.g. Fourier modes) and then applying Gram–Schmidt process. By considering such a base we will have

$$\vartheta(\mathbf{x}, t_e) = \sum_{i=1}^q a_i \vartheta_i(\mathbf{x}, t_e) \quad \text{with} \quad \sum_{i=1}^q a_i^2 = 1.$$

Then, using the linearity of the Frechet derivative with respect to ϑ we will have

$$\begin{aligned} \mathcal{Q}[\vartheta] &= \tilde{\mathcal{Q}}[a_1, \dots, a_q] \\ &= a_i a_j \left\langle E^\omega \left[\frac{\delta \mathcal{L}[\mathbf{u}(\bullet, t; \omega); \omega]}{\delta \mathbf{u}} [\vartheta_i(\bullet, t)] \right], \vartheta_j(\bullet, t) \right\rangle \\ &= \frac{1}{2} (Q_{ij} + Q_{ji}) a_i a_j \end{aligned}$$

where Q_{ij} is a $q \times q$ matrix whose elements are given by

$$Q_{ij} = \left\langle E^\omega \left[\frac{\delta \mathcal{L}[\mathbf{u}(\bullet, t; \omega); \omega]}{\delta \mathbf{u}} [\vartheta_i(\bullet, t)] \right], \vartheta_j(\bullet, t) \right\rangle.$$

Note that in the equation for $\mathcal{Q}[\vartheta]$ we have used the fact that for any matrix \mathbf{Q} and vector

\mathbf{x} we have

$$\mathbf{x}^T \mathbf{Q} \mathbf{x} = (\mathbf{x}^T \mathbf{Q} \mathbf{x})^T = \mathbf{x}^T \mathbf{Q}^T \mathbf{x} = \frac{1}{2} \mathbf{x}^T (\mathbf{Q} + \mathbf{Q}^T) \mathbf{x}$$

Therefore the problem has been reduced to the optimization of the quadratic function $\tilde{\mathcal{Q}}$ over the unit sphere $a_{ii}^2 = 1$. Note that the property $a_{ii}^2 = 1$ follows from the assumption of uniform variance for all the modes which are not included in the stochastic subspace. For the case where we had some information for the size of the various perturbations in the orthogonal complement we would have a weighted problem according to the variances of the individual modes in the orthogonal space.

The last optimization problem has always a solution since the unit sphere is a compact set. Moreover, since $\tilde{\mathcal{Q}}$ is quadratic we will have

$$\sigma_{t_e} [\mathbf{u}] = \lambda_{\max} [Q_{ij} + Q_{ji}]$$

where λ_{\max} denotes the maximum eigenvalue. Based on the above analysis we choose the new direction $\mathbf{u}_{s+1}^+(\mathbf{x}, t_e)$ in the expanded stochastic subspace as the critical direction $\vartheta_c(\mathbf{x}, t)$ for which maximum growth of variance will occur

$$\mathbf{u}_{s+1}^+(\mathbf{x}, t_e) = \vartheta_c(\mathbf{x}, t) = a_{c,i} \vartheta_i(\mathbf{x}, t)$$

where $\{a_{c,i}\}_{i=1}^q$ is the eigenvector of $Q_{ij} + Q_{ji}$ that corresponds to the maximum eigenvalue $\lambda_{\max} [Q_{ij} + Q_{ji}]$.

4.4 Update of the stochastic subspace using data and measurements

In many problems modeled through the stochastic framework, available data or measurements can improve significantly the accuracy of the stochastic solution. The scope of this section is to describe how this information can be merged with the numerically evolved stochastic fields within the context of DO equations.

Generally data and measurements are available in arbitrary locations in the domain of interest. The optimal estimation of gridded fields directly from the spatially irregular and multivariate data sets that are collected by varied instruments and sampling schemes is a problem studied in the context of objective analysis (see e.g. [160], [1], [2]) and will not be studied in this work. For schemes that utilize raw data to learn the dominant (multivariate) stochastic subspace, we refer to [73] and [75]. Here we assume that data or measurements information is expressed in field form known at particular time instants. Based on this assumption we first define some essential notation for the analysis that will follow.

4.4.1 Data and measurements formulation

We denote the time instant where data is available as t_o , the unbiased estimated field (through objective analysis) as $\hat{\mathbf{u}}(\mathbf{x}, t_o)$, and the covariance operator for the associated error $\mathcal{E}(\mathbf{x}, t_o; \omega) \equiv \hat{\mathbf{u}}(\mathbf{x}, t_o) - \mathbf{u}(\mathbf{x}, t_o; \omega)$ as

$$\mathbf{C}_{\mathcal{E}\mathcal{E}}(\mathbf{x}, \mathbf{y}) = E^\omega \left[\mathcal{E}(\mathbf{x}, t_o; \omega) \mathcal{E}(\mathbf{y}, t_o; \omega)^T \right].$$

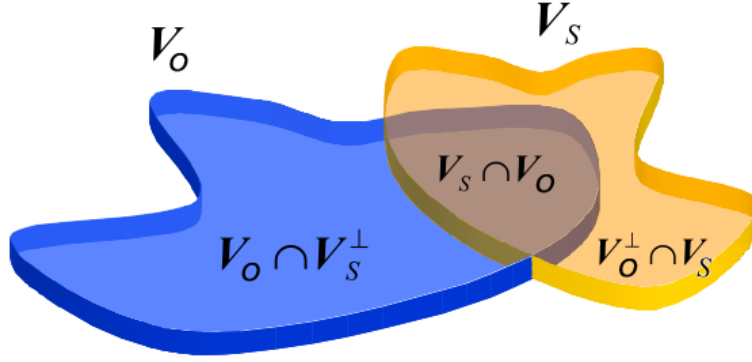


Figure 4-2: Decomposition of the stochastic subspace \mathbf{V}_S based on the data subspace \mathbf{V}_O .

For simplicity we also assume zero-mean Gaussian statistics for the estimated field. To express the available information in the DO framework we perform a spectrum analysis of the covariance operator by solving the following eigenvalue problem

$$\int_D \mathbf{C}_{\mathcal{E}\mathcal{E}}(\mathbf{x}, \mathbf{y}) v_{\mathcal{E},i}(\mathbf{x}) d\mathbf{x} = \lambda_{\mathcal{E},i}^2 v_{\mathcal{E},i}(\mathbf{y}), \quad \mathbf{y} \in D. \quad (4.3)$$

from which we obtain a set of eigenpairs $(\lambda_{\mathcal{E},i}^2, v_{\mathcal{E},i}(\mathbf{x}))$ $i = 1, 2, \dots$. Then, based on the critical variance threshold σ_{cr}^2 (below which stochasticity is negligible), we obtain the full-field *data subspace* defined as

$$\mathbf{V}_O = \text{span} \{v_{\mathcal{E},i}(\mathbf{x}) \mid \lambda_{\mathcal{E},i}^2 > \sigma_{cr}^2\}$$

defined as the span of all eigenfields $v_{\mathcal{E},i}(\mathbf{x})$ associated with important variance ($\lambda_{\mathcal{E},i}^2 > \sigma_{cr}^2$).

4.4.2 Update of the stochastic information inside \mathbf{V}_S

To update the stochastic information of the current state of the system we partition the stochastic subspace \mathbf{V}_S into two orthogonal (i.e. disjoint) linear subspaces as follows

$$\mathbf{V}_S = \mathbf{V}_S \cap \mathbf{V}_O \oplus \mathbf{V}_S \cap \mathbf{V}_O^\perp.$$

where \oplus denotes the direct sum of the two subspaces (Figure 4-1). Note that along the dimensions contained in the subspace $\mathbf{V}_S \cap \mathbf{V}_O^\perp \subset \mathbf{V}_S$, the available information from data and measurements guarantees accurate estimation since the associated data variance is less than σ_{cr}^2 . Therefore, for these directions, we may neglect those stochastic dimensions and update the stochastic subspace and the mean directly as

$$\begin{aligned} \mathbf{V}_S &\rightarrow \mathbf{V}_S \cap \mathbf{V}_O, \quad \text{and} \quad s \rightarrow \dim \mathbf{V}_S \cap \mathbf{V}_O \\ \bar{u}(\mathbf{x}, t_o) &\rightarrow \bar{u}(\mathbf{x}, t_o) - \mathbf{\Pi}_{\mathbf{V}_S \cap \mathbf{V}_O^\perp} [\bar{u}(\mathbf{x}, t_o)] + \mathbf{\Pi}_{\mathbf{V}_S \cap \mathbf{V}_O} [\hat{u}(\mathbf{x}, t_o)] \end{aligned}$$

where for the stochastic subspace we maintain only the directions lying on the intersection of the stochastic subspace and the data information. For the mean we substitute completely the information computed through the evolution equations with the measured information for which there is good accuracy, i.e. the information corresponding to eigendirections with $\lambda_{\mathcal{E},i}^2 \leq \sigma_{cr}^2$ which are contained in \mathbf{V}_O^\perp .

The next step of our analysis involves the update of the remaining stochastic coefficients $Y_i(t_o; \omega)$ that describe the probabilistic structure in the reduced-dimension stochastic subspace \mathbf{V}_S . We have by definition of \mathcal{E}

$$\hat{\mathbf{u}}(\mathbf{x}, t_o) = \mathcal{E}(\mathbf{x}, t_o; \omega) + \bar{\mathbf{u}}(\mathbf{x}, t_o) + Y_i(t_o; \omega) \mathbf{u}_i(\mathbf{x}, t_o)$$

By projecting the above equation to every basis element of the stochastic subspace we obtain for every $k = 1, \dots, s$

$$\langle \hat{\mathbf{u}}(\bullet, t_o), \mathbf{u}_k(\bullet, t_o) \rangle = \langle \mathcal{E}(\bullet, t_o; \omega), \mathbf{u}_k(\bullet, t_o) \rangle + \langle \bar{\mathbf{u}}(\bullet, t_o), \mathbf{u}_k(\bullet, t_o) \rangle + Y_k(t_o; \omega).$$

We shall now do a Bayes ‘data assimilation’ update in the \mathbf{Y} space. Using the above relation we can apply Bayes rule to update the probability density function describing the stochastic coefficients. More, specifically we will have

$$f_{\mathbf{Y}}(\mathbf{y}, t_o | \{\langle \hat{\mathbf{u}}(\bullet, t_o), \mathbf{u}_k(\bullet, t_o) \rangle\}_{k=1}^s) = \frac{f(\{\langle \hat{\mathbf{u}}(\bullet, t_o), \mathbf{u}_k(\bullet, t_o) \rangle\}_{k=1}^s | \mathbf{y}) f_{\mathbf{Y}}(\mathbf{y}, t_o)}{\int_{\mathbb{R}^s} f(\{\langle \hat{\mathbf{u}}(\bullet, t_o), \mathbf{u}_k(\bullet, t_o) \rangle\}_{k=1}^s | \mathbf{z}) f_{\mathbf{Y}}(\mathbf{z}, t_o) d\mathbf{z}}$$

where \mathbf{y} is the argument for the random variable $\mathbf{Y}(t_o; \omega)$ and $f_{\mathbf{Y}}$ is the corresponding probability density function (see Chapter 2 - Section 2.2). We have assumed Gaussian statistics for the error field $\mathcal{E}(\mathbf{x}, t_o; \omega)$. Therefore,

$$f(\{\langle \hat{\mathbf{u}}(\bullet, t_o), \mathbf{u}_k(\bullet, t_o) \rangle\}_{k=1}^s | \mathbf{y}) = \mathcal{N}(\langle \bar{\mathbf{u}}(\bullet, t_o), \mathbf{u}_k(\bullet, t_o) \rangle + y_k, \Xi_{ij})$$

where Ξ_{ij} is the covariance matrix defined as

$$\Xi_{ij} = \int_D \int_D \mathbf{u}_i^T(\mathbf{x}_1, t_o) \mathbf{C}_{\mathcal{E}\mathcal{E}}(\mathbf{x}_1, \mathbf{x}_2) \mathbf{u}_j(\mathbf{x}_2, t_o) d\mathbf{x}_1 d\mathbf{x}_2, \quad i, j = 1, \dots, s.$$

Thus, the pdf describing the updated stochastic coefficients will be

$$f_{\mathbf{Y}}(\mathbf{y}, t_o | \{\langle \hat{\mathbf{u}}(\bullet, t_o), \mathbf{u}_k(\bullet, t_o) \rangle\}_{k=1}^s) = \frac{\mathcal{N}(\langle \bar{\mathbf{u}}(\bullet, t_o), \mathbf{u}_k(\bullet, t_o) \rangle + y_k, \Xi_{ij}) f_{\mathbf{Y}}(\mathbf{y}, t_o)}{\int_{\mathbb{R}^s} \mathcal{N}(\langle \bar{\mathbf{u}}(\bullet, t_o), \mathbf{u}_k(\bullet, t_o) \rangle + y_k, \Xi_{ij}) f_{\mathbf{Y}}(\mathbf{z}, t_o) d\mathbf{z}}$$

To be consistent with the DO formulation we finally need to center the above density, so that the updated $Y_k(t_o; \omega)$ are zero mean (Figure 4-2). Specifically, we will have

$$\bar{u}(\mathbf{x}, t_o) \rightarrow \bar{u}(\mathbf{x}, t_o) + m_k \mathbf{u}_k(\mathbf{x}, t_o), \quad \text{with } m_k = \int_{\mathbb{R}^s} y_k f_{\mathbf{Y}}(\mathbf{y}, t_o | \{\langle \hat{\mathbf{u}}(\bullet, t_o), \mathbf{u}_k(\bullet, t_o) \rangle\}_{k=1}^s) d\mathbf{y}$$

$$f_{\mathbf{Y}}(\mathbf{y}, t_o) \rightarrow f_{\mathbf{Y}}(\mathbf{y} + \mathbf{m}, t_o | \{\langle \hat{\mathbf{u}}(\bullet, t_o), \mathbf{u}_k(\bullet, t_o) \rangle\}_{k=1}^s).$$

4.4.3 Expansion of the stochastic subspace \mathbf{V}_S

The second stage involves the consideration of the stochastic dimensions of \mathbf{V}_O which are not included into the stochastic subspace \mathbf{V}_S . More specifically, we consider the space $\mathbf{W}_O \equiv \mathbf{V}_O \cap \mathbf{V}_S^\perp$. This linear subspace contains directions with important uncertainty according to the estimation procedure and hence these should be included into the stochastic subspace \mathbf{V}_S . This can be done in more than one ways. One approach is the expansion of the stochastic subspace \mathbf{V}_S using all the new dimensions contained in \mathbf{W}_O . However, this method may involve significant cost. Another approach (ESSE learning) is to add only a single dimension for every synoptic batch of data [75].

A more efficient alternative is to combine the information for \mathbf{W}_O with the analytical arguments presented in the previous section in order to obtain the direction(s) in \mathbf{W}_O that tend to obtain larger values of variance according to the dynamics of the system. In this way, we may enhance \mathbf{V}_S only with the most unstable directions of the space \mathbf{W}_O .

If we select only the most unstable direction in \mathbf{W}_O , then according to the results of the last section this will be given by

$$\mathbf{u}_{s+1}(\mathbf{x}, t_o) = \sum_{i=1}^{\dim \mathbf{W}_O} a_i \mathbf{w}_i(\mathbf{x})$$

where $\mathbf{w}_i(\mathbf{x})$ is a basis that spans \mathbf{W}_O and $\{a_i\}_{i=1}^{s-m}$ is the eigenvector associated with the maximum eigenvalue of the matrix $Q_{ij} + Q_{ji}$, with

$$Q_{ij} = \left\langle E^\omega \left[\frac{\delta \mathcal{L}[\mathbf{u}(\bullet, t_o; \omega); \omega]}{\delta u} [\mathbf{w}_i(\bullet)] \right], \mathbf{w}_j(\bullet) \right\rangle.$$

Depending on the nature and scale of the problem and the size of the stochastic subspace a combination of the two approaches, i.e. adding those directions in \mathbf{W}_O with important variance as well as those which are most unstable, may result in more efficient results. Finally, the corresponding stochastic coefficients $Y_{s+1}(t_o; \omega)$ will follow Gaussian distribution with variance

$$\sigma_{Y_{s+1}}^2(t_o) = \int_D \int_D \mathbf{u}_{s+1}^T(\mathbf{x}_1, t_o) \mathbf{C}_{\mathcal{E}\mathcal{E}}(\mathbf{x}_1, \mathbf{x}_2) \mathbf{u}_{s+1}(\mathbf{x}_2, t_o) d\mathbf{x}_1 d\mathbf{x}_2$$

and mean

$$E^\omega [Y_{s+1}(t_o; \omega)] = \langle \hat{\mathbf{u}}(\bullet, t_o), \mathbf{u}_{s+1}(\bullet, t_o) \rangle$$

As we mentioned in the previous section appropriate modification of the mean field should be made so that $Y_{s+1}(t_o; \omega)$ is centered according to the DO formulation.

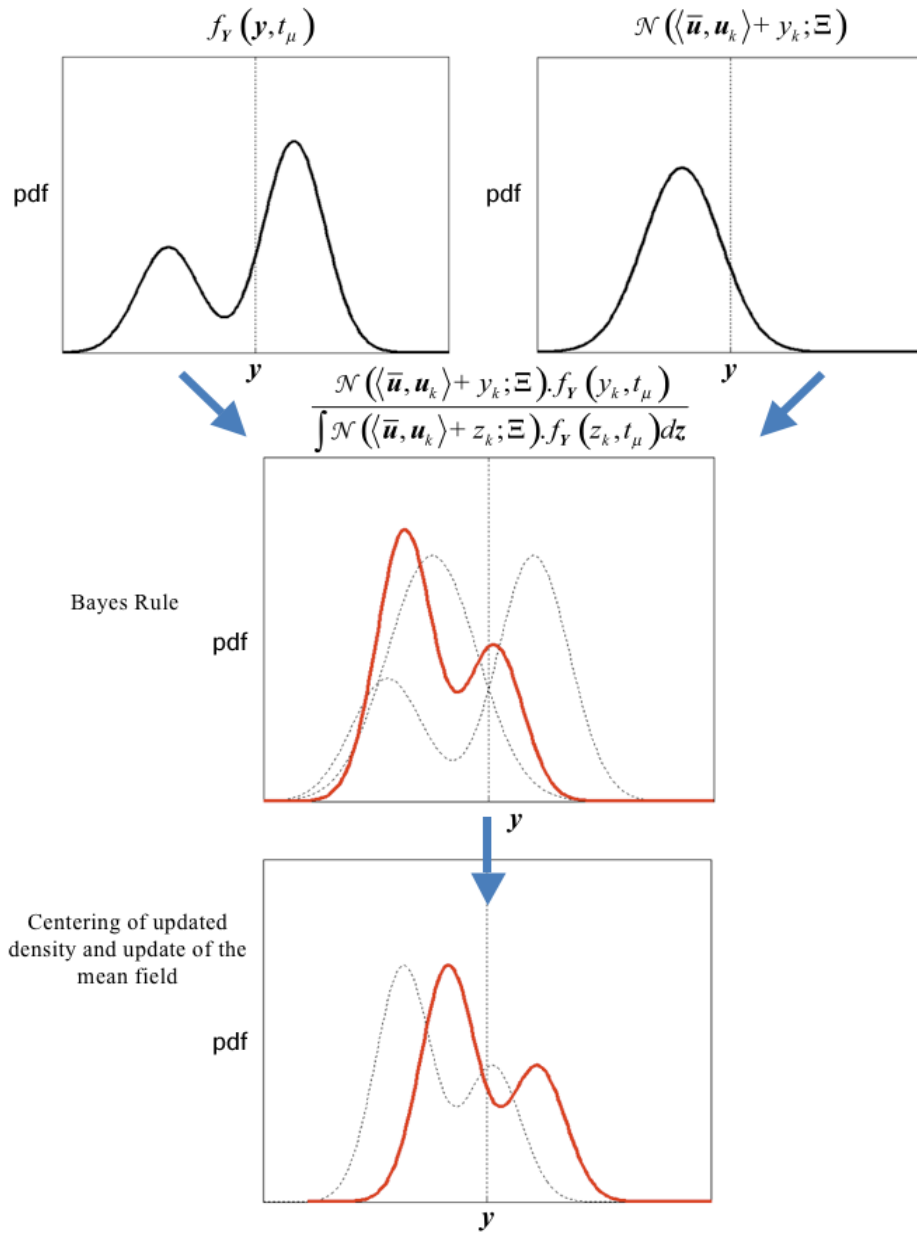


Figure 4-3: Update of the probability density function $f_Y(\mathbf{y}, t)$ using data or measurements.

Chapter 5

Application of dynamically orthogonal field equations to random fluid flows

Abstract

In this chapter we will apply the Dynamically Orthogonal field equations for the case of two dimensional random flows described by Navier-Stokes equations including the Coriolis force. The Navier-Stokes equations contain quadratic nonlinearities, which as we will see, are responsible for the transfer of energy from the mean flow to the various stochastic DO modes in the form of variance. The quadratic terms are also the cause of transfer of uncertainty among different DO modes. In what follows we will illustrate the above mechanisms through the consideration of special cases involving externally forced, forced through the boundary, and free systems. More specifically, in the first two sections we will formulate the problem and we will derive closed, evolution equations for the mean field, the scalar stochastic coefficients, and the DO modes. Note that the Navier-Stokes equations involve a diagnostic variable, the pressure, which is not described explicitly and hence special treatment is needed. In the third section we will discuss the case of stochastic boundary conditions and we will prove that this family of problems can always be reformulated as problems with deterministic boundary conditions and suitable random forcing. In Section 4 we will apply the methodology developed in Chapter 4 to express the most unstable mode and in Section 5 we will derive expressions for the transfer of energy from the mean flow to and among the stochastic modes. In the last three sections of the chapter we will present numerical results for specific geometries and forcing configurations and we will also examine convergence properties of the proposed methodology. The details for the numerical solution of the derived equations are included in Appendix B. Part of the material presented in the current chapter is contained in Sapsis and Lermusiaux, 2009 [129].

5.1 Formulation

We will now formulate the DO field equations for the special case of fluid flows governed by stochastic Navier-Stokes. The general equations, for an incompressible, two dimensional

fluid in a domain D in a rotating frame at frequency f have the form

$$\begin{aligned} \frac{\partial \mathbf{u}}{\partial t} &= -\nabla p + \frac{1}{\text{Re}} \Delta \mathbf{u} - \mathbf{u} \cdot \nabla \mathbf{u} - f \hat{\mathbf{k}} \times \mathbf{u} + \tau(\mathbf{x}, t) + \varphi(\mathbf{x}, t; \omega) \equiv \mathcal{L}[\mathbf{u}(\mathbf{x}, t; \omega); \omega] \\ 0 &= \text{div } \mathbf{u} \end{aligned}$$

where $\mathbf{u} = (u(\mathbf{x}, t; \omega), v(\mathbf{x}, t; \omega))$ is the flow velocity field, and $\hat{\mathbf{k}}$ is the unit vector for the z -direction. The pressure field is denoted with $p(\mathbf{x}, t; \omega)$, $f = f_0 + \beta_0 y$ is the Coriolis coefficient under the beta plane approximation, $\tau(\mathbf{x}, t) = (\tau_x(\mathbf{x}, t), \tau_y(\mathbf{x}, t))$ is the external deterministic stress acting on the fluid, and $\varphi(\mathbf{x}, t; \omega) = (\varphi_x(\mathbf{x}, t; \omega), \varphi_y(\mathbf{x}, t; \omega))$ is the zero-mean stochastic component of the stress for which we assume known the complete probabilistic information. In what follows we will use the DO field equations derived in Chapter 3 with inner product

$$\langle \mathbf{u}_1, \mathbf{u}_2 \rangle = \int_D (u_1 u_2 + v_1 v_2) d\mathbf{x}.$$

We consider the correlation operator for the stochastic part of the excitation $\mathbf{C}_{\varphi\varphi}(\mathbf{x}, \mathbf{y}) = E^\omega [\varphi(\mathbf{x}, t; \omega) \varphi(\mathbf{y}, t; \omega)^T]$. To diagonalize the probability measure associated with $\varphi(\mathbf{x}, t; \omega)$ we solve the following 2D-vector eigenvalue problem

$$\int_D \mathbf{C}_{\varphi\varphi}(\mathbf{x}, \mathbf{y}) \varphi_r(\mathbf{y}, t) d\mathbf{y} = \lambda_r^2 \varphi_r(\mathbf{x}, t)$$

In this way we obtain the principal directions over which the probability measure is spread in the variance sense. Retaining only the the first R terms we obtain the following approximation of the stochastic field $\varphi(\mathbf{x}, t; \omega)$

$$\varphi(\mathbf{x}, t; \omega) = \sum_{r=1}^R Z_r(t; \omega) \varphi_r(\mathbf{x}, t) = Z_r(t; \omega) \varphi_r(\mathbf{x}, t)$$

where R is defined by the order of truncation of the full series, and $Z_r(t; \omega)$ are the stochastic coefficients given by

$$Z_r(t; \omega) = \langle \varphi(\cdot, t; \omega), \varphi_r(\cdot, t) \rangle.$$

For simplicity we assume that the boundary conditions for the velocity are either deterministic Neumann or Dirichlet

$$\begin{aligned} \mathbf{u}(\xi, t; \omega) &= \mathbf{u}_{\partial D_1}(\xi, t), & \xi \in \partial D_1 \\ \frac{\partial \mathbf{u}}{\partial \mathbf{n}}(\xi, t; \omega) &= \mathbf{h}_{\partial D_2}(\xi, t), & \xi \in \partial D_2 \end{aligned}$$

The case of stochastic boundary conditions will be discussed Section 3.

Furthermore, we assume that the initial conditions are stochastic with known statistics given by

$$\mathbf{u}(\mathbf{x}, t_0; \omega) = \mathbf{u}_0(\mathbf{x}; \omega), \quad \mathbf{x} \in D, \quad \omega \in \Omega$$

5.2 Derivation of DO Navier-Stokes equations

We will first calculate the stochastic operator \mathcal{L} . By using the DO representation

$$\mathbf{u}(\mathbf{x}, t; \omega) = \bar{\mathbf{u}}(\mathbf{x}, t) + Y_i(t; \omega) \mathbf{u}_i(\mathbf{x}, t)$$

into Navier-Stokes equations we obtain

$$\begin{aligned} \mathcal{L}[\mathbf{u}(\mathbf{x}, t; \omega); \omega] = & -\nabla p + \frac{1}{\text{Re}} \Delta \bar{\mathbf{u}} - \bar{\mathbf{u}} \cdot \nabla \bar{\mathbf{u}} - f \hat{\mathbf{k}} \times \bar{\mathbf{u}} + \tau(\mathbf{x}, t) \\ & Y_i \left[\frac{1}{\text{Re}} \Delta \mathbf{u}_i - \mathbf{u}_i \cdot \nabla \bar{\mathbf{u}} - \bar{\mathbf{u}} \cdot \nabla \mathbf{u}_i - f \hat{\mathbf{k}} \times \mathbf{u}_i \right] \\ & - \frac{1}{2} Y_i Y_j [\mathbf{u}_i \cdot \nabla \mathbf{u}_j + \mathbf{u}_j \cdot \nabla \mathbf{u}_i] + Z_r(t; \omega) \varphi_r(\mathbf{x}, t) \end{aligned} \quad (5.2)$$

Moreover, by inserting the DO representation in the continuity equation we obtain

$$\text{div } \bar{\mathbf{u}} + Y_i(t; \omega) \text{div } \mathbf{u}_i = 0.$$

But since $Y_i(t; \omega)$ is random the above equation has the equivalent form

$$\begin{aligned} \text{div } \bar{\mathbf{u}} &= 0 \\ \text{div } \mathbf{u}_i &= 0, \quad i = 1, \dots, s. \end{aligned}$$

A very important property of Navier-Stokes equations that allow for the efficient applicability of the DO formulation is the analyticity of the evolution operator \mathcal{L} with respect to the argument $\mathbf{u}(\mathbf{x}, t; \omega)$. This property allows for the expression of the operator into a polynomial series that involve the unknown quantities of the DO representation (eq. 5.2). Through this property we are able to derive closed and exact evolution equations whose right hand side depends from moments of the stochastic coefficients, the DO modes and the mean.

Note, that for the case of a non-smooth operator \mathcal{L} we are not able to expand into a polynomial series therefore, even though the DO equations are valid, it is not possible to compute their right hand side efficiently using moments of the coefficients Y_i . Instead, in this case we need moments of the full field $\mathbf{u}(\mathbf{x}, t; \omega)$ which even though they are available (since the DO formulation includes the full probabilistic information) it is not straightforward to compute. For the case where the non-smoothness of the operator \mathcal{L} occurs in points where $\mathbf{u}(\mathbf{x}, t; \omega)$ has very low probability to exist we may approximate the operator by a polynomial series. We emphasize that the above described technical complication characterize in the same way every method that is based on an a priori representation of the solution (i.e. POD or PC). Monte-Carlo based methods are not sensitive to this point.

5.2.1 Stochastic pressure field

To derive an equation for the pressure we need to understand its role in the stochastic context of the operator \mathcal{L} given above. Pressure (for a flow with constant density) is the stochastic quantity which guarantees that every possible realization ω the evolved field $(u(\mathbf{x}, t; \omega), v(\mathbf{x}, t; \omega))$ is divergence-free (take the divergence of the momentum equation 5.2 and use the family of continuity equations to show this). Therefore, the stochastic pressure should be able to balance all the non-divergent contributions from the terms involved in

the operator \mathcal{L} (equation (5.2)). To this end we choose to represent the stochastic pressure field as

$$p = p_0 + Y_i(t; \omega) p_i - Y_i(t; \omega) Y_j(t; \omega) p_{ij} + Z_r(t; \omega) b_r$$

Based on the above discussion, the mean pressure field components should satisfy the following equation

$$\Delta p_0 = \operatorname{div} \left(-\bar{\mathbf{u}} \cdot \nabla \bar{\mathbf{u}} - f \hat{\mathbf{k}} \times \bar{\mathbf{u}} + \tau(\mathbf{x}, t) \right)$$

with boundary conditions often given by

$$\frac{\partial p_0}{\partial \mathbf{n}}(\xi, t) = 0, \quad \xi \in \partial D_1 \quad \text{and} \quad p_0(\xi, t) = \text{const.} \quad \xi \in \partial D_2$$

Note, that following common practice in fluid mechanics literature [28] we have chosen homogeneous Neumann condition for the pressure on the boundary ∂D_1 and piece-wise constant Dirichlet condition for the boundary ∂D_2 . As we will see, this property is key for simplifying the evolution equations for the stochastic coefficients and also for the numerical implementation using projection methods.

The stochastic terms in \mathcal{L} multiplied with $Y_i(t; \omega)$ will be balanced through the following equation

$$\Delta p_i = \operatorname{div} \left(-\mathbf{u}_i \cdot \nabla \bar{\mathbf{u}} - \bar{\mathbf{u}} \cdot \nabla \mathbf{u}_i - f \hat{\mathbf{k}} \times \mathbf{u}_i \right), \quad i = 1, \dots, s \quad (5.4)$$

with boundary conditions

$$\frac{\partial p_i}{\partial \mathbf{n}}(\xi, t) = 0, \quad \xi \in \partial D_1 \quad \text{and} \quad p_i(\xi, t) = 0, \quad \xi \in \partial D_2, \quad i = 1, \dots, s.$$

where the Dirichlet condition is taken to be homogeneous since the boundary conditions of the full problem have been assumed deterministic (the generalization for stochastic boundary conditions is presented in the next sections). Similarly, for the stochastic terms multiplied by $Y_i(t; \omega) Y_j(t; \omega)$ we will have

$$\Delta p_{ij} = \frac{1}{2} \operatorname{div} (\mathbf{u}_i \cdot \nabla \mathbf{u}_j + \mathbf{u}_j \cdot \nabla \mathbf{u}_i), \quad i, j = 1, \dots, s$$

and boundary conditions

$$\frac{\partial p_{ij}}{\partial \mathbf{n}}(\xi, t) = 0, \quad \xi \in \partial D_1 \quad \text{and} \quad p_{ij}(\xi, t) = 0, \quad \xi \in \partial D_2, \quad i, j = 1, \dots, s.$$

Finally, the forcing terms will be balanced through the family of equations

$$\Delta b_r = \operatorname{div} \varphi_r(\mathbf{x}, t), \quad r = 1, \dots, R.$$

with boundary conditions

$$\frac{\partial q_r}{\partial \mathbf{n}}(\xi, t) = 0, \quad \xi \in \partial D_1 \quad \text{and} \quad q_r(\xi, t) = 0, \quad \xi \in \partial D_2, \quad r = 1, \dots, R.$$

The above set of equations guarantees that for every realization ω the evolved field $(u(\mathbf{x}, t; \omega), v(\mathbf{x}, t; \omega))$

will always be incompressible. Moreover, the evolution operator \mathcal{L} will take the form

$$\begin{aligned} \mathcal{L} [\mathbf{u}(\mathbf{x}, t; \omega); \omega] &= -\nabla p_0 + \frac{1}{\text{Re}} \Delta \bar{\mathbf{u}} - \bar{\mathbf{u}} \cdot \nabla \bar{\mathbf{u}} - f \hat{\mathbf{k}} \times \bar{\mathbf{u}} + \tau(\mathbf{x}, t) \\ &Y_i \left[-\nabla p_i + \frac{1}{\text{Re}} \Delta \mathbf{u}_i - \mathbf{u}_i \cdot \nabla \bar{\mathbf{u}} - \bar{\mathbf{u}} \cdot \nabla \mathbf{u}_i - f \hat{\mathbf{k}} \times \mathbf{u}_i \right] \\ &- Y_i Y_j \left[-\nabla p_{ij} + \frac{1}{2} \mathbf{u}_i \cdot \nabla \mathbf{u}_j + \frac{1}{2} \mathbf{u}_j \cdot \nabla \mathbf{u}_i \right] + Z_r(t; \omega) [-\nabla b_r + \varphi_r(\mathbf{x}, t)] \end{aligned}$$

5.2.2 Evolution of the mean field $\bar{\mathbf{u}}(\mathbf{x}, t; \omega)$

Using the corresponding DO equation for the mean we obtain the set of deterministic PDEs

$$\frac{\partial \bar{\mathbf{u}}}{\partial t} = -\nabla p_0 + \frac{1}{\text{Re}} \Delta \bar{\mathbf{u}} - \bar{\mathbf{u}} \cdot \nabla \bar{\mathbf{u}} - f \hat{\mathbf{k}} \times \bar{\mathbf{u}} + \tau(\mathbf{x}, t) \quad (5.5a)$$

$$- \mathbf{C}_{Y_i(t)Y_j(t)} \left[-\nabla p_{ij} + \frac{1}{2} \mathbf{u}_i \cdot \nabla \mathbf{u}_j + \frac{1}{2} \mathbf{u}_j \cdot \nabla \mathbf{u}_i \right]$$

$$0 = \text{div } \bar{\mathbf{u}} \quad (5.5b)$$

with the following boundary conditions

$$\begin{aligned} \bar{\mathbf{u}}(\xi, t; \omega) &= \mathbf{u}_{\partial D_1}(\xi, t), \quad \xi \in \partial D_1 \\ \frac{\partial \bar{\mathbf{u}}}{\partial \mathbf{n}}(\xi, t; \omega) &= \mathbf{h}_{\partial D_2}(\xi, t), \quad \xi \in \partial D_2 \end{aligned}$$

5.2.3 Evolution of the stochastic subspace basis $\mathbf{u}_i(\mathbf{x}, t; \omega)$

We will first calculate the quantity $E^\omega [\mathcal{L} [\mathbf{u}(\mathbf{x}, t; \omega); \omega] Y_j(t; \omega)]$. We will have

$$\begin{aligned} E^\omega [\mathcal{L} [\mathbf{u}(\mathbf{x}, t; \omega); \omega] Y_j(t; \omega)] &= \mathbf{C}_{Y_m(t)Y_j(t)} \left[-\nabla p_m + \frac{1}{\text{Re}} \Delta \mathbf{u}_m - \mathbf{u}_m \cdot \nabla \bar{\mathbf{u}} - \bar{\mathbf{u}} \cdot \nabla \mathbf{u}_m - f \hat{\mathbf{k}} \times \mathbf{u}_m \right] \\ &- \mathbf{M}_{Y_j(t)Y_m(t)Y_n(t)} \left[-\nabla p_{mn} + \frac{1}{2} \mathbf{u}_m \cdot \nabla \mathbf{u}_n + \frac{1}{2} \mathbf{u}_n \cdot \nabla \mathbf{u}_m \right] \\ &+ \mathbf{C}_{Y_j(t)Z_r(t)} [-\nabla b_r + \varphi_r(\mathbf{x}, t)] \end{aligned}$$

Multiplying with the inverse matrix $\mathbf{C}_{Y_i(t)Y_j(t)}$ we will have (defining \mathbf{Q}_i)

$$\begin{aligned} \mathbf{Q}_i &\equiv \mathbf{C}_{Y_i(t)Y_j(t)}^{-1} E^\omega [\mathcal{L} [\mathbf{u}(\mathbf{x}, t; \omega); \omega] Y_j(t; \omega)] \\ &= \left[-\nabla p_i + \frac{1}{\text{Re}} \Delta \mathbf{u}_i - \mathbf{u}_i \cdot \nabla \bar{\mathbf{u}} - \bar{\mathbf{u}} \cdot \nabla \mathbf{u}_i - f \hat{\mathbf{k}} \times \mathbf{u}_i \right] \\ &- \mathbf{C}_{Y_i(t)Y_j(t)}^{-1} \mathbf{M}_{Y_j(t)Y_m(t)Y_n(t)} \left[-\nabla p_{mn} + \frac{1}{2} \mathbf{u}_m \cdot \nabla \mathbf{u}_n + \frac{1}{2} \mathbf{u}_n \cdot \nabla \mathbf{u}_m \right] \\ &+ \mathbf{C}_{Y_i(t)Y_j(t)}^{-1} \mathbf{C}_{Y_j(t)Z_r(t)} [-\nabla b_r + \varphi_r(\mathbf{x}, t)] \end{aligned}$$

Note that $\mathbf{C}_{Y_i(t)Y_j(t)}$ as a covariance matrix is always symmetric, positive-definite thus invertible. Using the last expression we obtain the evolution equations for the basis $\mathbf{u}_i(\mathbf{x}, t; \omega)$

$$\begin{aligned}\frac{\partial \mathbf{u}_i}{\partial t} &= \mathbf{Q}_i - \langle \mathbf{Q}_i, \mathbf{u}_m \rangle \mathbf{u}_m \\ 0 &= \operatorname{div} \mathbf{u}_i\end{aligned}$$

for $i = 1, \dots, s$. Moreover, we will have the following boundary conditions

$$\begin{aligned}\mathbf{u}_i(\xi, t) &= \mathbf{0}, \quad \xi \in \partial D_1 \\ \frac{\partial \mathbf{u}_i}{\partial \mathbf{n}}(\xi, t) &= \mathbf{0}, \quad \xi \in \partial D_2.\end{aligned}$$

5.2.4 Evolution of the stochastic coefficients $Y_i(\mathbf{x}, t; \omega)$

The set of evolution equations for the stochastic coefficients will take the form of a SDE

$$\begin{aligned}\frac{dY_i}{dt} &= \left\langle -\nabla p_m + \frac{1}{\operatorname{Re}} \Delta \mathbf{u}_m - \mathbf{u}_m \cdot \nabla \bar{\mathbf{u}} - \bar{\mathbf{u}} \cdot \nabla \mathbf{u}_m - f \hat{\mathbf{k}} \times \mathbf{u}_m, \mathbf{u}_i \right\rangle Y_m \\ &\quad - \left\langle -\nabla p_{mn} + \frac{1}{2} \mathbf{u}_m \cdot \nabla \mathbf{u}_n + \frac{1}{2} \mathbf{u}_n \cdot \nabla \mathbf{u}_m, \mathbf{u}_i \right\rangle (Y_m Y_n - \mathbf{C}_{Y_m(t)Y_n(t)}) \\ &\quad + \langle -\nabla b_r + \varphi_r(\mathbf{x}, t), \mathbf{u}_i \rangle Z_r(t; \omega)\end{aligned}$$

Using Gauss theorem [167] we have for every scalar field α and every divergent-free vector field \mathbf{F}

$$\int_D \nabla \alpha(\mathbf{x}) \cdot \mathbf{F}(\mathbf{x}) \, d\mathbf{x} = \int_{\partial D} \alpha(\xi) \mathbf{F}(\xi) \cdot \mathbf{n}(\xi) \, d\xi$$

Using this property for the velocity field, for part of the boundary ∂D_1 where homogeneous Dirichlet boundary conditions hold, the above integral vanishes because of the zero velocity of the modes on the boundary. Moreover, the zero boundary pressure associated with modes implies that the above integral will also vanish over the boundary ∂D_2 . Therefore, we will have

$$\langle \nabla p_m, \mathbf{u}_i \rangle = \langle \nabla p_{mn}, \mathbf{u}_i \rangle = \langle \nabla b_r, \mathbf{u}_i \rangle = 0 \quad (5.8)$$

Hence, the stochastic equation describing the evolution of the stochastic coefficients will be take the form

$$\begin{aligned}\frac{dY_i}{dt} &= \left\langle \frac{1}{\operatorname{Re}} \Delta \mathbf{u}_m - \mathbf{u}_m \cdot \nabla \bar{\mathbf{u}} - \bar{\mathbf{u}} \cdot \nabla \mathbf{u}_m - f \hat{\mathbf{k}} \times \mathbf{u}_m, \mathbf{u}_i \right\rangle Y_m \\ &\quad - \frac{1}{2} \langle \mathbf{u}_m \cdot \nabla \mathbf{u}_n + \mathbf{u}_n \cdot \nabla \mathbf{u}_m, \mathbf{u}_i \rangle (Y_m Y_n - \mathbf{C}_{Y_m(t)Y_n(t)}) \\ &\quad + \langle \varphi_r(\mathbf{x}, t), \mathbf{u}_i \rangle Z_r(t; \omega)\end{aligned}$$

We emphasize that the last property (5.8) is crucial since it allows us to apply projection methods (Guermont et al., [55], Ueckermann & Lermusiaux [personal communication]) for the numerical solution of the DO equations for Navier-Stokes. In this numerical framework the stochastic pressure does not need to be determined completely since the non-divergent requirement for the velocity field is enforced numerically. The last property that the pressure terms do not show up in the evolution equation for the stochastic coefficients, allows the

applicability of projection methods, leading to significantly smaller computational cost.

5.3 The case of stochastic boundary conditions

We shall now consider the problem of stochastic boundary conditions. We assume that the complete stochastic information for the boundary conditions is known. More specifically we have

$$\begin{aligned}\mathbf{u}(\xi, t; \omega) &= \mathbf{u}_{\partial D_1}(\xi, t) + \mathbf{u}'_{\partial D_1}(\xi, t; \omega), & \xi \in \partial D_1 \\ \frac{\partial \mathbf{u}}{\partial \mathbf{n}}(\xi, t; \omega) &= \mathbf{h}_{\partial D_2}(\xi, t) + \mathbf{h}'_{\partial D_2}(\xi, t; \omega), & \xi \in \partial D_2\end{aligned}$$

where $[\mathbf{u}'_{\partial D_1}(\xi, t; \omega), \mathbf{h}'_{\partial D_2}(\xi, t; \omega)]^T$ is the zero-mean stochastic part of the boundary conditions. We consider the correlation operator associated with the boundary conditions

$$\mathbf{C}_{\partial D \partial D}(\xi_1, \xi_2) = E^\omega \left[\begin{bmatrix} \mathbf{u}'_{\partial D_1}(\xi_1, t; \omega) \\ \mathbf{h}'_{\partial D_2}(\xi_1, t; \omega) \end{bmatrix} \begin{bmatrix} \mathbf{u}'_{\partial D_1}(\xi_2, t; \omega) \\ \mathbf{h}'_{\partial D_2}(\xi_2, t; \omega) \end{bmatrix}^T \right]$$

We formulate the eigenvalue problem to determine the principal directions where the probability is distributed in the variance sense

$$\int_{\partial D} \mathbf{C}_{\partial D \partial D}(\xi_1, \xi_2) \begin{bmatrix} \mathbf{u}_{\partial D_1, k}(\xi_2, t) \\ \mathbf{h}_{\partial D_2, k}(\xi_2, t) \end{bmatrix} d\xi_2 = \lambda_k^2 \begin{bmatrix} \mathbf{u}_{\partial D_1, k}(\xi_1, t) \\ \mathbf{h}_{\partial D_2, k}(\xi_1, t) \end{bmatrix}$$

Using this information we expand the stochastic boundary conditions as follows

$$\begin{aligned}\mathbf{u}(\xi, t; \omega) &= \mathbf{u}_{\partial D_1}(\xi, t) + \Xi_k(t; \omega) \mathbf{u}_{\partial D_1, k}(\xi, t), & \xi \in \partial D_1 \\ \frac{\partial \mathbf{u}}{\partial \mathbf{n}}(\xi, t; \omega) &= \mathbf{h}_{\partial D_2}(\xi, t) + \Xi_k(t; \omega) \mathbf{h}_{\partial D_2, k}(\xi, t), & \xi \in \partial D_2\end{aligned}$$

where k is an index taking values from $1, \dots, K$, the order of the truncation, and the stochastic coefficients are given by

$$\Xi_k(t; \omega) = \int_{\partial D_1} \mathbf{u}'_{\partial D_1}(\xi, t; \omega)^T \mathbf{u}_{\partial D_1, k}(\xi, t) d\xi + \int_{\partial D_2} \mathbf{h}'_{\partial D_2}(\xi, t; \omega)^T \mathbf{h}_{\partial D_2, k}(\xi, t) d\xi.$$

We will transform the above problem to an equivalent one having deterministic boundary conditions. In this case the effect of stochastic boundary conditions will come through the forcing terms. The idea is to handle the effect of stochastic boundary conditions through the partition of the solution into a component $\mathbf{u}_h(\mathbf{x}, t; \omega)$ that will satisfy the deterministic part of the boundary conditions, and a set of incompressible and irrotational components $\mathbf{u}_{b, k}(\mathbf{x}, t)$ that will satisfy the stochastic part of the boundary conditions. Specifically, we write the solution of the system as

$$\mathbf{u}(\mathbf{x}, t; \omega) = \mathbf{u}_h(\mathbf{x}, t; \omega) + \Xi_k(t; \omega) \mathbf{u}_{b, k}(\mathbf{x}, t)$$

Since the velocity fields $\mathbf{u}_{b,k}(\mathbf{x}, t)$ have been assumed irrotational and incompressible there will be a set of scalar potentials $\phi_{b,k}(\mathbf{x}, t)$ such that

$$\begin{aligned}\mathbf{u}_{b,k}(\mathbf{x}, t) &= \nabla\phi_{b,k}(\mathbf{x}, t) \\ \Delta\phi_{b,k}(\mathbf{x}, t) &= 0\end{aligned}$$

Moreover, each potential function $\phi_{b,k}(\mathbf{x}, t)$ will satisfy the following boundary conditions

$$\begin{aligned}\nabla\phi_{b,k}(\xi, t) &= \mathbf{u}_{\partial D_1, k}(\xi, t), & \xi \in \partial D_1 \\ \frac{\partial}{\partial \mathbf{n}}\nabla\phi_{b,k}(\xi, t) &= \mathbf{h}_{\partial D_2, k}(\xi, t), & \xi \in \partial D_2\end{aligned}$$

Note that time in the above elliptic equation act as a parameter; thus there is no need for initial conditions. With the above choice we have a well defined problem for the potentials $\phi_{b,k}(\mathbf{x}, t)$ and additionally our solution satisfies the stochastic part of the boundary conditions. Moreover, we require $\mathbf{u}_h(\mathbf{x}, t; \omega)$ to satisfy the deterministic part of the boundary conditions and we obtain the following problem for $\mathbf{u}_h(\mathbf{x}, t; \omega)$

$$\begin{aligned}\frac{\partial \mathbf{u}_h}{\partial t} &= \mathcal{L}[\mathbf{u}_h(\mathbf{x}, t; \omega) + \Xi_k(t; \omega) \nabla\phi_{b,k}(\mathbf{x}, t); \omega] - \frac{\partial}{\partial t}(\Xi_k(t; \omega) \nabla\phi_{b,k}(\mathbf{x}, t)) \\ 0 &= \text{div } \mathbf{u}_h\end{aligned}$$

with deterministic boundary conditions

$$\begin{aligned}\mathbf{u}_h(\xi, t; \omega) &= \mathbf{u}_{\partial D_1}(\xi, t), & \xi \in \partial D_1 \\ \frac{\partial \mathbf{u}_h}{\partial \mathbf{n}}(\xi, t; \omega) &= \mathbf{h}_{\partial D_2}(\xi, t), & \xi \in \partial D_2\end{aligned}$$

and initial conditions

$$\mathbf{u}_h(\mathbf{x}, t_0; \omega) = \mathbf{u}_0(\mathbf{x}; \omega) - \Xi_k(t_0; \omega) \nabla\phi_{b,k}(\mathbf{x}, t_0), \quad \mathbf{x} \in D, \quad \omega \in \Omega$$

Therefore, we have transformed the general problem to one with deterministic boundary conditions and stochastic forcing. We emphasize that the handling of the stochastic boundary conditions through the boundary is of special importance for the case of systems where the initial state is deterministic and uncertainty is introduced only through the boundary conditions (i.e. the stochastic subspace is initially an empty set). In this case the modes required to describe the current state of the system may be very few compared to those required to satisfy the stochastic boundary conditions. Using the above decomposition we create a new set of modes that depend exclusively on the stochastic characteristics of the boundary conditions and not on the system state. Hence, in this formulation the stochastic boundary conditions are satisfied a priori (since we have solved for the potentials $\phi_{b,k}(\xi, t)$) and we only need to solve for the uncertainty of the solution in the interior of the domain.

5.4 Unstable perturbations for Navier-Stokes equations

As we saw in Chapter 4 the application of adaptive criteria for the dimensionality of the stochastic subspace requires the determination of the most unstable perturbations. These perturbations should be normal to the current form of the stochastic subspace V_s . In Chapter

4 a closed expression for the determination of the most unstable direction was derived in terms of the Frechet derivative of the system operator. In this section we compute explicitly the form of the unstable mode and we prove that this depends only on the mean of the current state, while the dependence through the DO modes is indirect through the fact that the unknown mode should be normal to every existing DO mode.

We consider Navier-Stokes equations (5.1) and by computing the Frechet for the evolution operator \mathcal{L} we obtain the variation towards the deterministic state-space direction $\vartheta(\mathbf{x})$

$$\frac{\delta\mathcal{L}[\mathbf{u}(\bullet, t; \omega)]}{\delta\mathbf{u}}[\vartheta] = -\nabla\frac{\delta p}{\delta\mathbf{u}} + \frac{1}{\text{Re}}\Delta\vartheta - f\hat{\mathbf{k}} \times \vartheta - \vartheta \cdot \nabla\mathbf{u} - \mathbf{u} \cdot \nabla\vartheta.$$

Moreover, the continuity equation will take the form (since it must be satisfied for all variations $\delta\mathbf{u}$)

$$\text{div } \vartheta(\mathbf{x}) = 0$$

from which we can determine the variational derivative of the pressure $\frac{\delta p}{\delta\mathbf{u}}$

$$\Delta\left(\frac{\delta p}{\delta\mathbf{u}}\right) = \nabla \cdot \left(-f\hat{\mathbf{k}} \times \vartheta - \vartheta \cdot \nabla\mathbf{u} - \mathbf{u} \cdot \nabla\vartheta\right).$$

Applying the mean value operator E^ω we have

$$\Delta\left(E^\omega\left[\frac{\delta p}{\delta\mathbf{u}}\right]\right) = \nabla \cdot \left(-f\hat{\mathbf{k}} \times \vartheta - \vartheta \cdot \nabla\bar{\mathbf{u}} - \bar{\mathbf{u}} \cdot \nabla\vartheta\right).$$

Moreover,

$$E^\omega\left[\frac{\delta\mathcal{L}[\mathbf{u}(\bullet, t; \omega)]}{\delta\mathbf{u}}[\vartheta]\right] = -\nabla\left(E^\omega\left[\frac{\delta p}{\delta\mathbf{u}}\right]\right) + \frac{1}{\text{Re}}\Delta\vartheta - f\hat{\mathbf{k}} \times \vartheta - \vartheta \cdot \nabla\bar{\mathbf{u}} - \bar{\mathbf{u}} \cdot \nabla\vartheta.$$

Hence, from Chapter 4, Section 2 we will have the form of the functional $\mathcal{Q}[\vartheta]$ from which we will determine the most unstable mode

$$\begin{aligned} \mathcal{Q}[\vartheta] &= \left\langle E^\omega\left[\frac{\delta\mathcal{L}[\mathbf{u}(\bullet, t; \omega); \omega]}{\delta\mathbf{u}}[\vartheta(\bullet, t)]\right], \vartheta(\bullet, t) \right\rangle \\ &= -\left\langle \nabla\left(E^\omega\left[\frac{\delta p}{\delta\mathbf{u}}\right]\right), \vartheta \right\rangle + \frac{1}{\text{Re}}\langle \Delta\vartheta, \vartheta \rangle \\ &\quad - \langle \vartheta \cdot \nabla\bar{\mathbf{u}}, \vartheta \rangle - \langle \bar{\mathbf{u}} \cdot \nabla\vartheta, \vartheta \rangle - \langle f\hat{\mathbf{k}} \times \vartheta, \vartheta \rangle. \end{aligned}$$

The last Coriolis term $\langle f\hat{\mathbf{k}} \times \vartheta, \vartheta \rangle$ vanishes identically. Moreover, by using Gauss identity we have

$$\begin{aligned} \left\langle \nabla\left(E^\omega\left[\frac{\delta p}{\delta\mathbf{u}}\right]\right), \vartheta \right\rangle &= -\int_D E^\omega\left[\frac{\delta p}{\delta\mathbf{u}}\right] \text{div } \vartheta d\mathbf{x} + \int_{\partial D} E^\omega\left[\frac{\delta p}{\delta\mathbf{u}}\right] \vartheta \cdot \mathbf{n} dS \\ &= \int_{\partial D} E^\omega\left[\frac{\delta p}{\delta\mathbf{u}}\right] \vartheta \cdot \mathbf{n} dS \end{aligned}$$

where the last equality follows from the non-divergence property of ϑ . Note also, that using

same arguments with those used in the previous section we can show that $\int_{\partial D} E^\omega \left[\frac{\delta p}{\delta \mathbf{u}} \right] \vartheta \cdot \mathbf{n} dS =$

0. Thus we can avoid the solution of an inverse $(p - \mathbf{u})$ problem and express $\mathcal{Q}[\vartheta]$ explicitly in terms of the current mean velocity state of the system

$$\mathcal{Q}[\vartheta] = \frac{1}{\text{Re}} \langle \Delta \vartheta, \vartheta \rangle - \langle \vartheta \cdot \nabla \bar{\mathbf{u}}, \vartheta \rangle - \langle \bar{\mathbf{u}} \cdot \nabla \vartheta, \vartheta \rangle$$

Hence, the following expression for the matrix Q_{ij} can be written

$$Q_{ij} = \frac{1}{\text{Re}} \langle \Delta \vartheta_i, \vartheta_j \rangle - \langle \vartheta_i \cdot \nabla \bar{\mathbf{u}}, \vartheta_j \rangle - \langle \bar{\mathbf{u}} \cdot \nabla \vartheta_i, \vartheta_j \rangle$$

Following the analysis of Section 4.2.2 we have an expression for the most unstable mode

$$\vartheta_c(\mathbf{x}, t) = a_{c,i} \vartheta_i(\mathbf{x}, t)$$

where $a_{c,i}$ is the eigenvector that corresponds to the maximum eigenvalue of the matrix $Q_{ij} + Q_{ji}$.

We emphasize that in the computation of the matrix Q_{ij} used for the determination of the most unstable mode there is no contribution of the Coriolis terms (Coriolis force is locally orthogonal to the flow). This is physically justified by the fact that Coriolis force does not change the energy content of the system (it is a rotation term) and here the norm that we consider is the kinetic energy. However, other norms may be used to characterize the most unstable perturbation, e.g. growth of enstrophy, $\frac{1}{2} \int_D |\nabla \times \mathbf{u}|^2 d\mathbf{x}$. In the latter case, we will have a contribution of the Coriolis force due to the spatial variation of the Coriolis coefficient.

5.5 Transfer of energy in Navier-Stokes

We will now study energy exchange properties between different DO modes and the mean flow. As we saw in Chapter 3 the DO modes remain always orthogonal. Spatial orthogonality of these fields implies orthogonality of their spatial Fourier, Gabor, and Wavelet transforms [5], [35]. Therefore, different DO modes always contain different frequency-phase content at the same spatial locations. In what follows we will prove that the transfer of energy from the mean flow to the DO modes occurs through a linear mechanism and is triggered by linear instability of the mean flow. This causes transfer of energy content from the mean flow to the DO modes in the form of variance.

On the other hand, flow of energy among different DO modes occurs both in a linear and a non-linear way and is exclusively connected with the non-Gaussian statistics of the stochastic coefficients. As we will see, since different modes contain different frequency-phase content, the mutual interaction of the DO modes occurs in triads and it is not possible to specify the exact amount of energy transferred from one mode to another (we can only specify the total energy transferred from one mode to two others).

To illustrate these properties we consider a system that is not externally forced and which has homogeneous Dirichlet boundary conditions everywhere. More specifically, we

consider the system

$$\frac{\partial \mathbf{u}}{\partial t} = -\nabla p + \frac{1}{\text{Re}} \Delta \mathbf{u} - \mathbf{u} \cdot \nabla \mathbf{u} - f \hat{\mathbf{k}} \times \mathbf{u} \equiv \mathcal{L} [\mathbf{u}(\mathbf{x}, t; \omega)] \quad (5.9)$$

$$0 = \text{div } \mathbf{u} \quad (5.10)$$

$$\begin{aligned} \mathbf{u}(\xi, t; \omega) &= \mathbf{0}, & \xi \in \partial D \\ \mathbf{u}(\mathbf{x}, t_0; \omega) &= \mathbf{u}_0(\mathbf{x}; \omega), & \mathbf{x} \in D, \quad \omega \in \Omega \end{aligned} \quad (5.11)$$

5.5.1 Energy exchanges between the DO modes and the mean flow

To study the flow of energy among the mean flow and the DO modes we consider the DO equation for the stochastic coefficient $Y_i(t; \omega)$ since the fields $\mathbf{u}_i(\mathbf{x}, t)$ are normalized. We have, using Einstein notation

$$\begin{aligned} \frac{dY_i}{dt} &= \left\langle \frac{1}{\text{Re}} \Delta \mathbf{u}_m - \mathbf{u}_m \cdot \nabla \bar{\mathbf{u}} - \bar{\mathbf{u}} \cdot \nabla \mathbf{u}_m - f \hat{\mathbf{k}} \times \mathbf{u}_m, \mathbf{u}_i \right\rangle Y_m \\ &\quad - \frac{1}{2} \langle \mathbf{u}_m \cdot \nabla \mathbf{u}_n + \mathbf{u}_n \cdot \nabla \mathbf{u}_m, \mathbf{u}_i \rangle (Y_m Y_n - \mathbf{C}_{Y_m(t)Y_n(t)}) \end{aligned}$$

We assume that at the current time instant the correlation matrix $\mathbf{C}_{Y_m(t)Y_n(t)}$ is diagonalized (in this way we have energy on the diagonal components only) and we wish to study the transfer of energy from the mean flow to the mode i . Multiplying with Y_i and applying the mean value operator we obtain

$$\begin{aligned} \frac{1}{2} \frac{d}{dt} E^\omega [Y_i^2] &= \left\langle \frac{1}{\text{Re}} \Delta \mathbf{u}_i - \mathbf{u}_i \cdot \nabla \bar{\mathbf{u}} - \bar{\mathbf{u}} \cdot \nabla \mathbf{u}_i - f \hat{\mathbf{k}} \times \mathbf{u}_i, \mathbf{u}_i \right\rangle E^\omega [Y_i^2] \\ &\quad - \frac{1}{2} \langle \mathbf{u}_m \cdot \nabla \mathbf{u}_n + \mathbf{u}_n \cdot \nabla \mathbf{u}_m, \mathbf{u}_i \rangle E^\omega [Y_i Y_m Y_n] \end{aligned}$$

We have

$$\langle \bar{\mathbf{u}} \cdot \nabla \mathbf{u}_i, \mathbf{u}_i \rangle = \langle \bar{\mathbf{u}}, \nabla \mathcal{E}_i \rangle = 0 \quad (5.12)$$

where $\mathcal{E}_i = \frac{1}{2} \langle \mathbf{u}_i, \mathbf{u}_i \rangle$ and the last equation follows from Gauss identity and the chosen boundary conditions. Additionally we have

$$\langle f \hat{\mathbf{k}} \times \mathbf{u}_i, \mathbf{u}_i \rangle = 0$$

and from Gauss theorem and the chosen boundary conditions

$$\langle \Delta \mathbf{u}_i, \mathbf{u}_i \rangle = -\langle \nabla \mathbf{u}_i, \nabla \mathbf{u}_i \rangle.$$

Finally, we observe that

$$\langle \mathbf{u}_i \cdot \nabla \bar{\mathbf{u}}, \mathbf{u}_i \rangle = \int_D \mathbf{u}_i^T \mathbf{S}_{\bar{\mathbf{u}}} \mathbf{u}_i d\mathbf{x}$$

where $\{\mathbf{S}_{\bar{\mathbf{u}}}\}_{ij} = \frac{1}{2} \left(\frac{\partial \bar{u}_i}{\partial x_j} + \frac{\partial \bar{u}_j}{\partial x_i} \right)$. Hence, we will have

$$\begin{aligned} \frac{1}{2} \frac{d}{dt} E^\omega [Y_i^2] &= \left[-\frac{1}{\text{Re}} \langle \nabla \mathbf{u}_i, \nabla \mathbf{u}_i \rangle - \int_D \mathbf{u}_i^T \mathbf{S}_{\bar{\mathbf{u}}} \mathbf{u}_i dx \right] E^\omega [Y_i^2] \\ &\quad - \frac{1}{2} \langle \mathbf{u}_m \cdot \nabla \mathbf{u}_n + \mathbf{u}_n \cdot \nabla \mathbf{u}_m, \mathbf{u}_i \rangle E^\omega [Y_i Y_m Y_n] \end{aligned} \quad (5.13)$$

We observe that energy transfer between the stochastic mode i and the mean flow occurs in a linear way although the terms in the original equation which are responsible for this energy transfer are the nonlinear ones (it is the quadratic terms in Navier-Stokes that lead to the term $\mathbf{u}_i^T \mathbf{S}_{\bar{\mathbf{u}}} \mathbf{u}_i$ in equation (5.13)). Hence we have for the viscous dissipation

$$\varepsilon_{diss,i} = -\frac{1}{\text{Re}} E^\omega [Y_i^2] \langle \nabla \mathbf{u}_i, \nabla \mathbf{u}_i \rangle$$

and the rate of energy transferred to or from the mean flow to mode i in the form of stochastic energy (variance)

$$\varepsilon_{mean \rightarrow i} = -E^\omega [Y_i^2] \int_D \mathbf{u}_i^T \mathbf{S}_{\bar{\mathbf{u}}} \mathbf{u}_i dx.$$

We note that for small energy amplitudes $E^\omega [Y_i^2]$ (so that terms of $\mathcal{O}(Y^3)$ can be omitted) these two terms are those that mainly characterize the total energy variation of the mode \mathbf{u}_i , i.e. the total rate of energy change is given by

$$\begin{aligned} \varepsilon_{linear,i} &\equiv \varepsilon_{diss,i} + \varepsilon_{mean \rightarrow i} \\ &= - \left(\frac{1}{\text{Re}} \langle \nabla \mathbf{u}_i, \nabla \mathbf{u}_i \rangle + \int_D \mathbf{u}_i^T \mathbf{S}_{\bar{\mathbf{u}}} \mathbf{u}_i dx \right) E^\omega [Y_i^2] \end{aligned}$$

This is exactly the quantity that we maximize in order to choose the most unstable mode for the adaptation process described in Chapter 4 and in the previous section. Note that in this case the added mode has very small amplitude so the hypothesis that terms of $\mathcal{O}(Y^3)$ can be neglected is justified. We note that for the case where stochasticity is introduced only through the initial conditions, uncertainties are always reduced by the diffusion, but are either amplified or tapered by the nonlinear stretching of the mean flow.

5.5.2 Energy exchanges between the DO modes

To study energy exchanges among various modes we consider equation (5.13) derived in the previous subsection. By inspection, we observe that the rate of energy transferred to mode i from all the DO modes is given by

$$\varepsilon_{DO \rightarrow i} = -\frac{1}{2} \langle \mathbf{u}_m \cdot \nabla \mathbf{u}_n + \mathbf{u}_n \cdot \nabla \mathbf{u}_m, \mathbf{u}_i \rangle E^\omega [Y_i Y_m Y_n].$$

As it can be clearly seen the transfer of energy among different DO modes depends on the non-Gaussian characteristics of the probability measure and for the Gaussian case it vanishes (for Gaussian variables we always have $E^\omega [Y_i Y_m Y_n] = 0$). Note that the $m = n = i$

term vanishes (since the covariance operator is diagonal) so we have two remaining cases.

The first case where we have energy transferred directly from mode q to a different mode i (cases $m = q, n = i$, or $m = i, n = q$, or $n = m = q$). For that case, summing all non-zero contributions, we have the rate of energy transferred directly from mode q to mode i

$$\begin{aligned}
\varepsilon_{q \rightarrow i} &= -\langle \mathbf{u}_q \cdot \nabla \mathbf{u}_i + \mathbf{u}_i \cdot \nabla \mathbf{u}_q, \mathbf{u}_i \rangle E^\omega [Y_i^2 Y_q] - \frac{1}{2} \langle \mathbf{u}_q \cdot \nabla \mathbf{u}_q + \mathbf{u}_q \cdot \nabla \mathbf{u}_q, \mathbf{u}_i \rangle E^\omega [Y_q^2 Y_i] \\
&= -(\langle \mathbf{u}_i \cdot \nabla \mathbf{u}_q, \mathbf{u}_i \rangle + \langle \mathbf{u}_q \cdot \nabla \mathbf{u}_i, \mathbf{u}_i \rangle) E^\omega [Y_i^2 Y_q] - \langle \mathbf{u}_q \cdot \nabla \mathbf{u}_q, \mathbf{u}_i \rangle E^\omega [Y_q^2 Y_i] \\
&= -2 \left(\langle \mathbf{u}_i \cdot \nabla \mathbf{u}_q, \mathbf{u}_i \rangle + \frac{1}{2} \langle \mathbf{u}_q \cdot \nabla |\mathbf{u}_i|^2 \rangle \right) E^\omega [Y_i^2 Y_q] - \langle \mathbf{u}_q \cdot \nabla \mathbf{u}_q, \mathbf{u}_i \rangle E^\omega [Y_q^2 Y_i] \\
&= -\langle \mathbf{u}_i \cdot \nabla \mathbf{u}_q, \mathbf{u}_i \rangle E^\omega [Y_i^2 Y_q] + \langle \mathbf{u}_q \cdot \nabla \mathbf{u}_i, \mathbf{u}_q \rangle E^\omega [Y_q^2 Y_i] \\
&= -E^\omega [Y_i^2 Y_q] \int_D \mathbf{u}_i^T \mathbf{S}_{\mathbf{u}_q} \mathbf{u}_i d\mathbf{x} + E^\omega [Y_q^2 Y_i] \int_D \mathbf{u}_q^T \mathbf{S}_{\mathbf{u}_i} \mathbf{u}_q d\mathbf{x}.
\end{aligned}$$

In the above, we have used the equality $\langle \mathbf{u}_q \cdot \nabla \mathbf{u}_q, \mathbf{u}_i \rangle = -\langle \mathbf{u}_q \cdot \nabla \mathbf{u}_i, \mathbf{u}_q \rangle$ which follows from direct application of Gauss identity.

The remaining second case occurs when the energy transferred to mode i is due to its triple interaction with every other pair of DO modes. The rate of energy transfer due to this triple interaction with modes p and q has the form

$$\begin{aligned}
\varepsilon_{pq \rightarrow i} &= -\frac{1}{2} \langle \mathbf{u}_p \cdot \nabla \mathbf{u}_q + \mathbf{u}_q \cdot \nabla \mathbf{u}_p, \mathbf{u}_i \rangle E^\omega [Y_i Y_p Y_q] \\
&= \frac{1}{2} (\langle \mathbf{u}_q \cdot \nabla \mathbf{u}_p, \mathbf{u}_i \rangle + \langle \mathbf{u}_p \cdot \nabla \mathbf{u}_q, \mathbf{u}_i \rangle) E^\omega [Y_i Y_p Y_q] \\
&= \frac{1}{2} (\langle \mathbf{u}_q \cdot \nabla \mathbf{u}_i, \mathbf{u}_p \rangle + \langle \mathbf{u}_p \cdot \nabla \mathbf{u}_i, \mathbf{u}_q \rangle) E^\omega [Y_i Y_p Y_q] \\
&= \frac{1}{2} \left(\int_D \mathbf{u}_q^T \mathbf{S}_{\mathbf{u}_i} \mathbf{u}_p d\mathbf{x} + \int_D \mathbf{u}_p^T \mathbf{S}_{\mathbf{u}_i} \mathbf{u}_q d\mathbf{x} \right) E^\omega [Y_i Y_p Y_q] \\
&= \int_D \mathbf{u}_q^T \mathbf{S}_{\mathbf{u}_i} \mathbf{u}_p d\mathbf{x} E^\omega [Y_i Y_p Y_q].
\end{aligned}$$

5.5.3 Stochastic energy in Navier-Stokes

In the last two subsections we derived expressions characterizing the transform of energy to uncertainty (flow of energy from the mean to the modes) but also the variance exchange between the modes. Motivated by these results we define the following form of stochastic energy where energy of the mean and variance of the modes are considered in a unified way

$$\begin{aligned}
\mathcal{E}_S &= \frac{1}{2} E^\omega [\langle \mathbf{u}, \mathbf{u} \rangle] = \frac{1}{2} E^\omega [\langle \bar{\mathbf{u}} + Y_i \mathbf{u}_i, \bar{\mathbf{u}} + Y_i \mathbf{u}_i \rangle] \\
&= \frac{1}{2} \left(\|\bar{\mathbf{u}}\|^2 + \sum_{i=1}^s E^\omega [Y_i^2] \right).
\end{aligned}$$

The next step is to study the evolution of the above quantity. We have using the DO equations

$$\begin{aligned}
\frac{d\mathcal{E}_S}{dt} &= E^\omega [\langle \bar{\mathbf{u}}, \bar{\mathbf{u}}_t \rangle] + E^\omega \left[Y_i \frac{dY_i}{dt} \right] \\
&= E^\omega [\langle \bar{\mathbf{u}}, E^\omega [\mathcal{L}] \rangle] + E^\omega [Y_i \langle \mathcal{L} - E^\omega [\mathcal{L}], \mathbf{u}_i \rangle] \\
&= E^\omega [\langle \bar{\mathbf{u}}, E^\omega [\mathcal{L}] \rangle] + E^\omega [Y_i \langle \mathcal{L}, \mathbf{u}_i \rangle] \\
&= E^\omega [\langle \mathcal{L}, \bar{\mathbf{u}} \rangle] + E^\omega [\langle \mathcal{L}, Y_i \mathbf{u}_i \rangle] \\
&= E^\omega [\langle \mathcal{L}, \bar{\mathbf{u}} + Y_i \mathbf{u}_i \rangle] \\
&= E^\omega [\langle \mathcal{L}, \mathbf{u} \rangle]
\end{aligned}$$

Now, by directly computing the above quantity using Gauss identity (and equation (5.9)) we obtain

$$\begin{aligned}
\frac{d\mathcal{E}_S}{dt} &= E^\omega [\langle \mathcal{L}, \mathbf{u} \rangle] = E^\omega \left[\left\langle \frac{1}{\text{Re}} \Delta \mathbf{u}, \mathbf{u} \right\rangle \right] \\
&= -\frac{1}{\text{Re}} E^\omega [\langle \nabla \mathbf{u}, \nabla \mathbf{u} \rangle] \\
&= -\frac{1}{\text{Re}} (\langle \nabla \bar{\mathbf{u}}, \nabla \bar{\mathbf{u}} \rangle + E^\omega [Y_i^2] \langle \nabla \mathbf{u}_i, \nabla \mathbf{u}_i \rangle) \\
&= -\frac{1}{\text{Re}} \left(\|\nabla \bar{\mathbf{u}}\|^2 + E^\omega [Y_i^2] \|\nabla \mathbf{u}_i\|^2 \right)
\end{aligned}$$

Thus, the stochastic energy for homogeneous Navier-Stokes is dissipated due to viscosity in full analogy with the usual notion of energy for deterministic Navier-Stokes. All the other forms of energy transfer from the mean flow to the DO modes and among the DO modes are internal system interactions.

A summary of all the energy transfers is given in Figure 5-1 where the internal interactions among the DO modes (green and blue arrows) are shown. The black arrows show the energy exchanges between the mean flow and the modes. Finally, the red arrows represent the energy dissipation due to viscosity acting on both the mean flow and the DO modes.

5.6 Application I: Lid driven cavity flow with stochastic initial conditions

As a first application we present the results of the DO field equations applied to the numerical simulation of a lid-driven cavity flow described by the Navier-Stokes equations in a square domain. The stochasticity is introduced through the initial conditions. The physical configuration (Figure 5-2) consists of a square container filled with a fluid. The lid of the container moves at a given, constant velocity, thereby setting the fluid in motion. No-slip conditions are imposed on all four segments of the boundary with the exception of the upper boundary, along which the velocity u in the x -direction is set equal to the given lid velocity u_b to simulate the moving lid. The length of each side is $L = 1$ and the Reynolds number of the flow is taken to be $\text{Re} = 1000$. For the stochastic computation the lid velocity is taken to be $u_b = 1.5$ while in the DO expansion (3.10) we retain 5 modes which is equal to the stochastic dimension of the initial conditions. The flow fields associated with the initial conditions $u_0(\mathbf{x}; \omega)$ are shown in Figure 5-3 in terms of the streamfunction.

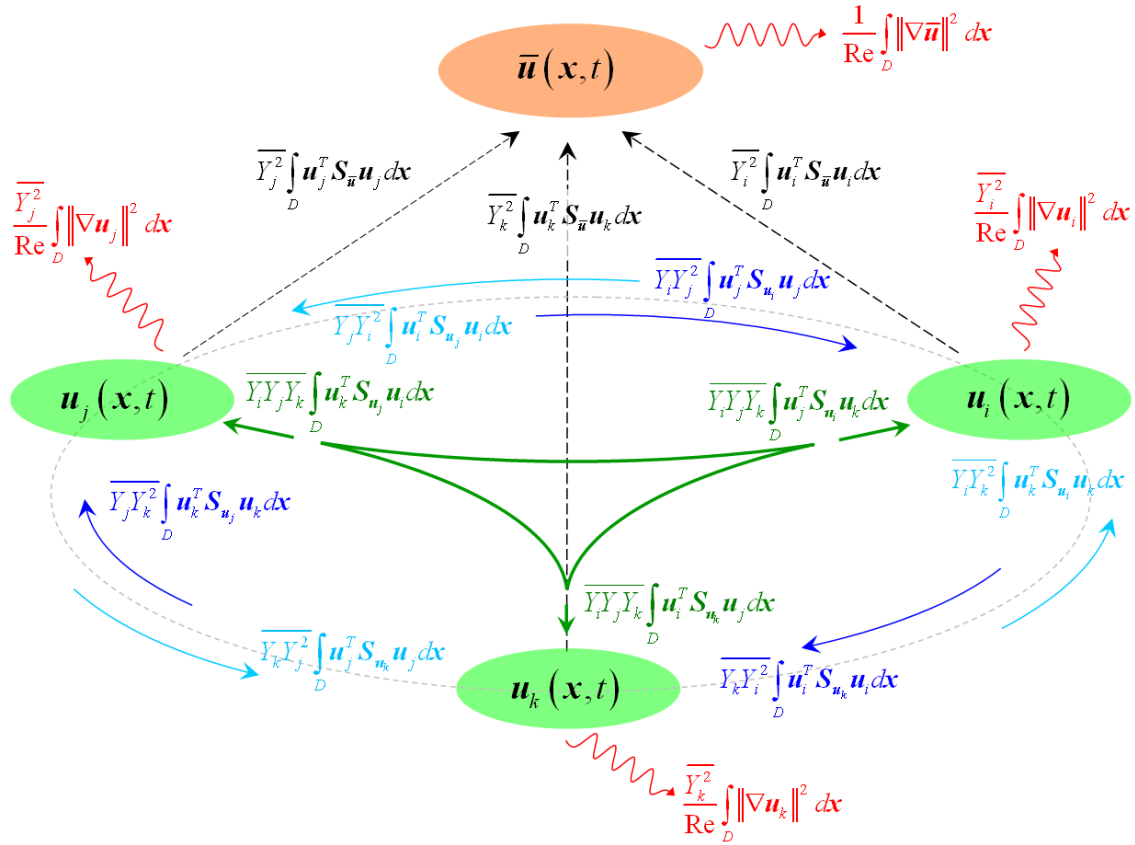


Figure 5-1: Energy exchanges between DO modes and the mean flow in stochastic, homogeneous, Navier-Stokes equations. The energy flow from the mean to the modes is characterized by the second order statistics while variance exchange among the modes is characterized by the third order statistics.

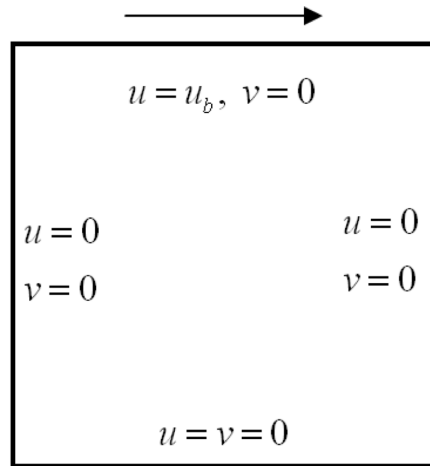


Figure 5-2: Driven cavity flow, problem configuration.

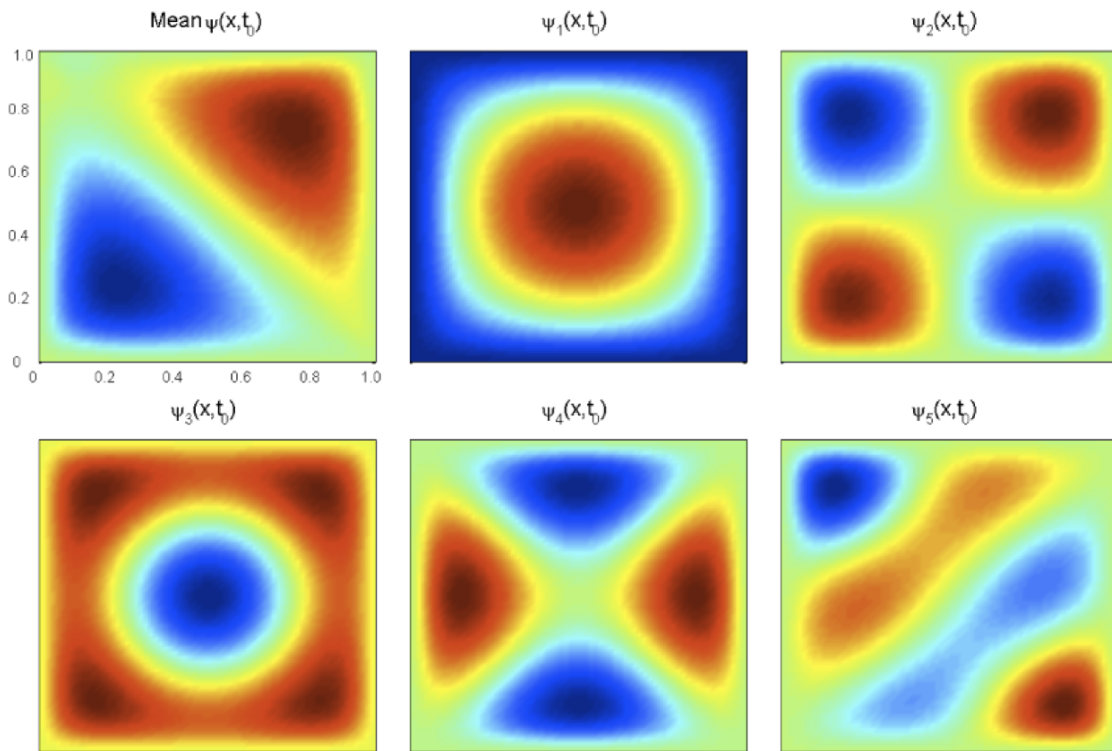


Figure 5-3: Initial conditions for the mean and the basis of the stochastic subspace V_S in terms of the field streamfunction.

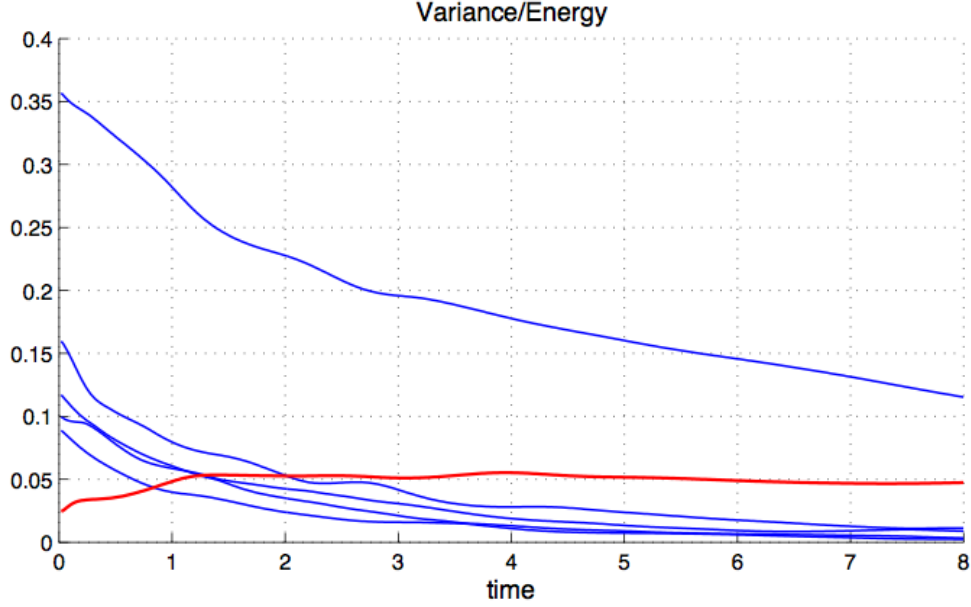


Figure 5-4: Evolution of principal variances $\sigma_i^2(t)$, $i = 1, \dots, 5$ (blue curves) and mean field energy (red curve) for the flow in a cavity.

By evolving all parameters of the system using the DO field equations we compute the complete 5-dimensional probabilistic structure of the stochasticity inside V_S . In Figure 5-4 we show the evolution of the principal variances $\sigma_i^2(t)$, $i = 1, \dots, 5$ which are the eigenvalues of the correlation operator $\mathbf{C}_{Y_i(t)Y_j(t)}$ (blue solid curves). They provide a direct measure of how the stochastic energy evolves with time. The red solid curve is associated with the deterministic kinetic energy of the mean flow field, i.e. the quantity $\langle \bar{u}(\bullet, t), \bar{u}(\bullet, t) \rangle$. We observe that the stochastic energy decays almost monotonically after some initial transient interactions, while the energy of the mean field slowly grows towards a steady limit. This is an expected behavior if we consider the fact that the deterministic cavity flow possess a stable attractor which is characterized by a steady velocity field. Therefore, in the absence of external stochastic excitation it is fully expected to have convergence of the system to this deterministic, one-dimensional attractor. The mean fields $\bar{\mathbf{u}}(\mathbf{x}, t)$ and orthonormal basis fields $\mathbf{u}_i(\mathbf{x}, t)$, $i = 1, \dots, 5$ are shown in Figure 5-5 and 5-6 for two different time instances both in terms of the streamfunction and vorticity. For the same time instances we present three out of the five two-dimensional marginals associated with the stochastic processes $\{Y_j(t; \omega)\}_{j=1}^5$.

Finally, in Figure 5-7 we compare the mean streamfunction computed using the 5-modes DO method with the one obtained by Monte-Carlo simulation initialized with the ESSE methodology and using 250 and 500 samples. We observe that as we increase the number of samples used for the Monte Carlo simulation we obtain better agreement with the DO mean estimate.

5.6.1 Evolution of a small stochastic perturbation

In this subsection we will study the convergence properties of the DO methodology for the lid driven cavity flow. The first feature that we want to examine is sensitivity of the flow

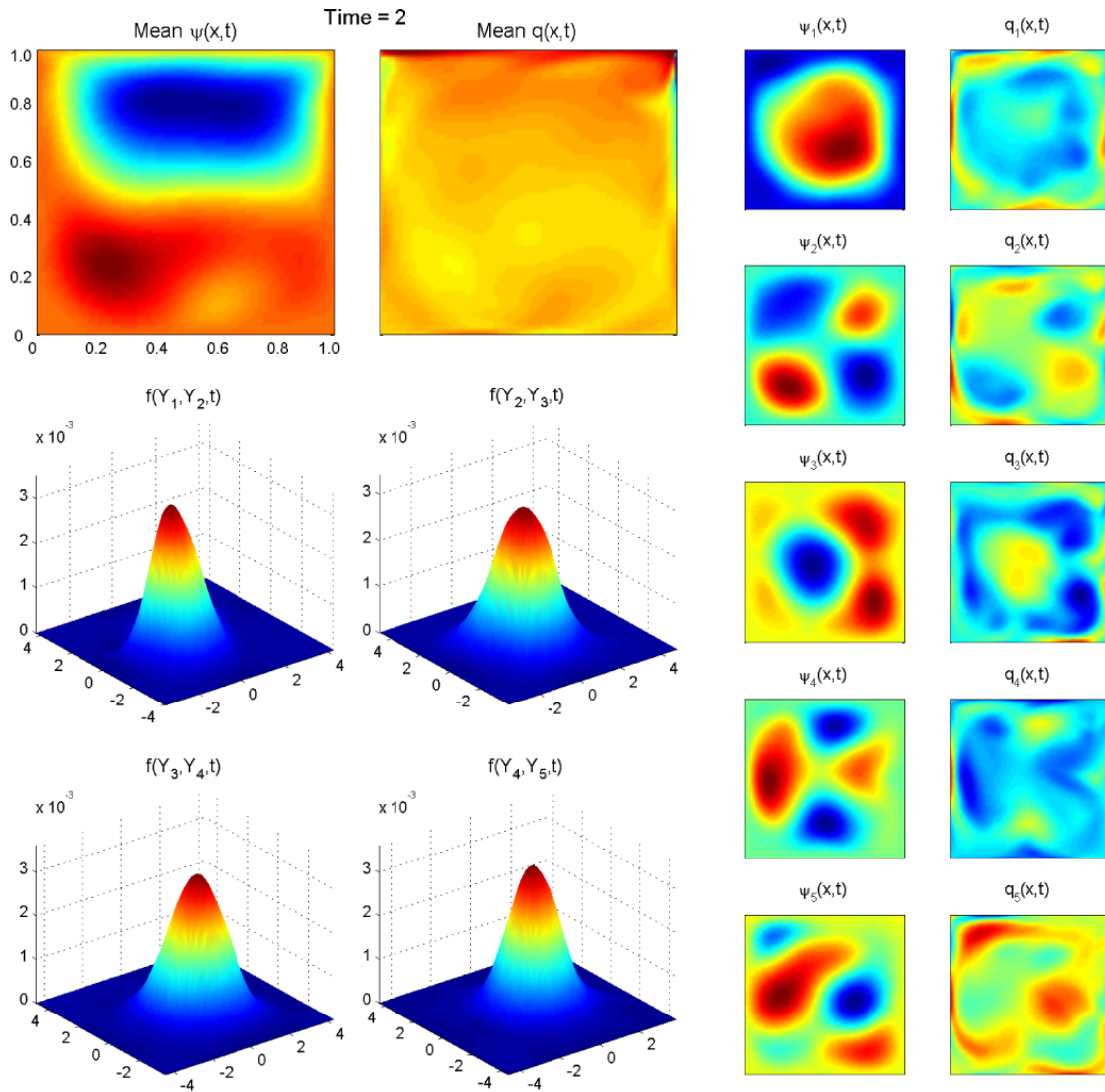


Figure 5-5: Mean field and basis of the stochastic subspace V_S in terms of the streamfunction and vorticity field; two-dimensional marginals of the five dimensional joint pdf $f(\mathbf{y}, t)$ at time $t = 2$.

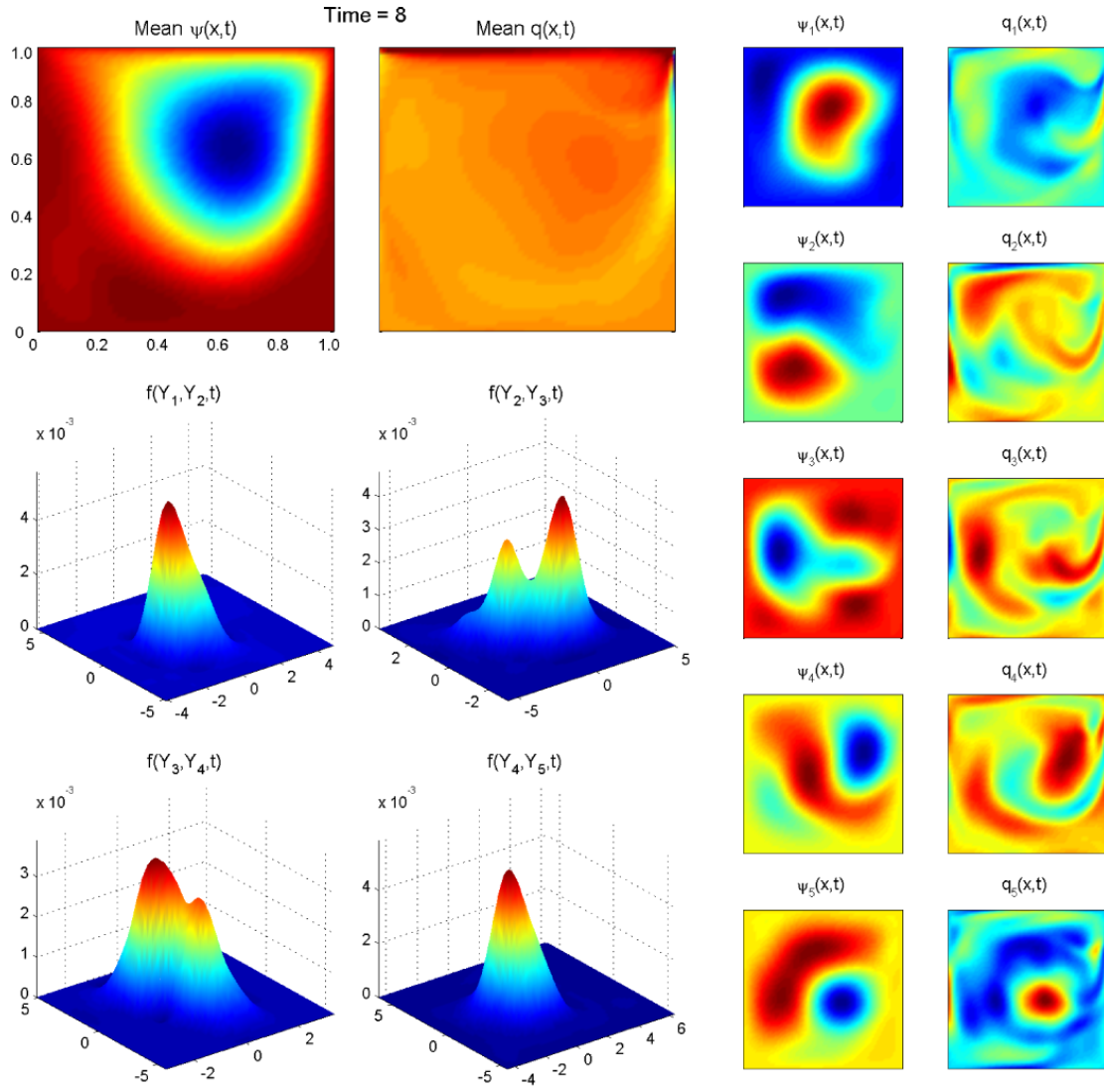


Figure 5-6: Mean field and basis of the stochastic subspace V_S in terms of the streamfunction and vorticity field; two-dimensional marginals of the five dimensional joint pdf $f(\mathbf{y}, t)$ at time $t = 8$.

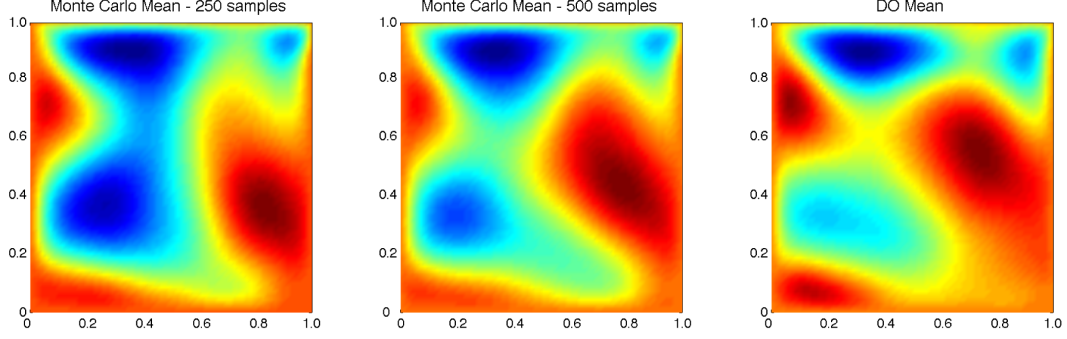


Figure 5-7: Mean velocity field (streamfunction) computed using Monte-Carlo method (250 and 500 samples) and the DO field equations ($s = 5$ modes) at $t = 1$.

in the addition of an extra stochastic mode having very small variance. In general the variance growth of an initially low-amplitude stochastic perturbation will depend on the stability properties of the dynamical system (as we saw in Chapter 4). For the lid-driven cavity flow there is a stable attractor where dynamics tend to converge after sufficiently large time. However, during the initial phase we have strong interactions between the DO modes and the mean flow.

We initiate the system with four stochastic modes in the first case and with the same four stochastic modes in the second case plus one extra that has variance $\sigma_5^2(t_0) = 10^{-6}$, i.e. much smaller than the stochasticity contained in the first four modes. We denote the first solution as $\mathbf{u}(\mathbf{x}, t; \omega) = \bar{\mathbf{u}}(\mathbf{x}, t) + Y_i(t; \omega) \mathbf{u}_i(\mathbf{x}, t)$ and the second solution as $\mathbf{v}(\mathbf{x}, t; \omega) = \bar{\mathbf{v}}(\mathbf{x}, t) + \Psi_i(t; \omega) \mathbf{v}_i(\mathbf{x}, t)$. After solving the corresponding set of DO equations for the two cases we project the stochastic solution $\mathbf{u}(\mathbf{x}, t; \omega)$ obtained with the four modes to the stochastic subspace computed in the second case using five modes. The results are shown for two different time instants in Figures 5-8 and 5-9. Specifically, the two upper plots represent the streamfunction of the mean flow for the case of four modes ($\psi_1(\mathbf{x}, t)$) and for the case of five modes ($\psi_2(\mathbf{x}, t)$). The red curves shown in the lower plot represent the time series for the variances $\sigma_i^2(t)$, $i = 1, \dots, 5$ of the five-modes solution $\mathbf{v}(\mathbf{x}, t; \omega)$. The blue curves represent the variance of the projection of the four-modes stochastic solution $\mathbf{u}(\mathbf{x}, t; \omega)$ to the stochastic subspace computed using the five modes solution, i.e. $\sigma_i^2(t) = \text{var}[\langle \mathbf{u}(\mathbf{x}, t; \omega), \mathbf{v}_i(\mathbf{x}, t) \rangle]$, $i = 1, \dots, 5$.

As we can observe the two sets of curves start initially very close having a very small difference due to initialization error (different Monte-Carlo samples). After time $t = 0.2$ the red curve describing the variance of the fifth mode for the solution $\mathbf{u}(\mathbf{x}, t; \omega)$ starts to grow due to an internal instability that causes transfer of energy from the mean flow to the stochastic perturbation (Figure 5-8). However, the mean flows for the two cases still compare satisfactory since the difference on the stochastic part of the solution is very small.

For larger times $t \sim 1 - 2$ the variance of the fifth stochastic mode (lower red curve) has increased more drastically causing an energy deviation for the other variance curves of the same order of magnitude (see Figure 5-9 e.g. the higher variance mode: red and blue curve). In this case, even though the topology of the mean flow remain the same there are some small differences caused by the different energy or variance distribution among the stochastic modes.

Therefore, we may conclude that the total error magnitude between the two stochastic solutions depends on the magnitude of the neglected part in the KL expansion. Depending on the stability properties of the fluid flow, the energy or the variance of a small perturbation may grow. However, the analytical criteria developed in Chapter 4 may be used to make sure that for every time instant the neglected part of the stochastic solution is smaller than an a priori chosen tolerance. This guarantees that our stochastic solution will have a given accuracy using the least number of stochastic modes at every time instant. These criteria will be illustrated in the third application involving an unstable double gyre flow which is initiated with deterministic initial conditions.

5.6.2 Convergence with respect to the stochastic dimensionality

We will now study the convergence properties of the stochastic solution with respect to the number of used modes. We use the same configuration as previously but with only one initial stochastic mode having important variance. Then we solve the DO equations each time using different number of modes (the extra modes are initiated using very small variance relative to the variance of the first mode). In Figures 5-10, 5-11, and 5-12 we present the mean flow for three time instants over different stochastic dimensionalities, $\dim(\mathbf{V}_S)$. We note that the general topological features of the fluid flow are common even for the case of very low dimensional stochastic subspace. However, for longer times a good degree of convergence is obtained using larger number of modes (see Figure 5-12).

In Figures 5-13, 5-14, and 5-15 we present the convergence properties of the stochastic subspace \mathbf{V}_S . Specifically, we show the four most energetic modes $\mathbf{u}_i(\mathbf{x}, t)$ and their associated variance $E^\omega [Y_i^2(t; \omega)]$ for different stochastic subspace dimensionalities. An interesting observation is that the robustness of the modes $\mathbf{u}_i(\mathbf{x}, t)$ is strongly related with the magnitude of their variance. Therefore the first mode that corresponds to the largest variance seems to converge much faster than the modes that correspond to lower magnitude of variance. The same observation can be made for the time series for the variances, $E^\omega [Y_i^2(t; \omega)]$. Specifically, the time series describing modes with larger variance seem to be more robust with respect to the stochastic dimensionality of the solution. These results are in agreement with those obtained with ESSE (e.g. [74], [75], [76]).

Finally, in Figure 5-16 we present two forms of error with respect to the number of used modes. The upper plot shows the instantaneous mean square error between the solution $\mathbf{u}_{\dim V_s}(\mathbf{x}, t; \omega)$ that utilizes s stochastic modes and the solution $\mathbf{u}_{12}(\mathbf{x}, t; \omega)$ that utilizes 12 stochastic modes. Therefore we have in the upper plot the time dependent norm

$$\|\mathbf{u}_{\dim V_s} - \mathbf{u}_{12}\|_t^2 = E^\omega [\langle \mathbf{u}_{\dim V_s}(\mathbf{x}, t; \omega) - \mathbf{u}_{12}(\mathbf{x}, t; \omega), \mathbf{u}_{\dim V_s}(\mathbf{x}, t; \omega) - \mathbf{u}_{12}(\mathbf{x}, t; \omega) \rangle]$$

and in the lower plot the global error

$$\|\mathbf{u}_{\dim V_s} - \mathbf{u}_{12}\|^2 = \frac{1}{T} \int_T \|\mathbf{u}_{\dim V_s} - \mathbf{u}_{12}\|_t^2 dt.$$

As we are able to observe the instantaneous error becomes maximum during the time interval $1 < t < 5$ where all the transient dynamics take place. Subsequently the flow begins to reach the steady state attractor and the error decays. In the lower plot we observe the convergence of the solution with respect to the number of modes. We note that after the stochastic subspace exceeds $\dim \mathbf{V}_S = 9$ the error decays rapidly and remains in very low

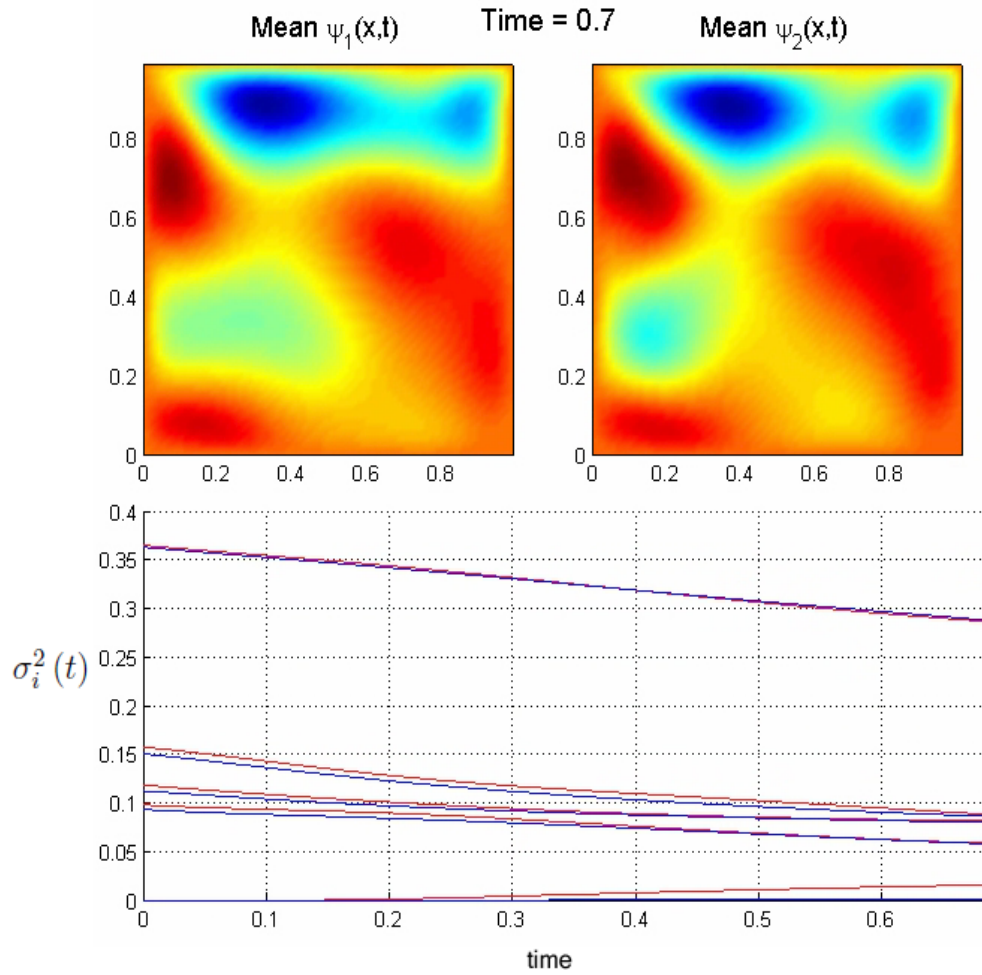


Figure 5-8: Upper plots: mean flow for $t = 0.7$ in terms of the streamfunction for i) the four modes solution and ii) the five modes solution. Lower plot: the red curves represent the time series for the variances $\sigma_i^2(t)$, $i = 1, \dots, 5$ of the five-modes solution $\mathbf{v}(\mathbf{x}, t; \omega)$ while the blue curves represent the projection of the four modes solution $\mathbf{u}(\mathbf{x}, t; \omega)$ to the modes $\mathbf{v}_i(\mathbf{x}, t)$.

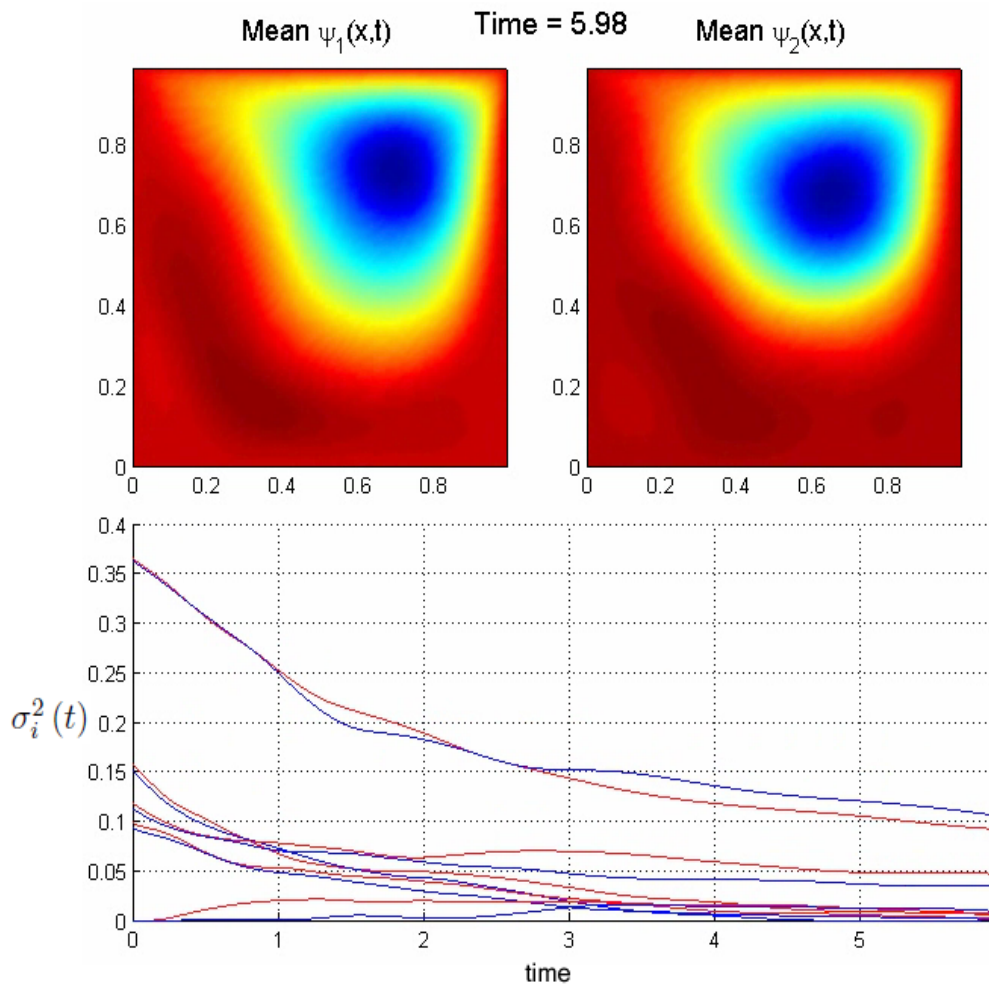


Figure 5-9: Upper plots: mean flow for $t = 5.98$ in terms of the streamfunction for i) the four modes solution and ii) the five modes solution. Lower plot: the red curves represent the time series for the variances $\sigma_i^2(t)$, $i = 1, \dots, 5$ of the five-modes solution $\mathbf{v}(\mathbf{x}, t; \omega)$ while the blue curves represent the projection of the four modes solution $\mathbf{u}(\mathbf{x}, t; \omega)$ to the modes $\mathbf{v}_i(\mathbf{x}, t)$.

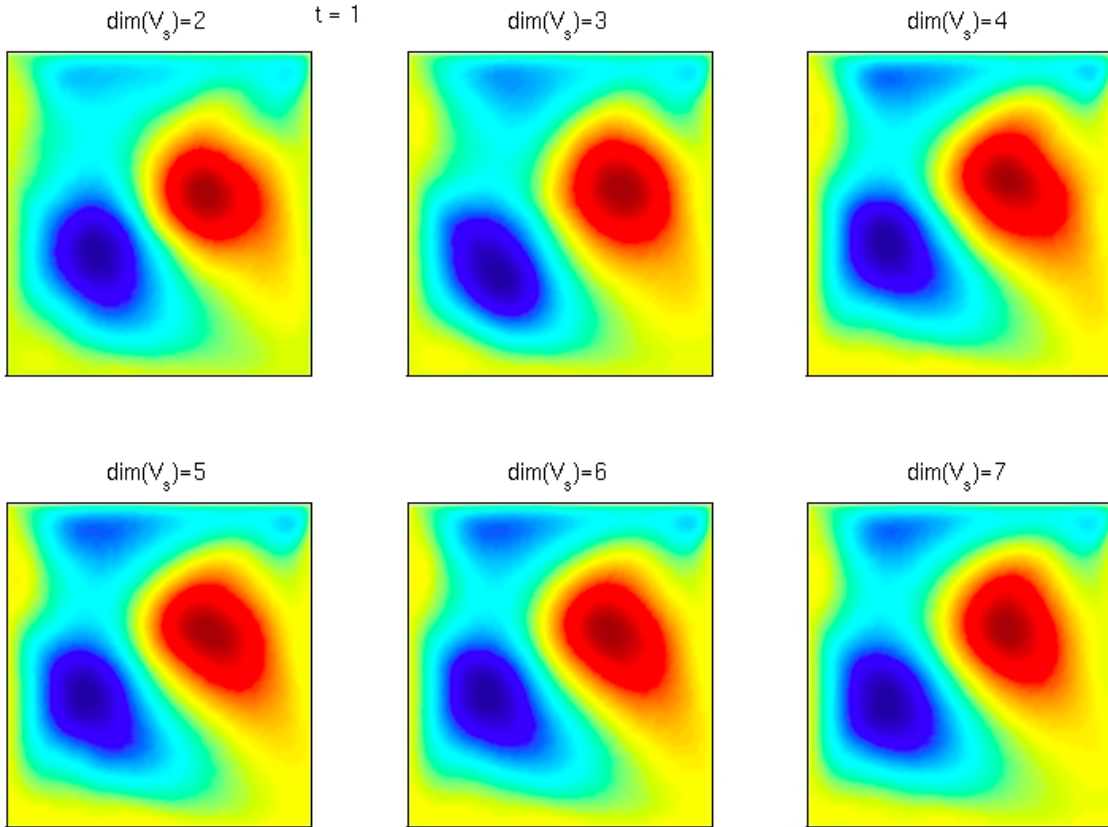


Figure 5-10: Mean flow for various stochastic dimensionalities and for $t = 1$.

levels; an indication that for this problem the stochastic dimensionality of the solution has finite dimension.

5.7 Application II: Flow past a circular disk with stochastic initial conditions

Here we consider the flow past a disk immersed in a channel. The inflow velocity at the left boundary has a parabolic profile with a maximum value $u = 1.5$; the disk measures $d = 1$ in diameter and is situated at a distance of 1.5 from the left and 1.6 from the upper boundary. It is well known that for two-dimensional flow past a circular cylinder, the first critical Reynolds number is around $Re \sim 40$, where the flow bifurcates from steady state to periodic vortex shedding [158]. Here, we consider the case of $Re = 100$. A typical realization for this case is shown in Figure 5-17. The stochastic initial conditions are described by the mean field and the stochastic subspace basis fields. They are all shown in terms of the streamfunction in Figure 5-18.

The principal variances $\sigma_i^2(t)$, $i = 1, \dots, 5$ (eigenvalues of $\mathbf{C}_{Y_i(t)Y_j(t)}$) (blue solid curves) and the kinetic energy of the mean flow field (red solid curve) are shown in Figure 5-19. In this case, we find a more complex evolution of the stochastic energy characterized by

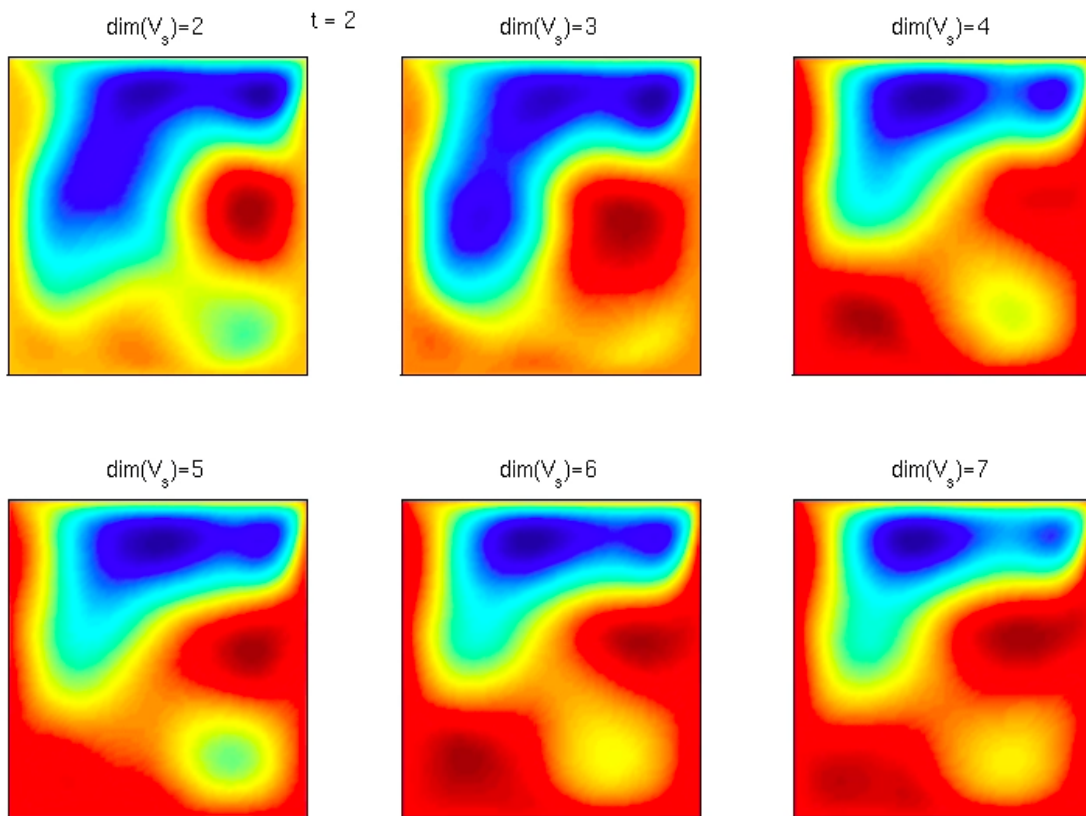


Figure 5-11: Mean flow for various stochastic dimensionalities and for $t = 2$.

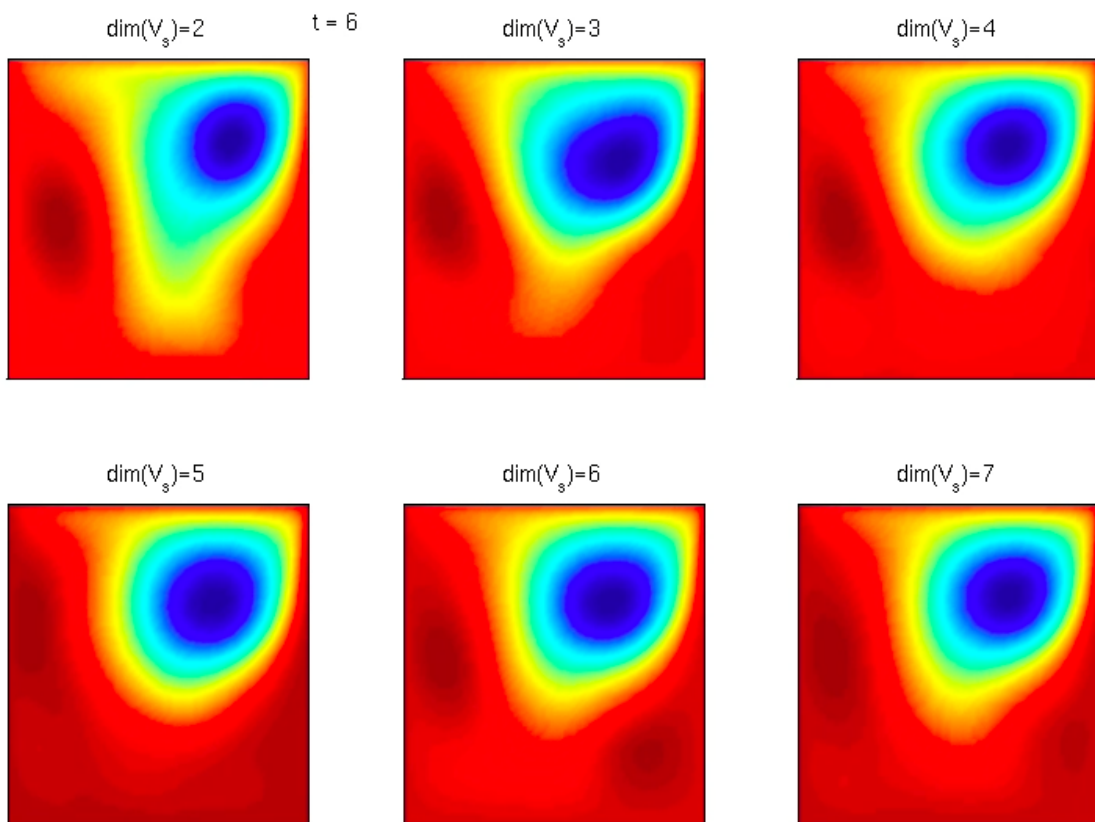


Figure 5-12: Mean flow for various stochastic dimensionalities and for $t = 6$.

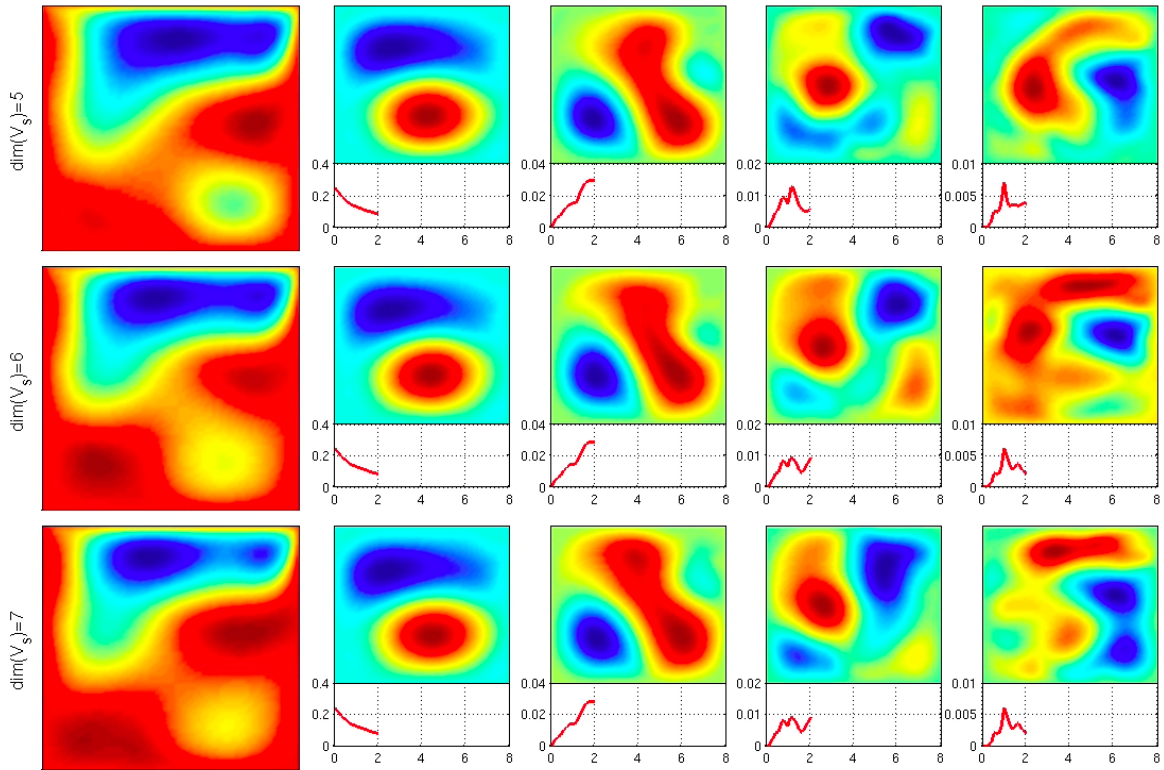


Figure 5-13: Left column: mean flow for various stochastic dimensionalities $\dim(\mathbf{V}_S)$ at $t = 2$. The four right columns on the right show the four most energetic modes $\mathbf{u}_i(\mathbf{x}, t)$ in terms of their streamfunction as well as their associated variance $E^\omega [Y_i^2(t; \omega)]$ as a function of time.

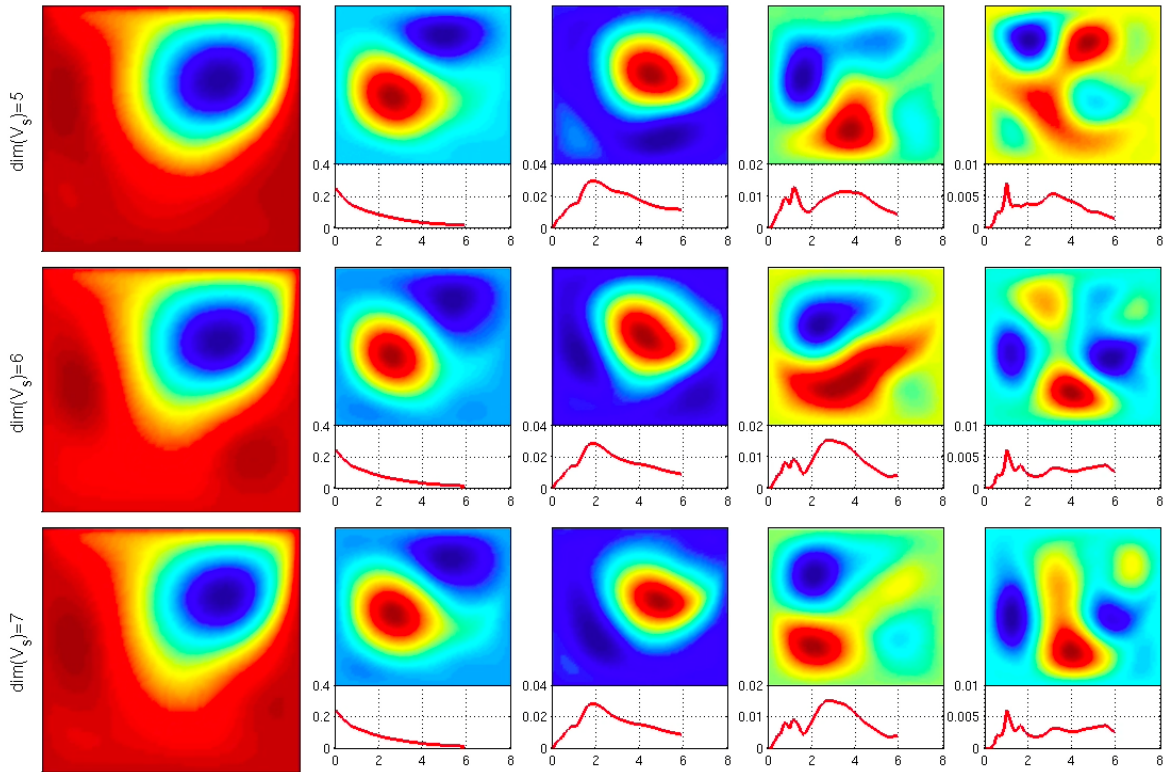


Figure 5-14: Left column: mean flow for various stochastic dimensionalities $\dim(\mathbf{V}_S)$ at $t = 6$. The four right columns on the right show the four most energetic modes $\mathbf{u}_i(\mathbf{x}, t)$ in terms of their streamfunction as well as their associated variance $E^\omega [Y_i^2(t; \omega)]$ as a function of time.

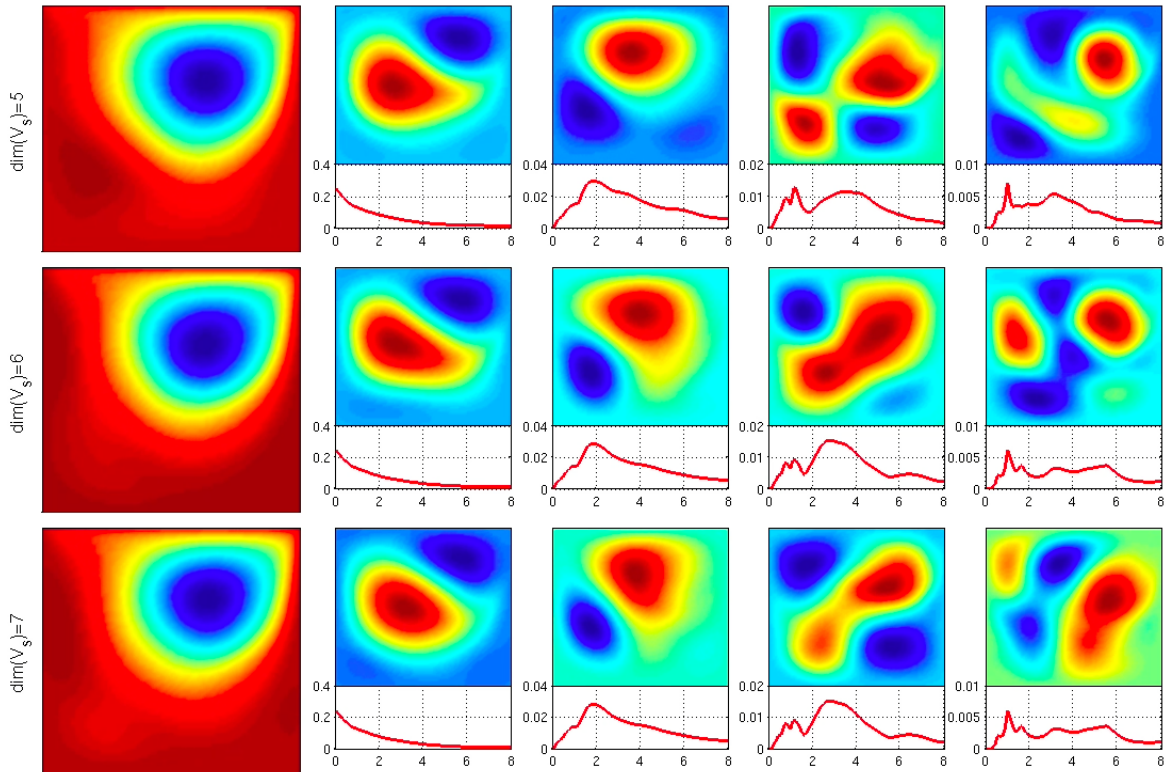


Figure 5-15: Left column: mean flow for various stochastic dimensionalities $\dim(\mathbf{V}_S)$ at $t = 8$. The four right columns on the right show the four most energetic modes $\mathbf{u}_i(\mathbf{x}, t)$ in terms of their streamfunction as well as their associated variance $E^\omega [Y_i^2(t; \omega)]$ as a function of time.

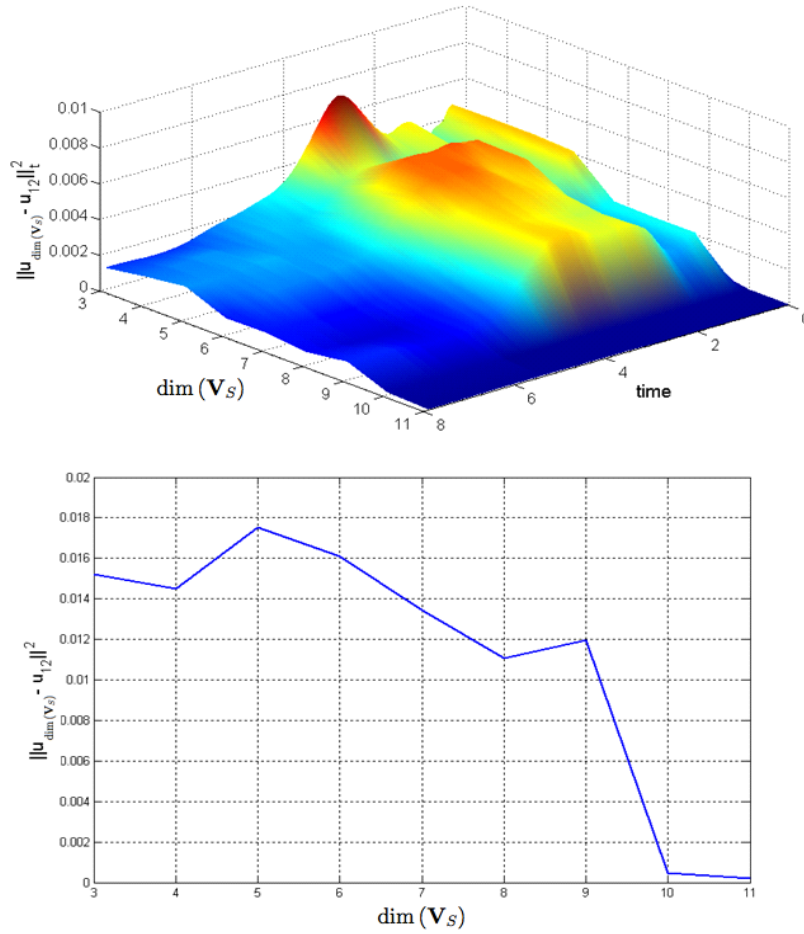


Figure 5-16: Upper plot: instantaneous error of the solution with respect to the number of modes used and time. Lower plot: time averaged error with respect to the number of DO modes.

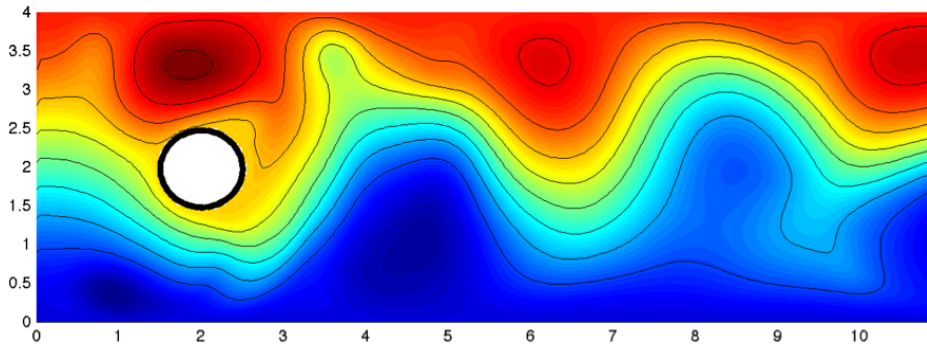


Figure 5-17: A typical realization of the flow past a circular disk.

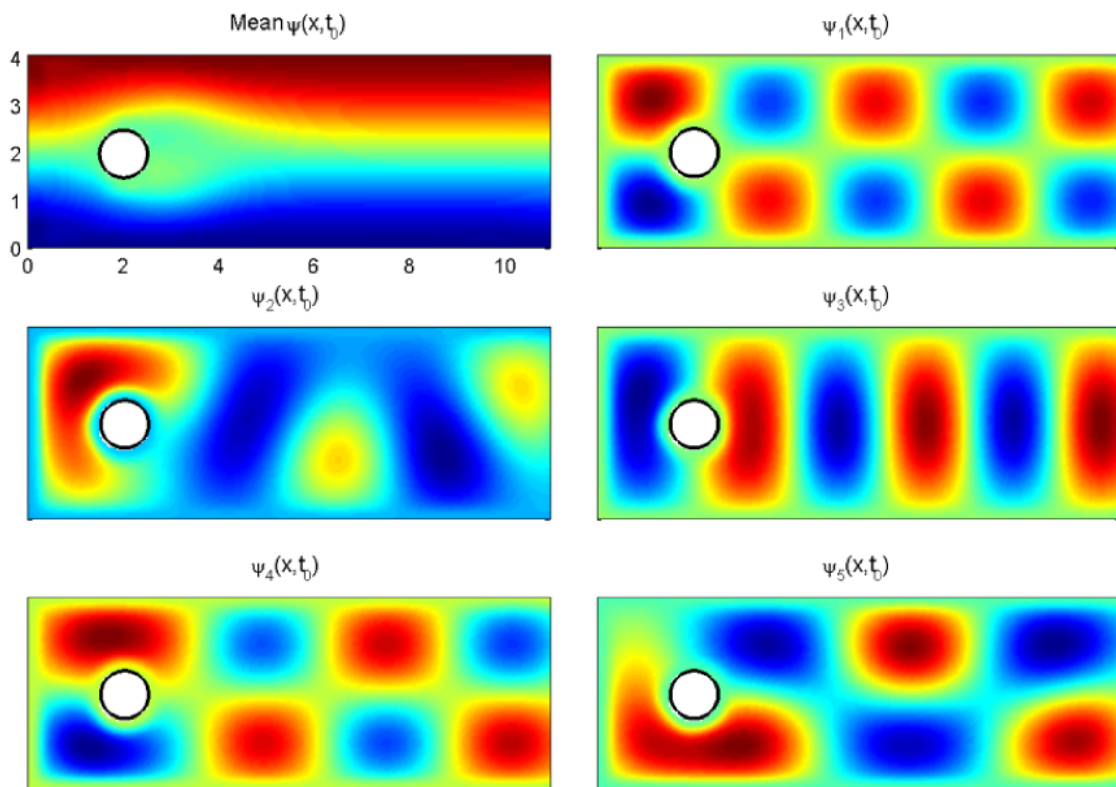


Figure 5-18: Initial conditions for the mean and the basis of the stochastic subspace V_S in terms of the field streamfunction.

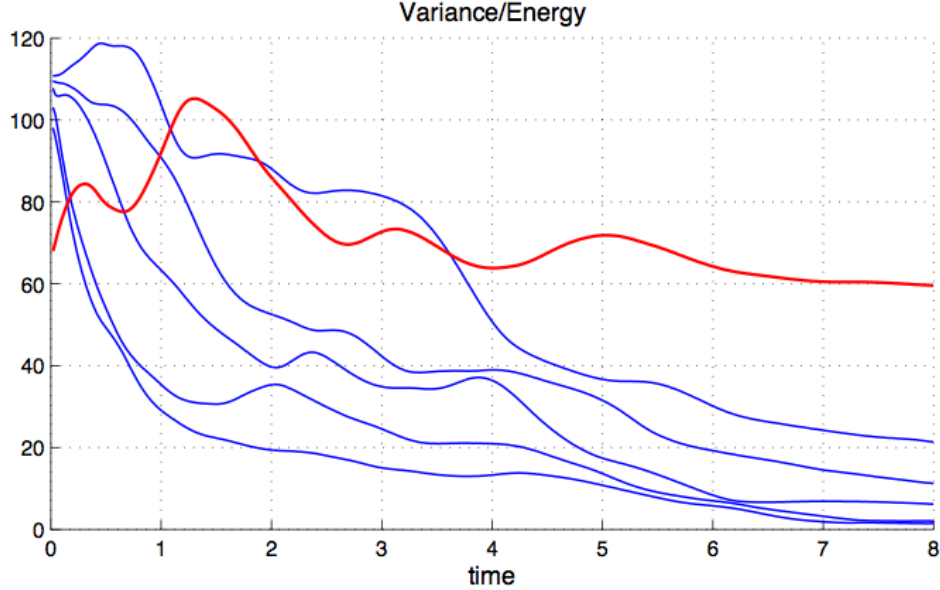


Figure 5-19: Evolution of principal variances $\sigma_i^2(t)$, $i = 1, \dots, 5$ (blue curves) and mean field energy (red curve) for the flow behind a disk.

oscillations and non-monotonic behavior. The evolution of the kinetic energy associated with the mean field is also more complex.

The mean fields $\bar{\mathbf{u}}(\mathbf{x}, t)$ and orthonormal basis fields $\mathbf{u}_i(\mathbf{x}, t)$, $i = 1, \dots, 5$ are shown in Figures 5-20 and 5-21 for two different time instances in terms of the streamfunction. For the same time instances we also present four out of the five two-dimensional marginals associated with the stochastic processes $\{Y_j(t; \omega)\}_{j=1}^5$. As we can observe, the basis fields $\mathbf{u}_i(\mathbf{x}, t)$ are mainly distorted at locations close to the solid boundaries indicating that the main interaction of the stochastic subspace V_S and the mean flow is taking place close to these locations and especially the circular obstacle. This behavior has also been reported in previous work based on generalized PC method ([162]). Larger interactions also occur where the mean vorticity is larger and where meanders and eddies form downstream.

Finally in Figure 5-22 we compare the mean streamfunction computed using the presented method with the one obtained by Monte-Carlo simulation initiated using ESSE methodology and 500 samples.

5.8 Application III: Instabilities in the forced double gyre flow in a basin

The third application that we consider is an idealized model for the description of the temporal variability of the wind-driven ocean circulation. Specifically, we consider the simplest model of the double-gyre circulation, that is a barotropic, single-layer QG model (see e.g. McCalpin and Haidvogel [99]; Chang et al. [27]). Simonnet and Dijkstra [133] used this simple double-gyre model to study instabilities of non-oscillatory modes that lead to the creation of a low-frequency gyre mode.

The aim of this section is to study the stochastic response of this model for different

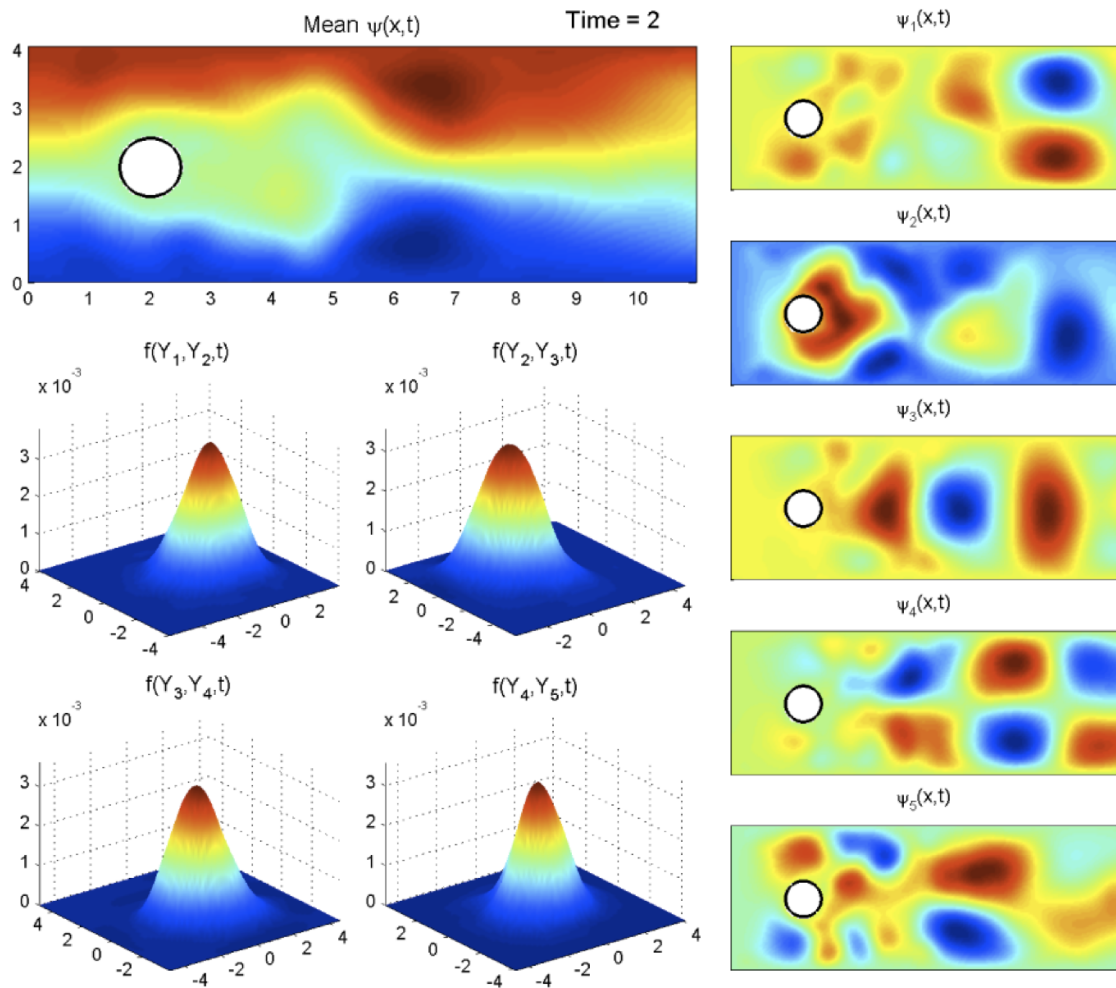


Figure 5-20: Mean field and basis of the stochastic subspace V_S in terms of the streamfunction; two-dimensional marginals of the five dimensional joint pdf $f(\mathbf{y}, t)$ at time $t = 2$.

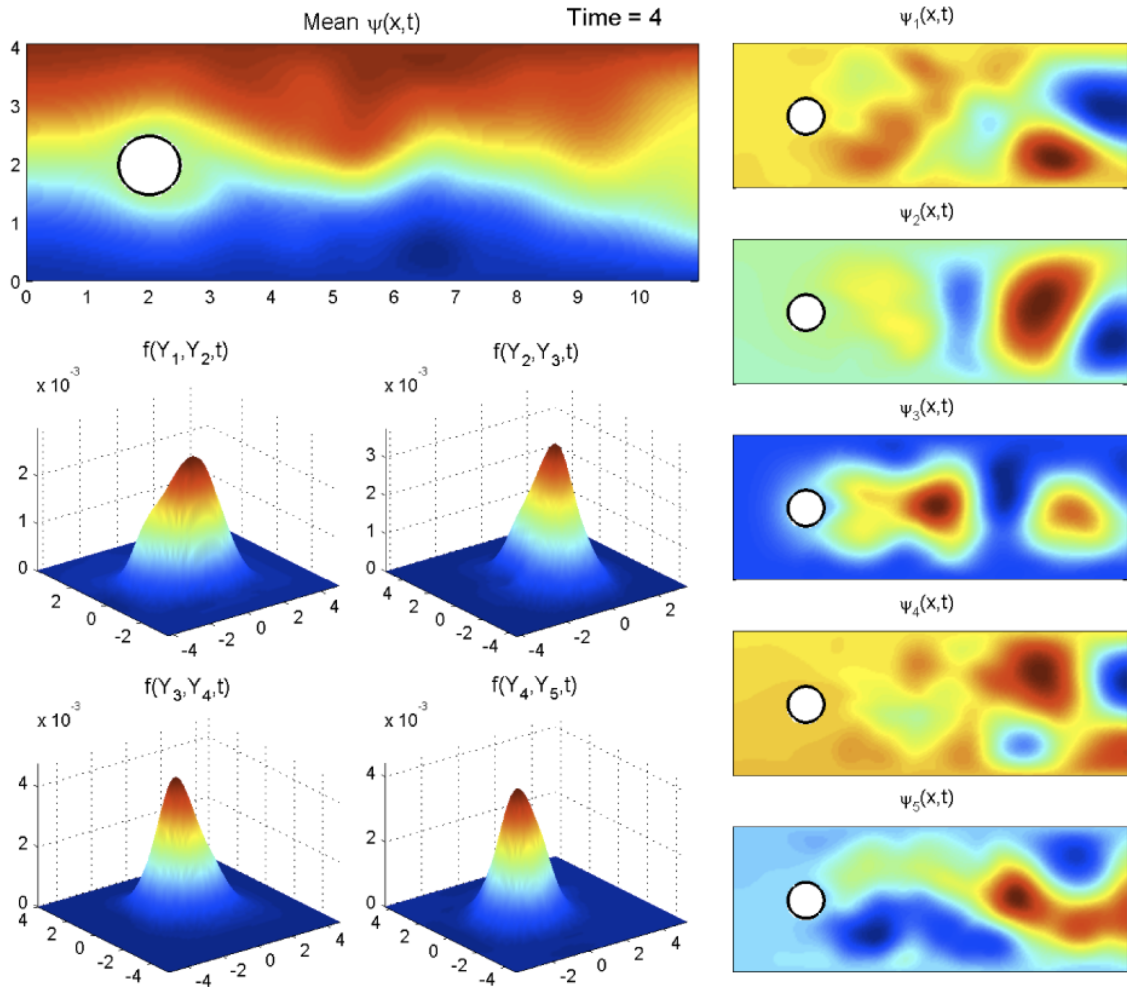


Figure 5-21: Mean field and basis of the stochastic subspace V_S in terms of the streamfunction; two-dimensional marginals of the five dimensional joint pdf $f(\mathbf{y}, t)$ at time $t = 4$.

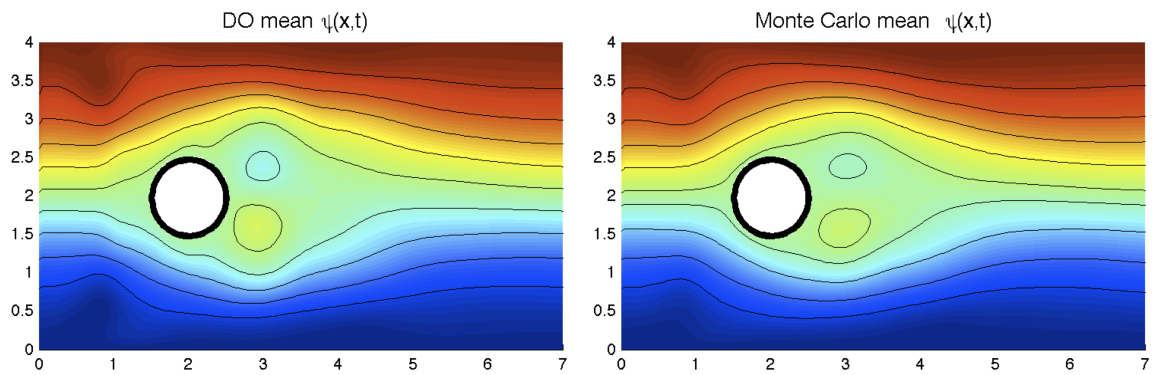


Figure 5-22: Mean velocity field (streamfunction) computed using the DO field equations ($s = 5$) and Monte-Carlo method (500 samples) at $t = 1$.

forcing parameters and Re regimes. After giving a detailed description of the model as well as an overview of the deterministic dynamics, we will examine what is the effect of a very small stochastic perturbation on the initial conditions of the problem. Through the developed stochastic framework we will prove that in the unstable regimes, as those are predicted by the deterministic theory, the system converges to a stochastic steady state response which is characterized by finite variance that is smaller than the energy of the mean flow. For larger Re this variance increases causing nonlinear interactions between the modes and the mean flow and resulting strongly non-Gaussian, non-stationary responses. The numerical results that follow are based on a finite-volume framework [148] suitably adjusted to model the two-dimensional DO equations. Other numerical frameworks such as Discontinuous Galerkin ([147], [149]) may also be applied for the solution of the DO equations.

5.8.1 Model

We use a barotropic single layer-model [37]. The ocean layer has a constant density ρ and mean thickness d and is confined to a square basin of horizontal dimensions $L \times L$. The flow in the basin is forced by a wind stress $(\tau_0 \tau^x, \tau_0 \tau^y)$, where τ_0 is a characteristic amplitude. Both bottom friction (with coefficient ε_0) and lateral (with coefficient A_H) are considered. Using characteristic horizontal and vertical scales L and d , a horizontal velocity scale U , a wind stress τ_0 , and a timescale L/U , the nondimensional equations become

$$\begin{aligned} \frac{\partial u}{\partial t} &= -\frac{\partial p}{\partial x} + \frac{1}{\text{Re}} \Delta u - \frac{\partial(u^2)}{\partial x} - \frac{\partial(uv)}{\partial y} - \mu u + f v + a \tau_x \\ \frac{\partial v}{\partial t} &= -\frac{\partial p}{\partial y} + \frac{1}{\text{Re}} \Delta v - \frac{\partial(vu)}{\partial x} - \frac{\partial(v^2)}{\partial y} - \mu v - f u + a \tau_y \\ 0 &= \frac{\partial u}{\partial x} + \frac{\partial v}{\partial y} \end{aligned}$$

where Re is the flow Reynolds number, $f = f_0 + \beta_0 y$ is the Coriolis coefficient, a the strength of the wind stress, and μ the bottom friction parameter. Their expression are given as

$$\text{Re} = \frac{UL}{A_H}; \quad a = \frac{\tau_0 L}{\rho d U^2}; \quad \beta = \frac{\beta_0 L^2}{U}; \quad \mu = \frac{L \varepsilon_0}{U}.$$

In the results shown below, we follow Simonnet and Dijkstra [133] and we set both μ and $F = \frac{f_0^2 L^2}{g d}$ to zero. The Reynolds number Re is used as the control parameter. The reference values of the other parameters are indicated in Table 5.1 (in dimensional form) and Table 5.2. The values of the dimensionless inertial and viscous boundary layer thickness, $\delta_I = L^{-1} \sqrt{U/\beta_0}$ and $\delta_M = L^{-1} (A_H/\beta_0)^{1/3}$ are also shown.

The flow in the basin is forced by an idealized zonal wind stress that is constant in time, given by

$$\tau_x = -\frac{1}{2\pi} \cos 2\pi y.$$

Free slip boundary conditions are imposed on the northern and southern walls ($y = 0, 1$) and no-slip boundary conditions on the eastern and western walls ($x = 0, 1$). In all the results that follow the system is initiated with zero mean flow and zero stochastic part. After a small time interval (10^{-2} non-dimensional time) a stochastic perturbation is added

Table 5.1: Reference values of parameters in the barotropic QG model (dimensional).

Parameter	Value	Parameter	Value
U	$7.1 \times 10^{-3} m.s^{-1}$	L	$1.0 \times 10^6 m$
L/U	$4.46 yr$	d	$2500 m$
τ_0	$1.26 \times 10^{-1} Pa$	β_0	$7.1 \times 10^{-12} (m.s)^{-1}$
ρ	$10^3 Kg.m^{-3}$	f_0	$5.0 \times 10^{-5} s^{-1}$

Table 5.2: Reference values of parameters in the barotropic QG model (non-dimensional).

Parameter	Value	Parameter	Value
a	1000	β	10^3
F	0	μ	0
δ_I	0.032	δ_M	0.02 – 0.04

with Gaussian statistics and variance equal to 10^{-6} of the mean energy. The shape of the perturbation is chosen according to the stability analysis arguments presented in Section 5.4. Subsequently we use the adaptive framework developed in Chapter 4 to add extra stochastic modes if this is necessary.

5.8.2 An overview of deterministic analysis

In this section we give a summary of the results presented in Simmonet and Dijkstra [133] that follow from deterministic stability analysis of the system. More specifically, it is shown that the considered QG model has a globally stable attractor for sufficiently low Re numbers. This can be seen in the bifurcation diagram in Figure 5-23 (published in [133]) where the vertical axis corresponds to the non-dimensional intensity of the subtropical gyre, that is $\psi_{subtropical} = \max_{\psi>0} \psi$ (with ψ being the flow streamfunction) and the horizontal axis corresponds to the Reynolds number.

As the Reynolds number increases and becomes larger than the critical value $Re = 29.7$ then a spatially symmetric mode (symmetry is meant in the sense of vorticity field), the P-mode (shown in Figure 5-24 top-left) becomes unstable causing the existence of multiple steady states. In Figure 5-24 (published in Simmonet and Dijkstra [133]) the eigenvalue corresponding to the P-mode is presented. As we are able to observe for Reynolds number between $Re = 29.7$ and $Re = 39.3$ the symmetric mode has an eigenvalue with a positive real part that leads to instabilities. However, even in this unstable regime the system converges to an attractor which, in contrary to the low Re regime, is stochastic (the authors describe it as a multiple steady state regime, [133]).

For higher Reynolds number the P-mode becomes stable with a negative growth-factor. This is the case for higher Reynolds numbers up to $Re = 71.5$ where the first Hopf bifurcation takes place and oscillations begin to occur. For even higher Reynolds numbers two more Hopf bifurcations take place as it is shown in 5-23 (points \mathbf{H}_1 , \mathbf{H}_{gyre} , \mathbf{H}_3). In the sections that follow we will give an exact probabilistic characterization of these regimes using the developed stochastic framework.

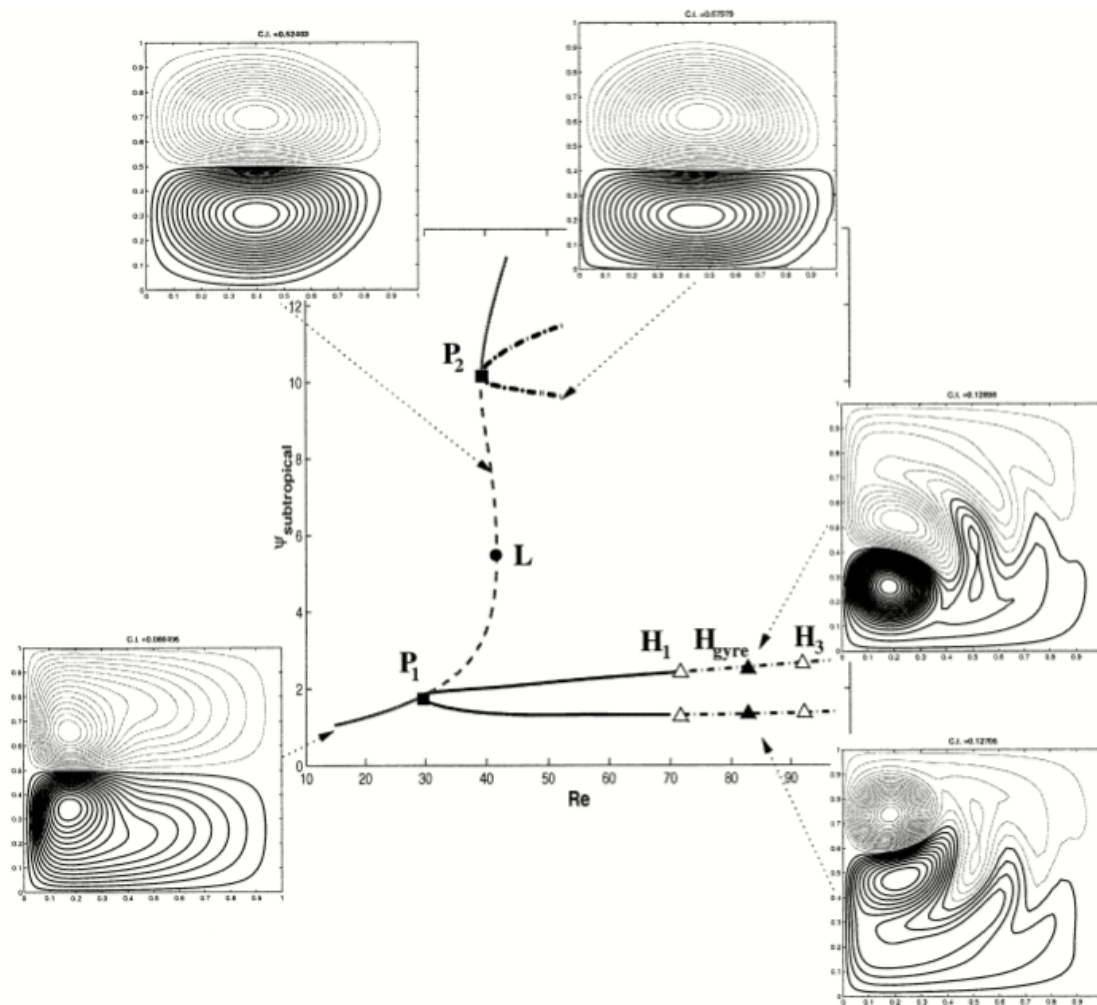


Figure 5-23: Bifurcation diagram for the QG model with values of the parameters as in Tables 5.1 and 5.2 (from Simonnet and Dijkstra [133]).

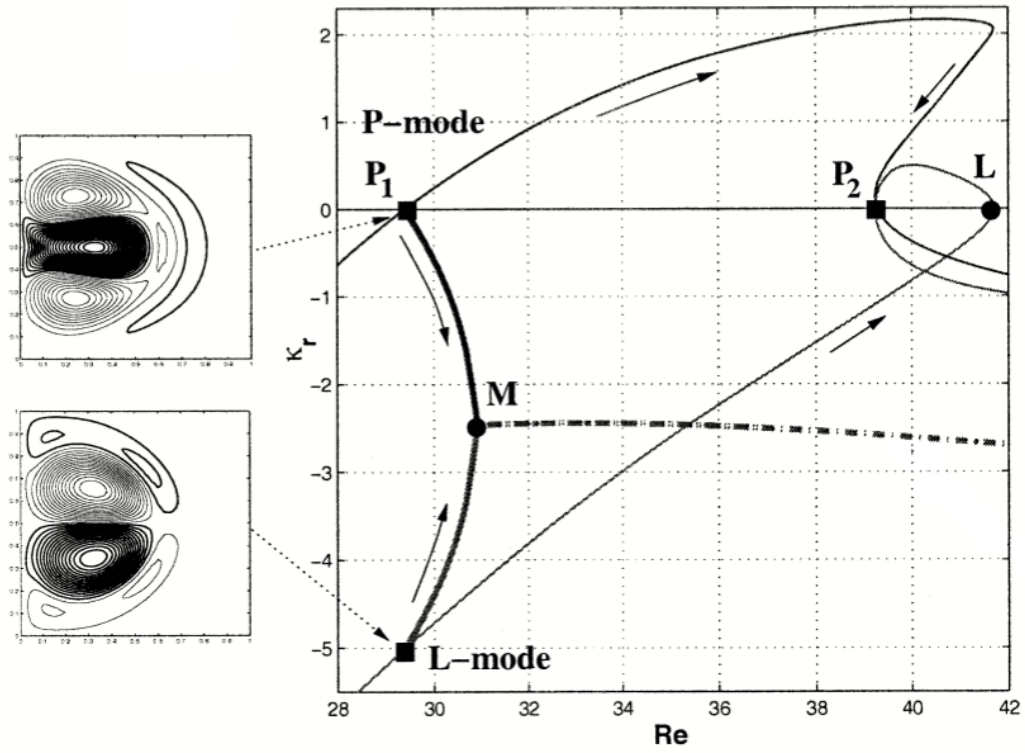


Figure 5-24: Spectral behavior of the eigenmodes involved into the various bifurcations of the anisymmetric branch for the barotropic QG model (from Simonnet and Dijkstra [133]).

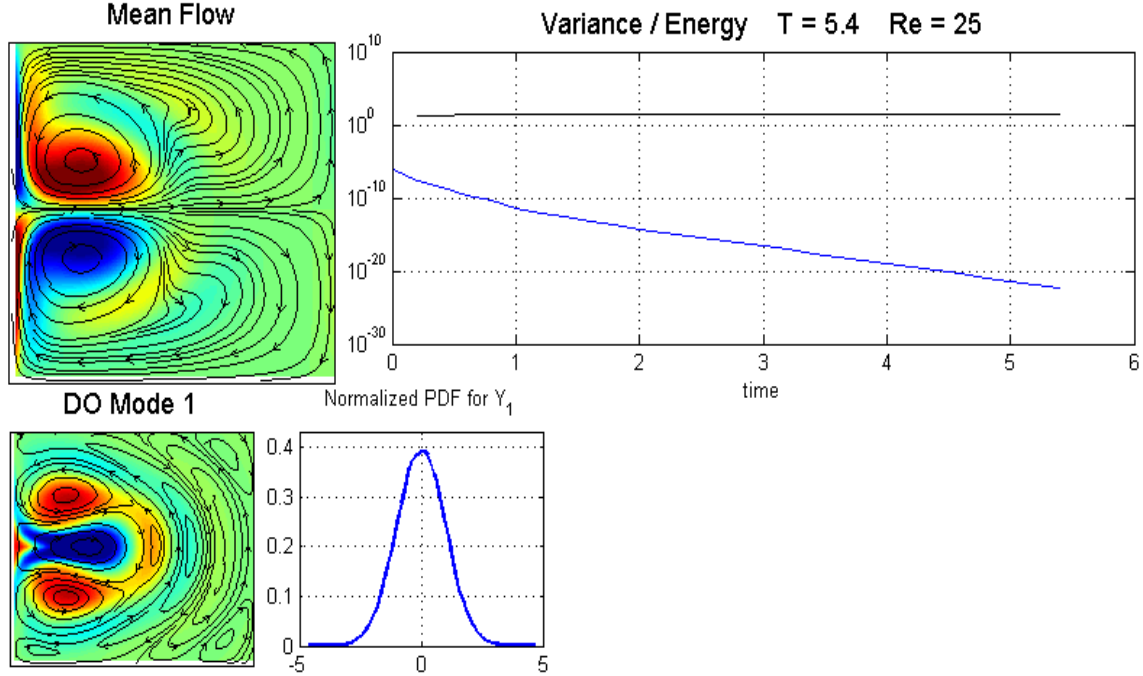


Figure 5-25: Stochastic response of the QG model for $Re = 25$. The left top plot shows the mean flow in terms of the vorticity (colormap) and the streamlines (black solid curves). The right-top plot indicates the energy of the mean flow (red curve) and the variance of the stochastic mode. The bottom plot indicates the first DO mode together with the pdf for the stochastic coefficient.

5.8.3 Bifurcation analysis of the stochastic response

We begin our probabilistic analysis in the stable regime, i.e. $Re < 29.7$. In Figure 5-25 we present the stochastic response of the system. The left-top plot shows the mean flow in terms of the vorticity (colormap) and the streamlines (black solid curves). The right-top plot indicates the energy of the mean flow (black curve) and the variance of the stochastic mode (blue curve). The bottom plot indicates the first DO mode together with the probability density function for the stochastic coefficient. In this case as we are able to observe the system state is stable and the system rapidly converges to a deterministic attractor since the variance of the stochastic perturbation decays monotonically. Therefore, in this regime the system behaves deterministically.

By numerically solving the DO field equations over various Re numbers we found that the deterministic regime is extended up to $Re \simeq 30.2$. A possible explanation for the numerical difference with the results by Simmonet and Dijkstra [133] is the different numerical schemes used but also the fact that very small linear growth rate may not be able to cause finite size stochastic perturbations.

As we increase the Reynolds number we observe in Figure 5-26 that the variance of the stochastic perturbation converges, in an oscillatory manner (see Figure 5-27), to a steady state. In this case we have one way interaction between the mean flow and the

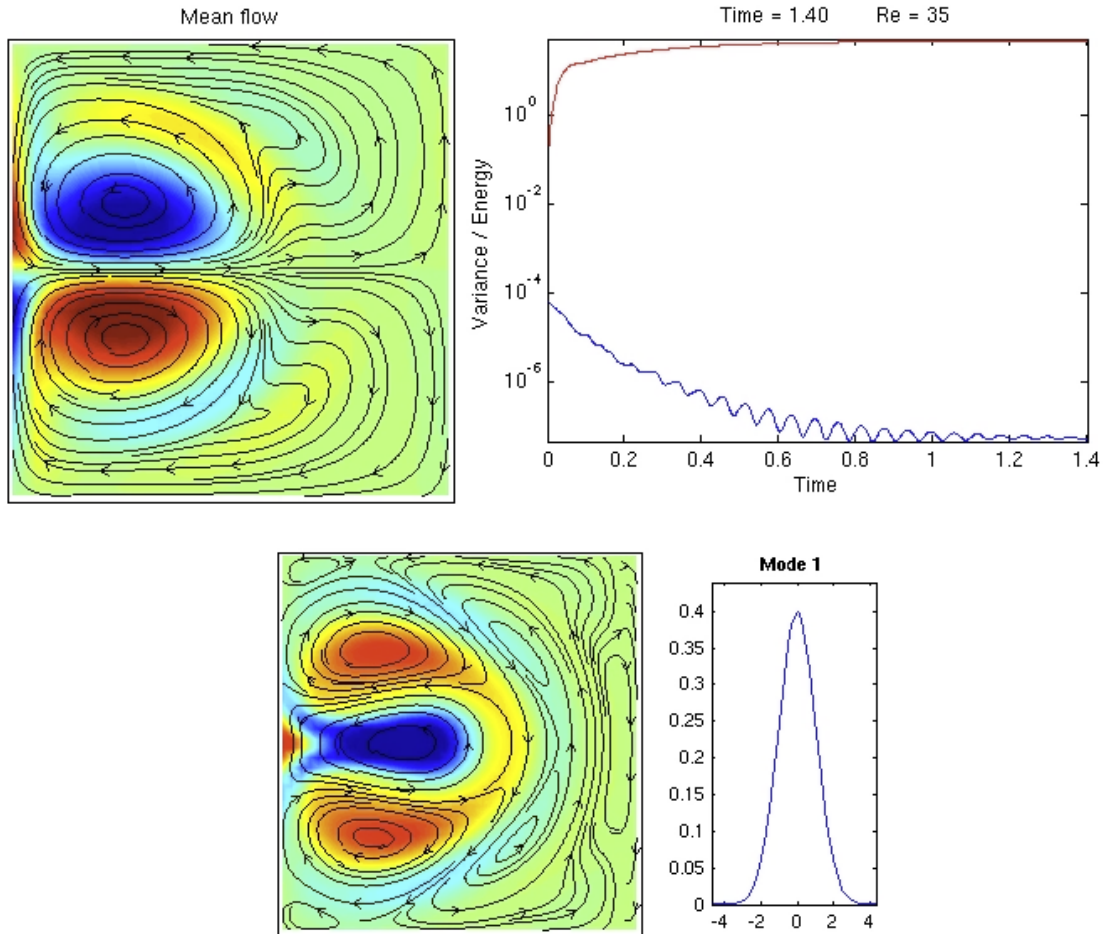


Figure 5-26: Stochastic response of the QG system for $Re = 35$ after the system has reached steady state statistics.

stochastic perturbation, since the steady state variance of the stochastic mode is pumping energy from the mean flow (since energy is continuously dissipated in the DO mode due to viscosity) while on the same time the mean flow preserves its antisymmetric character, i.e. it is not influenced by the symmetric perturbation. The statistics seem to preserve their original character, i.e. they have normal distribution. The spatial shape of the stochastic perturbation is strongly related with the linearly unstable mode computed in [133] (see Figure 5-24), i.e. the tripolar form of the perturbation presented in Simmonet and Dijkstra [133]. In this way we have obtained the complete statistical information for this family of multiple equilibria, reported in Simmonet and Dijkstra [133]. Also, we emphasize that the steady state statistics do not depend on the initial magnitude of the perturbation. The magnitude of the variance for the steady state regime increases monotonically with the Reynolds number. At $Re \simeq 38$ this growth is interrupted by the mutual interaction of the stochastic perturbation with the mean flow. More specifically, in Figure 5-28 we present the initial regime of the dynamics for $Re = 38$. At time $t = 3.46$ the existing stochastic mode exceeds the critical limit for variance causing the addition of a new mode (as it is described

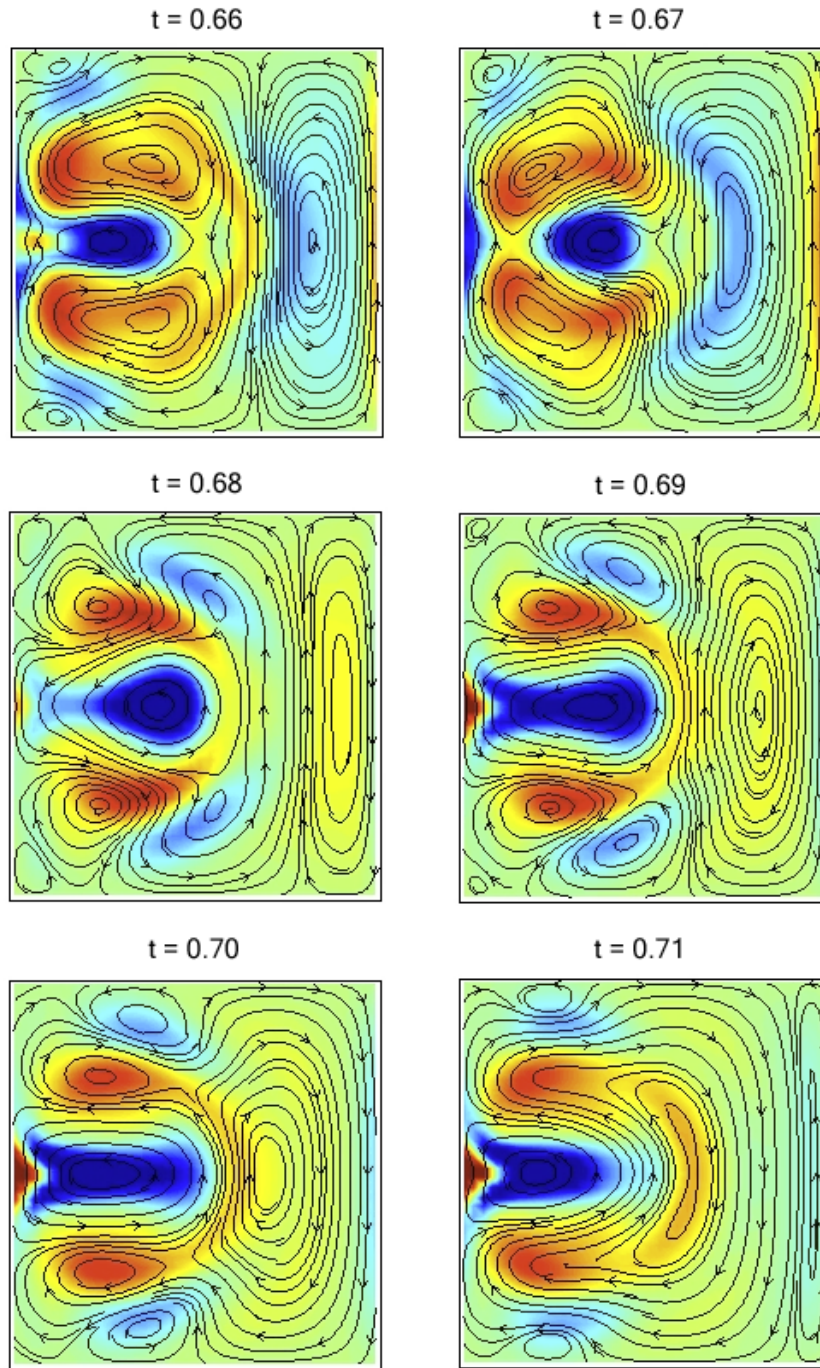


Figure 5-27: Oscillation of the DO mode during convergence to the steady state attractor for $Re = 35$.

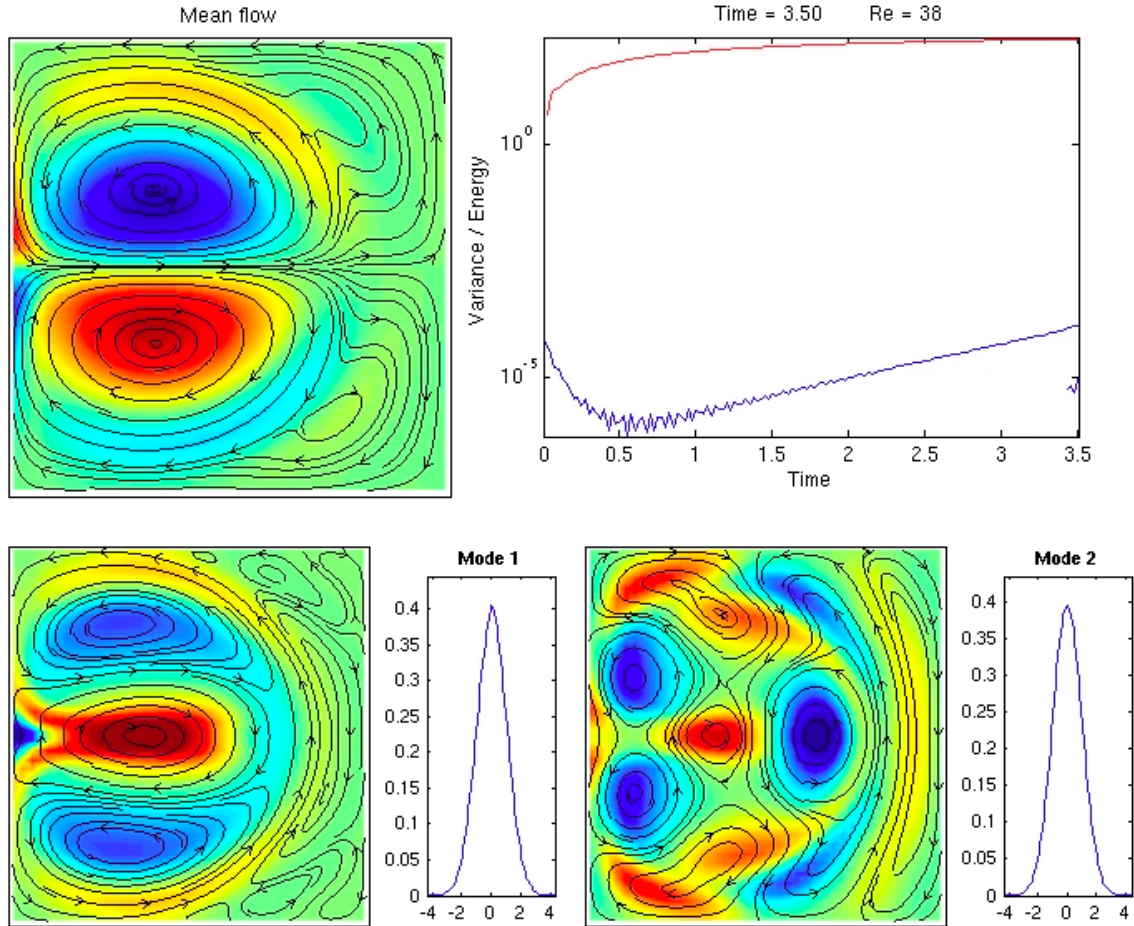


Figure 5-28: Addition of an extra mode at the time instant where the existing mode exceeds the predefined variance (Flow $Re = 38$).

in Chapter 4). This new mode, however, tends to decay, in an oscillatory manner as it is illustrated in Figure 5-29.

The P-mode continues to grow up the point where its variance becomes comparable with the energy of the mean flow. At this point we have a two-way interaction between the stochastic perturbation and the mean flow causing decay of the mean flow energy. Interestingly both the mean and the stochastic perturbation preserve their symmetric characteristics although both are deformed relative to the regime where their energies were not comparable. Subsequently, the system reaches a steady state that is time independent. This behavior is consistent with the description given in Simmonet and Dijkstra [133]. Here, we have also derived an exact description of the flow characteristics for the stochastic steady state regime.

At even higher Re number ($Re = 40$) the second mode becomes unstable causing its variance to grow similarly with the first mode. An interesting feature is the symmetry properties of the DO modes (Figure 5-32). We observe that the first one is spatially antisymmetric while its pdf retains its symmetric structure. The second mode however has

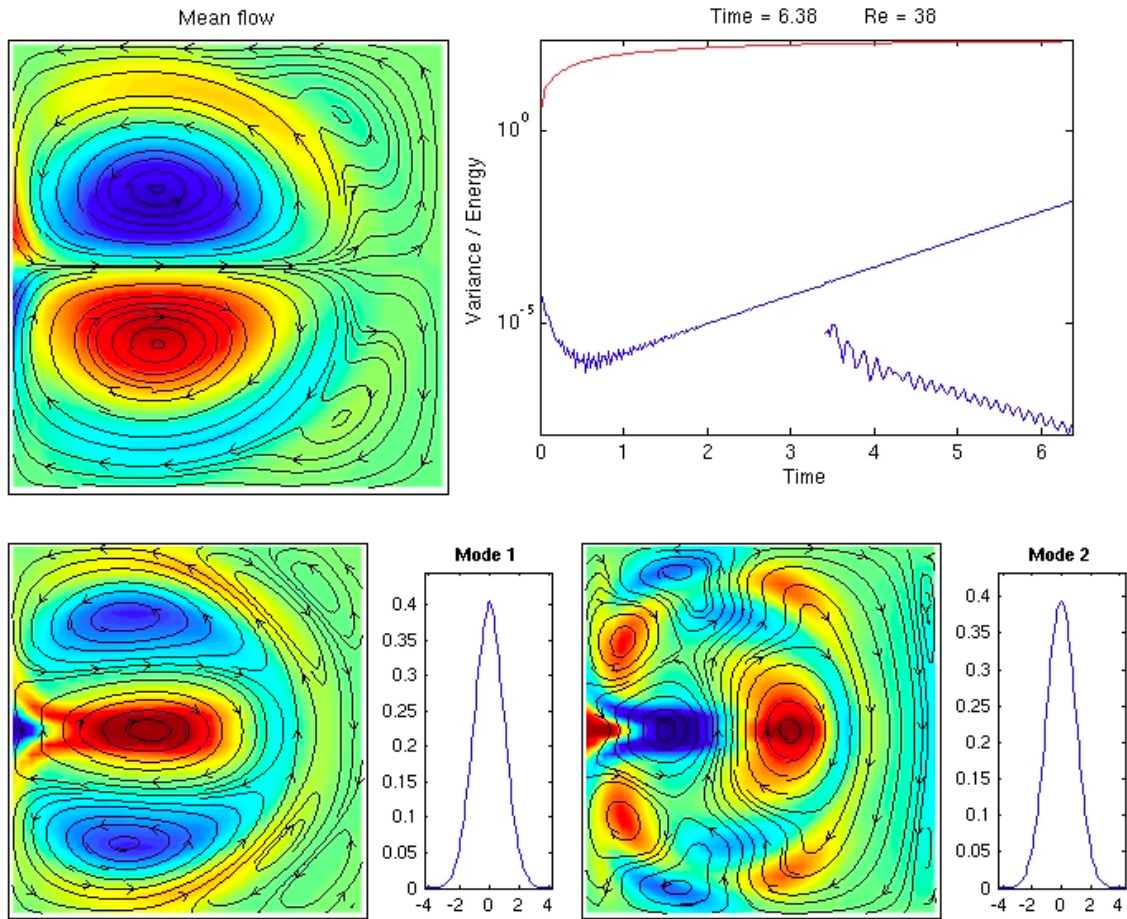


Figure 5-29: Mode removal due to very low variance (Flow $Re = 38$).

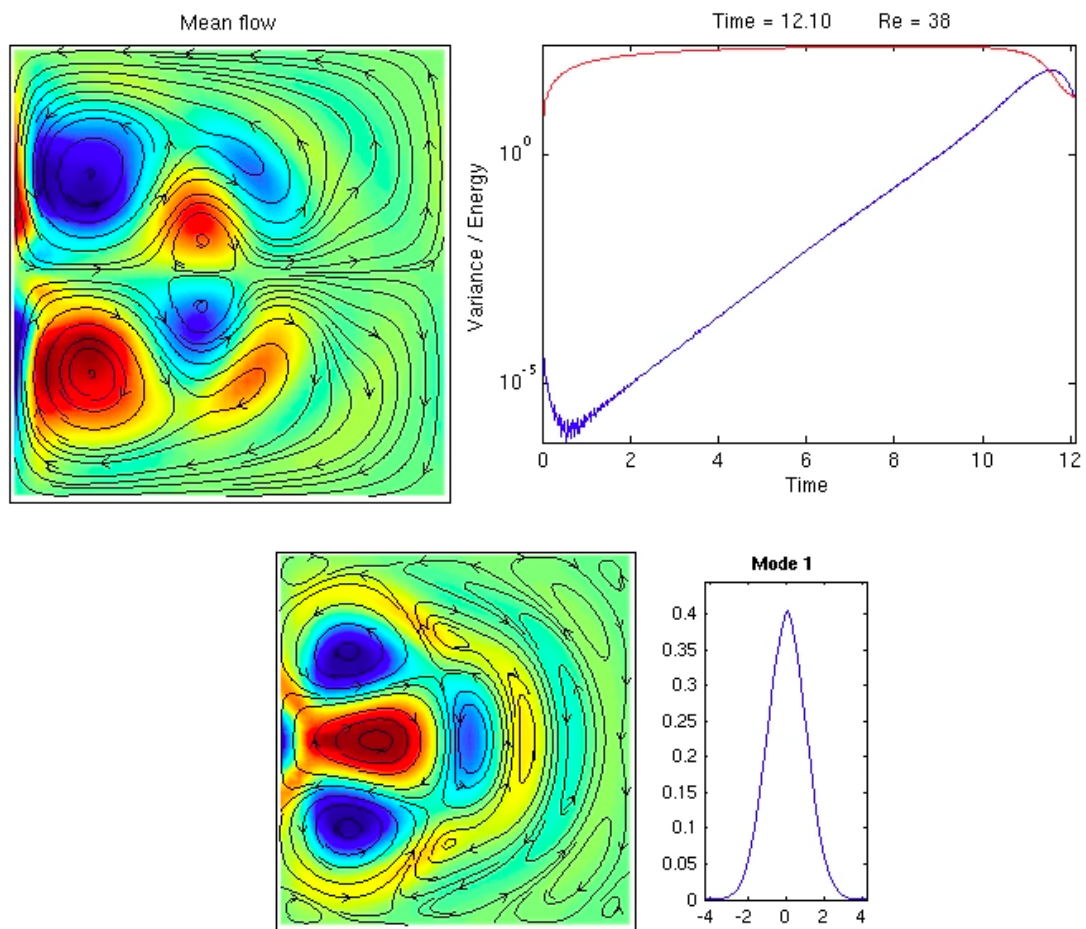


Figure 5-30: The variance of the stochastic perturbation becomes comparable with the energy of the mean flow. At this point mutual interactions between the mean flow and the perturbation begin to occur.

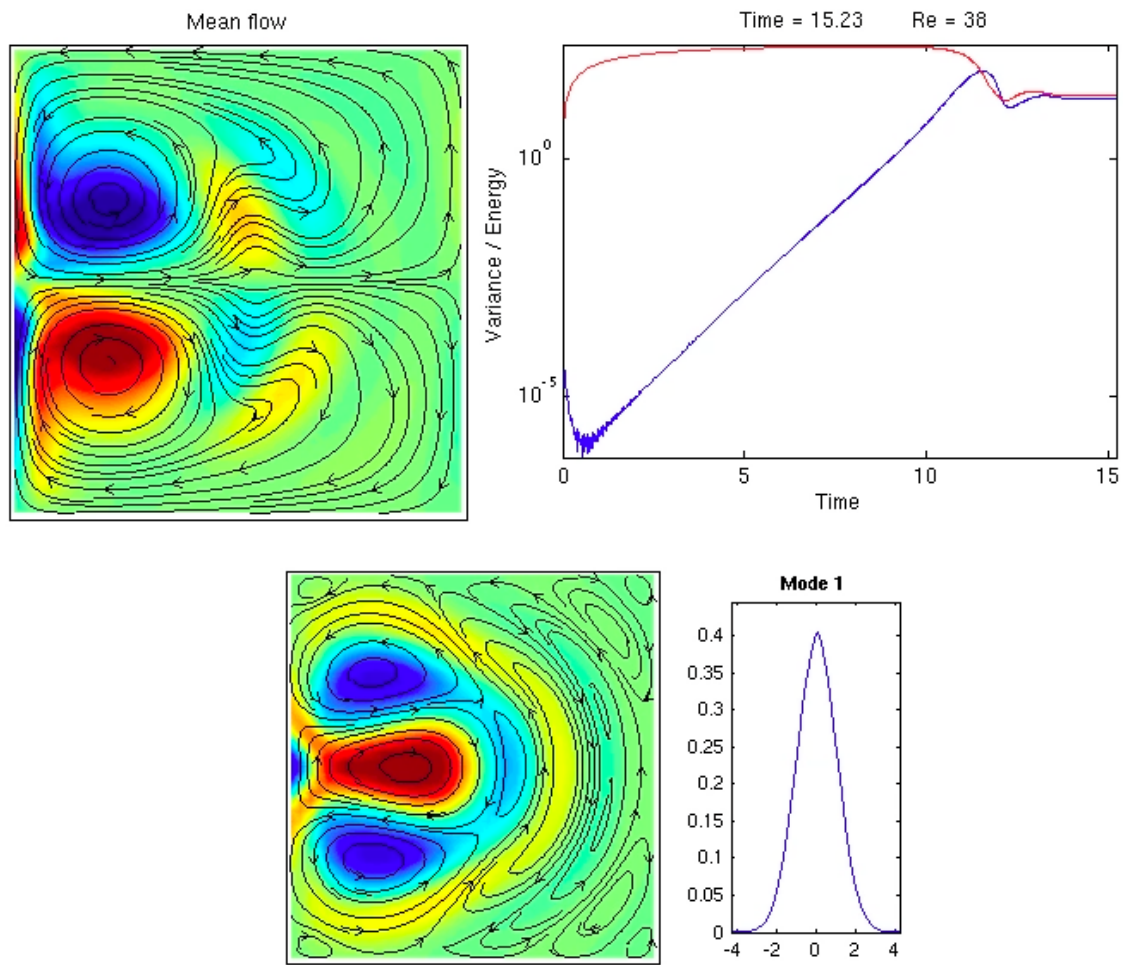


Figure 5-31: Steady state regime for $Re = 38$. Note that the perturbation retains its symmetric character even though the variance of the mode is comparable with energy of the mean flow.

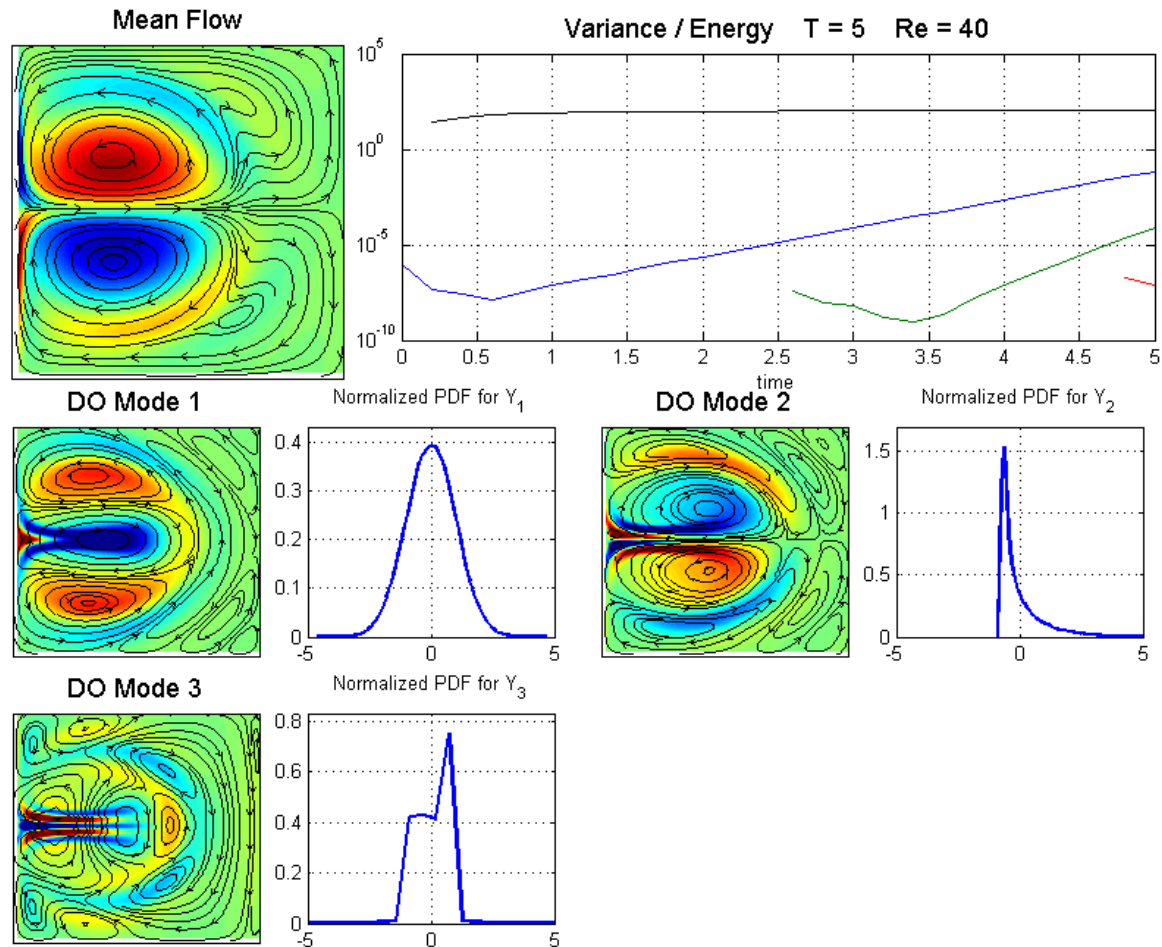


Figure 5-32: Stochastic response for $Re = 40$. Note that the first mode has symmetric spatial properties which are accompanied by symmetric pdf while the second mode has antisymmetric spatial properties with non-symmetric pdf.

the same type of symmetry with the mean flow (antisymmetric) while the corresponding stochastic coefficient has lost its initially symmetric structure (initially, when we add a new mode its density is assumed to be Gaussian - see Chapter 4).

For higher Re number ($Re = 55$) we obtain again stochastic instabilities. In this case, however, we observe that the mean flow has different characteristics with the vortices being completely detached from the left boundary. The response is initially Gaussian (Figure 5-33) but as time evolves, the statistics become more complicated with the first mode being described by a bimodal distribution (Figure 5-34). Therefore, in this case the flow has two most-probable stages around which the probability measure is distributed. Those stages are described completely through this approach. We emphasize that numerical simulations (which we do not present here) confirm that this picture is robust in terms of the initial distribution magnitude. More specifically, the shape of the modes as well as the shape of the distribution remains qualitatively the same independent of the initial magnitude of the perturbations confirming that the observed dynamics are caused by the nonlinear interactions with the mean flow and they are not the result of the growth of the perturbation

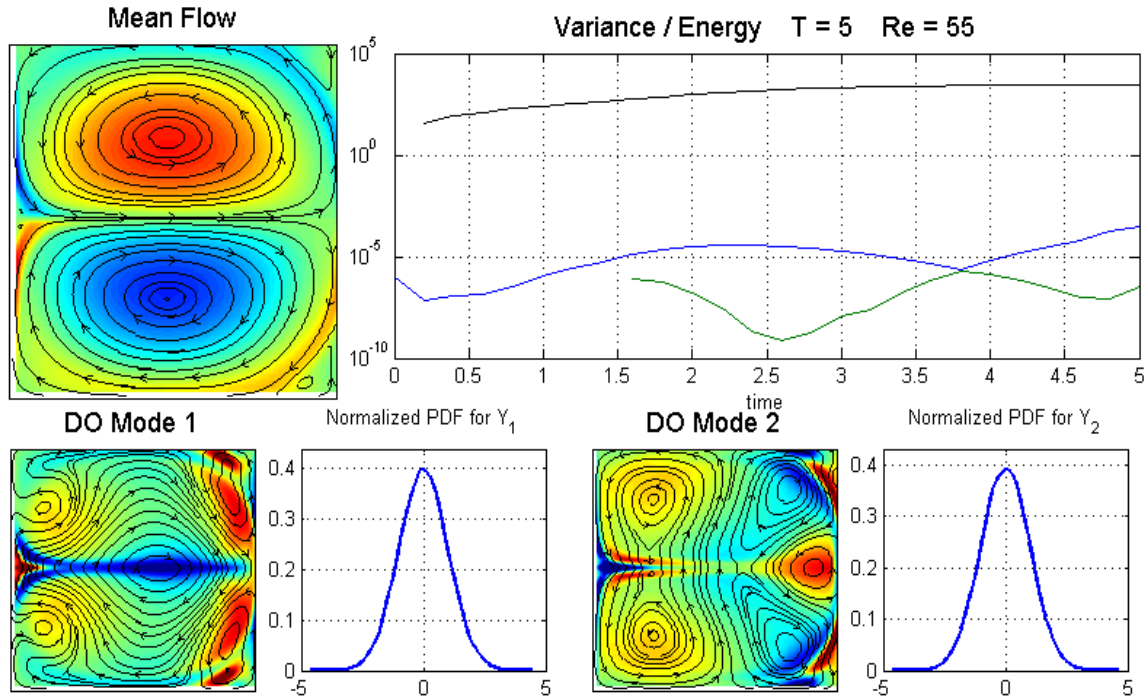


Figure 5-33: Initial stage of motion for $Re = 55$.

on the initial conditions.

As we increase the Reynolds number (exceeding $Re = 65$), the flow loses its stochastic features converging again to a deterministic attractor that is different from the one observed in the lower deterministic regime. The results are shown for $Re = 65$ in Figure 5-35. More specifically, in this regime the two gyres fill completely the domain while the stochastic perturbation tends to zero after an initial transient regime. The above behavior is consistent with the deterministic analysis that predicts stability for this regime. Note, that as we increase the Reynolds number the convergence of the stochastic mode to zero occurs more rapidly (before a critical Reynolds limit after which instabilities occur) as it can be seen in Figure 5-36 and 5-37.

For higher Reynolds number we enter the regime of unsteady behavior in the long term dynamics. The deterministic analysis predicts the occurrence of three Hopf bifurcations leading to periodic responses. Using the stochastic framework we found that for sufficiently small Re ($Re \leq 100$) we enter initially a stochastic regime that allows variance to increase temporarily. This is followed by a convergence to a deterministic attractor. However for larger Re (see Figure 5-38 for $Re = 200$) this deterministic behavior is interrupted by a sudden growth of the stochastic perturbation with energy pumped directly from the mean flow. This is followed by the addition of more DO modes according to the criteria developed in the previous Chapter. As we observe in this case the responses become strongly non-Gaussian illustrating very clearly the multiple equilibria that the system may reach.

The results presented in this section are summarized in the diagram of Figure 5-39. As we are able to observe, in agreement with the deterministic analysis, the system is characterized by two deterministic regimes. Between these two regimes we have the existence of a

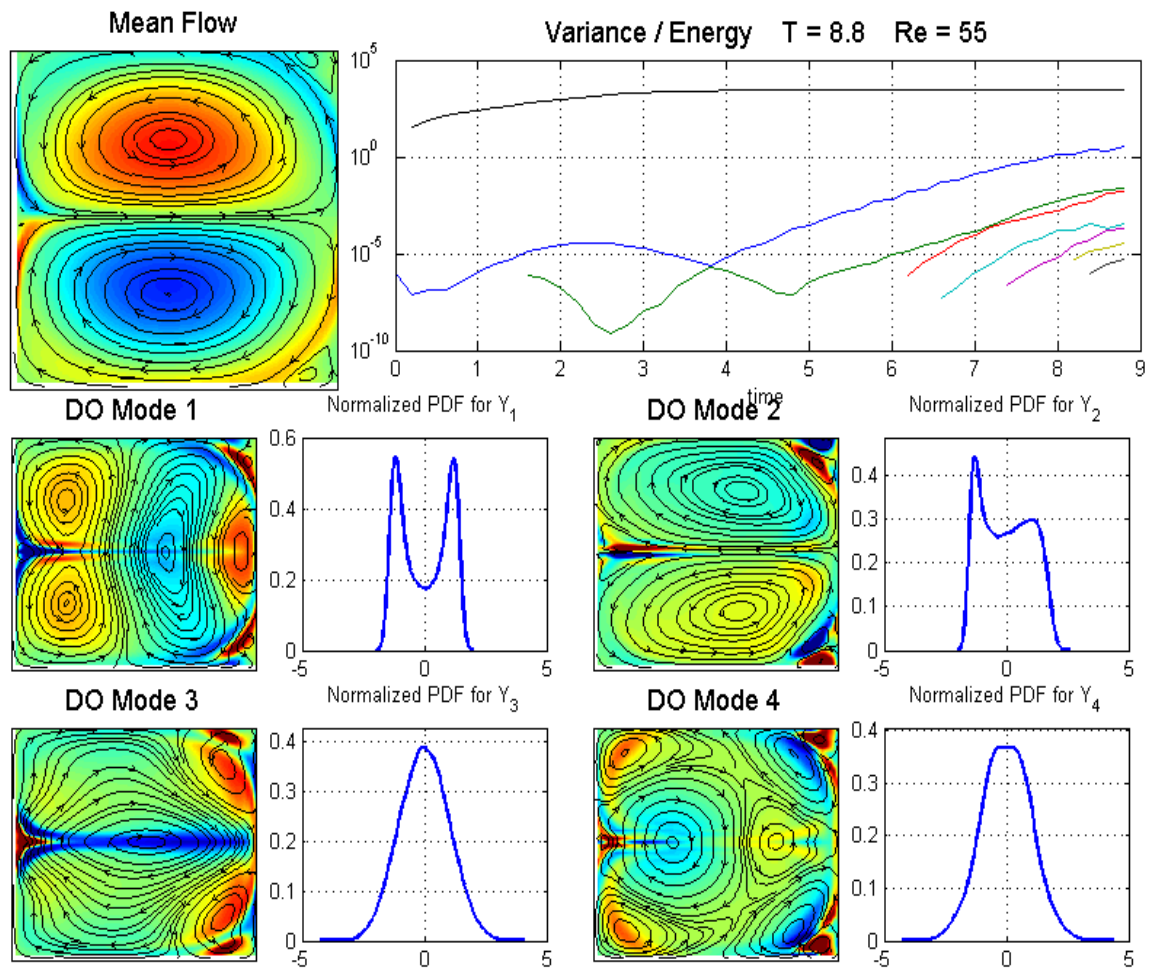


Figure 5-34: As time evolves more modes have to be added in order to achieve the given tolerance (in terms of variance).

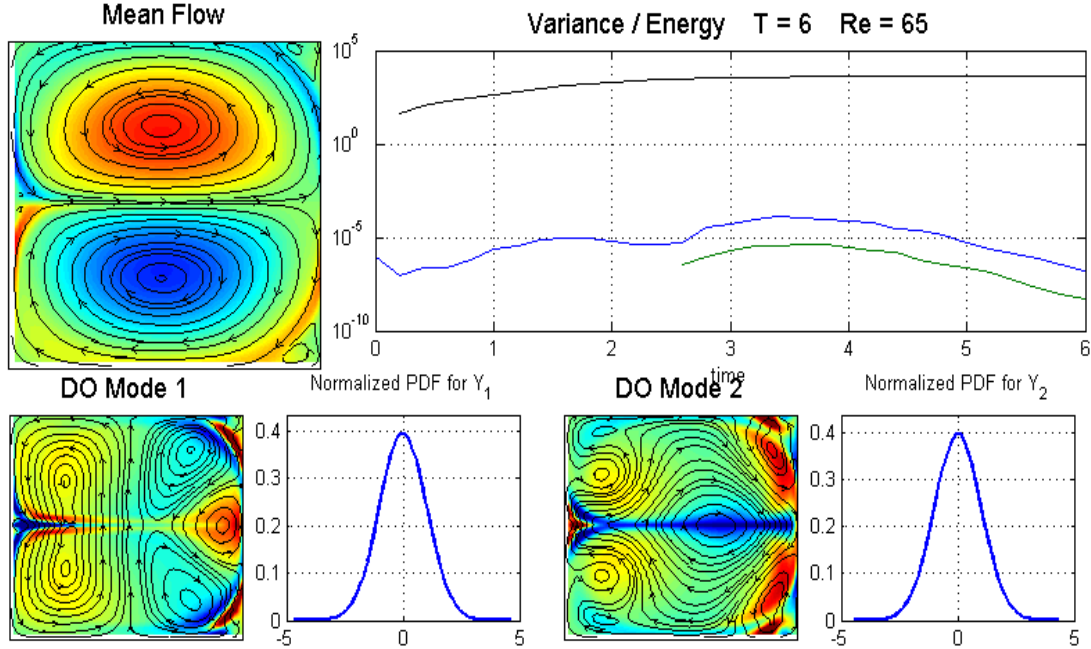


Figure 5-35: Convergence to a deterministic attractor after a transient stochastic regime for $Re = 65$.

linearly unstable mode leading to finite-amplitude, time-independent, stochastic perturbations for which we obtain an exact probabilistic description. For higher Reynolds number we still have the occurrence of the deterministic attractor. However, when the energy of the flow becomes sufficiently large then we have transfer of energy from the mean flow to the first DO mode enhancing its variance. This leads to the addition of more DO modes and to non-Gaussian transient responses.

In conclusion, we have illustrated how the DO field equations provide a natural framework for the partition of the problem into different dynamical components each one containing independent information. This is done without assuming anything on the nature of the response or its energy level. Moreover, the derived results are qualitatively consistent with the results predicted by linearization of the system in the deterministic framework. The modes extracted may be used for the setup of further reduced order models that take into account more efficiently the mutual interactions of modes and the finite-amplitude of the response. In the next section we will examine the qualitative changes occurring in the dynamics for larger Reynolds number.

5.8.4 Stochastic response for larger Reynolds number

We will now present results for the evolution of the flow with a much larger value of the Reynolds number. Specifically we consider the case of $Re = 10000$. As we observe in Figure 5-40 in the initial regime of the flow we have the formation of two antisymmetric small vortices. The DO mode follow these vortices, i.e. it localizes around them while its statistics remain Gaussian during this initial phase. As the energy of the mean flow increases so does the variance of the first DO mode causing the addition of new modes shown in Figure 5-41.

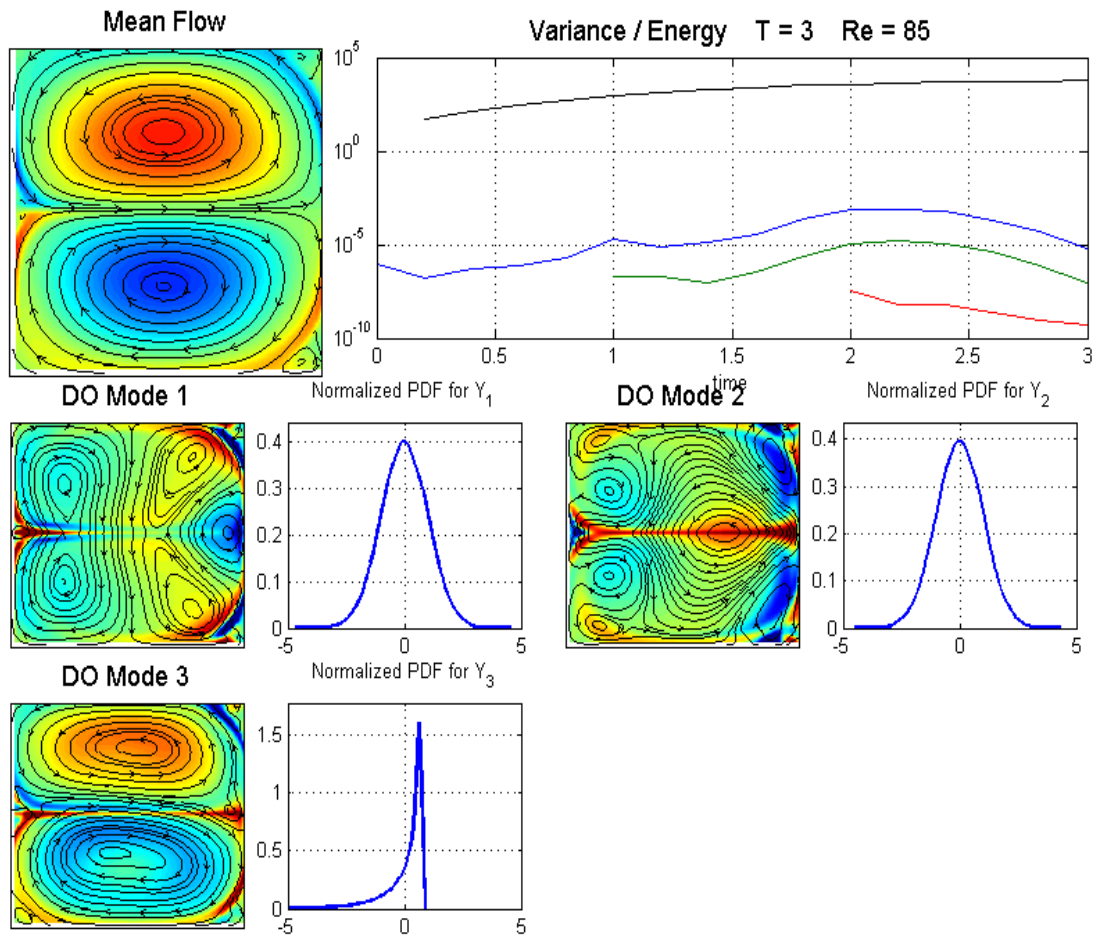


Figure 5-36: Response for $Re = 85$. In this case the convergence to the deterministic attractor occurs earlier with the initial stochastic regime being much shorter in time.

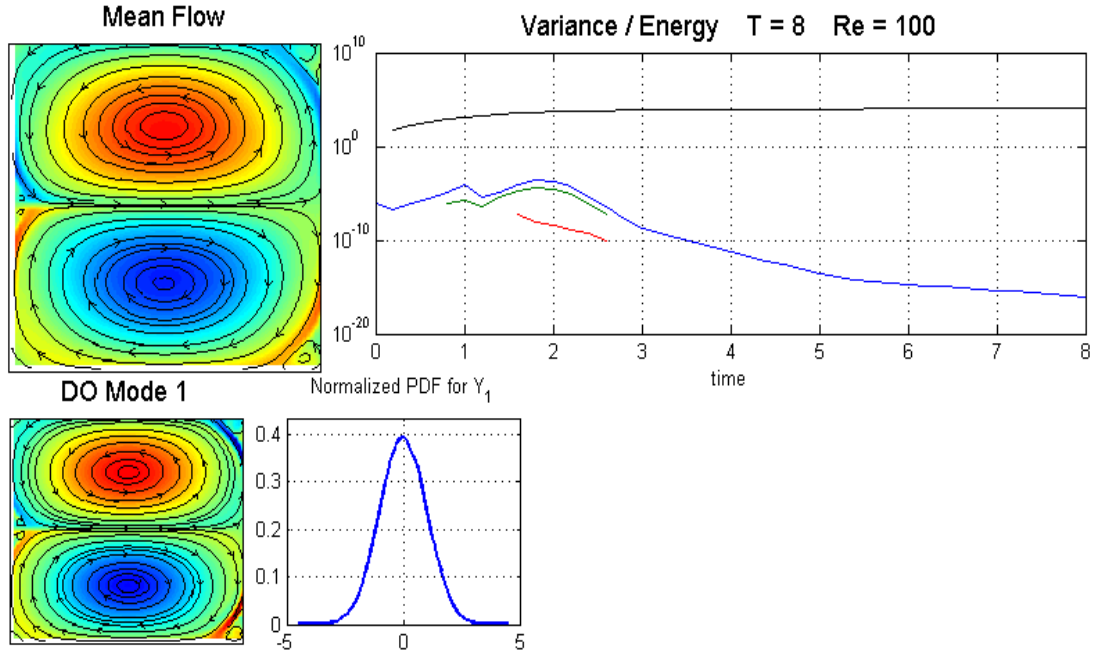


Figure 5-37: Convergence to a deterministic attractor for $Re = 100$.

Similarly with the first mode, the two new modes rapidly localize around the boundary of the vortices. Moreover, comparing with the lower Reynolds number results we see that in this case the DO modes present smaller spatial scales and sharper gradients. In the same time the variance of the modes continues to grow while the statistics remain Gaussian and their symmetry is preserved.

This picture of Gaussian statistics changes very suddenly with a nonlinear instability that causes the pdf of the third mode to lose its symmetry. This loss of symmetry is accompanied by change of the spatial symmetric properties of the corresponding mode. Note that results (not shown here) indicate that this loss of symmetry is connected with energy transfer between in the modes while the instabilities presented so far were connected with energy transfer from the mean flow to the modes. Specifically we observe that the mode loses its antisymmetric properties and becomes antisymmetric as the mean flow is. This non Gaussian behavior passes to the other modes very rapidly causing the system to reach a multi-equilibrium regime described very efficiently by the joint pdf function (whose marginals are shown in Figure 5-43).

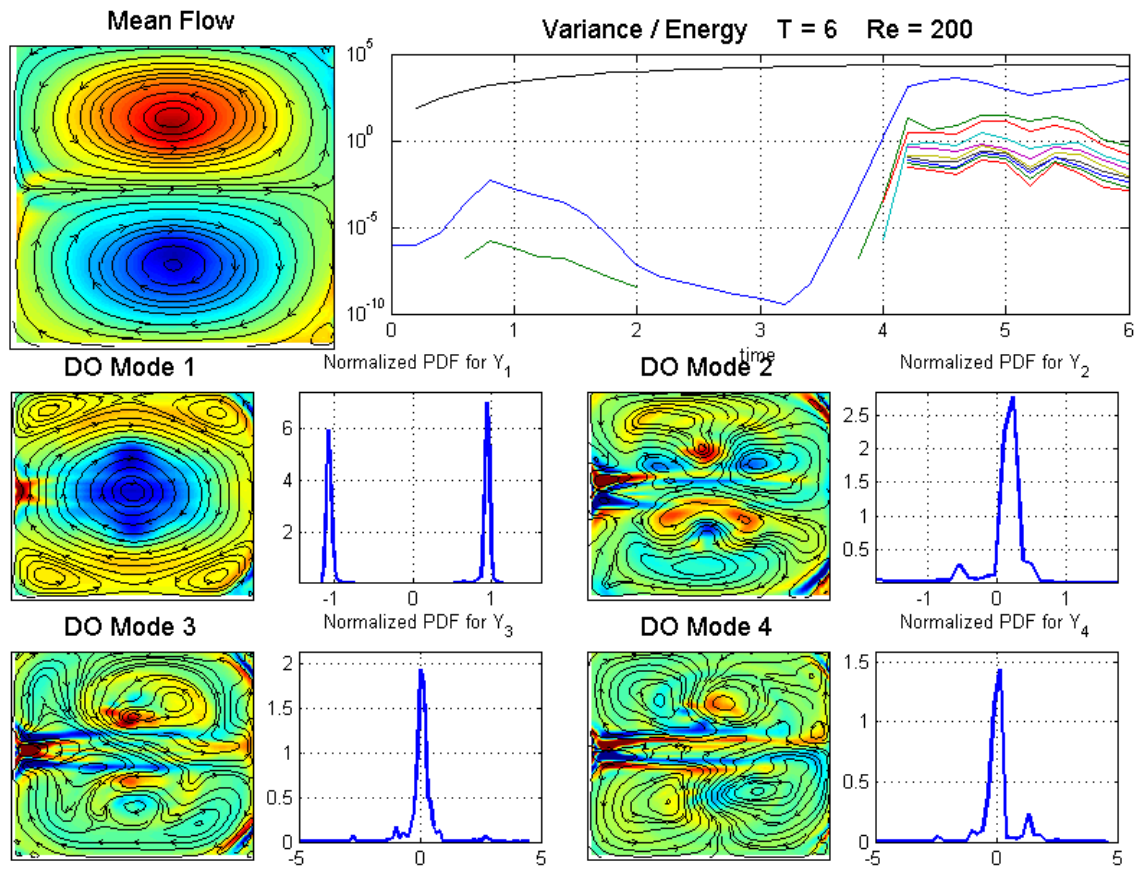


Figure 5-38: Stochastic attractor after a temporal convergence to deterministic dynamics ($Re = 200$).

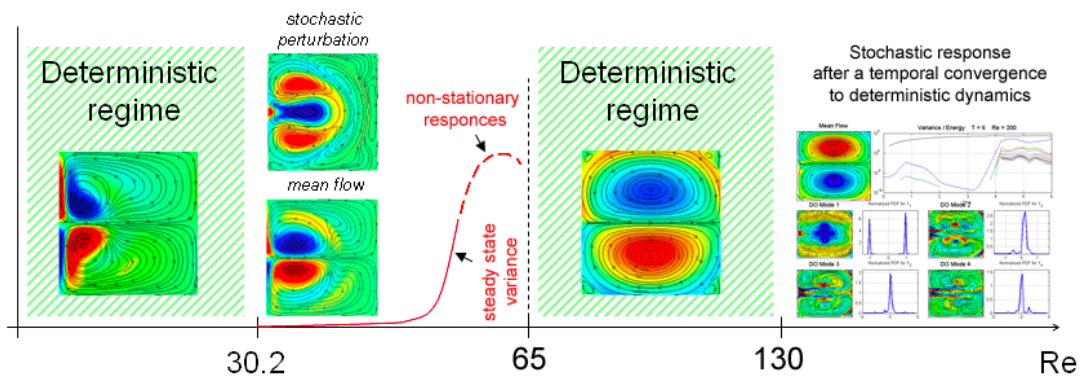


Figure 5-39: Summary of the stochastic analysis for the double gyre flow over various Reynolds numbers.

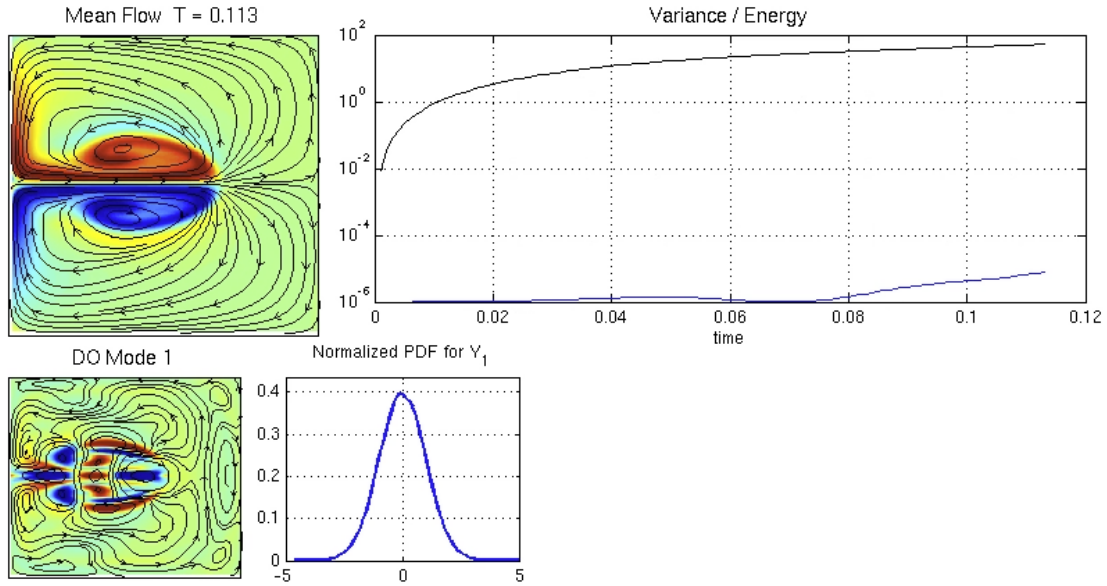


Figure 5-40: Initial regime of the stochastic response for $Re = 10^4$.

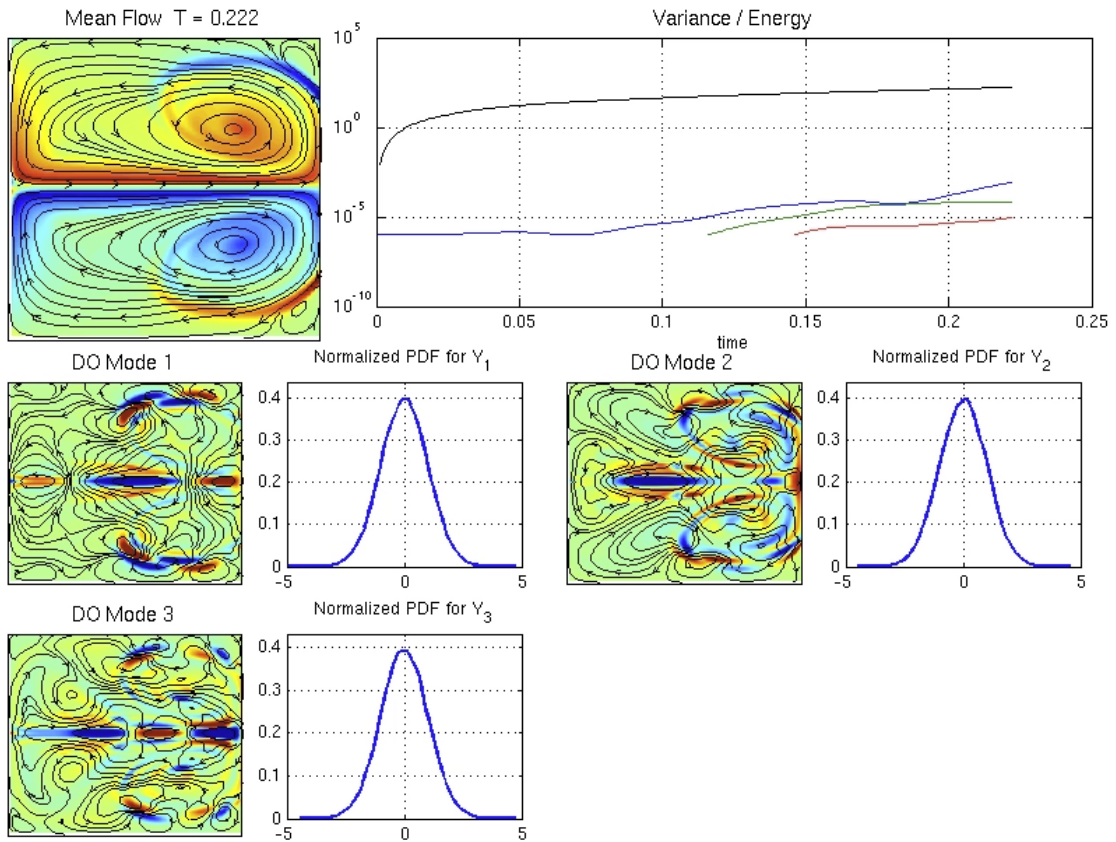


Figure 5-41: The modes added are localized around the boundary of the formed gyres of the mean flow.

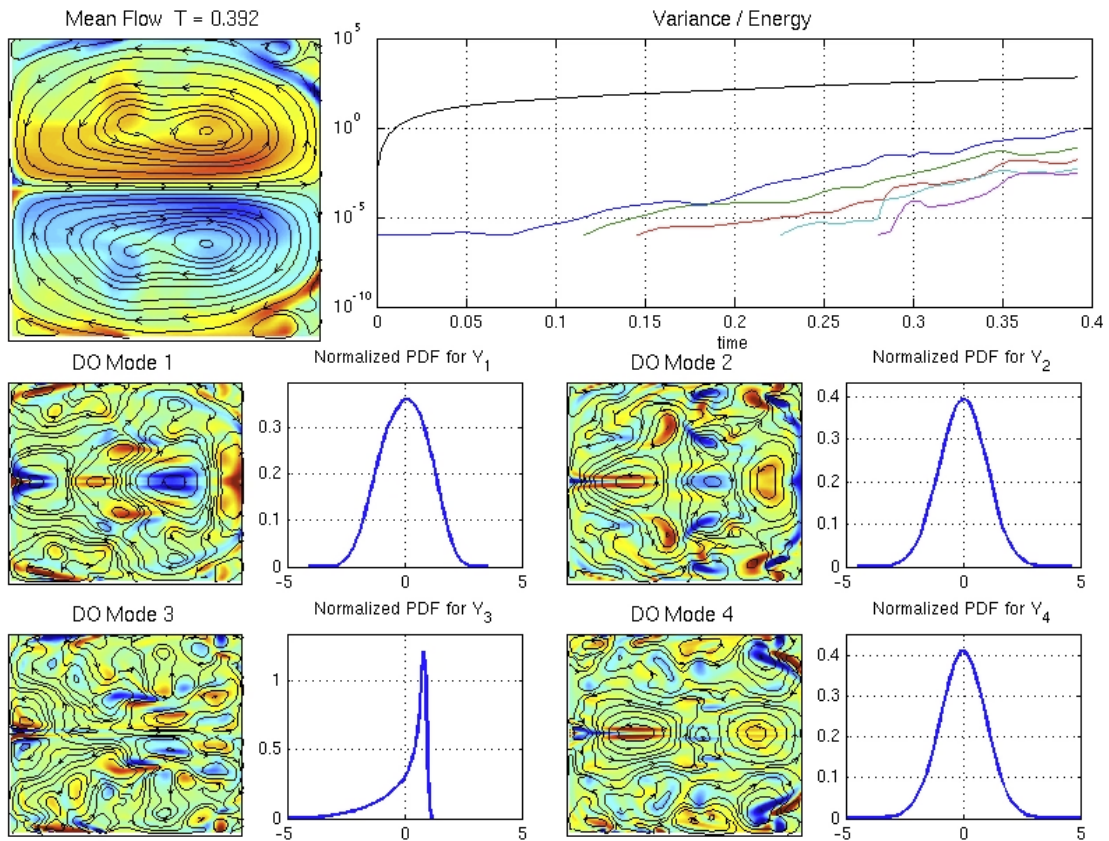


Figure 5-42: After the mean flow energy exceeds a certain limit an instability breaks the symmetry of the third mode as it is shown in the corresponding pdf plot.

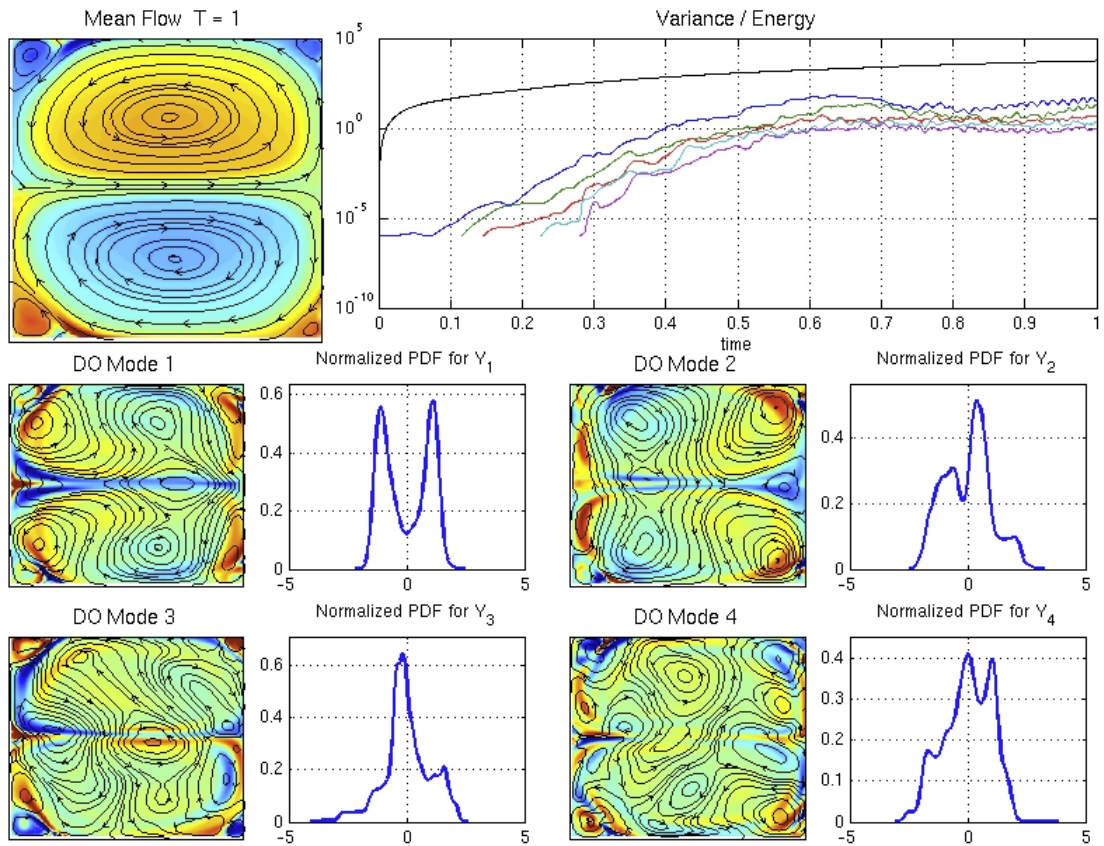


Figure 5-43: The instability shown in the previous figure is the starting point for the non-Gaussian statistics shown here.

Chapter 6

Finite-size particles in stochastic flows

Abstract

In this chapter we shall study the motion of finite-size particles in flows with uncertainty. Specifically, we will examine the coupled effects due to inertia and flow stochasticity. In the first part of the chapter we will summarize theoretical results for particles in deterministic flows. Subsequently we will present results for the stochastic case. Specifically, we will prove that the velocity of finite-size particles is governed by a stochastic slow manifold, a ‘layer’ of probability around the deterministic slow manifold derived previously for deterministic flows. Based on the stochastic reduction on this manifold we will derive a stochastic inertial equation that governs the motion of particles and which includes new terms expressing the coupled effect of particles inertia and stochasticity. In the second part of the chapter we will first illustrate numerically the convergence of the particles stochastic velocity to the stochastic slow manifold. We will validate the derived inertial equation for a specific example and we will analyze the coupled effects of particles inertia and flow stochasticity on the preferential concentration of particles.

6.1 Introduction

Dust, impurities, droplets, air bubbles, and other-finite size particles transported by incompressible flows are commonly encountered in many natural phenomena and industrial processes. Applications showing the importance of the phenomenon are pollutants transport in the ocean and atmosphere [146], [40], [62], rain initiation [114], [41], [131], coexistence between several species of plankton in the hydrosphere [119], [84], or planet formation by dust accretion in the solar system [155], [36]. In all of the above cases the flow velocity field may be characterized by uncertainties or stochasticity either because the flow dynamics is not fully resolved or because initial, boundary or parametric uncertainties are significant. Therefore, an important question is the analytical quantification of the effect of flow stochasticity on finite-size particle dynamics.

Several studies have been devoted for the above problem. In Maxey [97] the gravitational settling of aerosol particles in homogeneous and stationary random flow fields is studied. Using numerical simulations of Gaussian random fields it is shown that the coupled effect of particle inertia and flow stochasticity produces an increased settling velocity. These results

are then considered in terms of various asymptotic limits of either rapid settling or weak particle inertia.

Vasiliev and Neishtadt [151] consider the problem of finite-size particle transport in steady flows in the presence of small noise. It is shown that for the case of cell flow this effect is important at high viscosity and leads to a transition from bounded motion of the particles to diffusion-type chaotic motion.

Reynolds [117] derived for one dimensional flows, Lagrangian stochastic models for the prediction of fluid velocities along heavy-particle trajectories, by assuming the well-mixed condition. This approach ensures consistency with the Eulerian fluid velocity statistics. However, for higher dimensional flows additional assumptions are required for the unique definition of a Lagrangian stochastic model using this approach. The derived model is applied to simulate the trajectories of heavy particles in a vertical turbulent pipe flow.

In Pavliotis et al. [111] the problem of inertial particles in a random flow field with specified structure is considered. Specifically, the authors study the case of a time-dependent flow with stationary spatial structure and with random time dependence defined by a stationary Ornstein-Uhlenbeck process. Using homogenization theory they prove that under appropriate assumptions the large-scale, long-time behavior of the inertial particles is governed by an effective diffusion equation for the position variable alone.

Klyatskin and Elperin [64] and Klyatskin [65] study the problem of diffusion of a low-inertia particle in the field of a random force that is spatially homogeneous. In this case the authors prove that the problem admits an analytic solution which predicts that the particle velocity will be a Gaussian stochastic process with known covariance function. Bec et al. [12], [13] study the dynamics of very heavy particles suspended in incompressible flows with δ -correlated-in-time Gaussian statistics. Under these assumptions they derive a model which is used to single out the mechanisms leading to the preferential concentration of particles.

In what follows we will use recent results from stochastic singular perturbation theory [18] in combination with a Karhunen Loeve representation of the random flow, in order to derive a reduced order inertial equation that will describe the stochastic dynamics of inertial particles in arbitrary random flows. As it has been observed in the literature the random part of the fluid flow changes both the mean dynamics of the finite-size particles (an effect that is usually expressed through clustering) but also their diffusive dynamics (usually observed through reduced decorrelation time - also known as ‘crossing trajectories’ effect [164], [33]). Here, our primary aim is the study of the stochasticity of the flow on the mean dynamics of the particles. Specifically, through the reduced order stochastic dynamics we will study the result of a zero mean stochastic perturbation on the clustering properties of inertial particles. We will also validate and illustrate our theoretical findings through the stochastic double gyre flow presented in Chapter 5.

6.2 Summary of results for finite-size particles in deterministic flows

In this section we will summarize some recent results on the dynamics of finite-size particles in deterministic flows. These results will be essential for analyzing the motion of finite-size particles in stochastic flows. All the material, as well as proofs and applications in various settings are included in the following publications: Sapsis and Haller, 2008a,b, 2009, 2010a, b [128], [122], [123], [124], [125], and Haller and Sapsis 2008, 2010 [56], [57].

6.2.1 Reduced order dynamics

Let $\mathbf{u}(\mathbf{x}, t)$ denote the velocity field of a two- or three-dimensional fluid flow of density ρ_f , with \mathbf{x} referring to spatial locations and t denoting time. The fluid fills a compact (possibly time-varying) spatial region D with boundary ∂D ; we assume that D is a uniformly bounded smooth manifold for all times. We also assume $\mathbf{u}(\mathbf{x}, t)$ to be r times continuously differentiable in its arguments for some integer $r \geq 1$. We denote the material derivative of \mathbf{u} by

$$\frac{D\mathbf{u}}{Dt} = \mathbf{u}_t + (\nabla\mathbf{u})\mathbf{u}.$$

Let $\mathbf{x}(t)$ denote the path of a finite-size particle of density ρ_p immersed in the fluid. If the particle is spherical, its velocity $\mathbf{v}(t) = \dot{\mathbf{x}}(t)$ satisfies the equation of motion (cf. Maxey and Riley [98] and Babiano et al. [8])

$$\begin{aligned} \rho_p \dot{\mathbf{v}} = & \rho_f \frac{D\mathbf{u}}{Dt} & (6.1) \\ & + (\rho_p - \rho_f) \mathbf{g} \\ & - \frac{9\nu\rho_f}{2a^2} \left(\mathbf{v} - \mathbf{u} - \frac{a^2}{6} \Delta\mathbf{u} \right) \\ & - \frac{\rho_f}{2} \left[\dot{\mathbf{v}} - \frac{D}{Dt} \left(\mathbf{u} + \frac{a^2}{10} \Delta\mathbf{u} \right) \right] \\ & - \frac{9\rho_f}{2a} \sqrt{\frac{\nu}{\pi}} \int_0^t \frac{1}{\sqrt{t-s}} \left[\dot{\mathbf{v}}(s) - \frac{d}{ds} \left(\mathbf{u} + \frac{a^2}{6} \Delta\mathbf{u} \right)_{\mathbf{x}=\mathbf{x}(s)} \right] ds. \end{aligned}$$

Here ρ_p and ρ_f denote the particle and fluid densities, respectively, a is the radius of the particle, \mathbf{g} is the constant vector of gravity, and ν is the kinematic viscosity of the fluid. The individual force terms listed in separate lines on the right-hand side of (6.1) have the following physical meaning: (1) force exerted on the particle by the undisturbed flow (2) buoyancy force (3) Stokes drag (4) added mass term resulting from part of the fluid moving with the particle (5) Basset–Boussinesq memory term. The terms involving $a^2\Delta\mathbf{u}$ are usually referred to as the Fauxén corrections.

For simplicity, we assume that the particle is very small ($a \ll 1$), in which case the Fauxén corrections are negligible. We note that the coefficient of the Basset–Boussinesq memory term is equal to the coefficient of the Stokes drag term times $a/\sqrt{\pi\nu}$. Therefore, assuming that $a/\sqrt{\nu}$ is also very small, we neglect the last term in (6.1), following common practice in the related literature (Michaelides [100]). We finally rescale space, time, and velocity by a characteristic length scale L , characteristic time scale $T = L/U$ and characteristic velocity U , respectively, to obtain the simplified equations of motion

$$\dot{\mathbf{v}} - \frac{3R}{2} \frac{D\mathbf{u}}{Dt} = -\mu(\mathbf{v} - \mathbf{u}) + \left(1 - \frac{3R}{2} \right) \mathbf{g}, \quad (6.2)$$

with

$$R = \frac{2\rho_f}{\rho_f + 2\rho_p}, \quad \mu = \frac{R}{St}, \quad St = \frac{2}{9} \left(\frac{a}{L} \right)^2 \text{Re},$$

and with t , \mathbf{v} , \mathbf{u} and \mathbf{g} now denoting nondimensional variables. Variants of equation (6.2) have been studied by Babiano, Cartwright, Piro and Provenzale [8], Benczik, Toroczka and Tél [15], and Vilela, de Moura and Grebogi [152].

In equation (6.2), St denotes the particle Stokes number and $Re = UL/\nu$ is the Reynolds number. The density ratio R distinguishes neutrally buoyant particles ($R = 2/3$) from aerosols ($0 < R < 2/3$) and bubbles ($2/3 < R < 2$). In the limit of infinitely heavy particles ($R = 0$), equations (6.2) become the Maxey–Riley equations derived originally in [98]. The $3R/2$ coefficient represents the added mass effect: an inertial particle brings into motion a certain amount of fluid that is proportional to half of its mass. For neutrally buoyant particles, the equation of motion is simply $\frac{D}{Dt}(\mathbf{v} - \mathbf{u}) = -\mu(\mathbf{v} - \mathbf{u})$, i.e., the relative acceleration of the particle is equal to the Stokes drag acting on the particle.

Rubin, Jones and Maxey [121] studied (6.2) with $R = 0$ in the special case when \mathbf{u} describes a two-dimensional cellular steady flow model. They used a geometric singular perturbation approach developed by Fenichel [43] to understand particle settling in the flow. The same technique was employed by Burns et al. [24] in the study of particle focusing in the wake of a two-dimensional bluff body flow, which is steady in a frame co-moving with the von Kármán vortex street. Recently, Mograbi and Bar-Ziv [101] discussed this approach for general steady velocity fields and made observations about possible asymptotic behaviors in two dimensions.

Here we construct an attracting slow manifold that governs the asymptotic behavior of particles in system (6.2). We also obtain an explicit dissipative equation, the *inertial equation*, that describes the flow on the slow manifold. This equation has half the dimension of the Maxey–Riley equation; this fact simplifies both the qualitative analysis of inertial dynamics and the numerical tracking of finite-size particles.

Singular perturbation formulation

The derivation of the equation of motion (6.2) is only correct under the assumption $\mu \gg 1$, which motivates us to introduce the small parameter

$$\epsilon = \frac{1}{\mu} \ll 1,$$

and rewrite (6.2) as a first-order system of differential equations:

$$\begin{aligned} \dot{\mathbf{x}} &= \mathbf{v}, \\ \epsilon \dot{\mathbf{v}} &= \mathbf{u}(\mathbf{x}, t) - \mathbf{v} + \epsilon \frac{3R}{2} \frac{D\mathbf{u}(\mathbf{x}, t)}{Dt} + \epsilon \left(1 - \frac{3R}{2}\right) \mathbf{g}. \end{aligned} \quad (6.3)$$

This formulation shows that \mathbf{x} is a slow variable changing at $\mathcal{O}(1)$ speeds, while the fast variable \mathbf{v} varies at speeds of $\mathcal{O}(1/\epsilon)$.

To transform the above singular perturbation problem to a regular perturbation problem, we select an arbitrary initial time t_0 and introduce the fast time τ by letting

$$\epsilon\tau = t - t_0.$$

This type of rescaling is standard in singular perturbation theory with $t_0 = 0$. The new feature here is the introduction of a nonzero present time t_0 about which we introduce the new fast time τ . This trick enables us to extend existing singular perturbation techniques to unsteady flows.

Denoting differentiation with respect to τ by prime, we rewrite (6.3) as

$$\begin{aligned}
\mathbf{x}' &= \epsilon \mathbf{v}, \\
\phi' &= \epsilon, \\
\mathbf{v}' &= \mathbf{u}(\mathbf{x}, \phi) - \mathbf{v} \\
&\quad + \epsilon \frac{3R}{2} \frac{D\mathbf{u}(\mathbf{x}, \phi)}{Dt} \\
&\quad + \epsilon \left(1 - \frac{3R}{2}\right) \mathbf{g},
\end{aligned} \tag{6.4}$$

where $\phi \equiv t_0 + \epsilon\tau$ is a dummy variable that renders the above system of differential equations autonomous in the variables $(\mathbf{x}, \phi, \mathbf{v}) \in \mathcal{D} \times \mathbb{R} \times \mathbb{R}^n$; here n is the dimension of the domain of definition \mathcal{D} of the fluid flow ($n = 2$ for planar flows, and $n = 3$ for three-dimensional flows).

Slow manifold and inertial equation

The $\epsilon = 0$ limit of system (6.4),

$$\begin{aligned}
\mathbf{x}' &= \mathbf{0}, \\
\phi' &= 0, \\
\mathbf{v}' &= \mathbf{u}(\mathbf{x}, \phi) - \mathbf{v},
\end{aligned} \tag{6.5}$$

has an $n + 1$ -parameter family of fixed points satisfying $\mathbf{v} = \mathbf{u}(\mathbf{x}, \phi)$. More formally, for any time $T > 0$, the compact invariant set

$$M_0 = \{(\mathbf{x}, \phi, \mathbf{v}) : \mathbf{v} = \mathbf{u}(\mathbf{x}, \phi), \mathbf{x} \in \mathcal{D}, \phi \in [t_0 - T, t_0 + T]\}$$

is completely filled with fixed points of (6.5). Note that M_0 is a graph over the compact domain

$$D_0 = \{(\mathbf{x}, \phi) : \mathbf{x} \in \mathcal{D}, \phi \in [t_0 - T, t_0 + T]\};$$

we show the geometry of D_0 and M_0 in Figure 6-1.

Inspecting the Jacobian

$$\frac{d}{d\mathbf{v}} [\mathbf{u}(\mathbf{x}, \phi) - \mathbf{v}]_{M_0} = -\mathbf{I}_{n \times n},$$

we find that M_0 attracts nearby trajectories at a uniform exponential rate of $\exp(-\tau)$ (i.e., $\exp(-t/\epsilon)$ in terms of the original unscaled time). In fact, M_0 attracts all the solutions of (6.5) that satisfy $(\mathbf{x}(0), \phi(0)) \in \mathcal{D} \times [t_0 - T, t_0 + T]$; this can be verified using the last equation of (6.5), which is explicitly solvable for any constant value of \mathbf{x} and ϕ . Consequently, M_0 is a compact normally hyperbolic invariant set that has an open domain of attraction. Note that M_0 is not a manifold because its boundary

$$\partial M_0 = \partial \mathcal{D} \times [t_0 - T, t_0 + T] \cup \mathcal{D} \times \{t_0 - T\} \cup \mathcal{D} \times \{t_0 + T\}$$

has corners; $M_0 - \partial M_0$, however, is an $n + 1$ -dimensional normally hyperbolic invariant manifold.

By the results of Fenichel [43] for autonomous systems, any compact normally hyperbolic

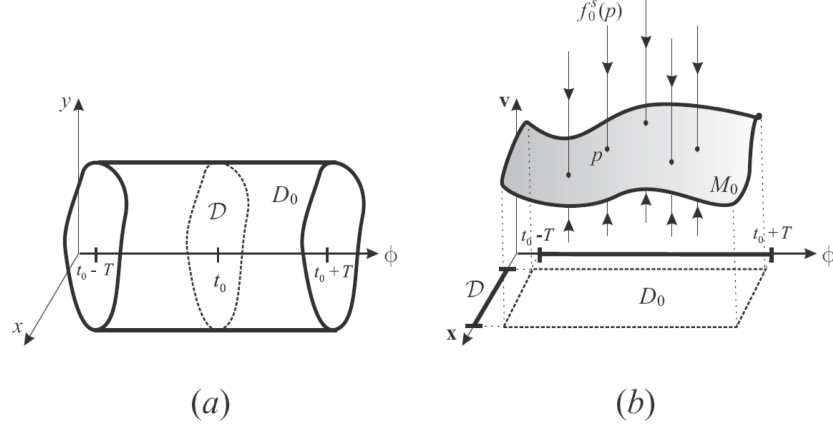


Figure 6-1: (a) The geometry of the domain D_0 (b) The attracting set of fixed points M_0 ; each point p in M_0 has a n -dimensional stable manifold $f_0^s(p)$ (unperturbed stable fiber at p) satisfying $(\mathbf{x}, \phi) = \text{const.}$

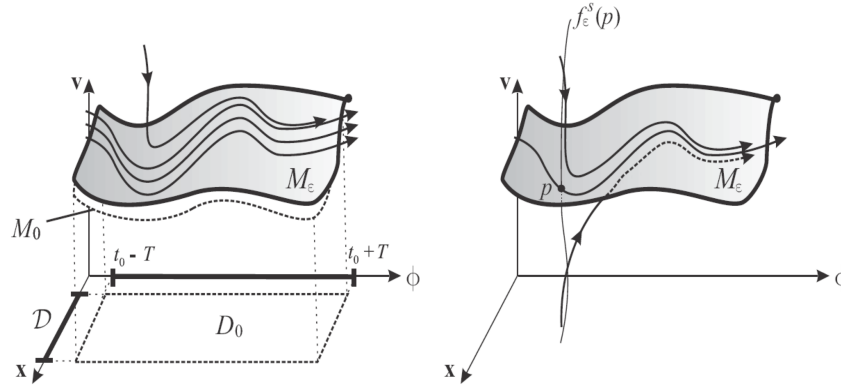


Figure 6-2: (a) The geometry of the slow manifold M_ϵ (b) A trajectory intersecting a stable fiber $f_\epsilon^s(p)$ converges to the trajectory through the fiber base point p .

set of fixed points on (6.5) gives rise to a nearby locally invariant manifold for system (6.4). (Local invariance means that trajectories can only leave the manifold through its boundary.) In our context, Fenichel's results guarantee the existence of $\epsilon_0(t_0, T) > 0$, such that for all $\epsilon \in [0, \epsilon_0)$, system (6.4) admits an attracting locally invariant manifold M_ϵ that is $\mathcal{O}(\epsilon)$ C^r -close to M_0 (See Figure 6-2). The manifold M_ϵ can be written in the form of a Taylor expansion

$$M_\epsilon = \{(\mathbf{x}, \phi, \mathbf{v}) : \mathbf{v} = \mathbf{u}(\mathbf{x}, \phi) + \epsilon \mathbf{u}^1(\mathbf{x}, \phi) + \dots + \epsilon^r \mathbf{u}^r(\mathbf{x}, \phi) + \mathcal{O}(\epsilon^{r+1}), (\mathbf{x}, \phi) \in D_0\}; \quad (6.6)$$

the functions $\mathbf{u}^k(\mathbf{x}, \phi)$ are as smooth as the right-hand side of (6.3). M_ϵ is a *slow manifold*,

because (6.4) restricted to M_ϵ is a slowly varying system of the form

$$\begin{aligned}\mathbf{x}' &= \epsilon \mathbf{v}|_{M_\epsilon} \\ &= \epsilon \left[\mathbf{u}(\mathbf{x}, \phi) + \epsilon \mathbf{u}^1(\mathbf{x}, \phi) + \dots + \epsilon^r \mathbf{u}^r(\mathbf{x}, \phi) + \mathcal{O}(\epsilon^{r+1}) \right].\end{aligned}\tag{6.7}$$

We find the functions $\mathbf{u}^k(\mathbf{x}, \phi)$ using the invariance of M_ϵ , which allows us to differentiate the equation defining M_ϵ in (6.6) with respect to τ . Specifically, differentiating

$$\mathbf{v} = \mathbf{u}(\mathbf{x}, \phi) + \sum_{k=1}^r \epsilon^k \mathbf{u}^k(\mathbf{x}, \phi) + \mathcal{O}(\epsilon^{r+1})$$

with respect to τ gives

$$\mathbf{v}' = \mathbf{u}_x \mathbf{x}' + \mathbf{u}_\phi \phi' + \sum_{k=1}^r \epsilon^k \left[\mathbf{u}_x^k \mathbf{x}' + \mathbf{u}_\phi^k \phi' \right] + \mathcal{O}(\epsilon^{r+1}),\tag{6.8}$$

on M_ϵ , while restricting the \mathbf{v} equations in (6.3) to M_ϵ gives

$$\begin{aligned}\mathbf{v}' &= \left[\mathbf{u} - \mathbf{v} + \epsilon \frac{3R}{2} \frac{D\mathbf{u}}{Dt} + \epsilon \left(1 - \frac{3R}{2} \right) \mathbf{g} \right]_{M_\epsilon} \\ &= - \sum_{k=1}^r \epsilon^k \mathbf{u}^k(\mathbf{x}, \phi) + \epsilon \frac{3R}{2} \frac{D\mathbf{u}}{Dt} + \epsilon \left(1 - \frac{3R}{2} \right) \mathbf{g}.\end{aligned}\tag{6.9}$$

Comparing terms containing equal powers of ϵ in (6.8) and (6.9), then passing back to the original time t , we obtain the following result.

Theorem 14 *For small $\epsilon > 0$, the equation of particle motion (6.7) on the slow manifold M_ϵ can be rewritten as*

$$\dot{\mathbf{x}} = \mathbf{u}(\mathbf{x}, t) + \epsilon \mathbf{u}^1(\mathbf{x}, t) + \dots + \epsilon^r \mathbf{u}^r(\mathbf{x}, t) + \mathcal{O}(\epsilon^{r+1}),\tag{6.10}$$

where r is an arbitrary but finite integer, and the functions $\mathbf{u}^i(\mathbf{x}, t)$ are given by

$$\begin{aligned}\mathbf{u}^1 &= \left(\frac{3R}{2} - 1 \right) \left[\frac{D\mathbf{u}}{Dt} - \mathbf{g} \right], \\ \mathbf{u}^k &= - \left[\frac{D\mathbf{u}^{k-1}}{Dt} + (\nabla \mathbf{u}) \mathbf{u}^{k-1} + \sum_{i=1}^{k-2} \left(\nabla \mathbf{u}^i \right) \mathbf{u}^{k-i-1} \right], \quad k \geq 2.\end{aligned}\tag{6.11}$$

We shall refer to (6.10) with the $\mathbf{u}^i(\mathbf{x}, t)$ defined in (6.11) as the *inertial equation* associated with the velocity field $\mathbf{u}(\mathbf{x}, t)$, because (6.10) gives the general asymptotic form of inertial particle motion induced by $\mathbf{u}(\mathbf{x}, t)$. A leading-order approximation to the inertial equations is given by

$$\dot{\mathbf{x}} = \mathbf{u}(\mathbf{x}, t) + \epsilon \left(\frac{3R}{2} - 1 \right) \left[\frac{D\mathbf{u}(\mathbf{x}, t)}{Dt} - \mathbf{g} \right];\tag{6.12}$$

this is the lowest-order truncation of (6.10) that has nonzero divergence, and hence is capable of capturing clustering or dispersion arising from finite-size effects.

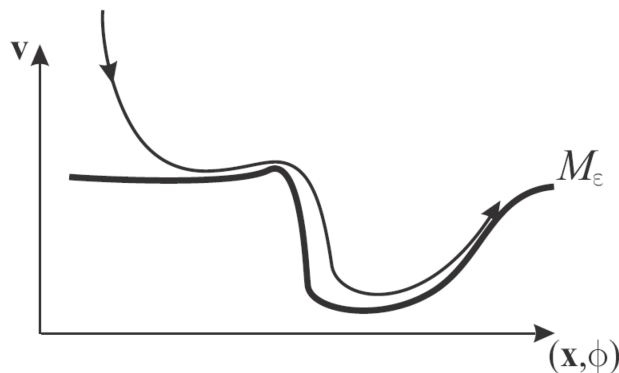


Figure 6-3: Sudden changes in the velocity field delay convergence to the slow manifold.

The above argument renders the slow manifold M_ϵ over the fixed time interval $[t_0 - T, t_0 + T]$. Since the choice of t_0 and T was arbitrary, we can extend the existence result of M_ϵ to an arbitrary long finite time interval.

Slow manifolds are typically not unique, but obey the same asymptotic expansion (6.11). Consequently, any two slow manifolds and the corresponding inertial equations are $\mathcal{O}(\epsilon^r)$ close to each other. Specifically, if $r = \infty$, then the difference between any two slow manifolds is exponentially small in ϵ . The case of neutrally buoyant particles ($R = 2/3$) turns out to be special: the slow manifold is the unique invariant surface

$$M_\epsilon = \{(\mathbf{x}, \phi, \mathbf{v}) : \mathbf{v} = \mathbf{u}(\mathbf{x}, \phi), \quad (\mathbf{x}, \phi) \in D_0\},$$

on which the dynamics coincides with those of infinitesimally small particles. This invariant surface survives for arbitrary $\epsilon > 0$, as noticed by Babiano et al. [8], but may lose its stability for larger values of ϵ .

Convergence to the slow manifold

The results of Fenichel [43] guarantee exponential convergence of solutions of (6.4) to the slow manifold M_ϵ . Translated to the original variables, exponential convergence with a uniform exponent to the slow manifold is only guaranteed over the compact time interval $[t_0 - T, t_0 + T]$.

Over finite time intervals, exponentially dominated convergence is not necessarily monotone. For instance, if the velocity field suddenly changes, say, at speeds comparable to $\mathcal{O}(1/\epsilon)$, then converged solutions may suddenly find themselves again at an increased distance from the slow manifold before they start converging again (cf. Figure 6-3). Again, this is the consequence of the lack of compactness in time, which results in a lack of uniform exponential convergence to the slow manifold over infinite times.

Where do solutions converging to the slow manifold tend asymptotically? Observe that for $\epsilon = 0$, each solution converging to M_0 is confined to an n -dimensional plane

$$f_0^s(p) = \{(\mathbf{x}_p, \phi_p, \mathbf{v}) : p = (\mathbf{x}_p, \phi_p, \mathbf{u}(\mathbf{x}_p, \phi_p)) \in M_0\}.$$

Fenichel refers to $f_0^s(p)$ as the *stable fiber* associated with the point p : each trajectory in

$f_0^s(p)$ converges to the base point of the fiber, p . More generally, a stable fiber has the property that each solution intersecting the fiber converges exponentially in time to the solution passing through the base point of the fiber. The collection of all fibers intersecting M_0 is called the stable foliation of M_0 , or simply the stable manifold of M_0 .

Fenichel [43] showed that the stable foliation of M_0 smoothly persists for small enough $\epsilon > 0$. Specifically, associated with each point $p \in M_\epsilon$, there is an n -dimensional manifold $f_\epsilon^s(p)$ such that any solution of (6.4) intersecting $f_\epsilon^s(p)$ will converge at an exponential rate to the solution that runs through the point p on M_ϵ . The persisting stable fibers $f_\epsilon^s(p)$ are C^r smooth in ϵ , hence they are $\mathcal{O}(\epsilon)$ C^r -close to the invariant planes $f_0^s(p)$, as indicated in Figure 6-2b.

6.2.2 Instabilities on the dynamics of finite-size particles

As we saw in the previous subsection the velocity of a finite-size spherical particle typically differs from the local velocity vector of the ambient fluid flow. In particular, we saw that an exponentially attracting slow manifold exists for general unsteady inertial particle motion as long as the particle Stokes number is small enough. We also derived an explicit reduced equation on the slow manifold (*inertial equation*) that governs the asymptotic behavior of particles. In the case of neutrally buoyant particles (suspensions), the inertial equation coincides with the equations of Lagrangian particle motion. This would seem to imply that neutrally buoyant particles should synchronize exponentially fast with Lagrangian particle dynamics for small Stokes numbers.

By contrast, Babiano *et al.* [8] and Vilela *et al.* [152] give numerical evidence that two-dimensional suspensions do not approach Lagrangian particle motions; instead, their trajectories scatter around unstable manifolds of the Lagrangian particle dynamics. Szeri *et al.* [139] present specific examples of suspended microstructures in two dimensional fluid flows where small changes of the modelling assumptions lead to drastically different dynamics. Babiano *et al.* [8] derive a criterion that characterizes the unstable regions in which scattering of inertial particles occurs. Their derivation follows an Okubo–Weiss-type heuristic reasoning, where it is assumed that the rate of change of the velocity gradient tensor calculated on a particle trajectory is small and hence can be neglected. However, as known counterexamples show (cf. Pierrehumbert and Yang [113] and Boffetta *et al.* [22]) such reasoning, in general, yields incorrect stability results except near fixed points of the flow field.

As we saw in the last subsection for $\epsilon > 0$ small enough, equation (6.2) admits a globally attracting invariant slow manifold. For neutrally buoyant particles, has the form

$$M_\epsilon = \{(\mathbf{x}, \phi, \mathbf{v}) : \mathbf{v} = \mathbf{u}(\mathbf{x}, \phi)\}; \quad (6.13)$$

for non-neutrally-buoyant particles, M_ϵ is given by a graph $\mathbf{v} = \mathbf{u}(\mathbf{x}, \phi) + \mathcal{O}(\epsilon)$.

The dynamics on M_ϵ is governed by the reduced Maxey-Riley equation (*inertial equation*)

$$\dot{\mathbf{x}} = \mathbf{u}(\mathbf{x}, t), \quad (6.14)$$

i.e., by the equation of motion for infinitesimal fluid elements.

Using an observation of Babiano *et al.* [8], we can conclude that the invariant manifold M_ϵ and the corresponding reduced equation (6.14) exists for all values of ϵ in the neutrally

buoyant case. Specifically, for $R = \frac{2}{3}$, equation (6.3) is equivalent to

$$\dot{\mathbf{v}} - \mathbf{u}_t - (\nabla \mathbf{u}) \mathbf{u} = -\mu (\mathbf{v} - \mathbf{u}).$$

As pointed out by Babiano *et al.* [8], this last equation can be recast in the form

$$\dot{\mathbf{v}} - \mathbf{u}_t - (\nabla \mathbf{u}) \mathbf{v} = -\mu (\mathbf{v} - \mathbf{u}) + (\nabla \mathbf{u}) (\mathbf{u} - \mathbf{v}),$$

or, equivalently,

$$\begin{aligned} \frac{d}{dt} [\mathbf{v} - \mathbf{u}(\mathbf{x}, t)] &= -[\nabla \mathbf{u}(\mathbf{x}, t) + \mu \mathbf{I}] [\mathbf{v} - \mathbf{u}(\mathbf{x}, t)], \\ \frac{d}{dt} \mathbf{x} &= \mathbf{v}. \end{aligned} \tag{6.15}$$

This shows that M_ϵ defined in (6.13) is an invariant manifold for any $\mu = 1/\epsilon$.

Global attractivity of the slow manifold

While M_ϵ exists for any $\epsilon > 0$, it is not guaranteed to be globally attracting for larger values of ϵ (i.e., for smaller values of μ). Here we give a sufficient condition under which the globally attractivity of M_ϵ is guaranteed.

Theorem 15 *Assume that for some fixed $\epsilon > 0$, the smallest eigenvalue field $\lambda_{\min}(\mathbf{x}, t)$ of the symmetric tensor field $\mathbf{I} + \epsilon \mathbf{S}(\mathbf{x}, t)$ is uniformly positive for all $\mathbf{x} \in \mathcal{D}$ and $t \in \mathbb{R}^+$. Then the invariant manifold M_ϵ is globally attracting, i.e., all neutrally buoyant particle motions synchronize exponentially fast with infinitesimal Lagrangian fluid trajectories.*

Proof: See Sapsis and Haller 2008 [128].

For two-dimensional incompressible flows, $\lambda_{\min}[\mathbf{I} + \epsilon \mathbf{S}]$ is the smaller root of the characteristic equation

$$\lambda^2 - 2\lambda + (1 + \epsilon^2 \det \mathbf{S}) = 0.$$

Therefore, the two-dimensional version of the sufficient condition in the above theorem requires that

$$\lambda_{\min} = 1 - \epsilon \sqrt{-\det \mathbf{S}(\mathbf{x}, t)} > 0,$$

or, equivalently,

$$\mu - \sqrt{|\det \mathbf{S}(\mathbf{x}, t)|} > 0 \tag{6.16}$$

holds uniformly for all $\mathbf{x} \in \mathcal{D}$ and $t \in \mathbb{R}$.

Note that Theorem 15 may be generalized for the case of non-neutrally buoyant particles by studying the normal stability of the manifold (6.6)

$$M_\epsilon = \{(\mathbf{x}, \phi, \mathbf{v}) : \mathbf{v} = \mathbf{u}(\mathbf{x}, \phi) + \epsilon \mathbf{u}^1(\mathbf{x}, \phi) + \dots + \epsilon^r \mathbf{u}^r(\mathbf{x}, \phi) + \mathcal{O}(\epsilon^{r+1}), (\mathbf{x}, \phi) \in D_0\}.$$

In this case the stability condition takes the form

$$\lambda_{\min} \left[\mathbf{S}(\mathbf{x}(t), t) + \frac{1}{\epsilon} \mathbf{I} \right] + \mathcal{O}(\epsilon) < 0. \tag{6.17}$$

See Appendix C for details.

6.2.3 Clustering of finite-size particles

A well-documented phenomenon displayed by inertial particles is clustering, i.e., concentration into narrow bands. Several studies have analyzed inertial particle dynamics in either analytically defined or numerically generated fluid flows (cf. Maxey and Riley [98], Tang et al. [140], Tio et al. [145], Marcu et al. [94], Martin and Meiburg [95], Marcu and Meiburg [93], Vasiliev and Neishtadt [151], Rubin et al. [121], Crowe et al. [32], Burns et al. [24]). These studies are based on the Maxey-Riley equations [98], the equation of motion for small spherical particles in an unsteady non-uniform flow velocity field.

The first systematic attempt to predict particle clustering appears to be by Rubin et al. [121], who study the settling of aerosol particles in a two-dimensional cellular flow field. Applying results of singular perturbation theory, they show the existence of a globally attracting slow manifold to which inertial particle velocities converge. Reduction to the slow manifold coupled with a subharmonic Melnikov calculation reveals that particles will be attracted to (and hence cluster around) an attracting periodic path as they settle downwards through a cellular flow field. Sedimentation patterns for Stokes particles in a weakly time-periodic flow have been studied by Angilella [4] using similar methods.

Burns et al. [24] investigate the motion of small, dilute spherical particles in the far wake of a bluff body flow model. Using the approach of Rubin et al. [121], they show numerically the existence of a periodic attractor, i.e., the location of clustering in the wake. A more recent numerical study by Vilela et al. [153] visualizes the attractor around which heavy particles cluster in a time-periodic flow.

The objective of the present subsection is to present a general criterion for predicting inertial particle clustering in three-dimensional steady velocity fields of the form

$$\mathbf{u} = (u(\mathbf{x}), v(\mathbf{x}), w(\mathbf{x})), \quad \mathbf{x} = (x, y, z) \in \mathbb{R}^3$$

and in two-dimensional time-periodic velocity fields of the form

$$\mathbf{u} = (u(\mathbf{x}), v(\mathbf{x}), \omega), \quad \mathbf{x} = (x, y, \phi) \in \mathbb{R}^2 \times S^1. \quad (6.18)$$

The latter velocity field is also represented as three-dimensional, including the third velocity component $\dot{\phi} = \omega$ in the three-dimensional extended phase space of the spatial variables (x, y) and the phase variable ϕ on the standard unit circle S^1 .

The main assumption we make is that the underlying fluid velocity field contains at least one closed two-dimensional stream surface. This certainly holds if \mathbf{u} describes a 3D steady Euler flow in which the Beltrami condition does not hold, i.e., vorticity and velocity are never parallel. In this case, the flow is integrable and the flow domain is foliated by continuous families of stream surfaces diffeomorphic cylinders or tori (Arnold and Keshin [6]). Isolated closed stream surfaces will also exist in three-dimensional nonintegrable flows; a well-known example is the non-integrable Arnold–Beltrami–Childress (ABC) flow which has KAM tori (Arnold and Keshin [6]). Finally, KAM tori typically exist in two-dimensional, incompressible flows; their signature is a closed invariant curve for the associated Poincaré map.

Under the above assumption, we use the inertial equation to reduce the full Maxey-Riley dynamics of small inertial particles to a three-dimensional slow manifold. Given the existence of a closed stream surface S_0 , we derive a necessary condition that guarantees the existence of a nearby particle attractor on the slow manifold. The criterion requires the

integral of the normal component of the material derivative

$$\frac{D\mathbf{u}}{Dt} = \mathbf{u}_t + (\nabla\mathbf{u})\mathbf{u}$$

over S_0 to vanish for a nearby attractor S_ϵ to exist for particles of mass ϵ . The vanishing of this integral on S_0 , therefore, predicts clustering on a nearby surface S_ϵ which is diffeomorphic to S_0 .

For the special case when the fluid particle motion is dense in S_0 , we use ergodic theory to reformulate our clustering criterion. The result is a simplified clustering criterion that only requires the evaluation of a line integral along a single fluid trajectory in S_0 . This formulation is particularly helpful for numerically or experimentally generated velocity fields, where exact expressions for closed stream surfaces are not readily available, but individual fluid trajectories are simple to generate.

Formulation

We consider the case of three-dimensional steady flows, and finite size particles for which the stability criterion (6.17) is everywhere valid. In this case a reduction of the dynamics to the slow manifold M_ϵ leads to the *inertial equation*

$$\dot{\mathbf{x}} = \mathbf{u}(\mathbf{x}) + \epsilon \left(\frac{3R}{2} - 1 \right) \left[\frac{D\mathbf{u}(\mathbf{x})}{Dt} - \mathbf{g} \right] + \mathcal{O}(\epsilon^2). \quad (6.19)$$

The above equation also holds for unsteady flows with the appropriate modifications. Specifically, for a two-dimensional velocity field $(u(x, y, \lambda t), v(x, y, \lambda t))$ that is $2\pi/\lambda$ -periodic in time, we let

$$\mathbf{x} = (x, y, \varphi), \quad \mathbf{u} = (u(\mathbf{x}), v(\mathbf{x}), \lambda), \quad (6.20)$$

and observe that the inertial equation (6.19) remains valid. As a result, particle trajectories of such two-dimensional flows approach asymptotically the trajectories of (6.19), as long as ϵ is small enough for condition (6.17) to hold on the domain of interest.

Necessary condition for clustering

For the setting described above, we have the following main result—a necessary condition—for the location of inertial particle clustering.

Assume that the three-dimensional vector field \mathbf{u} (defined as (6.20)) is incompressible, i.e., has zero divergence with respect to its arguments \mathbf{x} . Also assume that S_0 is a compact, two-dimensional stream surface for \mathbf{u} . Let us denote the outward unit normal of S_0 at point \mathbf{x} by $\mathbf{n}(\mathbf{x})$. Then the following hold:

Theorem 16 *Assume that the three-dimensional vector field \mathbf{u} (defined as (6.20)) is incompressible, i.e., has zero divergence with respect to its arguments \mathbf{x} . Also assume that S_0 is a compact, two-dimensional stream surface for \mathbf{u} . Let us denote the outward unit normal of S_0 at point \mathbf{x} by $\mathbf{n}(\mathbf{x})$. Then the following hold:*

(i) *A necessary condition for the existence of an inertial particle attractor S_ϵ that is $O(\epsilon)$ C^1 -close to S_0 is the following:*

$$\int_{S_0} \frac{D\mathbf{u}}{Dt} \cdot \mathbf{n} \, dA = 0, \quad (3R - 2) \int_{S_0} \nabla \left[\frac{D\mathbf{u}}{Dt} \cdot \mathbf{n} \right] \cdot \mathbf{n} \, dA < 0. \quad (6.21)$$

(ii) Assume that S_0 is a two-dimensional torus filled densely with the trajectories of the system $\dot{\mathbf{x}} = \mathbf{u}(\mathbf{x})$. Let $\xi(t)$ be one of these dense trajectories on S_0 . Then condition (6.21) is equivalent to

$$\begin{aligned} \lim_{T \rightarrow \infty} \frac{1}{T} \int_0^T |\dot{\xi}(t)| \left\{ \frac{D\mathbf{u}}{Dt} \cdot \mathbf{n} \right\}_{\mathbf{x}=\xi(t)} dt &= 0, \\ \lim_{T \rightarrow \infty} \frac{3R-2}{T} \int_0^T |\dot{\xi}(t)| \left\{ \nabla \left[\frac{D\mathbf{u}}{Dt} \cdot \mathbf{n} \right] \cdot \mathbf{n} \right\}_{\mathbf{x}=\xi(t)} dt &< 0. \end{aligned} \quad (6.22)$$

Proof: Sapsis and Haller, 2010 [124].

6.3 Dynamics of finite-size particles in stochastic flows

6.3.1 Stochastic velocity field

We will now study the motion of finite-size particles in the presence of flow uncertainty. We consider a random field $u(\mathbf{x}, t; \omega)$, $\mathbf{x} \in D \subseteq \mathbb{R}^n$, $n = 2, 3$, $t \in T$, $\omega \in \Omega$ and we assume that this can be written as the sum of a mean flow $\mathbf{U}(\mathbf{x}, t)$ and a zero-mean stochastic disturbance for which we utilize the stochastic expansion used in the previous chapters

$$\begin{aligned} \mathbf{u}(\mathbf{x}, t; \omega) &= \mathbf{U}(\mathbf{x}, t) + \sum_{i=1}^s Y_i(t; \omega) \mathbf{u}_i(\mathbf{x}, t), \quad \omega \in \Omega \\ &= \mathbf{U}(\mathbf{x}, t) + Y_i(t; \omega) \mathbf{u}_i(\mathbf{x}, t), \quad \omega \in \Omega \end{aligned}$$

Moreover, in what follows we will denote the correlation function that describes their second order characteristics as

$$C_{Y_i Y_j}(t_1, t_2) = E^\omega [Y_i(t_1; \omega) Y_j(t_2; \omega)]$$

Since our study will involve inertial particles it is necessary to consider the acceleration field given by

$$\begin{aligned} \frac{D\mathbf{u}(\mathbf{x}, t; \omega)}{Dt} &= (\nabla \mathbf{u}(\mathbf{x}, t; \omega)) \mathbf{u}(\mathbf{x}, t; \omega) + \mathbf{u}_t(\mathbf{x}, t; \omega) \\ &= \frac{D\mathbf{U}(\mathbf{x}, t)}{Dt} + \mathbf{a}(\mathbf{x}, t; \omega) \end{aligned} \quad (6.23)$$

where

$$\frac{D\mathbf{U}(\mathbf{x}, t)}{Dt} = \mathbf{U}_t(\mathbf{x}, t) + (\nabla \mathbf{U}(\mathbf{x}, t)) \mathbf{U}(\mathbf{x}, t)$$

and

$$\begin{aligned} \mathbf{a}(\mathbf{x}, t; \omega) &= Y_i(t; \omega) [(\nabla \mathbf{U}(\mathbf{x}, t)) \mathbf{u}_i(\mathbf{x}, t) + (\nabla \mathbf{u}_i(\mathbf{x}, t)) \mathbf{U}(\mathbf{x}, t) + \mathbf{u}_{i,t}(\mathbf{x}, t)] \\ &\quad + Y_{i,t}(t; \omega) \mathbf{u}_i(\mathbf{x}, t) \\ &\quad + Y_i(t; \omega) Y_j(t; \omega) (\nabla \mathbf{u}_i(\mathbf{x}, t)) \mathbf{u}_j(\mathbf{x}, t) \end{aligned}$$

with $Y_{i,t}(t; \omega) = \frac{\partial Y_i(t; \omega)}{\partial t}$ and $\mathbf{u}_{i,t}(\mathbf{x}, t) = \frac{\partial \mathbf{u}_i(\mathbf{x}, t)}{\partial t}$. Note that the consideration of a zero-mean random component in the velocity field introduces an extra non zero-mean term in

the acceleration field. Therefore it should be emphasized that

$$E^\omega [\mathbf{a}(\mathbf{x}, t; \omega)] = C_{Y_i Y_j}(t, t) (\nabla \mathbf{u}_i(\mathbf{x}, t)) \mathbf{u}_j(\mathbf{x}, t)$$

6.3.2 Markov (diffusion) approximation

Inserting representations (3.1), (6.23) for the flow velocity and acceleration fields into the equation of motion (6.3) we obtain

$$\epsilon \dot{\mathbf{v}} - \epsilon \frac{3R}{2} \left[\frac{D\mathbf{U}}{Dt} + C_{Y_i Y_j}(t, t) (\nabla \mathbf{u}_i(\mathbf{x}, t)) \mathbf{u}_j(\mathbf{x}, t) \right] = -(\mathbf{v} - \mathbf{U}) + \epsilon \left(1 - \frac{3R}{2} \right) \mathbf{g} + \zeta(\mathbf{x}, t; \omega) \quad (6.24)$$

where $\zeta(\mathbf{x}, t; \omega)$ is a zero-mean stochastic process defined as

$$\begin{aligned} \zeta(\mathbf{x}, t; \omega) = & \left[Y_i(t; \omega) + \epsilon \frac{3R}{2} Y_{i,t}(t; \omega) \right] \mathbf{u}_i(\mathbf{x}, t) \\ & + \frac{3\epsilon R}{2} [Y_i(t; \omega) Y_j(t; \omega) - C_{Y_i Y_j}(t, t)] (\nabla \mathbf{u}_i(\mathbf{x}, t)) \mathbf{u}_j(\mathbf{x}, t) \\ & + \frac{3\epsilon R}{2} Y_i(t; \omega) [(\nabla \mathbf{U}(\mathbf{x}, t)) \mathbf{u}_i(\mathbf{x}, t) + (\nabla \mathbf{u}_i(\mathbf{x}, t)) \mathbf{U}(\mathbf{x}, t) + \mathbf{u}_{i,t}(\mathbf{x}, t)] \end{aligned} \quad (6.25)$$

Note that in (6.24) the term $C_{Y_i Y_j}(t, t) (\nabla \mathbf{u}_i(\mathbf{x}, t)) \mathbf{u}_j(\mathbf{x}, t)$ can also be written as $\nabla_{\mathbf{x}} \mathbf{C}_{\mathbf{u}(\cdot, t) \mathbf{u}(\cdot, t)}(\mathbf{x}, \mathbf{y}) \Big|_{\mathbf{y}=\mathbf{x}}$. Equation (6.24) describes the stochastic dynamics of finite size particles in a random flow. The zero-mean stochastic process $\zeta(\mathbf{x}, t; \omega)$ has in general finite correlation length and therefore (6.24) is not an Ito Stochastic differential equation for which many analytical tools exist to derive equations describing the probability density function of the solution.

In what follows we will derive an Ito SDE that approximates the dynamics of (6.24). This derivation will be based on the assumption of small correlation time length for the stochastic process $\mathbf{Y}(t; \omega)$ (which is the only stochastic ingredient of $\zeta(\mathbf{x}, t; \omega)$) relative to the timescale of the mean flow $\mathbf{U}(\mathbf{x}, t)$, T . As correlation time length of the stochastic process $\mathbf{Y}(t; \omega)$ we define the time $\tau_{\mathbf{Y}}$ for which

$$\tau_{\mathbf{Y}}(t) = \max_{i,j} \tau_{ij}(t) \equiv \max_{i,j} C_{Y_i Y_j}^{-1}(t, t) \int_0^\infty C_{Y_i Y_j}(t, t + \tau) d\tau \quad (6.26)$$

This quantity is a measure of the memory of the stochastic process $\mathbf{Y}(t; \omega)$. For stationary fields the correlation time length is independent of time. For the general case we will assume that the statistical characteristics of the flow are slowly varying (with respect to the memory of the field $\tau_{\mathbf{Y}}$).

For the case where $\tau_{\mathbf{Y}}(t)$ is sufficiently small relative to the deterministic dynamics time scale, i.e. when $\tau_{\mathbf{Y}} < T$, Markov (or Diffusion) approximation can be applied to derive an approximate Ito SDE for the SDE (6.24). This methodology relies on the approximation of the stochastic process $\zeta(\mathbf{x}, t; \omega)$ by a process with independent increments with respect to time (e.g. Brownian motion). Therefore even if the process $\zeta(\mathbf{x}, t; \omega)$ may not possess the property of independent increments (i.e. zero correlation length) if the deterministic dynamics governing the evolution of \mathbf{x}, \mathbf{v} act on a slower time scale than the memory of the stochastic process ζ then the independent increment approximation is valid (Lin & Cai, 1995 [86], Klyatskin, 2005 [65]).

First we transform the above stochastic singular perturbation problem to a regular stochastic perturbation problem by selecting an arbitrary initial time t_0 and introduce the fast time τ by letting

$$\epsilon\tau = t - t_0.$$

Then equation (6.24) will take the form

$$\mathbf{v}' - \epsilon \frac{3R}{2} \left[\frac{D\mathbf{U}}{Dt} + C_{Y_i Y_j}(\phi, \phi) (\nabla \mathbf{u}_i(\mathbf{x}, \phi)) \mathbf{u}_j(\mathbf{x}, \phi) \right] = -(\mathbf{v} - \mathbf{U}) \quad (6.27)$$

$$+ \epsilon \left(1 - \frac{3R}{2} \right) \mathbf{g} + \zeta(\mathbf{x}, \phi; \omega)$$

$$\phi' = \epsilon \quad (6.28)$$

where we denote with prime the differentiation with respect to τ , and $\phi = t_0 + \epsilon\tau$. Then using diffusion approximation, the dynamics can be described by the following Ito SDE (Lin & Cai, 1995 [86], Klyatskin, 2005 [65])

$$d\mathbf{v}(\phi) = \epsilon \frac{3R}{2} \left[\frac{D\mathbf{U}}{Dt} + C_{Y_i Y_j}(\phi, \phi) (\nabla \mathbf{u}_i(\mathbf{x}, \phi)) \mathbf{u}_j(\mathbf{x}, \phi) \right] d\tau \quad (6.29)$$

$$+ \left[-(\mathbf{v} - \mathbf{U}) + \epsilon \left(1 - \frac{3R}{2} \right) \mathbf{g} \right] d\tau + \Sigma(\mathbf{x}, \mathbf{v}, \phi) d\mathbf{W}(\tau; \omega)$$

where in the above there is no drift correction since this is vanishing:

$$\mathcal{F}_i(x, \mathbf{v}, \phi) = \frac{1}{\tau_{\mathbf{Y}}} \int_{\phi}^{\phi + \tau_{\mathbf{Y}}} du \int_{\phi}^u E^{\omega} \left[\frac{\partial \zeta_i(\mathbf{x}, \phi; \omega)}{\partial v_j} \zeta_j(\chi(s; \mathbf{x}, \mathbf{v}, \phi), s; \omega) \right] ds = 0 \quad (6.30)$$

since $\zeta_i(\mathbf{x}, \phi; \omega)$ is independent of \mathbf{v} . Moreover, $\Sigma(\mathbf{x}, \mathbf{v}, \phi)$ is a matrix such that

$$\Sigma_{ik}(\mathbf{x}, \mathbf{v}, \phi) \Sigma_{jk}(\mathbf{x}, \mathbf{v}, \phi) = \frac{1}{\tau_{\mathbf{Y}}} \int_{\phi}^{\phi + \tau_{\mathbf{Y}}} du \int_{\phi}^{\phi + \tau_{\mathbf{Y}}} E^{\omega} [\zeta_i(\chi(u; \mathbf{x}, \mathbf{v}, \phi), u; \omega) \zeta_j(\chi(s; \mathbf{x}, \mathbf{v}, \phi), s; \omega)] ds \quad (6.31)$$

with $\chi(u; \mathbf{x}, \mathbf{v}, \phi_0)$ being the solution of the following deterministic system

$$\frac{d^2 \chi}{d\phi^2} - \epsilon \frac{3R}{2} \left[\frac{D\mathbf{U}}{Dt} + C_{Y_i Y_j}(\phi, \phi) (\nabla \mathbf{u}_i(\chi, \phi)) \mathbf{u}_j(\chi, \phi) \right] = - \left(\frac{d\chi}{d\phi} - \mathbf{U} \right) + \epsilon \left(1 - \frac{3R}{2} \right) \mathbf{g} \quad (6.32)$$

$$\chi(\phi_0) = \mathbf{x} \quad \text{and} \quad \dot{\chi}(\phi_0) = \mathbf{v}$$

We will now proceed to the asymptotic computation of the diffusion coefficient with respect to the correlation time length $\tau_{\mathbf{Y}}$. More specifically from equation (6.31) we may obtain the zero order approximation for the diffusion coefficient by first noting that

$$\tau_{\mathbf{Y}} \rightarrow 0 \Rightarrow C_{Y_i Y_j}(t, s) \rightarrow 2D_{ij}(t) \delta(t - s)$$

where (by direct integration from 0 to ∞ we obtain)

$$D_{ij}(\phi) = \int_0^{\infty} C_{Y_i Y_j}(\phi, \phi + \tau) d\tau. \quad (6.33)$$

The term $D_{ij}(\phi)$ expresses the statistical dependence of the field \mathbf{u}_i on the field \mathbf{u}_j over time and it can be seen as a measure of the intensity of the flow stochasticity. For the case of zero-correlation time length all this statistical dependence is concentrated in the current time instant and therefore we have an infinite correlation (Dirac function). However, this limit can still be used to obtain a zero-order approximation for the the diffusion coefficient. Thus, we will have from equations (6.25) and (6.31) for the diffusion coefficient

$$\begin{aligned} \Sigma_{ik}(\mathbf{x}, \phi) \Sigma_{jk}(\mathbf{x}, \phi) &= \frac{1}{\tau_{\mathbf{Y}}} \int_{\phi}^{\phi+\tau_{\mathbf{Y}}} du \int_{\phi}^{\phi+\tau_{\mathbf{Y}}} E^{\omega} [Y_l(\phi; \omega) Y_k(s; \omega) u_{l,i}(\mathbf{x}, \phi) u_{k,j}(\mathbf{x}, s)] ds + \mathcal{O}(\epsilon \sigma^2) \\ &= \lim_{\tau_{\mathbf{Y}} \rightarrow 0} \frac{1}{\tau_{\mathbf{Y}}} \int_{\phi}^{\phi+\tau_{\mathbf{Y}}} du \int_{\phi}^{\phi+\tau_{\mathbf{Y}}} C_{Y_l Y_k}(\phi, s) u_{l,i}(\mathbf{x}, \phi) u_{k,j}(\mathbf{x}, s) ds + \mathcal{O}\left(\epsilon \sigma^2, \frac{\tau_{\mathbf{Y}}}{T}\right) \\ &= 2D_{lk}(\phi) u_{l,i}(\mathbf{x}, \phi) u_{k,j}(\mathbf{x}, \phi) + \mathcal{O}\left(\epsilon \sigma^2, \frac{\tau_{\mathbf{Y}}}{T}\right) \\ &= 2 \int_0^{\infty} \mathbf{C}_{\mathbf{u}(\cdot, t) \mathbf{u}(\cdot, \phi + \tau)}(\mathbf{x}, \mathbf{x}) d\tau + \mathcal{O}\left(\epsilon \sigma^2, \frac{\tau_{\mathbf{Y}}}{T}\right) \\ &\equiv 2 \Sigma_0 \Sigma_0^T + \mathcal{O}\left(\epsilon \sigma^2, \frac{\tau_{\mathbf{Y}}}{T}\right) \end{aligned}$$

where $\sigma^2 = \max C_{Y_l Y_k}(\phi, \phi)$ expresses the order of the stochastic terms. The above approximation for diffusion coefficient coincide with those that describe the motion of fluid elements (zero-mass particles) in the limit of zero correlation length (see e.g. [65]). Hence, in this level of approximation (weakly stochastic flow) the effect of particle inertia does not enter through the diffusion term.

Using the above expression for the diffusion coefficient we obtain the equation of motion for the finite-size particles in the following form

$$\begin{aligned} d\mathbf{v}(\phi) &= \left[\frac{3\epsilon R}{2} \frac{D\mathbf{U}}{Dt} - (\mathbf{v} - \mathbf{U}) + \epsilon \left(1 - \frac{3R}{2} \right) \mathbf{g} + \frac{3\epsilon R}{2} C_{Y_i Y_j}(\phi, \phi) (\nabla \mathbf{u}_i(\mathbf{x}, \phi)) \mathbf{u}_j(\mathbf{x}, \phi) \right] d\tau \\ &\quad + \sqrt{2} \Sigma_0(\mathbf{x}, \phi) d\mathbf{W}(\tau; \omega) + \mathcal{O}\left(\epsilon, \frac{\tau_{\mathbf{Y}}}{T}\right) \end{aligned}$$

Reverting back to the original time t will result in

$$\begin{aligned} d\mathbf{v}(t) &= \left[\frac{3R}{2} \frac{D\mathbf{U}}{Dt} - \frac{1}{\epsilon} (\mathbf{v} - \mathbf{U}) + \left(1 - \frac{3R}{2} \right) \mathbf{g} + \frac{3R}{2} C_{Y_i Y_j}(t, t) (\nabla \mathbf{u}_i(\mathbf{x}, t)) \mathbf{u}_j(\mathbf{x}, t) \right] dt \\ &\quad + \frac{\sqrt{2}}{\sqrt{\epsilon}} \Sigma_0(\mathbf{x}, t) d\mathbf{W}(t; \omega) + \mathcal{O}\left(\sigma^2, \frac{\tau_{\mathbf{Y}}}{T}\right). \end{aligned} \quad (6.34)$$

Note, that the white noise term scales as

$$\frac{d\mathbf{W}(\tau;\omega)}{d\tau} = \frac{1}{\sqrt{\epsilon}} \frac{d\mathbf{W}(t;\omega)}{dt}$$

since $E^\omega [dW(\tau;\omega)^2] = d\tau$, and $E^\omega [dW(t;\omega)^2] = dt$ and therefore the above rescaling is the one that will give $d\tau = \epsilon dt$.

Examining more carefully equation (6.34), and comparing it with its deterministic counterpart (equation (6.3)) we see the addition of a white noise component but also a new term in the deterministic part of the equation. To understand better this new term we assume that the correlation time length is constant among different stochastic components Y_i . Then, using equation (6.33) as well as the definition of the correlation time length $\tau_{ij}(t)$ (equation (6.26)), we obtain

$$\begin{aligned} \frac{3R}{2} C_{Y_i Y_j}(t, t) (\nabla \mathbf{u}_i(\mathbf{x}, t)) \mathbf{u}_j(\mathbf{x}, t) &= \frac{3R}{2\tau_Y(t)} D_{ij}(t) (\nabla \mathbf{u}_i(\mathbf{x}, t)) \mathbf{u}_j(\mathbf{x}, t) \\ &= \frac{3R}{2\tau_Y(t)} \int_0^\infty \nabla_{\mathbf{x}} \mathbf{C}_{\mathbf{u}(\cdot, t) \mathbf{u}(\cdot, t+\tau)}(\mathbf{x}, \mathbf{y}) \Big|_{\mathbf{y}=\mathbf{x}} d\tau \end{aligned}$$

This term is related exclusively to the inertial dynamics of the finite-size particles and for sufficiently small correlation time length its effect can become comparable with the effect of the mean flow (or even more intense). Therefore, consideration of random fields that have zero correlation time length (i.e. Kraichnan fields [70]) will result unbounded acceleration on the right hand side of the equation of motion, except of the case of aerosol particles ($R = 0$) [12].

6.3.3 Stochastic slow manifold

For simplicity we will assume now that all stochastic components Y_i have the same correlation time length τ_Y which is assumed constant or sufficiently slowly varying. Then the equation describing the motion of finite size particles will have the form

$$d\mathbf{x} = \mathbf{v} dt \tag{6.35a}$$

$$\begin{aligned} d\mathbf{v} &= \left[\frac{3R}{2} \frac{D\mathbf{U}}{Dt} - \frac{1}{\epsilon} (\mathbf{v} - \mathbf{U}) + \left(1 - \frac{3R}{2} \right) \mathbf{g} + \frac{3R}{2} C_{Y_i Y_j}(t, t) (\nabla \mathbf{u}_i(\mathbf{x}, t)) \mathbf{u}_j(\mathbf{x}, t) \right] dt \\ &+ \frac{\sqrt{2}}{\sqrt{\epsilon}} \Sigma_0(\mathbf{x}, t) d\mathbf{W}(t;\omega) + \mathcal{O}\left(\sigma^2, \frac{\tau_Y}{T}\right) \end{aligned} \tag{6.35b}$$

where $\Sigma_0 \Sigma_0^T = \int_0^\infty \mathbf{C}_{\mathbf{u}(\cdot, t) \mathbf{u}(\cdot, t+\tau)}(\mathbf{x}, \mathbf{x}) d\tau$.

System (6.35) is a stochastic singular perturbation problem which in the absence of stochastic excitation and in the limit $\epsilon = 0$ admits a globally attracting invariant manifold (see Section 1 of current chapter). Therefore, from Berglund and Gentz, 2003 [17] we have the existence of a stochastic slow manifold

$$\mathcal{M}_\epsilon^\omega = \{(\mathbf{x}, \mathbf{v}) \mid \mathbf{v} = \mathbf{u}_\epsilon(\mathbf{x}, t, \epsilon; \omega)\}$$

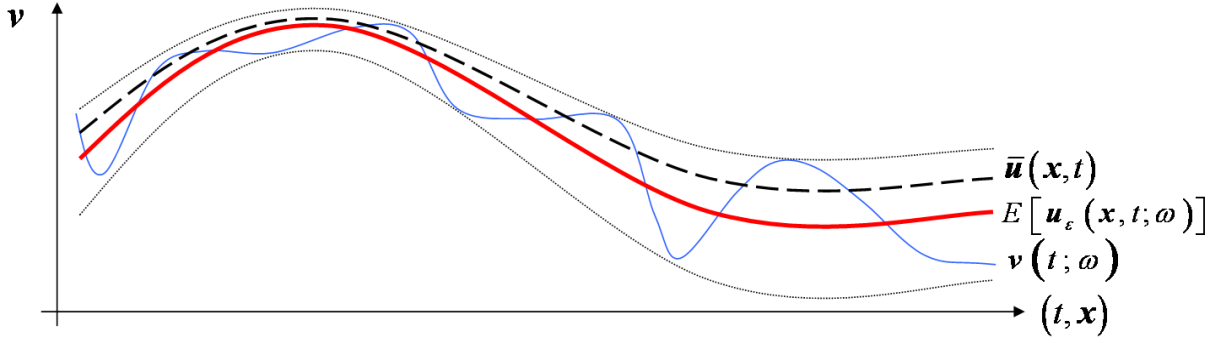


Figure 6-4: Particle velocity (blue solid curve) attracted by a concentrated layer of probability, a stochastic slow manifold. The red solid curve denotes the mean of the manifold and the dotted curves define the local spread of probability around the mean.

which has the form of a concentrated probability measure around the deterministic slow manifold and which attract solutions of the stochastic differential equation (6.35) (Figure 6-4). In what follows we will determine the second order stochastic characteristics of the stochastic slow manifold, i.e. mean and variance.

Mean of the stochastic slow manifold

To determine the mean of the stochastic slow manifold we use the invariance property of $\mathbf{u}_\epsilon(\mathbf{x}, t, \epsilon; \omega)$ and apply the mean value operator to equation (6.35b). The last term vanishes because of the non-anticipative property of white-noise [136]. Therefore we obtain

$$\begin{aligned} \frac{d\bar{\mathbf{v}}}{dt} &= \frac{3R}{2} \frac{D\mathbf{U}}{Dt} - \frac{1}{\epsilon} (\bar{\mathbf{v}} - \mathbf{U}) + \left(1 - \frac{3R}{2}\right) \mathbf{g} \\ &+ \frac{3R}{2} C_{Y_i Y_j}(t, t) (\nabla \mathbf{u}_i(\mathbf{x}, t)) \mathbf{u}_j(\mathbf{x}, t) \end{aligned} \quad (6.36)$$

Expanding in the same way we did in the proof of Theorem 14 the mean of the stochastic slow manifold, $\bar{\mathbf{v}}$ with respect to ϵ we obtain

$$\begin{aligned} \bar{\mathbf{u}}_\epsilon(\mathbf{x}, t, \epsilon) &= \mathbf{U} + \epsilon \left(1 - \frac{3R}{2}\right) \left[\mathbf{g} - \frac{D\mathbf{U}}{Dt} - C_{Y_i Y_j}(t, t) (\nabla \mathbf{u}_i(\mathbf{x}, t)) \mathbf{u}_j(\mathbf{x}, t) \right] \\ &+ \mathcal{O}\left(\epsilon^2, \epsilon\sigma^2, \frac{\tau Y}{T}\right) \end{aligned} \quad (6.37)$$

Variance of the stochastic slow manifold

To determine the variance of the probability measure around the mean value of the stochastic slow manifold we consider equation (6.35b). with $\mathbf{v} = \mathbf{u}_\epsilon$ (\mathbf{u}_ϵ is invariant manifold for (6.35b)) and we subtract from it equation (6.36). Then by setting $\xi_s = \mathbf{v} - \bar{\mathbf{u}}_\epsilon$ we obtain

$$d\xi_s = -\frac{1}{\epsilon} \xi_s dt + \frac{\sqrt{2}}{\sqrt{\epsilon}} \Sigma_0(\mathbf{x}, t) d\mathbf{W}(t; \omega) + \mathcal{O}\left(\epsilon, \sigma^2, \frac{\tau Y}{T}\right) \quad (6.38)$$

Now, from equation (6.38) we have

$$\begin{aligned}\xi_s(t + \Delta t) &= \xi_s(t) - \frac{1}{\epsilon} \xi_s(t) \Delta t + \frac{\sqrt{2}}{\sqrt{\epsilon}} \Sigma_0(\mathbf{x}, t) \Delta \mathbf{W}(t; \omega) \Rightarrow \\ \overline{\xi_s^2(t + \Delta t)} &= \overline{\xi_s^2(t)} - \frac{2}{\epsilon} \overline{\xi_s^2(t)} \Delta t + \frac{2}{\epsilon} \Sigma_0^T(\mathbf{x}, t) \Sigma_0(\mathbf{x}, t) \Delta t\end{aligned}$$

where $\overline{\xi_s^2(t)} = E^\omega \left[\xi_s(t; \omega) \xi_s(t; \omega)^T \right]$. Therefore, in the limit $\Delta t \rightarrow 0$ we have

$$\frac{d\overline{\xi_s^2}}{dt} = -\frac{2}{\epsilon} \overline{\xi_s^2} + \frac{2}{\epsilon} \Sigma_0^T(\mathbf{x}, t) \Sigma_0(\mathbf{x}, t)$$

From the last equation we obtain the zero-order approximation for the variance of the stochastic slow manifold

$$\overline{\xi_s^2}(\mathbf{x}, t, \epsilon) = \Sigma_0^T(\mathbf{x}, t) \Sigma_0(\mathbf{x}, t) + \mathcal{O}\left(\epsilon \sigma^2, \frac{\tau_Y}{T}\right). \quad (6.39)$$

The last equation describes the local variance of the stochastic slow manifold.

6.3.4 Stochastic inertial equation

The next step of our analysis will involve the formulation of a reduced order stochastic differential equation, a stochastic inertial equation, that will describe the reduced order dynamics on the stochastic slow manifold. Taking into account equation (6.37), (6.39) and the fact that we are already in the delta correlated regime we have the following Ito stochastic differential equation approximating the dynamics of the full slow fast system for order 1 timescales ([18])

$$\begin{aligned}d\mathbf{x} &= \mathbf{U} dt + \epsilon \left(1 - \frac{3R}{2}\right) \left[\mathbf{g} - \frac{D\mathbf{U}}{Dt} \right] dt \\ &- \epsilon \left(1 - \frac{3R}{2}\right) C_{Y_i Y_j}(t, t) (\nabla \mathbf{u}_i(\mathbf{x}, t)) \mathbf{u}_j(\mathbf{x}, t) dt \\ &+ \Sigma_0^T(\mathbf{x}, t) \nabla \Sigma_0(\mathbf{x}, t) dt + \sqrt{2} \Sigma_0(\mathbf{x}, t) d\mathbf{W}(t; \omega) + \mathcal{O}\left(\epsilon^2, \epsilon \sigma^2, \frac{\tau_Y}{T}\right)\end{aligned} \quad (6.40)$$

where the new term on the deterministic part of the right hand side is the Wong-Zakai correction ([159], [86]) due to the spatial dependence of $\Sigma_0(\mathbf{x}, t)$. For $\epsilon = 0$ the above inertial equation is reduced to the delta-correlated approximation for the description of fluid elements in random flows ([65]). On the other hand for zero stochasticity of the flow we recover the corresponding approximation of the deterministic inertial equation derived in the first section.

Analyzing the terms on the right hand side we have for each line: i) the deterministic effect of particles inertia, ii) the coupled effect of particles inertia and flow uncertainty, iii) the effect of the random flow. Thus, the diffusion coefficient and the associated drift correction, in this level of approximation, do not take into account the effect of particles inertia. The coupled effect of particles inertia and flow stochasticity is expressed through the term $\epsilon \left(\frac{3R}{2} - 1\right) C_{Y_i Y_j}(t, t) (\nabla \mathbf{u}_i(\mathbf{x}, t)) \mathbf{u}_j(\mathbf{x}, t)$ and as we shall see in the applications it plays an important role for the formation of clustering regions for finite-size particles different than those predicted by the mean flow.

Using this equation we can directly obtain a transport equation for the probability density function describing the evolution of finite-size tracers in a random field. Specifically, the stochastic inertial equation is equivalent with the following Fokker-Planck-Kolmogorov equation [136] describing the probability density function or the concentration $c(\mathbf{x}, t)$ of finite-size tracers

$$\begin{aligned} & \frac{\partial c}{\partial t} + \frac{\partial}{\partial x_i} \left[c \left(\overline{u_{\epsilon,i}}(\mathbf{x}, t, \epsilon) + \Sigma_{0,jm}(\mathbf{x}, t) \frac{\partial}{\partial x_j} \Sigma_{0,im}(\mathbf{x}, t) \right) \right] \\ &= \frac{\partial^2}{\partial x_i \partial x_j} (\Sigma_{0,ik}(\mathbf{x}, t) \Sigma_{0,jk}(\mathbf{x}, t) c) \end{aligned}$$

Note, that

$$\begin{aligned} \frac{\partial^2}{\partial x_i \partial x_j} (\Sigma_{0,ik}(\mathbf{x}, t) \Sigma_{0,jk}(\mathbf{x}, t) c) &= \frac{\partial}{\partial x_i} \left(\frac{\partial}{\partial x_j} [\Sigma_{0,ik}(\mathbf{x}, t) \Sigma_{0,jk}(\mathbf{x}, t)] c \right) \\ &+ \frac{\partial}{\partial x_i} \left(\Sigma_{0,ik}(\mathbf{x}, t) \Sigma_{0,jk}(\mathbf{x}, t) \frac{\partial c}{\partial x_j} \right) \end{aligned}$$

However,

$$\begin{aligned} \frac{\partial}{\partial x_j} [\Sigma_{0,ik}(\mathbf{x}, t) \Sigma_{0,jk}(\mathbf{x}, t)] &= D_{lk}(t) \frac{\partial}{\partial x_j} u_{l,i}(\mathbf{x}, t) u_{k,j}(\mathbf{x}, t) \\ &= D_{lk}(t) \left[\frac{\partial u_{l,i}(\mathbf{x}, t)}{\partial x_j} u_{k,j}(\mathbf{x}, t) + \frac{\partial u_{k,j}(\mathbf{x}, t)}{\partial x_j} u_{l,i}(\mathbf{x}, t) \right] \\ &= D_{lk}(t) \frac{\partial u_{l,i}(\mathbf{x}, t)}{\partial x_j} u_{k,j}(\mathbf{x}, t) \tag{6.41} \\ &= \Sigma_{0,jm}(\mathbf{x}, t) \frac{\partial}{\partial x_j} \Sigma_{0,im}(\mathbf{x}, t). \end{aligned}$$

where the last term in the second line vanishes due to incompressibility of $\mathbf{u}_k(\mathbf{x}, t)$. Therefore, the transport equation will take the form

$$\begin{aligned} & \frac{\partial c}{\partial t} + \frac{\partial}{\partial x_i} \left[c \left(U_i + \epsilon \left(1 - \frac{3R}{2} \right) \left[\mathbf{g} - \frac{DU_i}{Dt} - C_{Y_k Y_l}(t, t) \frac{\partial u_{k,i}(\mathbf{x}, t)}{\partial x_m} u_{l,m}(\mathbf{x}, t) \right] \right) \right] \\ &= \frac{\partial}{\partial x_i} \left(\Sigma_{0,ik}(\mathbf{x}, t) \Sigma_{0,jk}(\mathbf{x}, t) \frac{\partial c}{\partial x_j} \right) \end{aligned}$$

or equivalently

$$\begin{aligned} & \frac{\partial c}{\partial t} + \frac{\partial}{\partial x_i} \left[c \left(U_i + \epsilon \left(1 - \frac{3R}{2} \right) \left[\mathbf{g} - \frac{DU_i}{Dt} - C_{Y_k Y_l}(t, t) \frac{\partial u_{k,i}(\mathbf{x}, t)}{\partial x_m} u_{l,m}(\mathbf{x}, t) \right] \right) \right] \\ &= \frac{\partial}{\partial x_i} \left(\frac{\partial c}{\partial x_j} \int_0^\infty \mathbf{C}_{u_i(\cdot, t) u_j(\cdot, t+\tau)}(\mathbf{x}, \mathbf{x}) d\tau \right). \end{aligned}$$

The last equation describes the forward evolution of the concentration for finite-size particles with given characteristics ϵ, R under the assumption of small correlation time length for the stochasticity of the velocity field relative to the mean field dynamics.

6.3.5 Stochastic source inversion

The stochastic inertial equation may also be used for the source-inversion of finite-size particles in the presence of diffusion or flow uncertainty. More specifically, as it is shown in Haller and Sapsis, 2008 [56] the reduced order inertial equation for deterministic flows can be inverted since the reduction to the slow manifold does not allow for numerical instabilities; this is not the case if we use the full set of dynamical equations (6.3) since the strong attraction to the invariant slow manifold (in forward time) will cause numerical blow-ups if we try to solve these equations backwards.

This is also the case for stochastic flows. Equation (6.40) is numerically well defined both in forward and backward time since the vector field on the right hand side is a small deformation of passive scalar advection due to the inertial terms and the presence of noise. This allows us to obtain the initial position of inertial particles with some uncertainty due to the randomness of the flow.

6.4 Higher order Lagrangian stochastic models

In the previous section we derived a Lagrangian stochastic model based on the diffusion approximation of the random terms. As we saw in the first level approximation inertia does not modify the effect of diffusivity. Therefore, inertial particles diffuse in the same manner as fluid particles. This is not the case for the deterministic terms of the inertial equation where the effect of particles finite-size enters explicitly. The expression for the diffusion coefficient was derived based on the assumption of very small correlation time length for the stochastic term, which allowed us to apply diffusion approximation. However, other methods may also be used for the description of the diffusive dynamics.

Methods which are based on the well-mixed condition [144] allows us to derive higher order Lagrangian models for the description of the diffusive dynamics of fluid elements. In this framework it is assumed that the Eulerian velocity that the particle ‘feels’ evolves in a Markovian manner. Based on these assumptions Thomson [144] considered models of fluid particle trajectories in which the trajectories in the (\mathbf{x}, \mathbf{v}) –space are Markovian, continuous and have the same local structure as a process with independent increments. Such processes can be represented as solutions of Ito stochastic differential equations (cf. [138]). Based on the same arguments, we may assume that the evolution of inertial particles is described by the stochastic model

$$\begin{aligned} d\mathbf{x} &= \mathbf{U}dt + \epsilon \left(1 - \frac{3R}{2}\right) \left[\mathbf{g} - \frac{D\mathbf{U}}{Dt}\right] dt \\ &\quad - \epsilon \left(1 - \frac{3R}{2}\right) C_{Y_i Y_j}(t, t) (\nabla \mathbf{u}_i(\mathbf{x}, t)) \mathbf{u}_j(\mathbf{x}, t) dt + v dt \\ dv &= \mathbf{f}(t, \mathbf{x}, v) dt + \sigma_v \mathbf{F}(t, \mathbf{x}, v) d\mathbf{W}(t; \omega) \end{aligned} \quad (6.42)$$

where the drift and diffusion coefficients \mathbf{f}, \mathbf{F} are defined based on the well-mixed condition ([144], see also [20]) which essentially guarantees that the produced process $v(t; \omega)$ will have at every time instant the exact same statistics with the Eulerian velocity field $\mathbf{u}(\mathbf{x}, t; \omega)$ at the location $\mathbf{x} = \mathbf{x}(t; \omega)$, where the particle is currently moving.

The main difference of the inertial particle model (6.42) with (6.40) is the addition of more memory in the diffusive dynamics, by increasing the order of the model (two stochastic equations instead of one). However, this is also the main disadvantage of equation (6.42)

since the formulation of a transport equation for the concentration field of inertial particles will lead to an advection-diffusion equation involving six spatial variables (three for the position and three for the velocity). Therefore, higher order inertial particle models may only be solved through Monte-Carlo simulation.

A final remark on the above discussion is that through the above method inertial effects may also be taken into account in the diffusive dynamics if one applies the well-mixed condition directly to the statistics of the Eulerian field $\zeta(\mathbf{x}, t; \omega)$ (see equation (6.25) for definition) instead of the Eulerian statistics of the flow field $\mathbf{u}(\mathbf{x}, t; \omega)$ (which is the first level of approximation for the diffusivity of inertial tracers as shown in Section 6.3.2).

6.5 Clustering due to stochasticity of the flow

In this section we will discuss the coupled effect of flow stochasticity and particles inertia on the clustering properties of finite-size particles. By clustering of finite-size particles in random flows we mean the formation of narrow zones in the physical phase space where the concentration of finite-size particles becomes very important. In Section 6.2.3 we saw that in deterministic flows the cause for the formation of these zones is the dissipative dynamics induced by the order ϵ terms in the inertial equation.

For the case of random flows, as we saw in Section 6.3.4, we have the dissipative term $\epsilon \left(1 - \frac{3R}{2}\right) \left[\mathbf{g} - \frac{D\mathbf{U}}{Dt}\right]$ found also in the deterministic analysis, the white noise term with the associated drift correction $\Sigma_0^T(\mathbf{x}, t) \nabla \Sigma_0(\mathbf{x}, t)$, but also the new term $\epsilon \left(1 - \frac{3R}{2}\right) C_{Y_i Y_j}(t, t) (\nabla \mathbf{u}_i(\mathbf{x}, t)) \mathbf{u}_j(\mathbf{x}, t)$ which expresses (to the first order) the coupled effect of particles inertial and flow stochasticity. The combined effect of the deterministic terms on the right hand side of (6.40) causes particles to be attracted by critical manifolds in the flow which are, in general, different by those of the mean flow alone. On the other hand the existence of noise prevents the particles to cluster on lower dimensional manifolds (which is the case in deterministic flows) since it induces diffusive behavior. The result is particles to concentrate smoothly around the critical manifolds defined by the deterministic part of the right hand side of (6.40).

In what follows we will analyze more rigorously this behavior. Before we proceed to this analysis let us understand better the physical effect of the new term $\epsilon \left(1 - \frac{3R}{2}\right) C_{Y_i Y_j}(t, t) (\nabla \mathbf{u}_i(\mathbf{x}, t)) \mathbf{u}_j(\mathbf{x}, t)$ on the deterministic part of the inertial equation by considering the following simplified case. Assume we have a zero mean random flow field which has the following form

$$\mathbf{u}(\mathbf{x}, t; \omega) = Y(t; \omega) \mathbf{u}_0(\mathbf{x}, t) \quad (6.43)$$

where $Y(t; \omega)$ is a zero mean Gaussian process and $\mathbf{u}_0(\mathbf{x}, t)$ is a deterministic flow field for which the deterministic clustering criterion presented previously can be applied. Furthermore, we assume that there is a manifold S_0 in the physical phase space such that the clustering criterion (in the following form; see Sapsis and Haller 2010 [124] for details) holds, i.e.

$$\int_{\text{Int}(S_0)} \nabla \cdot \frac{D\mathbf{u}}{Dt} dV = 0$$

The above condition can also be written as

$$\int_{\text{Int}(S_0)} \nabla \cdot [(\nabla \mathbf{u}_0) \mathbf{u}_0] dV = 0.$$

An interesting feature of the last condition is its independence of the sign of the flow.

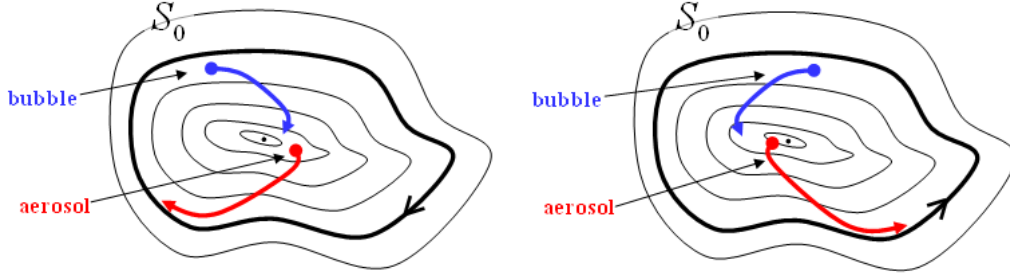


Figure 6-5: Clustering manifold is independent from the flow direction.

Additionally, a similar argument on the second condition

$$(3R - 2) \int_{S_0} \nabla \left[\frac{D\mathbf{u}}{Dt} \cdot \mathbf{n} \right] \cdot \mathbf{n} dA < 0,$$

which defines the kind of the particles (bubbles or aerosols) that will cluster around S_0 , reveals that particles (either bubbles or aerosols) will cluster around S_0 independently from the direction of the flow. Therefore, returning to the stochastic flow field (6.43), we conclude that the same kind of clustering (i.e. same kind of particles and same location) will occur for both the cases where $Y(t; \omega)$ is positive and negative (Figure 6-5).

Thus, a zero mean stochastic perturbation on the flow velocity field can induce non-zero probability for particles clustering, assuming that the geometry of the perturbation has a suitable spatial form to cause clustering. This is exactly the effect that the coupling term $\epsilon \left(1 - \frac{3R}{2}\right) C_{Y_i Y_j}(t, t) (\nabla \mathbf{u}_i(\mathbf{x}, t)) \mathbf{u}_j(\mathbf{x}, t)$ expresses in the inertial equation. It induces clustering of particles and depends on the covariance of the stochastic coefficients and the geometry of the stochastic perturbations.

For the general case of two-dimensional, random, periodic flows (or three dimensional random time-independent flows) we will use the unified setting described in Section 6.2.3. For this case we first consider the following deterministic system (using the notation defined in (6.20))

$$\begin{aligned} \dot{\mathbf{x}} = v(\mathbf{x}, \varphi) \equiv & \mathbf{U}(\mathbf{x}, \varphi) - \epsilon \left(1 - \frac{3R}{2}\right) C_{Y_i Y_j}(\varphi, \varphi) (\nabla \mathbf{u}_i(\mathbf{x}, \varphi)) \mathbf{u}_j(\mathbf{x}, \varphi) \\ & + \Sigma_0^T(\mathbf{x}, \varphi) \nabla \Sigma_0(\mathbf{x}, \varphi) + \epsilon \left(1 - \frac{3R}{2}\right) \left[\mathbf{g} - \frac{D\mathbf{U}}{Dt}(\mathbf{x}, \varphi) \right] \end{aligned} \quad (6.44)$$

The last equation is the deterministic part of the stochastic inertial equation. Theorem 5.1.6 from Berglund and Gentz [18] guarantees that an attracting manifold for a deterministic system such as (6.44) will persist as a domain of high concentration in the presence of additive noise, i.e. for the full inertial stochastic equation (i.e. including the white-noise term), assuming that the noise intensity does not exceed in size (order of magnitude) the deterministic terms.

Therefore, it is sufficient to describe the clustering regions for the dissipative deterministic dynamical system (6.44). This can be done with direct numerical integration of

equation (6.44) or by assuming a decomposition of the vector field $v(\mathbf{x}, \varphi)$ in the form of an irrotational and incompressible component. Specifically, if we assume that there is a potential $\phi(\mathbf{x}, \varphi)$ and a streamfunction $\psi(\mathbf{x}, \varphi)$ such that

$$v(\mathbf{x}, \varphi) = \nabla \times \psi(\mathbf{x}, \varphi) + \nabla \phi(\mathbf{x}, \varphi)$$

then we will have $\psi \sim \mathcal{O}(1)$ (since this term will contain the effect of the incompressible field $\mathbf{U}(\mathbf{x}, \varphi)$) while $\phi \sim \mathcal{O}(\epsilon)$. Based on this decomposition we are able to apply directly the analytical results of Theorem 16 and predict whether an invariant manifold for the incompressible flow $\dot{\mathbf{x}} = \nabla \times \psi(\mathbf{x}, \varphi)$ will persist as a clustering manifold for equation (6.44) and thus for the full stochastic inertial equation.

We emphasize that the invariant manifolds (if those exist) for the incompressible flow $\dot{\mathbf{x}} = \nabla \times \psi(\mathbf{x}, \varphi)$ are in general different from those predicted by the mean field equation $\dot{\mathbf{x}} = \mathbf{U}(\mathbf{x}, \varphi)$ since there are terms that constitute $v(\mathbf{x}, \varphi)$, other than $\mathbf{U}(\mathbf{x}, \varphi)$, which are incompressible and therefore they contribute to the streamfunction ψ . This will be also illustrated in the numerical example presented in the following section.

6.6 Application: Particles in the double gyre flow

To illustrate our theoretical findings we consider the stochastic double gyre flow analyzed in Chapter 5. Specifically, we consider the case presented in Section 5.8.3 for $\text{Re} = 25$ with different parameters. After computing the stochastic flow field we rescale time by a factor of 100. The dimensional parameters of the flow are presented in 6.1.

In Figure 6-6 we present the stochastic flow field. Specifically, the mean flow field $\mathbf{U}(\mathbf{x}, t)$ is shown in the left-top plot (the colormap indicates the vorticity and the solid curves the streamlines of the flow). For this case of parameters we have two stochastic perturbations $\mathbf{u}_i(\mathbf{x}, t)$, $i = 1, 2$ shown in the lower plots along with the corresponding probability density functions of the stochastic coefficients $Y_i(t; \omega)$. The variance $E^\omega [Y_i^2(t; \omega)]$ of each of the stochastic perturbations is shown in the right-top plot as blue solid curves. The red curve indicates the energy of the mean flow, $\frac{1}{2} \int |\mathbf{U}(\mathbf{x}, t)|^2 d\mathbf{x}$.

We will study the motion of finite-size particles for $t = 100$ where the a typical stochastic perturbation has an order of magnitude of 10% of the typical amplitude of the mean flow; therefore in this regime we expect the effect of flow uncertainty to be comparable with the effect of inertia. After $t = 100$ the dynamics of the mean flow have converged to a stationary regime, while the most energetic stochastic mode has converged to a periodic attractor with period of oscillation ($T \sim 2$) comparable with the time scale of motion for the finite-size particles. Therefore, this is a case of unsteady flow with non-stationary statistics.

Note, that for particles having size $\epsilon = 10^{-2}$ or smaller the stability criterion (6.17) is satisfied for almost every flow realization ω , everywhere in the domain. Therefore, the reduction to the stochastic inertial manifold is valid.

6.6.1 Stochastic slow manifold in the flow

We consider heavy particles with $\epsilon = 0.001$ and $R = 0.4$. In Figure 6-7 we present the modulus of the velocity of the slow manifold $|\bar{\mathbf{u}}_\epsilon(\mathbf{x}, t, \epsilon)|$ with respect to the horizontal dimensions x and y and for $t = 100$. In this time regime the mean flow has converged to a steady form even though the stochastic perturbations perform a periodic oscillation. This

Table 6.1: Reference values of parameters in the barotropic QG model used for the study of finite-size particles (dimensional).

Parameter	Value	Parameter	Value
U	$7.1 \times 10^{-1} m.s^{-1}$	L	$1.0 \times 10^6 m$
L/U	16.27 days	D	2500 m
τ_0	$1.26 \times 10^{-1} Pa$	β_0	$7.1 \times 10^{-12} (m.s)^{-1}$
ρ	$10^3 Kg.m^{-3}$	f_0	$5.0 \times 10^{-5} s^{-1}$

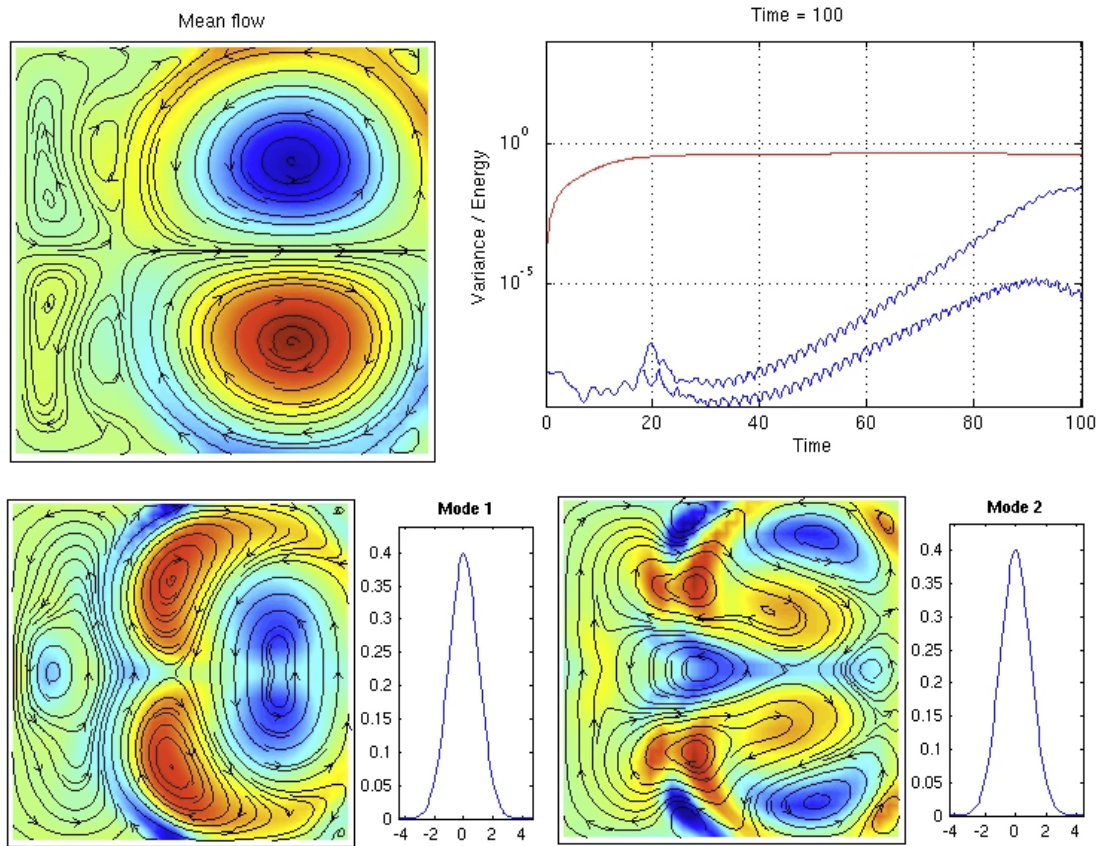


Figure 6-6: Stochastic double gyre for the illustration of the inertial particles motion; $Re = 25$ (See chapter 5 for details).

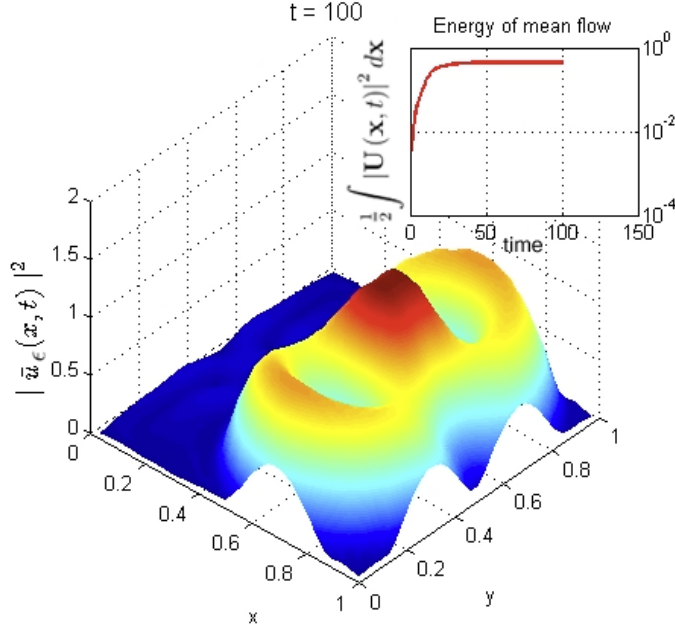


Figure 6-7: Mean value of the stochastic slow manifold governing the motion of inertial particles for the double gyre stochastic flow.

is clearly seen from the top-right plot where we present the energy of the mean flow (red curve).

In Figures 6-8 and 6-9 we show the spatial distribution of uncertainty in the stochastic slow manifold by plotting the quantity

$$\sigma_s(\mathbf{x}, t) = \frac{1}{\text{trace}[\mathbf{C}_{\mathbf{Y}(t)}\mathbf{Y}(t)]} \int_0^\infty \|\mathbf{C}_{\mathbf{u}(\cdot, t)\mathbf{u}(\cdot, t+\tau)}(\mathbf{x}, \mathbf{x})\| d\tau$$

for different time instants, where $\|\cdot\|$ denotes the Euclidean matrix norm. The above quantity is a weighted average of uncertainty of the slow manifold due to stochasticity coming from different modes. The total variance of the slow manifold, at every time instant can be characterized by the global quantity $\text{trace}[\mathbf{C}_{\mathbf{Y}(t)}\mathbf{Y}(t)]$ which is shown in the top-right plot as a function of time. In the considered time regime the variance of the slow manifold is of order 10^{-2} of the energy of the mean flow. Therefore, a stochastic fluctuation will have a typical magnitude of 10% relative to the mean flow.

The mean value of the stochastic slow manifold depends on both the mean flow and the stochastic fluctuations. However, since the energy of the mean flow is an order of magnitude higher than the stochastic fluctuations, the mean value of the stochastic slow manifold appears almost stationary. On the other hand, the typical deviations of particle velocities from the mean slow manifold depend strongly on both space and time. Therefore, in accordance with the plots 6-8 and 6-9 we expect higher deviations from the mean value of the stochastic slow manifold in locations and time instants where $\sigma_s(\mathbf{x}, t)$ is higher.

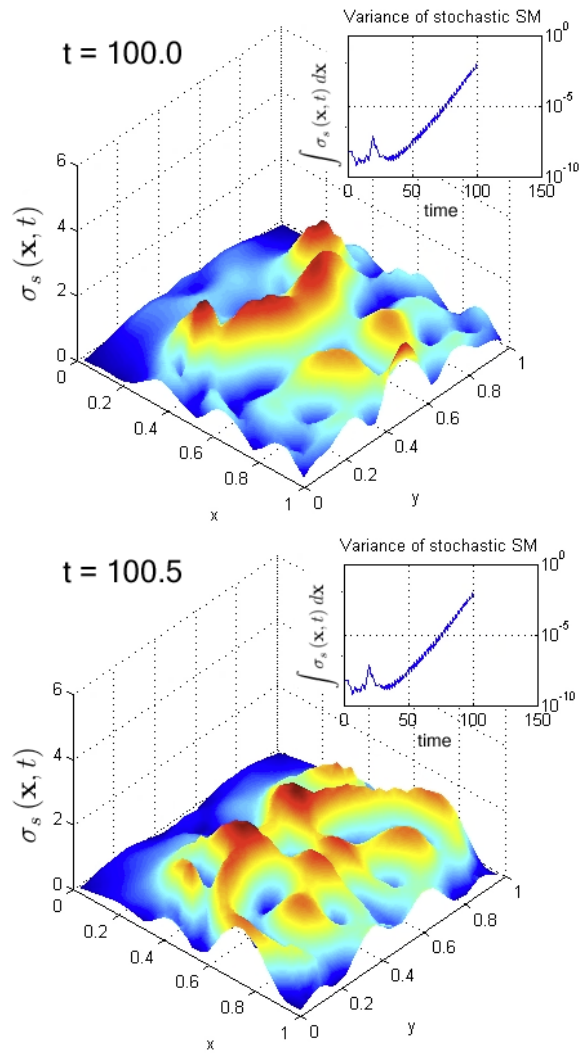


Figure 6-8: Variance of the stochastic slow manifold describing motion inertial particles for $t = 100.0$ and $t = 100.5$.

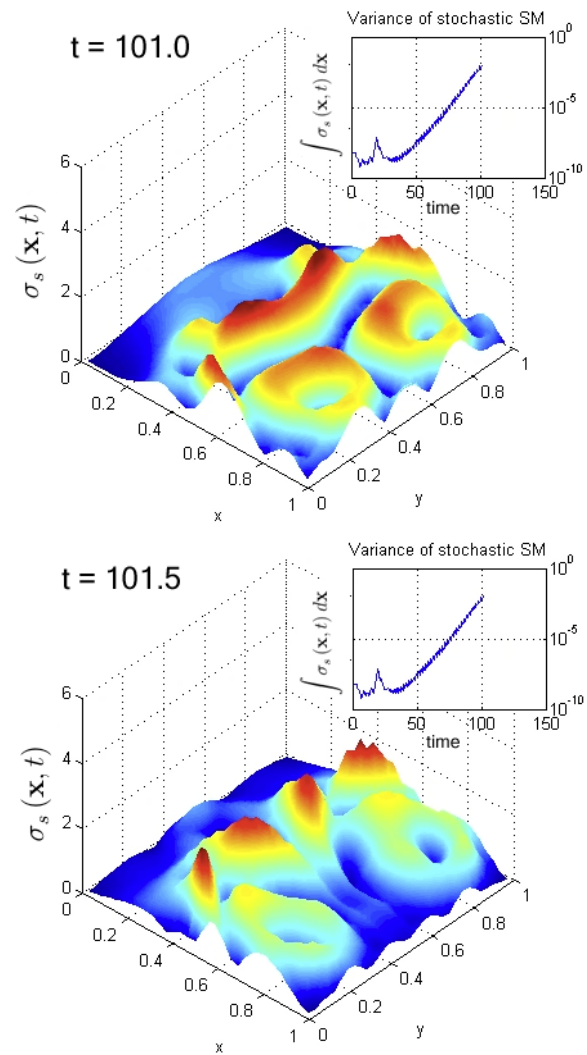


Figure 6-9: Variance of the stochastic slow manifold describing motion inertial particles for $t = 101.0$ and $t = 101.5$.

6.6.2 Convergence to the stochastic slow manifold

We shall now illustrate the convergence of the stochastic dynamics in the concentrated layer of probability that defines the stochastic slow manifold. We consider a specific flow realization ω_i and we solve the deterministic Maxey-Riley equation with very high accuracy. We initiate an inertial particle with $\epsilon = 10^{-3}$ and $R = 0.4$ with initial velocity away from the stochastic manifold.

In Figure 6-10a we present the distance from the stochastic slow manifold

$$z(t) = |E^\omega [\mathbf{u}_\epsilon(\mathbf{x}, t, \epsilon; \omega)] - \mathbf{v}(t; \omega_i)|$$

with respect to the horizontal position of the particle. The black dot indicates the projection of the particle on the mean of the stochastic slow manifold. The colormap shows the instantaneous local variance of the stochastic slow manifold, $\sigma_s(\mathbf{x}, t)$. In Figure 6-10b we present with blue solid curve the x -component of the particle velocity. The red curves show the typical spread (two typical deviations) of probability around the mean of the stochastic slow manifold. Specifically, they are defined by the quantity

$$u_{x, \pm 2\sigma}(t) = u_\epsilon(\mathbf{x}(t), t, \epsilon; \omega) \pm \frac{2}{\text{trace}[\mathbf{C}_{\mathbf{Y}(t)\mathbf{Y}(t)}]} \int_0^\infty \|\mathbf{C}_{u(\cdot, t)u(\cdot, t+\tau)}(\mathbf{x}, \mathbf{x})\| d\tau$$

and they illustrate the location where most of the probability measure is concentrated. In Figure 6-10c we present directly the distance from the slow manifold,

$$z_x(t) = v_x(t; \omega_i) - E^\omega [u_{\epsilon x}(\mathbf{x}, t, \epsilon; \omega)]$$

together with the curves

$$z_{x, \pm 2\sigma}(t) = \pm \frac{2}{\text{trace}[\mathbf{C}_{\mathbf{Y}(t)\mathbf{Y}(t)}]} \int_0^\infty \|\mathbf{C}_{u(\cdot, t)u(\cdot, t+\tau)}(\mathbf{x}, \mathbf{x})\| d\tau.$$

As we are able to observe, during the initial phase of motion we have rapid convergence into the layer of probability that defines the stochastic slow manifold. Subsequently, the particle continue to move inside the stochastic slow manifold, with its velocity fluctuating (see Figure 6-11). Note that the magnitude of the jumps from the mean of the stochastic slow manifold are in full accordance with the bounds defined by the curves $z_{x, \pm 2\sigma}(t)$ (Figure 6-11c).

6.6.3 Validation of stochastic inertial equation

The next step of our analysis involves the validation of the reduced order, stochastic, inertial equation (6.40). We consider an initial distribution of inertial particles (heavy particles with $\epsilon = 10^{-3}$ and $R = 0.4$) that is described by a Gaussian probability density function (see Figure 6-12-top plot). We first create a large number ($N = 10^4$) of particles positions that follow the initial Gaussian distribution. We advect those particles by solving the stochastic inertial equation (6.40). For the numerical solution of the stochastic differential equation we use the Euler-Maruyama method (see e.g. [58], [49]). Then we advect the initial sample set of particles (which approximate the initial distribution) using the deterministic inertial

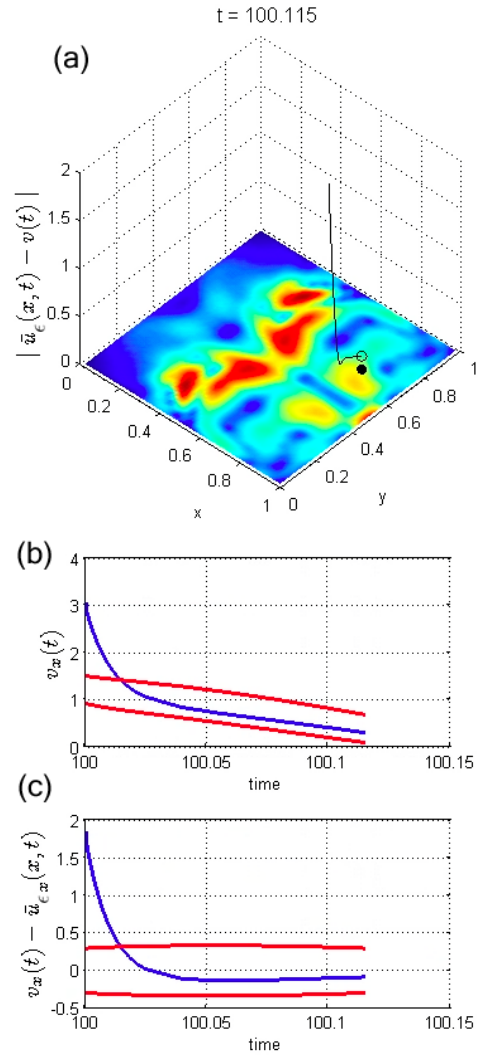


Figure 6-10: (a) Rapid convergence to the stochastic slow manifold during the initial phase of motion. The colormap denotes the local variance of the slow manifold $\sigma_s(\mathbf{x}, t)$. The vertical coordinate shows the distance of the stochastic dynamics from the mean slow manifold. (b) x - component of the particle velocity, resolved according to Maxey-Riley equation for a particular flow realization (blue solid curve). The red lines indicate the local spread of probability around the mean slow manifold at the particle's location. (c) same as (b) but now the distance from the slow manifold is shown.

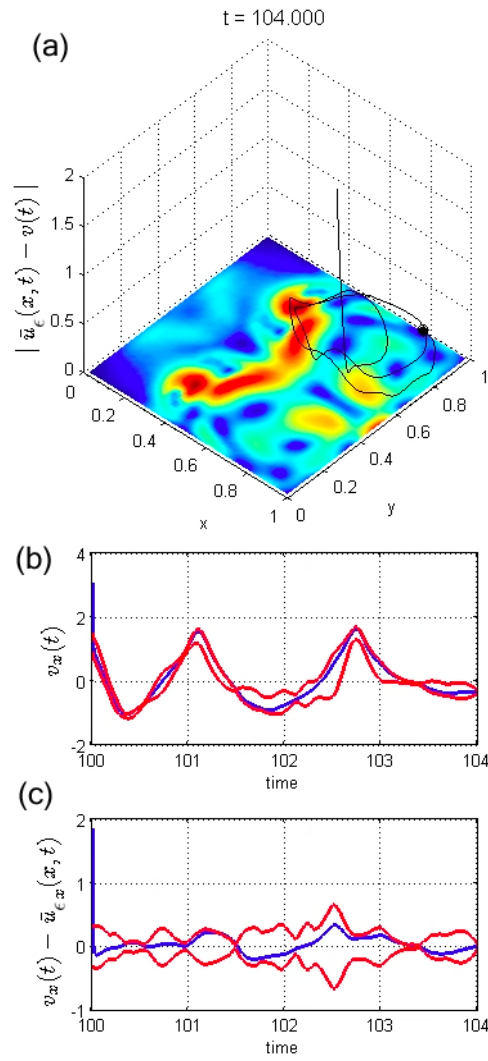


Figure 6-11: Same as 6-10 but for a later time instant.

equation for $M = 500$ realizations of the random flow field.

The results are shown in Figures 6-12, 6-13 for 5 time instants. In the left column we present the results from simulating the stochastic inertial equation, while in the right column we show the Monte-Carlo simulation. Note that the computational time required for the Monte-Carlo simulation was almost 500 times higher since we had to advect the probability density function for every flow realization. As we are able to observe the full Monte-Carlo simulation is slightly more diffusive relative to the stochastic inertial equation. However, the results compare satisfactory even for larger times.

6.6.4 Clustering due to the combined effect of inertial and flow stochasticity

We will now comment on the effect of flow stochasticity on the clustering properties of heavy particles. In Figure 6-14 we present the particles concentration (particles have the same parameters as in the previous section) for two different time instants. The blue lines represent the streamlines for the mean flow $\mathbf{U}(\mathbf{x}, t)$ and the red curves represent the clustering manifolds predicted by the deterministic part of the stochastic inertial equation (6.44).

During the initial phase of motion, the initially Gaussian blob is transported according to the mean flow. Additionally, we observe a stretching, normal to the mean flow, caused by the existence of the stochastic perturbation (Figure 6-14 top). As we are able to observe the stretching of the probability density function, i.e. concentration field occurs in accordance with the clustering manifolds for the deterministic part of the stochastic inertial equation (red curves).

In a later time instant the concentration field has been transported by the mean flow while it has also aligned according to the clustering manifolds of the stochastic perturbation (Figure 6-14 bottom). We observe the formation of a closed ring of particles (on the right of the plot) which is not consistent with the mean flow but it is fully justified by the clustering regions of the full stochastic flow.

Therefore, zero mean stochastic perturbations, even of low intensity (in this case the variance of the perturbation is 1% of the mean flow energy), are capable to influence drastically, the evolution of the concentration field. Through the developed framework we have identified the geometry of these deformations and we have correlate their form with the characteristics of the stochastic part of the flow.

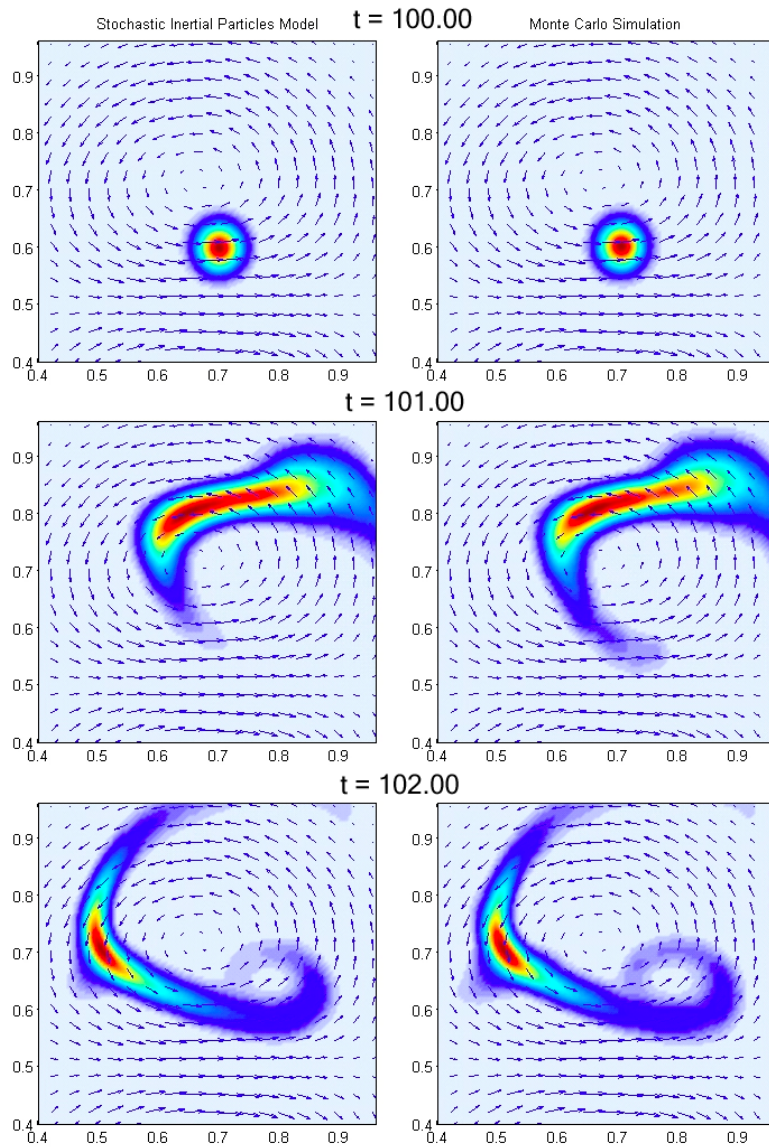


Figure 6-12: Comparison of stochastic inertial equation (6.40) and direct Monte-Carlo simulation for $t = 100, 101, 102$.

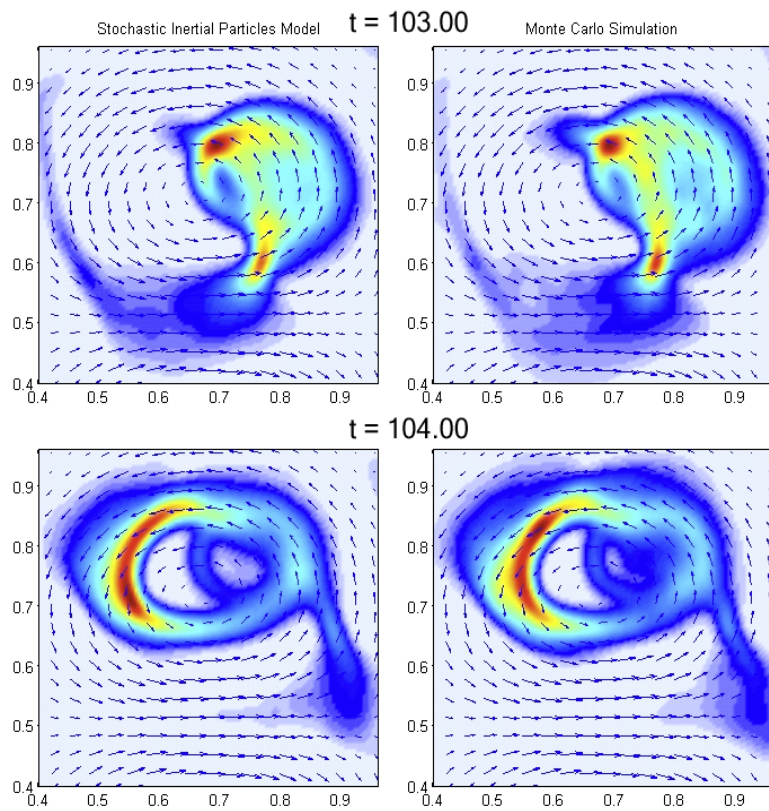


Figure 6-13: Same as Figure 6-12 for $t = 103, 104$.

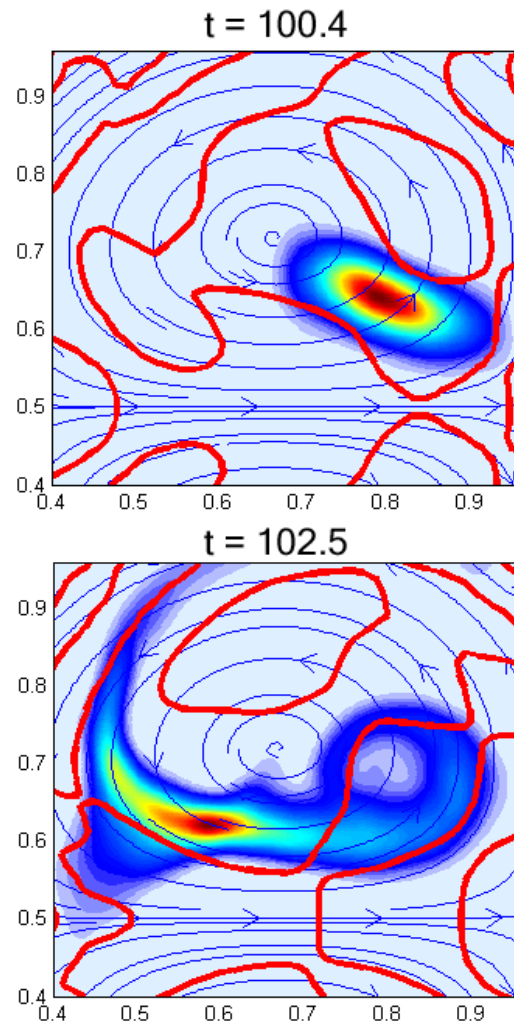


Figure 6-14: Concentration field for finite size particles (heavy particles) for two different time instants. The blue lines indicate streamlines for the mean flow. The red lines indicate clustering manifolds for the stochastic flow field.

Chapter 7

Conclusions

In this chapter we will summarize our contributions and results obtained within the context of this Ph.D. thesis.

Dynamically orthogonal field equations: We have derived an exact, closed set of equations that determine the evolution of continuous stochastic fields described by a SPDE. By hypothesizing a finite order dynamical expansion (DO expansion) we derived directly from the original SPDE a system of differential equations consisting of a PDE for the mean field, a family of PDEs for the orthonormal basis where the stochasticity ‘lives’ as well as a system of SDEs that describes how the stochasticity evolves in the time varying stochastic subspace. Therefore, we do not assume an a priori representation neither for the stochastic coefficients, nor for the spatial structure of the solution; all this information is obtained directly by the system equations, boundary and initial conditions. We have also illustrated that under appropriate assumptions the DO approach generates both the equations obtained by the Proper-Orthogonal-Decomposition method and by the Polynomial-Chaos method; thus it unifies the two methodologies. Even though the developed framework is valid for non-smooth systems its efficient numerical properties are limited by the order of the non-linearity (infinite for non-smooth systems), similarly with the other analytical approaches (PC or POD method). The above results have been published in the article Sapsis and Lermusiaux, *Physica D*, 2009 [129].

Adaptive criteria for stochastic dimensionality: To treat the strongly transient responses characterizing complex systems such as those found in oceanic applications we have developed a set of adaptive criteria that controls the size of the stochastic subspace where the reduction of the full dynamics is performed in the context of the DO method. Those criteria are based on the covariance operator of the system response as well as on the stochastic operator expressing the dynamics of the system. The above material is included in Sapsis and Lermusiaux, 2010 [126].

Computational code for 2D stochastic Navier-Stokes: We have developed and validated a computational code in Matlab that implements the DO field equations for 2D Navier-Stokes in general geometries. This code is based on the finite-differences numerical scheme and also incorporates the adaptive criteria for the stochastic dimensionality of the solution. We used this code for the validation of DO methodology by solving the stochastic fluid flow in a cavity and behind a cylinder (material included in Sapsis and Lermusiaux, *Physica D*, 2009 [129]). This code also served as a basis for the development of a more accurate and optimized version based on the finite-volume approach (in collaboration with Mr. Matt Ueckermann). Using the finite-volume code we obtained the stochastic response of an idealized ‘double

gyre' model, which has elements of ocean, atmospheric and climate instability behaviors, and we illustrated its response over different dynamical regimes.

Dynamics of finite-size particles with applications: The derivation of the Lagrangian stochastic model presented in Chapter 6 was based on our own work on the deterministic dynamics of finite-size particles. More specifically, for finite-size particles in deterministic flows we derived a reduced order inertial equations that describes accurately the dynamics of finite-size particles for sufficiently small size (Haller and Sapsis, *Physica D*, 2008 [56]). These results were also extended and applied to large scale geophysical flows in Sapsis and Haller, *J. Atm. Sc.*, 2009 [123]. Dispersion properties of finite-size particles were studied analytically in Sapsis and Haller, *Physics of Fluids*, 2008 [128] and Haller and Sapsis, *SIAM J. Appl. Dyn. Syst.*, 2010 [57]. Also, analytical criteria were derived for the description of clustering regions for finite-size particles in Sapsis and Haller, *Chaos*, 2010 [124].

Lagrangian Stochastic transport model for finite-size particles: Based on the deterministic analysis for finite-size particles as well as on our DO representation of the stochastic flow, we derived a reduced order Lagrangian stochastic model describing the motion of finite-size particles in arbitrary random flows. We validated this model for a specific random flow through the comparison with direct Monte-Carlo simulations. Also, using the reduced order stochastic inertial equation we illustrate the combined effect of inertia and flow uncertainty on the clustering properties of finite-size particles.

7.1 Future directions

Future directions include the application of the developed framework to complex systems characterized by uncertainty, others than those considered in the context of this thesis. Applications of this kind include for example the analysis and identification of structural systems subjected to random excitations (e.g. water waves), wave propagation in random media, as well as biological systems (such as population models) in environments with uncertainty.

Based on the work related to the idealized climate model an interesting direction would be the analysis of the effect of stochasticity directly introduced from the external forcing which in this study was modeled as deterministic. Another promising research direction will be the stochastic analysis of the flow transition from deterministic to stochastic states characterized by a large number of modes (turbulence). The study of energy flow among the modes and between the mean field, in combination with the DO formulation may be used for the development of reduced order dynamical systems that will contain the essential dynamics that characterize this transition.

DO may also be used for characterization and prediction of more realistic systems (oceanic and atmospheric flows). For realistic numerical studies, non-intrusive schemes (e.g. [90], [103]) based on our DO expansion should also be investigated. Research is underway for developing DO schemes for data assimilation [80] or Bayesian inference [96] in idealized and realistic dynamical systems. Adaptive modeling and adaptive sampling are also promising directions (e.g. [78], [110]).

Related to the work on finite-size particles an interesting future direction is the development of transport models that take into account, apart of the finite-size, the interaction between finite-size particles due to clustering that occurs because of inertia (as it is described in the current work). Development of such models will play a very important role on the understanding of cloud formation and rain initiation (where both the particles finite-

size and their interaction play an important role) [114], [41], [131] as well as in the problem of coexistence between several species of plankton in the hydrosphere [119], [84]. Another potential application of interest is planet formation by dust accretion in the solar system [155], [36].

Research is underway for the experimental validation of the developed models in chaotic fluid flows using PIV techniques [108], [107]. To this end an interesting direction for future research will be the extension of the present theory in more complex models describing particles motion such as dynamical equations that include the effect of non-spherical shapes, take into account memory effects (Basset-Boussinesq terms), and/or contain non-Stokes (i.e. non-linear) drag forces.

Appendix A

DO equations for 3D Navier-Stokes in component wise form

In this appendix we will present in detail the DO field equations for the special case of fluid flows governed by stochastic Navier-Stokes. All the results will be presented in component-wise form which is most suitable for the development of computational code. The general equations, for an incompressible fluid in a domain D have the form

$$\begin{aligned}
\frac{\partial u}{\partial t} &= -\frac{\partial p}{\partial x} + \frac{1}{\text{Re}}\Delta u - \frac{\partial(u^2)}{\partial x} - \frac{\partial(uv)}{\partial y} - \frac{\partial(uw)}{\partial z} + fv + \tau_x(\mathbf{x}, t) + \varphi_x(\mathbf{x}, t; \omega) \\
&\equiv \mathcal{L}_u[\chi(\mathbf{x}, t; \omega); \omega] \\
\frac{\partial v}{\partial t} &= -\frac{\partial p}{\partial y} + \frac{1}{\text{Re}}\Delta v - \frac{\partial(vu)}{\partial x} - \frac{\partial(v^2)}{\partial y} - \frac{\partial(vw)}{\partial z} - fu + \tau_y(\mathbf{x}, t) + \varphi_y(\mathbf{x}, t; \omega) \\
&\equiv \mathcal{L}_v[\chi(\mathbf{x}, t; \omega); \omega] \\
\frac{\partial w}{\partial t} &= -\frac{\partial p}{\partial z} + \frac{1}{\text{Re}}\Delta w - \frac{\partial(wu)}{\partial x} - \frac{\partial(wv)}{\partial y} - \frac{\partial(w^2)}{\partial z} - g\rho + \tau_z(\mathbf{x}, t) + \varphi_z(\mathbf{x}, t; \omega) \\
&\equiv \mathcal{L}_w[\chi(\mathbf{x}, t; \omega); \omega] \\
\frac{\partial \rho}{\partial t} &= -\frac{\partial(u\rho)}{\partial x} - \frac{\partial(v\rho)}{\partial y} - \frac{\partial(w\rho)}{\partial z} + \kappa\Delta\rho \equiv \mathcal{L}_\rho[\chi(\mathbf{x}, t; \omega); \omega] \\
0 &= \frac{\partial u}{\partial x} + \frac{\partial v}{\partial y} + \frac{\partial w}{\partial z}
\end{aligned}$$

where

$$\chi = (u(\mathbf{x}, t; \omega), v(\mathbf{x}, t; \omega), w(\mathbf{x}, t; \omega), \rho(\mathbf{x}, t; \omega))$$

is the state vector with $(u(\mathbf{x}, t; \omega), v(\mathbf{x}, t; \omega), w(\mathbf{x}, t; \omega))$ being the flow velocity field and $\rho(\mathbf{x}, t; \omega)$ the density. The pressure field is denoted with $p(\mathbf{x}, t; \omega)$, $f = f_0 + \beta_0 y$ is the Coriolis coefficient, $(\tau_x(\mathbf{x}, t), \tau_y(\mathbf{x}, t), \tau_z(\mathbf{x}, t))$ is the external deterministic stress acting on the fluid, and $(\varphi_x(\mathbf{x}, t; \omega), \varphi_y(\mathbf{x}, t; \omega), \varphi_z(\mathbf{x}, t; \omega))$ is the zero-mean stochastic component of the stress for which we assume known the complete statistical information. In what follows we will use the DO field equations derived in the previous chapter with inner product

$$\langle \chi_1, \chi_2 \rangle = \int_D [u_1 u_2 + v_1 v_2 + w_1 w_2 + \rho_1 \rho_2] d\mathbf{x}.$$

We will also use the notation

$$\{\alpha_1, \alpha_2\} = \int_D \alpha_1(\mathbf{x}) \alpha_2(\mathbf{x}) d\mathbf{x}.$$

By performing a Karhunen-Loeve expansion on the stochastic field $\varphi(\mathbf{x}, t; \omega)$ we may approximate it as

$$\varphi(\mathbf{x}, t; \omega) = \sum_{r=1}^R Z_r(t; \omega) \varphi_r(\mathbf{x}, t) = Z_r(t; \omega) \varphi_r(\mathbf{x}, t),$$

where R is defined by the order of truncation of the KL series for the field $\varphi(\mathbf{x}, t; \omega)$.

For simplicity we assume that the boundary conditions are either deterministic Neumann or Dirichlet for the velocity field and Neumann for the density field

$$\begin{aligned} \mathbf{u}(\xi, t; \omega) &= \mathbf{u}_{\partial D_1}(\xi, t), & \xi \in \partial D_1 \\ \frac{\partial \mathbf{u}}{\partial \mathbf{n}}(\xi, t; \omega) &= \mathbf{h}_{\mathbf{u}, \partial D_2}(\xi, t), & \xi \in \partial D_2 \\ \frac{\partial \rho}{\partial \mathbf{n}}(\xi, t; \omega) &= h_{\rho, \partial D}(\xi, t), & \xi \in \partial D. \end{aligned}$$

As it is shown in chapter 5 the case of stochastic boundary conditions can always be transformed into a problem with deterministic boundary conditions and suitable stochastic forcing.

Furthermore, we assume that the initial conditions are known and given by

$$\begin{aligned} \mathbf{u}(\mathbf{x}, t_0; \omega) &= \mathbf{u}_0(\mathbf{x}; \omega), & \mathbf{x} \in D, \quad \omega \in \Omega \\ \rho(\mathbf{x}, t_0; \omega) &= \rho_0(\mathbf{x}; \omega), & \mathbf{x} \in D, \quad \omega \in \Omega. \end{aligned}$$

We will first calculate the stochastic operator \mathcal{L} . By using the DO representation

$$\chi(\mathbf{x}, t; \omega) = \bar{\chi}(\mathbf{x}, t) + Y_i(t; \omega) \chi_i(\mathbf{x}, t)$$

into Navier-Stokes equations we obtain

$$\begin{aligned} \mathcal{L}_u[\chi(\mathbf{x}, t; \omega); \omega] &= -\frac{\partial p}{\partial x} + F_0 + Y_i F_i - Y_i Y_j F_{ij} + Z_r(t; \omega) \varphi_{xr}(\mathbf{x}, t) \\ \mathcal{L}_v[\chi(\mathbf{x}, t; \omega); \omega] &= -\frac{\partial p}{\partial y} + G_0 + Y_i G_i - Y_i Y_j G_{ij} + Z_r(t; \omega) \varphi_{yr}(\mathbf{x}, t) \\ \mathcal{L}_w[\chi(\mathbf{x}, t; \omega); \omega] &= -\frac{\partial p}{\partial z} + H_0 + Y_i H_i - Y_i Y_j H_{ij} + Z_r(t; \omega) \varphi_{zr}(\mathbf{x}, t) \\ \mathcal{L}_\rho[\chi(\mathbf{x}, t; \omega); \omega] &= R_0 + Y_i R_i - Y_i Y_j R_{ij} \end{aligned}$$

where the fields on the right hand side are given by

$$F_0 = \frac{1}{\text{Re}} \Delta \bar{u} - \frac{\partial (\bar{u}^2)}{\partial x} - \frac{\partial (\bar{u}\bar{v})}{\partial y} - \frac{\partial (\bar{u}\bar{w})}{\partial z} + f\bar{v} + \tau_x(\mathbf{x}, t)$$

$$\begin{aligned}
G_0 &= \frac{1}{\text{Re}} \Delta \bar{v} - \frac{\partial(\bar{v}\bar{u})}{\partial x} - \frac{\partial(\bar{v}^2)}{\partial y} - \frac{\partial(\bar{v}\bar{w})}{\partial z} - f\bar{u} + \tau_y(\mathbf{x}, t) \\
H_0 &= \frac{1}{\text{Re}} \Delta \bar{w} - \frac{\partial(\bar{w}\bar{u})}{\partial x} - \frac{\partial(\bar{w}\bar{v})}{\partial y} - \frac{\partial(\bar{w}^2)}{\partial z} - g\bar{\rho} + \tau_z(\mathbf{x}, t) \\
R_0 &= \kappa \Delta \bar{\rho} - \frac{\partial(\bar{u}\bar{\rho})}{\partial x} - \frac{\partial(\bar{v}\bar{\rho})}{\partial y} - \frac{\partial(\bar{w}\bar{\rho})}{\partial z}
\end{aligned}$$

and,

$$\begin{aligned}
F_i &= \frac{1}{\text{Re}} \Delta u_i - 2 \frac{\partial(u_i \bar{u})}{\partial x} - \frac{\partial(v_i \bar{u} + u_i \bar{v})}{\partial y} - \frac{\partial(w_i \bar{u} + u_i \bar{w})}{\partial z} + f v_i \\
G_i &= \frac{1}{\text{Re}} \Delta v_i - \frac{\partial(v_i \bar{u} + u_i \bar{v})}{\partial x} - 2 \frac{\partial(v_i \bar{v})}{\partial y} - \frac{\partial(w_i \bar{v} + v_i \bar{w})}{\partial z} - f u_i \\
H_i &= \frac{1}{\text{Re}} \Delta w_i - \frac{\partial(w_i \bar{u} + u_i \bar{w})}{\partial x} - \frac{\partial(w_i \bar{v} + v_i \bar{w})}{\partial y} - 2 \frac{\partial(w_i \bar{w})}{\partial z} - g \rho_i \\
R_i &= \kappa \Delta \rho_i - \frac{\partial(\rho_i \bar{u} + u_i \bar{\rho})}{\partial x} - \frac{\partial(\rho_i \bar{v} + v_i \bar{\rho})}{\partial y} - \frac{\partial(\rho_i \bar{w} + w_i \bar{\rho})}{\partial z}
\end{aligned}$$

for $i = 1, \dots, s$, and

$$\begin{aligned}
F_{ij} &= \frac{\partial(u_i u_j)}{\partial x} + \frac{\partial(u_i v_j)}{\partial y} + \frac{\partial(u_i w_j)}{\partial z} \\
G_{ij} &= \frac{\partial(v_i u_j)}{\partial x} + \frac{\partial(v_i v_j)}{\partial y} + \frac{\partial(v_i w_j)}{\partial z} \\
H_{ij} &= \frac{\partial(w_i u_j)}{\partial x} + \frac{\partial(w_i v_j)}{\partial y} + \frac{\partial(w_i w_j)}{\partial z} \\
R_{ij} &= \frac{\partial(\rho_i u_j)}{\partial x} + \frac{\partial(\rho_i v_j)}{\partial y} + \frac{\partial(\rho_i w_j)}{\partial z}
\end{aligned}$$

with $i, j = 1, \dots, s$.

Moreover, by inserting the DO representation in the continuity equation we obtain

$$\frac{\partial \bar{u}}{\partial x} + \frac{\partial \bar{v}}{\partial y} + \frac{\partial \bar{w}}{\partial z} + Y_i(t; \omega) \left(\frac{\partial u_i}{\partial x} + \frac{\partial v_i}{\partial y} + \frac{\partial w_i}{\partial z} \right) = 0.$$

But since $Y_i(t; \omega)$ is random the above equation has the equivalent form

$$\begin{aligned}
\frac{\partial \bar{u}}{\partial x} + \frac{\partial \bar{v}}{\partial y} + \frac{\partial \bar{w}}{\partial z} &= 0 \\
\frac{\partial u_i}{\partial x} + \frac{\partial v_i}{\partial y} + \frac{\partial w_i}{\partial z} &= 0, \quad i = 1, \dots, s.
\end{aligned}$$

A.1 Stochastic pressure field

To derive an equation for the pressure we need to understand its role in the stochastic context of the operator \mathcal{L} given above. Pressure is the stochastic quantity which guarantees that for every possible realization ω the evolved field $(u(\mathbf{x}, t; \omega), v(\mathbf{x}, t; \omega), w(\mathbf{x}, t; \omega))$ is incompressible. Therefore, the stochastic pressure should be able to balance all the non-divergent contributions from the terms involved in the operator \mathcal{L} . To this end we choose

to represent the stochastic pressure field as

$$p = p_0 + Y_i(t; \omega) p_i - Y_i(t; \omega) Y_j(t; \omega) p_{ij} + Z_r(t; \omega) b_r$$

Based on the above discussion, the mean pressure field components should satisfy the following equation

$$\Delta p_0 = \frac{\partial F_0}{\partial x} + \frac{\partial G_0}{\partial y} + \frac{\partial H_0}{\partial z} = 0$$

with boundary conditions given by

$$\frac{\partial p_0}{\partial \mathbf{n}}(\xi, t; \omega) = 0, \quad \xi \in \partial D_1 \quad \text{and} \quad p_0 = \text{const.} \quad \xi \in \partial D_2$$

The stochastic terms in \mathcal{L} multiplied with $Y_i(t; \omega)$ will be balanced through the following equation

$$\Delta p_i = \frac{\partial F_i}{\partial x} + \frac{\partial G_i}{\partial y} + \frac{\partial H_i}{\partial z} = 0, \quad i = 1, \dots, s$$

and boundary conditions

$$\frac{\partial p_i}{\partial \mathbf{n}}(\xi, t; \omega) = 0, \quad \xi \in \partial D_1 \quad \text{and} \quad p_i = 0, \quad \xi \in \partial D_2, \quad i = 1, \dots, s.$$

Similarly, for the stochastic terms multiplied by $Y_i(t; \omega) Y_j(t; \omega)$ we will have

$$\Delta p_{ij} = \frac{\partial F_{ij}}{\partial x} + \frac{\partial G_{ij}}{\partial y} + \frac{\partial H_{ij}}{\partial z} = 0, \quad i, j = 1, \dots, s$$

and boundary conditions

$$\frac{\partial p_{ij}}{\partial \mathbf{n}}(\xi, t; \omega) = 0, \quad \xi \in \partial D_1 \quad \text{and} \quad p_{ij} = 0, \quad \xi \in \partial D_2, \quad i, j = 1, \dots, s.$$

Finally, the forcing terms will be balanced through the family of equations

$$\Delta b_r = \frac{\partial \varphi_{xr}}{\partial x} + \frac{\partial \varphi_{yr}}{\partial y} + \frac{\partial \varphi_{zr}}{\partial z} = 0, \quad r = 1, \dots, R.$$

with boundary conditions

$$\frac{\partial q_r}{\partial \mathbf{n}}(\xi, t; \omega) = 0, \quad \xi \in \partial D_1 \quad \text{and} \quad q_r = 0, \quad \xi \in \partial D_2, \quad r = 1, \dots, R.$$

The above set of equations guarantees that for every realization ω the evolved field $(u(\mathbf{x}, t; \omega), v(\mathbf{x}, t; \omega), w(\mathbf{x}, t; \omega))$ will always be incompressible. Moreover, the evolution operator \mathcal{L} will take the form

$$\begin{aligned} \mathcal{L}_u[\chi(\mathbf{x}, t; \omega); \omega] = & \left[-\frac{\partial p_0}{\partial x} + F_0 \right] + Y_i \left[-\frac{\partial p_i}{\partial x} + F_i \right] \\ & - Y_i Y_j \left[-\frac{\partial p_{ij}}{\partial x} + F_{ij} \right] + Z_r(t; \omega) \left[-\frac{\partial q_r}{\partial x} + \varphi_{xr}(\mathbf{x}, t) \right] \end{aligned}$$

$$\begin{aligned}\mathcal{L}_v [\chi(\mathbf{x}, t; \omega); \omega] &= \left[-\frac{\partial p_0}{\partial y} + G_0 \right] + Y_i \left[-\frac{\partial p_i}{\partial y} + G_i \right] \\ &\quad - Y_i Y_j \left[-\frac{\partial p_{ij}}{\partial y} + G_{ij} \right] + Z_r(t; \omega) \left[-\frac{\partial q_r}{\partial y} + \varphi_{yr}(\mathbf{x}, t) \right]\end{aligned}$$

$$\begin{aligned}\mathcal{L}_w [\chi(\mathbf{x}, t; \omega); \omega] &= \left[-\frac{\partial p_0}{\partial z} + H_0 \right] + Y_i \left[-\frac{\partial p_i}{\partial z} + H_i \right] \\ &\quad - Y_i Y_j \left[-\frac{\partial p_{ij}}{\partial z} + H_{ij} \right] + Z_r(t; \omega) \left[-\frac{\partial q_r}{\partial z} + \varphi_{zr}(\mathbf{x}, t) \right]\end{aligned}$$

$$\mathcal{L}_\rho [\chi(\mathbf{x}, t; \omega); \omega] = R_0 + Y_i R_i - Y_i Y_j R_{ij}$$

A.2 Evolution of the mean field $\bar{\mathbf{u}}(\mathbf{x}, t; \omega)$

Using the corresponding DO equation for the mean we obtain the set of deterministic PDEs

$$\begin{aligned}\frac{\partial \bar{u}}{\partial t} &= -\frac{\partial p_0}{\partial x} + F_0 - \mathbf{C}_{Y_i(t)Y_j(t)} \left(-\frac{\partial p_{ij}}{\partial x} + F_{ij} \right) + \tau_x(\mathbf{x}, t) \\ \frac{\partial \bar{v}}{\partial t} &= -\frac{\partial p_0}{\partial y} + G_0 - \mathbf{C}_{Y_i(t)Y_j(t)} \left(-\frac{\partial p_{ij}}{\partial y} + G_{ij} \right) + \tau_y(\mathbf{x}, t) \\ \frac{\partial \bar{w}}{\partial t} &= -\frac{\partial p_0}{\partial z} + H_0 - \mathbf{C}_{Y_i(t)Y_j(t)} \left(-\frac{\partial p_{ij}}{\partial z} + H_{ij} \right) + \tau_z(\mathbf{x}, t) \\ \frac{\partial \bar{\rho}}{\partial t} &= R_0 - \mathbf{C}_{Y_i(t)Y_j(t)} R_{ij} \\ 0 &= \frac{\partial \bar{u}}{\partial x} + \frac{\partial \bar{v}}{\partial y} + \frac{\partial \bar{w}}{\partial z}\end{aligned}$$

with the following boundary conditions

$$\begin{aligned}\bar{\mathbf{u}}(\xi, t; \omega) &= \mathbf{u}_{\partial D_1}(\xi, t), \quad \xi \in \partial D_1 \\ \frac{\partial \bar{\mathbf{u}}}{\partial \mathbf{n}}(\xi, t; \omega) &= \mathbf{h}_{\partial D_2}(\xi, t), \quad \xi \in \partial D_2 \\ \frac{\partial \bar{\rho}}{\partial \mathbf{n}}(\xi, t; \omega) &= h_{\rho, \partial D}(\xi, t), \quad \xi \in \partial D\end{aligned}$$

A.3 Evolution of the stochastic subspace basis $\chi_i(\mathbf{x}, t; \omega)$

We will first calculate the quantity $E^\omega [\mathcal{L}[u(\mathbf{x}, t; \omega); \omega] Y_j(t; \omega)]$. We will have

$$\begin{aligned}E^\omega [\mathcal{L}_u [\chi(\mathbf{x}, t; \omega); \omega] Y_j(t; \omega)] &= \mathbf{C}_{Y_m(t)Y_j(t)} \left[-\frac{\partial p_m}{\partial x} + F_m \right] \\ &\quad - \mathbf{M}_{Y_j(t)Y_m(t)Y_n(t)} \left[-\frac{\partial p_{mn}}{\partial x} + F_{mn} \right] \\ &\quad + \mathbf{C}_{Y_j(t)Z_r(t)} \left[-\frac{\partial q_r}{\partial x} + \varphi_{xr}(\mathbf{x}, t) \right]\end{aligned}$$

$$\begin{aligned}
E^\omega [\mathcal{L}_v [\chi (\mathbf{x}, t; \omega) ; \omega] Y_j (t; \omega)] &= \mathbf{C}_{Y_m(t)Y_j(t)} \left[-\frac{\partial p_m}{\partial y} + G_m \right] \\
&\quad - \mathbf{M}_{Y_j(t)Y_m(t)Y_n(t)} \left[-\frac{\partial p_{mn}}{\partial y} + G_{mn} \right] \\
&\quad + \mathbf{C}_{Y_j(t)Z_r(t)} \left[-\frac{\partial q_k}{\partial y} + \varphi_{yr} (\mathbf{x}, t) \right]
\end{aligned}$$

$$\begin{aligned}
E^\omega [\mathcal{L}_w [\chi (\mathbf{x}, t; \omega) ; \omega] Y_j (t; \omega)] &= \mathbf{C}_{Y_m(t)Y_j(t)} \left[-\frac{\partial p_m}{\partial z} + H_m \right] \\
&\quad - \mathbf{M}_{Y_j(t)Y_m(t)Y_n(t)} \left[-\frac{\partial p_{mn}}{\partial z} + H_{mn} \right] \\
&\quad + \mathbf{C}_{Y_j(t)Z_r(t)} \left[-\frac{\partial q_k}{\partial z} + \varphi_{zr} (\mathbf{x}, t) \right]
\end{aligned}$$

$$E^\omega [\mathcal{L}_\rho [\chi (\mathbf{x}, t; \omega) ; \omega] Y_j (t; \omega)] = \mathbf{C}_{Y_m(t)Y_j(t)} R_m - \mathbf{M}_{Y_j(t)Y_m(t)Y_n(t)} R_{mn}$$

Multiplying with the inverse matrix $\mathbf{C}_{Y_i(t)Y_j(t)}^{-1}$ we will have

$$\begin{aligned}
Q_{ui} &\equiv E^\omega [\mathcal{L}_u [\chi (\mathbf{x}, t; \omega) ; \omega] Y_j (t; \omega)] \mathbf{C}_{Y_i(t)Y_j(t)}^{-1} \\
&= \left[-\frac{\partial p_i}{\partial x} + F_i \right] - \mathbf{C}_{Y_i(t)Y_j(t)}^{-1} \mathbf{M}_{Y_j(t)Y_m(t)Y_n(t)} \left[-\frac{\partial p_{mn}}{\partial x} + F_{mn} \right] \\
&\quad + \mathbf{C}_{Y_i(t)Y_j(t)}^{-1} \mathbf{C}_{Y_j(t)Z_r(t)} \left[-\frac{\partial q_r}{\partial x} + \varphi_{xr} (\mathbf{x}, t) \right] \\
Q_{vi} &\equiv E^\omega [\mathcal{L}_v [\chi (\mathbf{x}, t; \omega) ; \omega] Y_j (t; \omega)] \mathbf{C}_{Y_i(t)Y_j(t)}^{-1} \\
&= \left[-\frac{\partial p_i}{\partial y} + G_i \right] - \mathbf{C}_{Y_i(t)Y_j(t)}^{-1} \mathbf{M}_{Y_j(t)Y_m(t)Y_n(t)} \left[-\frac{\partial p_{mn}}{\partial y} + G_{mn} \right] \\
&\quad + \mathbf{C}_{Y_i(t)Y_j(t)}^{-1} \mathbf{C}_{Y_j(t)Z_r(t)} \left[-\frac{\partial q_r}{\partial y} + \varphi_{yr} (\mathbf{x}, t) \right] \\
Q_{wi} &\equiv E^\omega [\mathcal{L}_w [\chi (\mathbf{x}, t; \omega) ; \omega] Y_j (t; \omega)] \mathbf{C}_{Y_i(t)Y_j(t)}^{-1} \\
&= \left[-\frac{\partial p_i}{\partial z} + H_i \right] - \mathbf{C}_{Y_i(t)Y_j(t)}^{-1} \mathbf{M}_{Y_j(t)Y_m(t)Y_n(t)} \left[-\frac{\partial p_{mn}}{\partial z} + H_{mn} \right] \\
&\quad + \mathbf{C}_{Y_i(t)Y_j(t)}^{-1} \mathbf{C}_{Y_j(t)Z_r(t)} \left[-\frac{\partial q_r}{\partial z} + \varphi_{zr} (\mathbf{x}, t) \right] \\
Q_{\rho i} &\equiv E^\omega [\mathcal{L}_\rho [\chi (\mathbf{x}, t; \omega) ; \omega] Y_j (t; \omega)] \mathbf{C}_{Y_i(t)Y_j(t)}^{-1} \\
&= R_i - \mathbf{C}_{Y_i(t)Y_j(t)}^{-1} \mathbf{M}_{Y_j(t)Y_m(t)Y_n(t)} R_{mn}
\end{aligned}$$

Using the above expressions we obtain the evolution equations for the basis $\mathbf{u}_i (\mathbf{x}, t; \omega)$, $\rho_i (\mathbf{x}, t; \omega)$

$$\begin{aligned}
\frac{\partial u_i}{\partial t} &= Q_{ui} - (\{Q_{ui}, u_m\} + \{Q_{vi}, v_m\} + \{Q_{wi}, w_m\} + \{Q_{\rho i}, \rho_m\}) u_m \\
\frac{\partial v_i}{\partial t} &= Q_{vi} - (\{Q_{ui}, u_m\} + \{Q_{vi}, v_m\} + \{Q_{wi}, w_m\} + \{Q_{\rho i}, \rho_m\}) v_m
\end{aligned}$$

$$\begin{aligned}\frac{\partial w_i}{\partial t} &= Q_{wi} - (\{Q_{ui}, u_m\} + \{Q_{vi}, v_m\} + \{Q_{wi}, w_m\} + \{Q_{\rho_i}, \rho_m\}) w_m \\ 0 &= \frac{\partial u_i}{\partial x} + \frac{\partial v_i}{\partial y} + \frac{\partial w_i}{\partial z} \\ \frac{\partial \rho_i}{\partial t} &= Q_{\rho_i} - (\{Q_{ui}, u_m\} + \{Q_{vi}, v_m\} + \{Q_{wi}, w_m\} + \{Q_{\rho_i}, \rho_m\}) \rho_m\end{aligned}$$

for $i = 1, \dots, s$. Moreover, we will have the following boundary conditions

$$\begin{aligned}\mathbf{u}_i(\xi, t) &= \mathbf{0}, \quad \xi \in \partial D_1 \\ \frac{\partial \mathbf{u}_i}{\partial \mathbf{n}}(\xi, t) &= \mathbf{0}, \quad \xi \in \partial D_2. \\ \frac{\partial \rho_i}{\partial \mathbf{n}}(\xi, t) &= \mathbf{0}, \quad \xi \in \partial D\end{aligned}$$

A.4 Evolution of the stochastic coefficients $Y_i(\mathbf{x}, t; \omega)$

The set of evolution equations for the stochastic coefficients will take the form of a SDE

$$\begin{aligned}\frac{dY_i}{dt} &= (\{u_i, F_m\} + \{v_i, G_m\} + \{w_i, H_m\} + \{\rho_i, R_m\}) Y_m \\ &\quad - (\{u_i, F_{mn}\} + \{v_i, G_{mn}\} + \{w_i, H_{mn}\} + \{\rho_i, R_{mn}\}) (Y_m Y_n - \mathbf{C}_{Y_m(t)Y_n(t)}) \\ &\quad + (\{\varphi_{xr}(\mathbf{x}, t), u_i\} + \{\varphi_{yr}(\mathbf{x}, t), v_i\} + \{\varphi_{zr}(\mathbf{x}, t), w_i\}) Z_r(t; \omega) \\ &\quad - \left(\left\langle u_i, \frac{\partial p_m}{\partial x} \right\rangle + \left\langle v_i, \frac{\partial p_m}{\partial y} \right\rangle + \left\langle w_i, \frac{\partial p_m}{\partial z} \right\rangle \right) Y_m \\ &\quad + \left(\left\langle u_i, \frac{\partial p_{mn}}{\partial x} \right\rangle + \left\langle v_i, \frac{\partial p_{mn}}{\partial y} \right\rangle + \left\langle w_i, \frac{\partial p_{mn}}{\partial z} \right\rangle \right) (Y_m Y_n - \mathbf{C}_{Y_m(t)Y_n(t)}) \\ &\quad - \left(\left\langle u_i, \frac{\partial q_r}{\partial x} \right\rangle + \left\langle v_i, \frac{\partial q_r}{\partial y} \right\rangle + \left\langle w_i, \frac{\partial q_r}{\partial z} \right\rangle \right) Z_r(t; \omega)\end{aligned}$$

Using Gauss theorem we have for every scalar field α and every divergent-free vector field β

$$\int_D \nabla \alpha(\mathbf{x}) \cdot \beta(\mathbf{x}) d\mathbf{x} = \int_{\partial D} \alpha(\xi) \beta(\xi) \cdot \mathbf{n}(\xi) d\xi$$

Applying the above property for the pressure p_m and the vector field \mathbf{u}_i and by using (without loss of generality) the boundary conditions of section 5.2 we obtain

$$\left\langle u_i, \frac{\partial p_m}{\partial x} \right\rangle + \left\langle v_i, \frac{\partial p_m}{\partial y} \right\rangle + \left\langle w_i, \frac{\partial p_m}{\partial z} \right\rangle = 0.$$

Furthermore, by applying the same argument for the pressure fields p_{mn} and q_k and the vector fields \mathbf{u}_i we also obtain

$$\begin{aligned}\left\langle u_i, \frac{\partial p_{mn}}{\partial x} \right\rangle + \left\langle v_i, \frac{\partial p_{mn}}{\partial y} \right\rangle + \left\langle w_i, \frac{\partial p_{mn}}{\partial z} \right\rangle &= 0 \\ \left\langle u_i, \frac{\partial q_r}{\partial x} \right\rangle + \left\langle v_i, \frac{\partial q_r}{\partial y} \right\rangle + \left\langle w_i, \frac{\partial q_r}{\partial z} \right\rangle &= 0.\end{aligned}$$

Hence, the stochastic equation describing the evolution of the stochastic coefficients will be take the form

$$\begin{aligned} \frac{dY_i}{dt} = & (\{u_i, F_m\} + \{v_i, G_m\} + \{w_i, H_m\} + \{\rho_i, R_m\}) Y_m \\ & - (\{u_i, F_{mn}\} + \{v_i, G_{mn}\} + \{w_i, H_{mn}\} + \{\rho_i, R_{mn}\}) (Y_m Y_n - \mathbf{C}_{Y_m(t)Y_n(t)}) \\ & + (\{\varphi_{xr}(\mathbf{x}, t), u_i\} + \{\varphi_{yr}(\mathbf{x}, t), v_i\} + \{\varphi_{zr}(\mathbf{x}, t), w_i\}) Z_r(t; \omega). \end{aligned}$$

Appendix B

Numerical implementation of 2D DO for Navier-Stokes

In the following paragraphs we will give a brief description of the numerical components used in the computational algorithm. The numerical implementation of the DO field equations for the description of stochastic fluid flows (Chapter 5) was performed in Matlab. In Figure B-1 we present the diagram describing the computational algorithm.

B.1 Initial conditions formulation

The first component of the algorithm is the formulation of the initial conditions. This is done by numerically solving the eigenvalue problem of Section 2.5 (Theorem 7). We use the covariance matrix describing the spatial stochastic information of the initial conditions. After spatial discretization of the domain the continuous eigenvalue problem takes the form of a finite-dimensional eigenvalue problem, with symmetric matrix (symmetry follows from the properties of the covariance matrix). Note that for a domain discretized using M^2 the size of the matrix to be diagonalized is M^4 . Therefore to avoid excessive computational cost it is essential to use a coarser grid for the diagonalization of the covariance matrix and then interpolate on the finer computational grid.

Through the diagonalization procedure we obtain a set of eigenvectors ($\mathbf{u}_{i0}(\mathbf{x})$, $i = 1, 2, \dots$) and the corresponding eigenvalues. As it was discussed in Section 2.5 the eigenvalues represent the variance along the direction defined by the corresponding eigenvector. By a choosing a critical amount of variance below which uncertainty is considered negligible we obtain the initial dimension of the stochastic subspace, s .

The next step is the representation of the stochastic coefficients $Y_{0i}(\omega)$, $i = 1, 2, \dots, s$ which can be in general non-Gaussian. To represent their arbitrary stochastic structure we use a random number generator for the following random vector

$$Y_{0i}(\omega) = \langle \mathbf{u}_0(\mathbf{x};\omega), \mathbf{u}_{i0}(\mathbf{x}) \rangle, \quad i = 1, 2, \dots, s.$$

Note, that the relatively small size of s (i.e. $s \sim 10$) allows for the use of a large number of random samples to represent the random vector.

B.1.1 Storage of orthonormal basis

For the application of the adaptive criteria it is essential to have a basis that will be able to approximate satisfactory any flow realization. The eigenvectors produced by the diagonalization of the initial conditions covariance matrix are spatially smooth but also consist an orthonormal basis that can approximate (up to the ability given by the computational grid) any flow realization. To this end we use the set of basis elements obtained from the previous diagonalization process. Note that, assuming the initial conditions respect the boundary conditions of the problem, the obtained base from the diagonalization process respects the geometry and boundary conditions of the problem as well.

B.2 Evolution of stochastic state

Having the initial stochastic conditions for the DO equations we may now proceed for their numerical solution. We have to solve a stochastic ODE having dimensionality s coupled with $s + 1$ deterministic PDEs (see Chapter 5). For the spatial discretization of the deterministic PDEs we use a C-grid in combination with a central difference scheme (see [54]). For the solution of the involved pressure equations we use the Gauss-Seidel method also described in [54]. Time discretization is performed using Euler's method which employs first-order difference quotients.

For the solution of the stochastic differential equation we evolve each one of the random samples (in a deterministic sense) created previously for the representation of the stochastic coefficients $Y_{0i}(\omega)$, $i = 1, 2, \dots, s$. Note that because of the low dimensionality, s , the computational cost involved in the solution of the stochastic differential equation is negligible relative to the evolution of the $s + 1$ deterministic fields. Using the statistics of the evolved random samples we are able to compute all the moments required for the evolution of the deterministic fields.

At the end of each time step we orthonormalize the stochastic subspace basis elements $\mathbf{u}_i(\mathbf{x}, t)$, $i = 1, 2, \dots, s$. Even though the orthonormality is theoretically preserved by the DO equations we reenforce it numerically at the end of each time step to avoid round-off errors. The numerical algorithm that we use is the modified Gram-Schmidt method which guarantees smaller errors in finite-precision arithmetic (see e.g. [11]).

B.3 Diagonalization of covariance matrix - Adaptive criteria

We evolve the stochastic state as described above for N time steps. where N is a small integer number (usually chosen between 10 and 100). After N time steps the solution is expressed in the special reference frame where the the stochastic coefficients $Y_i(t; \omega)$, $i = 1, 2, \dots, s$ are uncorrelated. This is done by diagonalizing the low-dimensional matrix \mathbf{C}_{YY} and subsequently rotating the stochastic coefficients and the stochastic subspace basis elements as described in Section 4.3.1.

At this point the stochastic state of the system is expressed in suitable form so that the adaptive criteria can be applied (Chapter 4). Specifically, the diagonal form of \mathbf{C}_{YY} allows for the removal of the mode with the smallest variance (if the corresponding criteria are satisfied) or the addition of a the most unstable mode (if the variance of the modes satisfies the corresponding criteria). In the latter case the computation of the most unstable mode is performed using the orthonormal base computed at the beginning but also the current

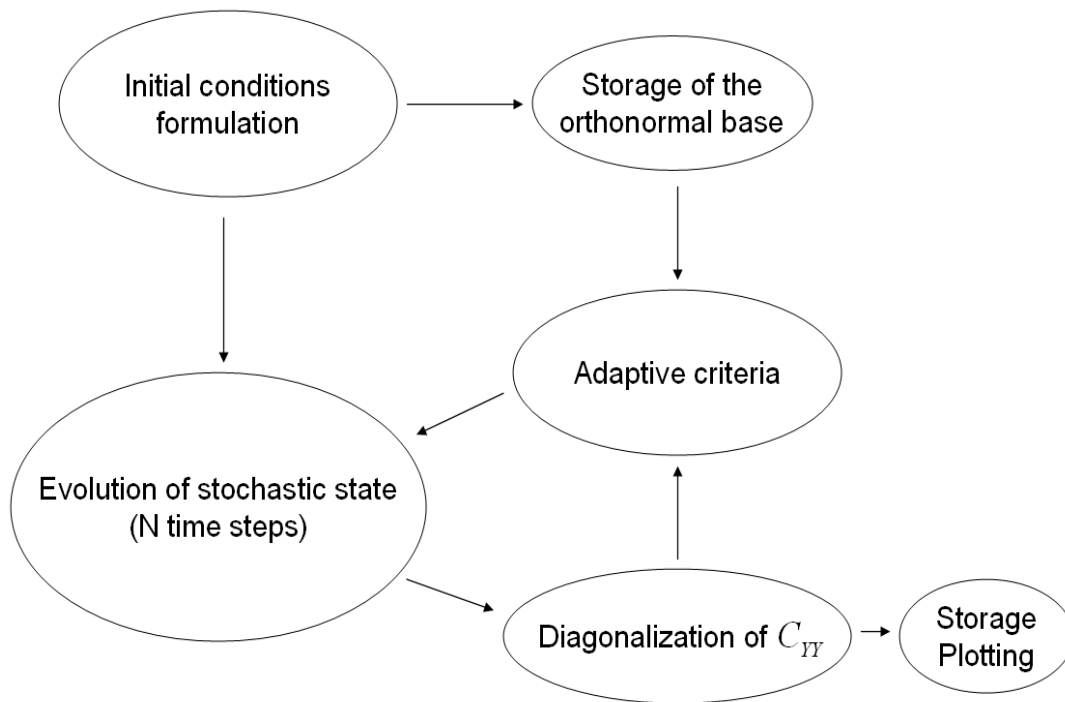


Figure B-1: Computational algorithm for the adaptive DO equations.

state of the system.

After the application of the adaptive criteria the updated form of the system state returns to the ‘evolution’ component of the algorithm.

B.4 Storage - Plotting

The storage and plotting is performed after the diagonalization of the covariance matrix and the rotation of the stochastic state in the corresponding reference frame. We store i) the random samples for the stochastic coefficients $Y_i(t; \omega)$, $i = 1, 2, \dots, s$, ii) the mean field, and iii) the stochastic subspace basis elements $\mathbf{u}_i(\mathbf{x}, t)$, $i = 1, 2, \dots$. The flow fields are visualized using either the streamfunction or the vorticity function. The samples for the stochastic coefficients are used to obtain the corresponding probability density function. This is done using a kernel smoothing density estimate method (see [23]) that allows us to obtain smooth probability density functions of general form.

Appendix C

Normal local stability of general invariant manifolds

In this appendix we will first state a general result describing the normal stability properties of invariant manifolds and then we will apply it to generalize the results presented in section 6.2.2 for the stability of neutrally buoyant particles. The results presented in the current section are part of the publication [57].

Invariant manifolds are distinguished sets of trajectories that organize the global geometry of trajectories in a dynamical system. Even if an invariant manifold is attracting (i.e., all close enough trajectories ultimately converge to the manifold), it may admit localized regions of instability where nearby trajectories temporarily depart from the manifold. These departures and later returns may manifest themselves in spectacular jumps along the manifold. Such transient jumps are often important to locate in applications.

In this section, we extend the ideas from the specialized setting considered in section 6.2.2 to identify localized transverse instability and attraction on general invariant manifolds. Our main tool in achieving this is the normal infinitesimal Lyapunov exponent (NILE), defined as the leading order short-term stretching or contraction rate at points of an invariant manifold. We derive a general explicit formula for the NILE, and hence for the normally stable and unstable domains of an invariant manifold. Subsequently, we apply our results to characterize the stability properties of the dynamics of non-neutrally buoyant particles.

C.1 Set-up and definitions

Consider a dynamical system of the form

$$\dot{X} = \mathcal{F}(X, t), \quad X \in \mathbb{R}^n, \quad (\text{C.1})$$

with $n \geq 2$, and with a smooth function $\mathcal{F}: \mathbb{R}^n \times \mathbb{R} \rightarrow \mathbb{R}^n$. A trajectory $X(t; t_0, X_0)$ of this system is a solution of the initial value problem $X(t_0) = X_0$. The flow map associated with (C.1) is a two-parameter family of transformations defined as

$$\begin{aligned} F_{t_0}^t: \mathbb{R}^n &\rightarrow \mathbb{R}^n, \\ X_0 &\mapsto X(t; t_0, X_0), \end{aligned}$$

The linearized flow map $DF_{t_0}^t$ is defined as

$$DF_{t_0}^t : T\mathbb{R}^n \rightarrow T\mathbb{R}^n, \\ (p, v) \mapsto (F_{t_0}^t(p), D_{X_0}X(t; t_0, p)v),$$

mapping vectors v based at a point p to vectors $D_{X_0}X(t; t_0, p)v$ based at the point $F_{t_0}^t(p)$. The notation $T\mathbb{R}^n$ refers to the tangent bundle of \mathbb{R}^n ; a local fiber of this bundle at a point $p \in \mathbb{R}^n$ will be denoted by $T_p\mathbb{R}^n$.

We assume that $M(t) \subset \mathbb{R}^n$ be a k -dimensional differentiable manifold that is locally invariant over under the map $F_{t_0}^t$ over the time interval $[t_1, t_2]$. This means that

$$F_{t_0}^t(M(t_0)) \subset M(t), \tag{C.2}$$

for all times $t_0, t \in [t_1, t_2]$ with $t \geq t_0$.

Beyond invariance and smoothness, we make no further assumption about the manifold $M(t)$. We do note that $M(t)$ will typically only be of interest in physical applications if it is robust, i.e., persists under small perturbations. As Fenichel [42] showed, such persistence is ensured if $M(t)$ is time-independent, compact, and normally hyperbolic.

C.2 Normally stable and normally unstable subsets

Instead of the asymptotic behavior along $M(t)$, our focus here is the instantaneous behavior of trajectories close to $M(t)$. Specifically, we would like to locate points on $M(t)$ at which most transverse perturbations to $M(t)$ start growing in norm over infinitesimally short times. (A measure zero set of transverse perturbations are allowed to decrease at such points due to the presence of stable directions.) The union of such points will form the *normally unstable subset* $M_u(t)$ of $M(t)$. Similarly, the *normally stable subset* $M_s(t)$ of $M(t)$ is the union of points in $M(t)$ at which all transverse perturbations to $M(t)$ decay over infinitesimally short times.

Note that $M_s(t)$ and $M_u(t)$ are typically not invariant subsets of $M(t)$: trajectories in $M(t)$ will generally either avoid both of these subsets, or simply cross them. Likewise, trajectories near $M(t)$ may either stay away from the subsets $M_s(t)$ and $M_u(t)$ of $M(t)$, or pass over these regions. In the latter case, however, the passing trajectories will break away from $M(t)$ while near $M_u(t)$, and approach $M(t)$ while near $M_s(t)$ (see Fig. C-1).

If $M_s(t) \equiv M(t)$, then $M(t)$ is a normally hyperbolic locally invariant manifold that only admits stable normal directions; in this case, $M(t)$ has an n -dimensional stable manifold (or domain of attraction). If $M_u(t) \equiv M(t)$, then $M(t)$ is a normally hyperbolic locally invariant manifold that only admits unstable normal directions; in this case, $M(t)$ has an n -dimensional unstable manifold.

The stable and unstable subsets described above have a major impact on the dynamics near $M(t)$. As it turns out below, locating them is possible from explicit calculations, and hence they offer a feasible alternative to Lyapunov-type numbers in the analysis of impact of $M(t)$ on phase space geometry. We make these ideas more precise below.

Definition 17 Let $T_pM(t)$ and $N_pM(t)$ denote the tangent and normal space of $M(t)$ at

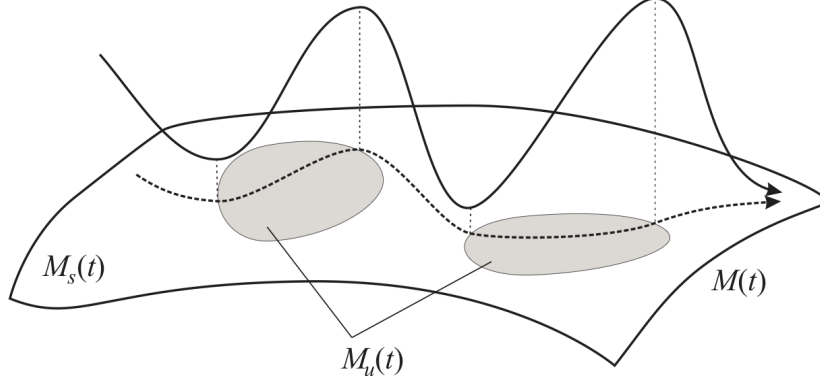


Figure C-1: Trajectories jump away from $M(t)$ over the unstable subset $M_u(t)$, but return to $M(t)$ over the stable subset $M_s(t)$. The figure assumes that $M(t)$ is a normally hyperbolic attracting manifold, in which case the jumping trajectory keeps approaching the same underlying trajectory on $M(t)$ by the invariant foliation of the stable manifold $W^s(M(t))$.

$p \in M(t)$, respectively. Also, let

$$\begin{aligned} \Pi_p^t: T_p \mathbb{R}^n = T_p M(t) \oplus N_p M(t) &\rightarrow N_p M(t), \\ (u, v) &\mapsto v, \end{aligned}$$

denote the natural projection from $T_p \mathbb{R}^n$, the tangent space of \mathbb{R}^n at p , to $N_p M(t)$. We then define the normal infinitesimal Lyapunov exponent (NILE) at a point $p \in M(t)$ as

$$\sigma(p; t) = \lim_{s \rightarrow +0} \frac{1}{s} \log \left\| \Pi_{F_t^{t+s}(p)}^{t+s} D F_t^{t+s} \Big|_{N_p M(t)} \right\|. \quad (\text{C.3})$$

The limit in the definition of $\sigma(p; t)$ exists for any v by the differentiability of the linearized flow map $D F_{t_0}^t$ and of the normal projection $\Pi_{F_{t_0}^t(p)}^t$ in t . Also note that the limit is finite because $D F_t^t \equiv I$ by definition, and hence $D F_t^{t+s} - I = \mathcal{O}(s)$. The action of the operator $\Pi_{F_t^{t+s}(p)}^{t+s} D F_t^{t+s}$ on a vector $v_0 \in N_p M(t)$ is shown in Fig. C-2.

Next, we want to argue that exponent $\sigma(p; t)$ is independent of the choice of the transverse bundle in which we seek to measure growth rates from $M(t)$. To describe this independence in more precise terms, we let $\tilde{N}M(t)$ be another smoothly varying n -dimensional vector bundle that is a fibration over $M(t)$; we require this bundle to be transverse to $M(t)$, by which we mean $\tilde{N}_p M(t) \cap T_p M(t)$ within $T_p \mathbb{R}^n$, for all $p \in M(t)$.

We can then view $T_p \mathbb{R}^n$ as the direct sum of $\tilde{N}_p M(t)$ and $T_p M(t)$,

$$T_p \mathbb{R}^n = \tilde{N}_p M(t) \oplus T_p M(t),$$

and define the natural projection from $T_p \mathbb{R}^n$ onto $\tilde{N}_p M(t)$ as

$$\begin{aligned} \tilde{\Pi}_p^t: T_p \mathbb{R}^n = T_p M(t) \oplus \tilde{N}_p M(t) &\rightarrow \tilde{N}_p M(t), \\ (\tilde{u}, \tilde{v}) &\mapsto \tilde{v}. \end{aligned}$$

We require each fiber $\tilde{N}_p M(t)$ to have the same constant position relative to the tangent

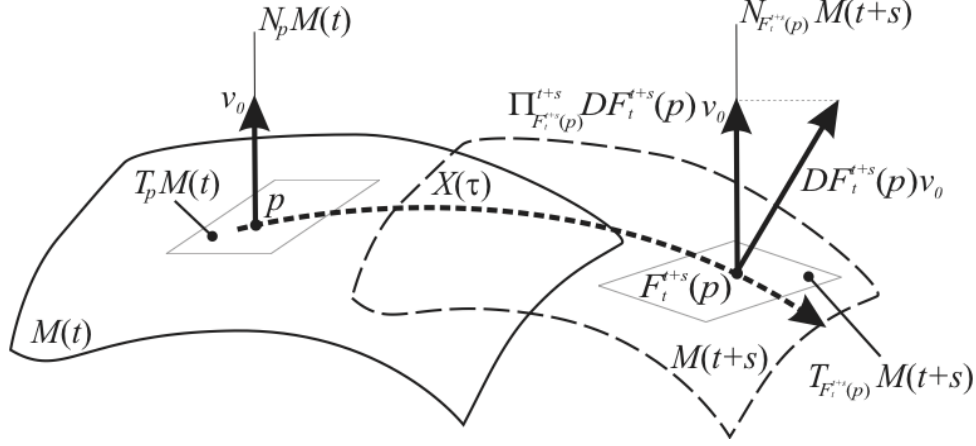


Figure C-2: The operator $\Pi_{F_t^{t+s}(p)}^{t+s} DF_t^{t+s}|_{N_p M(t)}$ maps vectors in the normal space $N_p M(t)$ to vectors in the normal space $N_{F_t^{t+s}(p)} M(t+s)$. The NILE $\sigma(p; t)$ is the exponential rate at which the norm of the above operator grows in the limit of infinitesimally small s . Therefore, $\sigma(p; t)$ measures the exponential rate at which the normal component of vectors normal to the manifold $M(t)$ grows over very short times. (The time τ is arbitrary within the interval $[t, t+s]$.)

space $T_p M(t)$ and the normal space and normal space $N_p M(t)$. Specifically, we require $\tilde{N}M(t)$ to be such that the tangential projection from $\tilde{N}_p M(t)$ to $N_p M(t)$,

$$\begin{aligned} Q: \tilde{N}_p M(t) &\rightarrow N_p M(t), \\ Q &= \Pi_p^t|_{\tilde{N}_p M(t)}, \end{aligned} \tag{C.4}$$

is independent of t and p . This latter condition is important, otherwise the value of the NILE computed on $\tilde{N}M(t)$ would be affected by the s -dependence of the fiber family $\tilde{N}_{F_t^{t+s}(p)} M(t+s)$ along the trajectory $F_t^{t+s}(p)$ starting from p at time t .

Proposition 18 *If we define*

$$\tilde{\sigma}(p; t) = \lim_{s \rightarrow +0} \frac{1}{s} \log \left\| \tilde{\Pi}_{F_t^{t+s}(p)}^{t+s} DF_t^{t+s} \Big|_{\tilde{N}_p M(t)} \right\|,$$

then we have $\tilde{\sigma}(p; t) \equiv \sigma(p; t)$

Proof: See Haller and Sapsis, 2010 [57].

We conclude that the $\sigma(p; t)$ is independent of the choice of transverse directions to the invariant manifold, and hence gives an intrinsic characterization of the local stability of $M(t)$ at t . Motivated by this observation, we introduce the following definition of normally stable and unstable subsets of $M(t)$.

Definition 19 *We define the normally unstable subset of $M(t)$ as*

$$M_u(t) = \{p \in M \mid \sigma(p; t) > 0\},$$

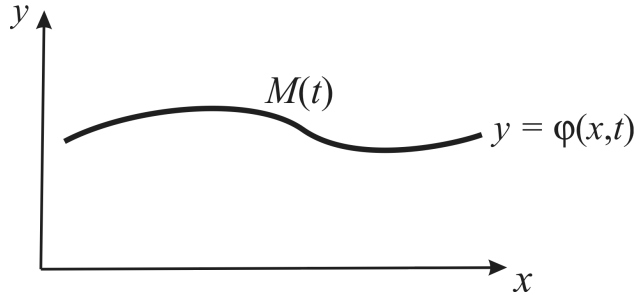


Figure C-3: The manifold $M(t)$ as a local graph over the x variables.

and the normally stable subset of $M(t)$ as

$$M_s(t) = \{p \in M \mid \sigma(p; t) < 0\}.$$

The subsets $M_u(t)$ and $M_s(t)$ —described informally above—are now defined precisely through the Lyapunov-type number $\sigma(p; t)$. Unlike the Lyapunov-type numbers arising in Fenichel’s theory, however, $\sigma(p; t)$ turns out to be computable explicitly. Consequently, $M_u(t)$ and $M_s(t)$ can be identified in any application, provided the invariant manifold $M(t)$ is known to exist.

C.3 Computing the NILE

In this section, we give two alternative expressions that can be used for computing the NILE in specific examples. The first expression will assume the explicit knowledge of normal vectors along the manifold $M(t)$. The resulting form of the NILE reveals that—in the language of mechanics— $\sigma(p, t)$ is equal to the maximal normal rate of strain relative to $M(t)$ at the point $p \in M(t)$.

The second expression will utilize a local coordinate representation of $M(t)$. In appropriate coordinates $(x, y) \in \mathbb{R}^k \times \mathbb{R}^{n-k}$, the k -dimensional invariant manifold $M(t)$ can always be written locally as a smooth graph:

$$M(t) = \left\{ (x, y) \in \mathbb{R}^k \times \mathbb{R}^{n-k} : y = \varphi(x, t), \quad x \in D(t) \right\}, \quad t \in [t_1, t_2]; \quad (\text{C.5})$$

here $D(t)$ is an open domain on which the local coordinate x is defined at time t (see Fig. C-3). The vector variable x may contain some parameters (dummy variables) on which the dynamical system depends; this is why we have suppressed any explicit parameter dependence in (C.1) and (C.6).

In the local variables (x, y) , the dynamical system (C.1) takes the form

$$\begin{aligned} \dot{x} &= f(x, y, t), \\ \dot{y} &= g(x, y, t), \end{aligned} \quad (\text{C.6})$$

where f and g are sufficiently smooth functions of their arguments.

Theorem 20 (i) Let $n(p, t)$ be a unit normal vector field to $M(t)$, that is smooth both in $p \in M(t)$ and in t . We then have

$$\sigma(p, t) = \max_{n(p, t) \in N_p M(t)} \langle n(p, t), D\mathcal{F}(p, t)n(p, t) \rangle,$$

with $\langle \cdot, \cdot \rangle$ denoting the standard Euclidean inner product.

(ii) Using the local form $y = \varphi(x, t)$ of $M(t)$ and the vector field (C.6), we define the matrix field

$$\Gamma(x, t) = g_y(x, \varphi(x, t), t) - \varphi_x(x, t)f_y(x, \varphi(x, t), t), \quad (\text{C.7})$$

where the subscript refers to differentiation with respect to the variable in the subscript.

We then have

$$\sigma(x, t) = \lambda_{\max} [\Gamma(x, t) + \Gamma^T(x, t)] / 2,$$

where $\lambda_{\max}[\cdot]$ refers to the largest eigenvalue of a symmetric matrix.

Proof: See Haller and Sapsis, 2010 [57].

C.4 Locating stable and unstable neighborhoods of $M(t)$

The normally stable and unstable subsets partition $M(t)$ into subsets in which infinitesimally small perturbations transverse to $M(t)$ start decaying or growing, respectively. The norm of such small perturbations is instantaneously constant on the boundary between $M_s(t)$ and $M_u(t)$.

As trajectories leave the vicinity of $M(t)$, the growth of their distance is no longer captured accurately by the linearized flow along $M(t)$. To locate finite-size neighborhoods of $M(t)$ where trajectories increase their distances from $M(t)$, we again assume that $M(t)$ is given locally in the form of a graph (C.5). As in the proof of Theorem 20, we use the change of coordinates

$$z = y - \varphi(x, t)$$

to transform $M(t)$ to the $z = 0$ plane. In the transformed coordinates, the flow satisfies

$$\begin{aligned} \dot{x} &= f(x, z + \varphi(x, t), t), \\ \dot{z} &= g(x, z + \varphi(x, t), t) - \varphi_x(x, t)f(x, z + \varphi(x, t), t) - \varphi_t(x, t). \end{aligned}$$

Taking the inner product of the second equation with z gives

$$\frac{1}{2} \frac{d}{dt} |z|^2 = \langle g(x, z + \varphi(x, t), t) - \varphi_x(x, t)f(x, z + \varphi(x, t), t) - \varphi_t(x, t), z \rangle.$$

The boundary between domains of instantaneous growth from, and decay to, the $\{z = 0\}$ plane is given by the *instantaneous stability boundary*

$$B(t) = \{(x, z) : \langle g(x, z + \varphi(x, t), t) - \varphi_x(x, t)f(x, z + \varphi(x, t), t) - \varphi_t(x, t), z \rangle = 0\}. \quad (\text{C.8})$$

The stable and unstable neighborhoods of $M(t)$ are given by

$$\begin{aligned} S(t) &= \{(x, z) : \langle g(x, z + \varphi(x, t), t) - \varphi_x(x, t)f(x, z + \varphi(x, t), t) - \varphi_t(x, t), z \rangle < 0\}, \\ U(t) &= \{(x, z) : \langle g(x, z + \varphi(x, t), t) - \varphi_x(x, t)f(x, z + \varphi(x, t), t) - \varphi_t(x, t), z \rangle > 0\}. \end{aligned}$$

Note that

$$\begin{aligned}
& \langle g(x, z + \varphi(x, t), t) - \varphi_x(x, t) f(x, z + \varphi(x, t), t) - \varphi_t(x, t), z \rangle \\
&= \langle [g_y(x, \varphi(x, t), t) - \varphi_x(x, t) f_y(x, \varphi(x, t), t)] z, z \rangle + O(|z|^3) \\
&= |z|^2 \left[\left\langle \frac{1}{2} [\Gamma(x, t) + \Gamma^T(x, t)] e_z, e_z \right\rangle + O(|z|) \right], \tag{C.9}
\end{aligned}$$

therefore

$$\begin{aligned}
M(t) \cap S(t) &= \left\{ (x, z) : z = 0, \quad \lambda_{\max} \left[\frac{1}{2} [\Gamma(x, t) + \Gamma^T(x, t)] \right] < 0 \right\}, \\
M(t) \cap U(t) &= \left\{ (x, z) : z = 0, \quad \lambda_{\max} \left[\frac{1}{2} [\Gamma(x, t) + \Gamma^T(x, t)] \right] > 0 \right\}.
\end{aligned}$$

As a result, we conclude that

$$\begin{aligned}
M_s(t) &\equiv M(t) \cap S(t), \\
M_u(t) &\subset M(t) \cap U(t).
\end{aligned}$$

Also note that by (C.8) and (C.9), both the instantaneous stability boundary $B(t)$ and the cylindrical surface

$$\mathcal{B}(t) = \{(x, z) : \sigma(x, t) = 0\} \tag{C.10}$$

have the same intersection with the manifold $M(t)$. Therefore, near the manifold $M(t)$, the condition $\sigma(x, t) = 0$ gives an approximation to the instantaneous stability boundary $B(t)$; the error of the approximation grows linearly in the order of the distance from the manifold. This error can be decreased to quadratic in the distance if we also include the $O(|z|^3)$ term in (C.9) in our calculations. In that case, the calculated dividing surface $B(t)$ will have a quadratic tangency with $\mathcal{B}(t)$ along $M(t)$.

The instantaneous stability boundary $B(t)$ between stable and unstable neighborhoods of $M(t)$ can also be computed directly from (C.8) without Taylor expansion in the z variable. Specifically, for any fixed z value, we can locate the curve of x values satisfying (C.8). Putting all these curves together, we obtain the surface $B(t)$.

C.5 Stability properties of non-neutrally buoyant particles

Note that (6.3) is of the form (C.6) with $x = \mathbf{x} \in \mathbb{R}^2$, $y = \mathbf{v} \in \mathbb{R}^2$, and with

$$\begin{aligned}
f(\mathbf{x}, \mathbf{v}, t) &= \mathbf{v}, \\
g(\mathbf{x}, \mathbf{v}, t) &= -\frac{1}{\epsilon} [\mathbf{v} - \mathbf{u}(\mathbf{x}, t)] + \frac{3R}{2} \frac{D\mathbf{u}(\mathbf{x}, t)}{Dt} + \left(1 - \frac{3R}{2}\right) \mathbf{g}. \tag{C.11}
\end{aligned}$$

In chapter 6 we proved that for any fixed $\epsilon > 0$ small enough, equation (6.3) admits a globally attracting two-dimensional invariant manifold of the form

$$M(t) = \left\{ (\mathbf{x}, \mathbf{v}) \in \mathbb{R}^4 : \mathbf{v} = \mathbf{u}(\mathbf{x}, t) + \epsilon \left[\frac{3R}{2} - 1 \right] \left[\frac{D\mathbf{u}(\mathbf{x}, t)}{Dt} - \mathbf{g} \right] + O(\epsilon^2) \right\}. \tag{C.12}$$

By comparison with the general form (C.5), formula (C.12) yields

$$\varphi(\mathbf{x}, t) = \mathbf{u}(\mathbf{x}, t) + \epsilon \left[\frac{3R}{2} - 1 \right] \left[\frac{D\mathbf{u}(\mathbf{x}, t)}{Dt} - \mathbf{g} \right] + \mathcal{O}(\epsilon^2). \quad (\text{C.13})$$

We apply Theorem 20 to identify the stable and unstable subsets of $M(t)$. Using (C.11) and (C.13), we obtain that the matrix $\Gamma(\mathbf{x}, t)$ satisfies

$$\begin{aligned} \Gamma(\mathbf{x}, t) &= [g_{\mathbf{v}} - \varphi_{\mathbf{x}} f_{\mathbf{v}}]_{\mathbf{v}=\varphi(\mathbf{x}, t)} \\ &= \left[-\frac{1}{\epsilon} I - \varphi_{\mathbf{x}} \right] \\ &= -\frac{1}{\epsilon} I - \nabla \mathbf{u}(\mathbf{x}, t) + \mathcal{O}(\epsilon), \end{aligned}$$

and hence the NILE can be written as

$$\begin{aligned} \sigma(\mathbf{x}, t) &= \lambda_{\max} [\Gamma^T(\mathbf{x}, t) + \Gamma(\mathbf{x}, t)] / 2 \\ &= \lambda_{\max} \left[-\frac{1}{\epsilon} I - \frac{1}{2} (\varphi_{\mathbf{x}}(\mathbf{x}, t) + \varphi_{\mathbf{x}}(\mathbf{x}, t)^T) \right] \\ &= -\frac{1}{\epsilon} I + \frac{1}{2} \lambda_{\max} [\nabla \mathbf{u}(\mathbf{x}, t) + \nabla \mathbf{u}(\mathbf{x}, t)^T] + \mathcal{O}(\epsilon). \end{aligned}$$

Here we used the fact that by incompressibility of the flow, the two-dimensional symmetric matrix $\nabla \mathbf{u}(\mathbf{x}, t) + \nabla \mathbf{u}(\mathbf{x}, t)^T$ has zero trace; as a result, its eigenvalues have opposite signs.

Up to an order $\mathcal{O}(\epsilon)$ error, therefore, the stable and unstable subsets of $M(t)$ satisfy

$$\begin{aligned} M_s(t) &\approx \left\{ (\mathbf{x}, \mathbf{v}) \in M(t) : \lambda_{\max} \left[\frac{\nabla \mathbf{u}(\mathbf{x}, t) + \nabla \mathbf{u}(\mathbf{x}, t)^T}{2} \right] < \frac{1}{\epsilon} \right\}, \\ M_u(t) &\approx \left\{ (\mathbf{x}, \mathbf{v}) \in M(t) : \lambda_{\max} \left[\frac{\nabla \mathbf{u}(\mathbf{x}, t) + \nabla \mathbf{u}(\mathbf{x}, t)^T}{2} \right] > \frac{1}{\epsilon} \right\}. \end{aligned} \quad (\text{C.14})$$

Bibliography

- [1] A. Agarwal. *Statistical Field Estimation and Scale Estimation for Complex Coastal Regions and Archipelagos*. MIT, MSc Thesis, 2009.
- [2] A. Agarwal and P. F. J. Lermusiaux. Statistical field estimation for complex coastal regions and archipelagos. *in preperation*, 2010.
- [3] S. Albeverio, F. Flandoli, and Y. Sinai. *SPDE in Hydrodynamic: Recent Progress and Prospects*. Springer-Verlag, 2008.
- [4] J.R. Angilella. Asymptotic analysis of chaotic particle sedimentation and trapping in the vicinity of a vertical upward streamline. *Phys. Fluids*, 19:073302, 2007.
- [5] J.-P. Antoine, R. Murenzi, P. Vandergheynst, and S.T. Ali. *Two-dimensional wavelets and their relatives*. Cambridge University Press, 2004.
- [6] V.I. Arnold and B. Keshin. *Topological methods in hydrodynamics*. Springer-Verlag, 1998.
- [7] G. Athanassoulis. *Stochastic Modeling and Prediction of Ocean Systems*. National Technical University of Athens, Greece, 2002.
- [8] A. Babiano, J.H. Cartwright, O. Piro, and A. Provenzale. Dynamics of a small neutrally buoyant sphere in a fluid and targeting in hamiltonian systems. *Physical Review Letters*, 84(25):5764, 2000.
- [9] G. K. Batchelor. *The theory of homogeneous turbulence*. Cambridge University Press, 1959.
- [10] G.K. Batchelor. *An Introduction to Fluid Dynamics*. Cambridge University Press, 2000.
- [11] D. Bau III and N. Trefethen. *Numerical linear algebra*. Society of Industrial and Applied Mathematics, 1997.
- [12] J. Bec, M. Cencini, and R. Hillerbrand. Heavy particles in incompressible flows: the large stokes number asymptotics. *Physica D*, 226:11–22, 2007.
- [13] J. Bec, M. Cencini, R. Hillerbrand, and K. Turitsyn. Stochastic suspensions of heavy particles. *Physica D*, 237:2037–2050, 2008.
- [14] R. Bellman. *Dynamic Programming*. Princeton University Press, 1957.

- [15] I.J. Benczik, Z. Toroczka, and T. Tel. Selective sensitivity of open chaotic flows on inertial tracer advection: Catching particles with a stick. *Phys. Rev. Lett.*, 89(16):164501, Sep 2002.
- [16] M. Beran. *Statistical Continuum Theories*. Interscience Publishers, 1968.
- [17] N. Berglund and B. Gentz. Geometric singular perturbation theory for stochastic differential equations. *Journal of Differential Equations*, 191(1):1–54, June 2003.
- [18] N. Berglund and B. Gentz. *Noise-Induced Phenomena in Slow-Fast Dynamical Systems*. Springer-Verlag, 2006.
- [19] G. Berkooz, P. Holmes, and J. Lumley. The proper orthogonal decomposition in the analysis of turbulent flows. *Annual Reviews of Fluid Mechanics*, 25:539–575, 1993.
- [20] P.S. Berloff and J.C. McWilliams. Material transport in oceanic gyres. Part II: Hierarchy of stochastic models. *Journal of Physical Oceanography*, 32(3):797–830, March 2002.
- [21] H.N. Najm B.J. Debusschere, P.P. Pebay, O.M. Knio, R.G. Ghanem, and O.P. Le Maitre. Numerical challenges in the use of Polynomial Chaos representations for stochastic processes. *SIAM J. Sci. Comput.*, 26:698 – 719, 2004.
- [22] G. Boffetta, G. Lacorata, G. Redaelli, and A. Vulpiani. Detecting barriers to transport: a review of different techniques. *Physica D*, 159:58, 2001.
- [23] A.W. Bowman and A. Azzalini. *Applied smoothing techniques for data analysis*. New York: Oxford University Press, 1997.
- [24] T.J. Burns, R.W. Davis, and E.F. Moore. A perturbation study of particle dynamics in a plane wake flow. *J. Fluid. Mech.*, 384:1–26, 1999.
- [25] R.H. Cameron and W.T. Martin. The orthogonal development of nonlinear functionals in series of Fourier-Hermite functionals. *Ann. Math.*, 48:385–392, 1947.
- [26] H. Cartan. *Differential Calculus*. Kershaw Publishing Company LTD, 1971.
- [27] K. I. Chang, K. Ide, M. Ghil, and C.-C.A. Lai. Transition to aperiodic variability in a wind-driven double gyre circulation model. *J. Phys. Oceanography*, 31:1260–1286, 2001.
- [28] S.A. Chapra and R.P. Canale. *Numerical Methods for Engineers*. McGraw-Hill, 6th edition edition, 2010.
- [29] E. Chatzi and A. Smyth. The unscented Kalman filter and particle filter methods for nonlinear structural system identification with non-collocated heterogeneous sensing. *Struct. Control and Health Monit.*, 16:99–123, 2009.
- [30] D. Chen and J. Liu. Mixture Kalman filters. *J. Roy. Stat. Soc. A*, 62:493–508, 2000.
- [31] A.J. Chorin. Gaussian fields and random flow. *J. Fluid. Mech.*, 85:325–347, 1974.
- [32] C. Crowe, T. Troutt, and J. Chung. Numerical models for two-phase turbulent flows. *Annu. Rev. Fluid Mech.*, 28:11, 1996.

- [33] G. T. Csanady. Turbulent diffusion of heavy particles in the atmosphere. *J. Atmos. Sci.*, 20:201–208, 1963.
- [34] S. Das, R. Ghanem, and S. Finette. Polynomial chaos representation of spatio-temporal random fields from experimental measurements. *J. Comput. Phys.*, In Press, 2009.
- [35] I. Daubechies. *Ten lectures on wavelets*. Society of Industrial and Applied Mathematics, 1992.
- [36] I. dePater and J. Lissauer. *Planetary Science*. Cambridge University Press, 2001.
- [37] H. Dijkstra and C.A. Katsman. Temporal variability of the wind-driven quasi-geostrophic double gyre ocean circulation: Basic bifurcation diagrams. *Geophys. Astrophys. Fluid Dynamics*, 85:195–232, 1997.
- [38] A. Doucet, N. de Freitas, and N. Gordon. *Sequential Monte-Carlo methods in practice*. Springer-Verlag, 2001.
- [39] A.D. Egorov, P.I. Sobolevsky, and L.A. Yanovich. *Functional Integrals: Approximate Evaluation and Applications*. Kluwer Academic Publishers, 1993.
- [40] V. Etyemezian, S. Ahonen, D. Nikolic, J. Gillies, H. Kuhns, D. Gillete, and J. Veranth. Deposition and removal of fugitive dust in the arid southwestern united states: measurements and model results. *Journal of air and waste managment*, 54:1099–1111, 2004.
- [41] G. Falkovich, A. Fouxon, and M. G. Stepanov. Acceleration of rain initiation by cloud turbulence. *Nature*, 419:151, 2002.
- [42] N. Fenichel. Persistence and smoothness of invariant manifolds for flows. *Ind. Univ. Math. J.*, 21:193–225, 1971.
- [43] N. Fenichel. Geometric singular perturbation theory for ordinary differential equations. *Journal of Differential Equations*, 31(1):53–98, January 1979.
- [44] C. Foias. A functional approach to turbulence. *Russian Mathematical Surveys*, 29:293–326, 1974.
- [45] J. Fouque, J. Garnier, G. Papanicolaou, and K. Solna. *Wave propagation and time reversal in randomly layered media*. Springer-Verlag, 2007.
- [46] U. Frisch. *Turbulence, The Legacy of A. N. Kolmogorov*. Cambridge University Press, 1996.
- [47] B. Ganapathysubramanian and N. Zabarar. Modeling diffusion in random heterogeneous media: Data-driven models, stochastic collocation and the variational multiscale method. *J. Comp. Phys.*, 226(1):326 – 353, 2007.
- [48] B. Ganapathysubramanian and N. Zabarar. A non-linear dimension reduction methodology for generating data-driven stochastic input models. *J. Comp. Phys.*, 227(13):6612 – 6637, 2008.
- [49] T.C. Gard. *Introduction to stochastic differential equations*. Marcel Dekker, 1988.

- [50] D. Gay and H. Ray. Identification and control of distributed parameter systems by means of the singular value decomposition. *Chemical Engineering Science*, 50:1519–1539, 1995.
- [51] R. Ghanem and J. Red-Horse. Propagation of probabilistic uncertainty in complex physical systems using a stochastic finite element approach. *Physica D*, 133(1-4):137–144, 1999.
- [52] R. Ghanem and P. Spanos. Stochastic finite elements: a Spectral Approach. *Springer-Verlag*, 1991.
- [53] P. Grassberger and I. Procaccia. Measuring the strangeness of strange attractors. *Physica D*, 9:189–208, 1983.
- [54] M. Griebel, T. Dornseifer, and T. Neunhoeffler. *Numerical Simulation in Fluid Dynamics*. Society of Industrial and Applied Mathematics, 1997.
- [55] J.L. Guermond, P. Mineev, and J. Shen. An overview of projection methods for incompressible flows. *Computer methods in applied mechanics and engineering*, 195:6011–6045, 2006.
- [56] G. Haller and T.P. Sapsis. Where do inertial particles go in fluid flows? *Physica D: Nonlinear Phenomena*, 237:573, 2008.
- [57] G. Haller and T.P. Sapsis. Localized instability and attraction along invariant manifolds. *SIAM J. of Appl. Dynamical Systems*, 9:611–633, 2010.
- [58] D. J. Higham. An algorithmic introduction to numerical simulation of stochastic differential equations. *SIAM Review*, 43(3):525–546, 2001.
- [59] P. Holmes, J. Lumley, and G. Berkooz. *Turbulence, Coherent Structures, Dynamical Systems and Symmetry*. Cambridge University Press, 1996.
- [60] E. Hopf. Statistical hydromechanics and functional calculus. *Journal of Rational Mechanics and Analysis*, 1:87–123, 1952.
- [61] I. Hoteit, D. Pham, G. Triantafyllou, and G. Korres. A new approximate solution of the optimal nonlinear filter for data assimilation in meteorology and oceanography. *Monthly Weather Review*, 136:317–334, 2008.
- [62] J. A. Hubbard, J. S. Haglund, and O. A. Exekoye. Simulation of the evolution of particle size distributions containing coarse particulate in the atmospheric surface layer with a simple convection-diffusion-sedimentation model. *Atmospheric Environment*, 43:4435–4443, 2009.
- [63] E. Kalnay. *Atmospheric modeling, Data assimilation and Predictability*. Cambridge University Press, 2002.
- [64] V. I. Klyatskin and T. Elperin. Diffusion of low-inertia particles in a field of random forces and the kramers problem. *Izvestiya, Atmospheric and Oceanic Physics*, 38(6):2002, 2002.
- [65] V.I. Klyatskin. *Stochastic equations through the eye of the physicist*. Elsevier Publishing Company, 2005.

- [66] O.M. Knio and O.P. Le Maitre. Uncertainty propagation in CFD using polynomial chaos decomposition. *Fluid Dynamics Research*, 38:616–640, 2006.
- [67] A. Kolmogorov. *Foundations of the Theory of Probability*. Chelsea Publishing Company, 1956.
- [68] V. Konotop and L. Vazquez. *Nonlinear Random Waves*. World Scientific, 1994.
- [69] Z. Kotulski. Equations for the characteristic functional and moments of the stochastic evolutions with an application. *SIAM J. Appl. Math.*, 49:296–313, 1989.
- [70] R. H. Kraichnan. Small-scale structure of a scalar field convected by turbulence. *Phys. Fluids*, 11:945–953, 1968.
- [71] J.A. Lee and M. Verleysen. *Nonlinear Dimensionality Reduction*. Springer-Verlag, 2007.
- [72] L.C. Lee. Wave propagation in a random medium. a complete set of the moment equations with different wavenumbers. *J. Math. Phys.*, 15:1431–1435, 1974.
- [73] P.F.J. Lermusiaux. *Error Subspace Data Assimilation Methods for Ocean Field Estimations: Theory, Validation, and Applications*. Harvard University, PhD Thesis, 1997.
- [74] P.F.J. Lermusiaux. Data assimilation via Error Subspace Statistical Estimation. Part II: Middle Atlantic Bight shelfbreak front simulations and ESSE validation. *Monthly Weather Review*, 127:1408 – 1432, 1999.
- [75] P.F.J. Lermusiaux. Estimation and study of mesoscale variability in the Strait of Sicily. *Dynamics of Atmospheres and Oceans*, 29:255 – 303, 1999.
- [76] P.F.J. Lermusiaux. Evolving the subspace of the three-dimensional multiscale ocean variability: Massachusetts Bay. *Journal of Marine Systems*, 29:385 – 422, 2001.
- [77] P.F.J. Lermusiaux. Uncertainty estimation and prediction for interdisciplinary ocean dynamics. *J. Comp. Phys.*, 217:176–199, 2006.
- [78] P.F.J. Lermusiaux. Adaptive Modeling, Adaptive Data Assimilation and Adaptive Sampling. *Physica D*, 230:172 – 196, 2007.
- [79] P.F.J. Lermusiaux, C.-S. Chiu, G.G. Gawarkiewicz, P. Abbot, A.R. Robinson, R.N. Miller, P.J. Haley, W.G. Leslie, S.J. Majumdar, A. Pang, and F. Lekien. Quantifying Uncertainties in Ocean Predictions. *Oceanography*, 19:92 – 105, 2006.
- [80] P.F.J. Lermusiaux, P. Malanotte-Rizzoli, D. Stammer, J. Carton, J. Cummings, and A.M. Moore. Progress and Prospects of U.S. Data Assimilation in Ocean Research. *Oceanography*, 19:172 – 183, 2006.
- [81] P.F.J. Lermusiaux and A.R. Robinson. Data assimilation via Error Subspace Statistical Estimation. Part I: Theory and schemes. *Monthly Weather Review*, 127:1385 – 1407, 1999.

- [82] P.F.J. Lermusiaux, A.R. Robinson, P.J. Haley, and W.G. Leslie. Advanced interdisciplinary data assimilation: Filtering and smoothing via error subspace statistical estimation. In *The OCEANS 2002 MTS/IEEE*. Holland Publications, 2002.
- [83] M. Leutbecher and T. N. Palmer. Ensemble forecasting. *J. Comput. Phys.*, 227:3515, 2008.
- [84] D. Lewis and T. Pedley. Planktonic contact rates in homogeneous isotropic turbulence: Theretic predictions and kinematic simulations. *J. Theor. Biol.*, 205:377, 2000.
- [85] R. Lewis and R. Kraichnan. A space - time functional formalism for turbulence. *Communications on Pure and Applied Mathematics*, 15:397–411, 1962.
- [86] Y.K. Lin and C.Q. Cai. *Probabilistic Structural Dynamics*. McGraw-Hill, Inc., 1995.
- [87] M. Loeve. *Probability Theory II*. Springer-Verlag, 1978.
- [88] D. Lucor, D. Xiu, and G. Karniadakis. Spectral representations of uncertainty in simulations: Algorithms and applications. *ICOSAHOM-01, Uppsala Sweden*, June 11-15, 2001.
- [89] J.L. Lumley. *Stochastic Tools in Turbulence*. Academic-Press, 1971.
- [90] O. Le Maitre, M. Reagan, H. Najm, R. Ghanem, and O. Knio. A stochastic projection method for fluid flow II. Random process. *J. Comput. Phys.*, 181:9 – 44, 2002.
- [91] O.P. Le Maitre, O. M. Knio, H. Najm, and R. Ghanem. A stochastic projection method for fluid flow: Basic formulation. *J. Comp. Phys.*, 173:481–511, 2001.
- [92] G.D. Manolis and C.Z. Karakostas. A Green’s function method to SH-wave motion in a random continuum. *Eng. Anal. Bound. Elements*, 27(2):93 – 100, 2003.
- [93] B. Marcu and E. Meiburg. The effect of streamwise braid vortices on the particle dispersion in a plane mixing layer. i. equilibrium points and their stability. *Phys. Fluids*, 8:715, 1996.
- [94] B. Marcu, E. Meiburg, and P. Newton. Dynamics of heavy particles in a burgers vortex. *Phys. Fluids*, 7:400, 1995.
- [95] J. Martin and E. Meiburg. The accumulation and dispersion of heavy particles in forced two-dimensional mixing layers: I. the fundumantal and subharmonic cases. *Phys. Fluids*, 6:1116, 1994.
- [96] Y. Marzouk, H. Najm, and L. Rahn. Stochastic spectral methods for efficient bayesian solution of inverse problems. *J. Comput. Phys.*, 224:560 – 586, 2007.
- [97] M. R. Maxey. The gravitational settling of aerosol particles in homogeneous turbulence and random flow fields. *J. Fluid Mech.*, 174:441–465, 1987.
- [98] M. R. Maxey and J. J. Riley. Equation of motion for a small rigid sphere in a nonuniform flow. *Physics of Fluids*, 26(4):883–889, 1983.
- [99] J. McCalpin and D. Haidvogel. Phenomenology of the low-frequency variability in a reduced-gravity, quasi-geostrophic double-gyre model. *J. Phys. Oceanography*, 26:739–752, 1996.

- [100] E.E. Michaelides. The transient equation of motion for particles, bubbles, and droplets. *J. Fluids Eng.*, 119:223, 1997.
- [101] E. Mograbi and E. Bar-Ziv. On the asymptotic solution of the maxey-riley equation. *Phys. Fluids*, 18:051704, 2006.
- [102] A. Monin and A. Yaglom. *Statistical Fluid Mechanics: Mechanics of turbulence, vol. I,II*. MIT Press, 1971, 1975.
- [103] H.N. Najm. Uncertainty quantification and polynomial chaos techniques in computational fluid dynamics. *Annu. Rev. Fluid Mech.*, 41:35 – 52, 2009.
- [104] A. Naylor and G. Sell. *Linear Operator Theory in Engineering and Science*. Springer-Verlag, 1982.
- [105] J. C. Nihoul and S. Djenidi. Hierarchy and scales in marine ecohydrodynamics. *Earth Sci. Rev.*, 31:255–277, 1991.
- [106] M. Ochi. *Ocean Waves: The Stochastic Approach*. Cambridge University Press, 1998.
- [107] N. T. Ouellette and J. P. Gollub. Dynamic topology in spatiotemporal chaos. *Phys. Fluids*, 20:064104, 2008.
- [108] N. T. Ouellette, P. J. J. O’Malley, and J. P. Gollub. Transport of finite-sized particles in chaotic flow. *Phys. Rev. Lett.*, 101:174504, 2008.
- [109] A. Papoulis. *Probability, Random Variables and Stochastic Processes*. McGraw-Hill, 1965.
- [110] N.M. Patrikalakis, P.F.J. Lermusiaux, C. Evangelinos, J.J. McCarthy, A.R. Robinson, H. Schmidt, P.J. Haley, S. Lalis, R. Tian, W.G. Leslie, and W. Cho. *Towards Dynamic Data Driven Systems for Rapid Adaptive Interdisciplinary Ocean Forecasting. Invited paper in ‘Dynamic Data-Driven Application Systems’*. Springer, 2009.
- [111] G. A. Pavliotis, A. M. Stuart, and K. C. Zygalakis. Homogenization for inertial particles in a random flow. *Commun. Math. Sci.*, 5:507–531, 2007.
- [112] Y.B. Pesin. *Dimension Theory in Dynamical Systems: Contemporary Views and Applications*. The University of Chicago, 1998.
- [113] R.T. Pierrehumbert and H. Yang. Global chaotic mixing on isentropic surfaces. *J. Atmos. Sci.*, 50:2462, 1993.
- [114] M. Pinsky and A. Khain. Turbulence effects on droplets growth and size distribution in clouds - a review. *J. Aerosol Science*, 28:1177, 1997.
- [115] S.M. Prigarin. *Spectral Models of Random Fields in Monte Carlo Methods*. VSP BV, 2001.
- [116] V.S. Pugachev and I.N. Sinityn. *Stochastic Differential Systems*. John Wiley and Sons, 1987.
- [117] A. M. Reynolds. On the formulation of lagrangian stochastic models for heavy-particle trajectories. *Journal of Colloid and Interface Science*, 232:260–268, 2000.

- [118] J. Roberts and P. Spanos. *Random Vibration and Statistical Linearization*. Dover Publications, 2003.
- [119] B. J. Rothschild and T. R. Osborn. Small scale turbulence and plankton contact rates. *J. Plankton Res.*, 10:465, 1988.
- [120] Yu.A. Rozanov. *Random Fields and Stochastic Partial Differential Equations*. Kluwer Academic Publishers, 1996.
- [121] J. Rubin, C.K.R.T. Jones, and M. Maxey. Settling and asymptotic motion of aerosol particles in a cellular flow field. *J. Nonlinear Sci.*, 5:337–358, 1995.
- [122] T. Sapsis and G. Haller. Inertial particle’s motion in geophysical fluid flows. *6th EUROMECH Conference ENOC 2008, St. Petersburg, Russia*, 2008.
- [123] T. P. Sapsis and G. Haller. Inertial particle dynamics in a hurricane. *J. Atmos. Sci.*, 66:2481–2492, 2009.
- [124] T. P. Sapsis and G. Haller. Clustering criterion for inertial particles in two-dimensional time-periodic and three-dimensional steady flows. *Chaos*, 20:017515, 2010.
- [125] T. P. Sapsis, G. Haller, and J. Peng. Predator prey interactions in jellyfish feeding. *Bulletin of Mathematical Biology - In press*, 2010.
- [126] T. P. Sapsis and P. F. J. Lermusiaux. Dynamical criteria for the evolution of the stochastic dimensionality in flows with uncertainty. *in preperation*, 2010.
- [127] T.P. Sapsis and G.A. Athanassoulis. New partial differential equations governing the joint, response-excitation, probability distributions of nonlinear systems, under general stochastic excitation. *Probab. Eng. Mech.*, 23(2-3):289 – 306, 2008.
- [128] T.P. Sapsis and G. Haller. Instabilities in the dynamics of neutrally buoyant particles. *Physics of Fluids*, 20:017102, 2008.
- [129] T.P. Sapsis and P.F.J. Lermusiaux. Dynamically orthogonal field equations for continuous stochastic dynamical systems. *Physica D*, 238:2347–2360, 2009.
- [130] A. Sarkar and R. Ghanem. Mid-frequency structural dynamics with parameter uncertainty. *Comput. Meth. Appl. Mech. and Eng.*, 191(47-48):5499 – 5513, 2002.
- [131] R. A. Shaw. Particle turbulence interactions in atmospheric clouds. *Ann. Rev. of Fluid Mech.*, 35:183, 2003.
- [132] S. Shvartsman and Y. Kevrekidis. Nonlinear model reduction for control of distributed systems: A computer-assisted study. *A.I.Ch.E. Journal*, 44:1579–1595, 1998.
- [133] E. Simmonet and H. Dijkstra. Spontaneous generation of low-frequency modes of variability in the wind-driven ocean circulation. *J. Phys. Oceanography*, 32:1747–1762, 2002.
- [134] L. Sirovich. Turbulence and the dynamics of coherent structures, parts I, II and III. *Quart. Appl. Math.*, XLV:561–590, 1987.
- [135] K. Sobczyk. *Stochastic Wave Propagation*. Elsevier Publishing Company, 1985.

- [136] K. Sobczyk. *Stochastic Differential Equations*. Kluwer Academic Publishers, 1991.
- [137] T. Soong and M. Grigoriu. *Random Vibration of Mechanical and Structural Systems*. PTR Prentice Hall, 1993.
- [138] D. Stroock. *Markov Processes from K. Ito's Perspective*. Princeton University Press, 2003.
- [139] A. J. Szeri, S. Wiggins, and L. G. Leal. On the dynamics of suspended microstructures in unsteady, spatially inhomogeneous, two-dimensional fluid flows. *J. Fluid Mech.*, 228:207, 1991.
- [140] L. Tang, F. Wen, Y. Yang, C. Crowe, J. Chung, and T. Troutt. Self-organizing particle dispersion mechanism in a plane wake. *Phys. Fluids A*, 4:2244, 1992.
- [141] V.I. Tatarskii. The light propagation in a medium with random inhomogeneities of the refractive index and the markov process approximation. *J. Exp. Theor. Phys.*, 56:2106–2117, 1969.
- [142] V.I. Tatarskii. Characteristic functional for one class of non-gaussian random functions. *Waves in Random Media*, 5:243–252, 1995.
- [143] H. Tennekes and J.L. Lumley. *A first course in turbulence*. MIT Press, 1972.
- [144] D.J. Thomson. Criteria for the selection of stochastic models of particle trajectories in turbulent flows. *Journal of Fluid Mechanics Digital Archive*, 180(-1):529–556, 1987.
- [145] K. K. Tio, A. Linan, J. Lasheras, and A. Ganan-Calvo. On the dynamics of buoyant and heavy particles in a periodic stuart vortex flow. *J. Fluid. Mech.*, 253:671, 1993.
- [146] M. Y. Tsai, K. Elgethun, J. Ramaprasad, M. G. Yost, A. S. Felsot, V. R. Hebert, and R. A. Fenske. The washington aerial spray drift study: modeling pesticide spray drift deposition from an aerial application. *Atmospheric Environment*, 39:6194–6203, 2005.
- [147] M. Ueckermann. Towards next generation ocean models: Novel discontinuous galerkin schemes for 2D unsteady biogeochemical models. Master's thesis, MIT, 2009.
- [148] M. Ueckermann and P.F.J. Lermusiaux. Manual for finite-volume code used for mit course 2.29, 2009.
- [149] M. Ueckermann and P.F.J. Lermusiaux. High order schemes for 2D unsteady biochemical ocean models. *Ocean Dynamics*, 2010, In Press.
- [150] R. van der Merwe and E. Wan. Gaussian mixture sigma-point particle filters for sequential probabilistic inference in dynamic state-space models. *Proceedings of the International Conference on Acoustics, Speech, and Signal Processing (ICASSP), Hong-Kong*, 2003.
- [151] A.A. Vasiliev and A.I. Neishtadt. Regular and chaotic transport of impurities in steady flows. *Chaos*, 4:673, 1994.

- [152] R.D. Vilela, A.P.S. de Moura, and C. Grebogi. Finite-size effects on open chaotic advection. *Physical Review E (Statistical, Nonlinear, and Soft Matter Physics)*, 73(2), 2006.
- [153] R.D. Vilela and A. Motter. Can aerosols be trapped in open flows. *Phys. Rev. Lett.*, 99:264101, 2007.
- [154] M. J. Vishik and A.V. Fursikov. *Mathematical Problems of Statistical Hydromechanics*. Kluwer Academic Publishers, 1988.
- [155] Weidenschilling. Aerodynamics of solid bodies in the solar nebula. *Mont. Not. R. Astr. Soc.*, 180:57, 1977.
- [156] N. Wiener. The homogeneous chaos. *Am. J. Math.*, 60:897–936, 1938.
- [157] N. Wiener. *Nonlinear Problems in Random Theory*. MIT Technology Press and John Wiley and Sons, 1958.
- [158] C.H.K. Williamson. Vortex dynamics in the cylinder wake. *Annu. Rev. Fluid Mech.*, 28:477 – 539, 1996.
- [159] E. Wong and M. Zakai. On the relation between ordinary and stochastic equations. *International Journal of Engineering Sciences*, 3:213–229, 1965.
- [160] C. Wunsch. *Discrete Inverse and State Estimation Problems with Geophysical Fluid Applications*. Cambridge University Press, 2006.
- [161] D. Xiu and G. Karniadakis. The Wiener-Askey polynomial chaos for stochastic differential equations. *SIAM J. Sci. Comp.*, 24:619–644, 2002.
- [162] D. Xiu and G. Karniadakis. Modeling uncertainty in flow simulations via generalized polynomial chaos. *J. Comp. Phys.*, 187:137–167, 2003.
- [163] A.M. Yaglom. *Correlation Theory of Stationary and Related Random Functions, Volume I: Basic Results*. Springer-Verlag, 1986.
- [164] M. I. Yudine. Physical considerations of heavy-particle diffusion. *Atmospheric diffusion and air pollution, Advances in geophysics*, 6:185–191, 1959.
- [165] D. Zhang. *Stochastic Methods for Flow in Porous Media*. Academic-Press, 2001.
- [166] Y. Zhang, M. Henson, and Y. Kevrekidis. Nonlinear model reduction for dynamic analysis of cell population models. *Chemical Engineering Science*, 58:429–445, 2003.
- [167] V.A. Zorich. *Mathematical Analysis II*. Springer-Verlag, 2004.